Amazon hydrology from space: scientific advances and future challenges

Alice César Fassoni-Andrade[1,2,3], Ayan Santos Fleischmann[3], Fabrice Papa[1,2], Rodrigo Cauduro Dias de Paiva[3], Sly Wongchuig[4], John M. Melack[5], Adriana Aparecida Moreira[3], Adrien Paris[6,1], Anderson Ruhoff[3], Claudio Barbosa[7], Daniel Andrade Maciel[7], Evlyn Novo[7], Fabien Durand[1,2], Frédéric Frappart[1], Filipe Aires[8], Gabriel Medeiros Abrahão[9], Jefferson Ferreira-Ferreira[10], Jhan Carlo Espinoza[4], Leonardo Laipelt[3], Marcos Heil Costa[9], Raul Espinoza-Villar[11], Stéphane Calmant[1], Victor Pellet[12,8]

[1] Laboratoire d'Etudes en Géophysique et Océanographie Spatiales (LEGOS), Université Toulouse, IRD, CNRS, CNES, UPS, Toulouse, France.

[2] Institute of Geosciences, University of Brasília (UnB), Campus Universitário Darcy Ribeiro, Brasília, Brazil.

[3] Institute of Hydraulic Research, Federal University of Rio Grande do Sul (UFRGS), Porto Alegre, Brazil.

[4] Univ. Grenoble Alpes, IRD, CNRS, Grenoble INP, Institut des Géosciences de l'Environnement (IGE, UMR 5001), 38000, Grenoble, France.

[5] Earth Research Institute, University of California, Santa Barbara.

[6] Ocean Next, La Terrasse, 38660 Grenoble, France.

[7] Instrumentation Lab for Aquatic Systems (LabISA), Earth Observation Coordination of National Institute for Space Research (INPE), São José dos Campos, SP, Brazil.

[8] Laboratoire d'Etudes du Rayonnement et de la Matière en Astrophysique et Atmosphères, Observatoire de Paris, UMR 8112, Paris, France.

[9] Federal University of Viçosa (UFV), Viçosa, MG, Brazil.

[10] Mamirauá Institute for Sustainable Development, Tefé, AM, Brazil.

[11] Departamento de Ordenamiento Territorial y Construcción, Universidad Nacional Agraria La Molina (UNALM), Av. La Molina s/n Lima 12, Perú.

[12] Institute of Industrial Science, The University of Tokyo, Tokyo, Japan.

Corresponding author: Alice Fassoni-Andrade (alice.fassoni@gmail.com, alice.fassoni@legos.obs-mip.fr)

Key points:

- Integrated view of scientific advances in Amazon hydrology with remote sensing
- Expected progresses to understand the water cycle, aquatic ecosystems and environmental changes with upcoming hydrology-oriented missions
- Need to translate advance knowledge from RS to support water management and environmental governance

Abstract

As the largest river basin on Earth, the Amazon is of major importance to the world's climate and water resources. Over the past decades, advances in satellite-based remote sensing (RS) have brought our understanding of its terrestrial water cycle and the associated hydrological processes to a new era. Here, we review major studies and the various techniques using satellite RS in the Amazon. We show how RS played a major role in supporting new research and key findings regarding the Amazon water cycle, and how the region became a laboratory for groundbreaking investigations of new satellite retrievals and analyses. At the basin-scale, the understanding of several hydrological processes was only possible with the advent of RS observations, such as the characterization of "rainfall hotspots" in the Andes-Amazon transition, evapotranspiration rates, and variations of surface waters and groundwater storage. These results strongly contribute to the recent advances of hydrological models and to our new understanding of the Amazon water budget and aquatic environments. In the context of upcoming hydrology-oriented satellite missions, which will offer the opportunity for new synergies and new observations with finer space-time resolution, this review aims to guide future research agenda towards an integrated monitoring and understanding of the Amazon water from space. Integrated multidisciplinary studies, fostered by international collaborations, set up future directions to tackle the great challenges the Amazon is currently facing, from climate change to increased anthropogenic pressure.

Plain Language Summary

The Amazon basin is the largest river basin in the world, characterized by complex hydrological processes that connect high rates of precipitation, extensive floodplains, dense tropical forests, complex topography, and large variations in freshwater storage and discharge. It plays a key role in the water, energy and carbon cycles and interacts with the global climate system. Earth observations have played a major role in supporting research in Amazon hydrology, and the characterization of several hydrological processes was only possible with the help of remote sensing data. The basin is now facing great risk under current climate change and increased anthropogenic pressure and the resulting environmental alterations require a better understanding of the overall basin’s water cycle across scales. We review the strengths and limitations of observations from satellites in the context of the current and upcoming hydrology-oriented satellite missions, and we make recommendations for improving satellite observations of the Amazon basin water cycle, along with an interdisciplinary and stepwise approach to guide research for the next decades.

Table of contents

1. Introduction

The Amazon River basin (AB) is the major hydrological system of the world (~6 million km^2) with a diverse rivers, floodplains and wetlands (Latrubesse et al., 2017; **Figure 1**). It spans over seven countries and it hosts four of the ten largest rivers in the world, namely the Solimões-Amazonas, Madeira, Negro, and Japurá rivers (**Figure 2**). It receives high annual rainfall rates (~2200 mm yr^{-1} , Builes-Jaramillo & Poveda, 2018; Espinoza et al., 2009) and around half of the precipitation in the AB is recycled by local evapotranspiration (Salati et al., 1979; Satyamurty, da Costa, & Manzi, 2013) providing moisture to southern parts of South America. The Amazon River then flows into the Atlantic Ocean with an average annual discharge of 206 x 10^3 m^{3}s^{-1} (Callède et al., 2010), amounting to almost 20% of the total global freshwater reaching the ocean annually and exports the largest sedimentary supply to the ocean (1.1 x 10^9 tons per year; Armijos et al., 2020).

The high rates of precipitation, evapotranspiration, and large variations in freshwater storage and river discharge make the AB a key player in the global climate system, with large contributions to the water, energy, and carbon cycles (Gash et al., 2013; Nagy et al., 2016). Amazon surface waters, for instance, are a major source and sink of carbon dioxide (Abril et al., 2014; Amaral et al., 2020; Guilhen et al., 2020; Raymond et al., 2013; Richey et al., 2002) and the largest natural geographic source of methane in the tropics (Kirschke et al., 2013; Melack et al., 2004; Pangala et al., 2017; Pison et al., 2013). Seasonal variations in water contribute to the formation of tropical forests (Leite et al., 2012), maintain high aquatic productivity (Melack & Forsberg, 2001) and biodiversity (Junk, 1997; Junk et al., 2010), and influence fish distributions and fisheries yield (Junk et al., 2010; Lobón-Cerviá et al., 2015). The AB hosts ~40% of the world tropical forest and ~15% of global land biodiversity (Marengo et al., 2018). AB is the home of local people that rely on rivers as transportation corridors, and utilize these environments for their subsistence (A. B. Anderson et al., 1991; Campos-Silva et al., 2020; Endo et al., 2016). AB also serves the broader South American population in terms of energy, food and other forest products

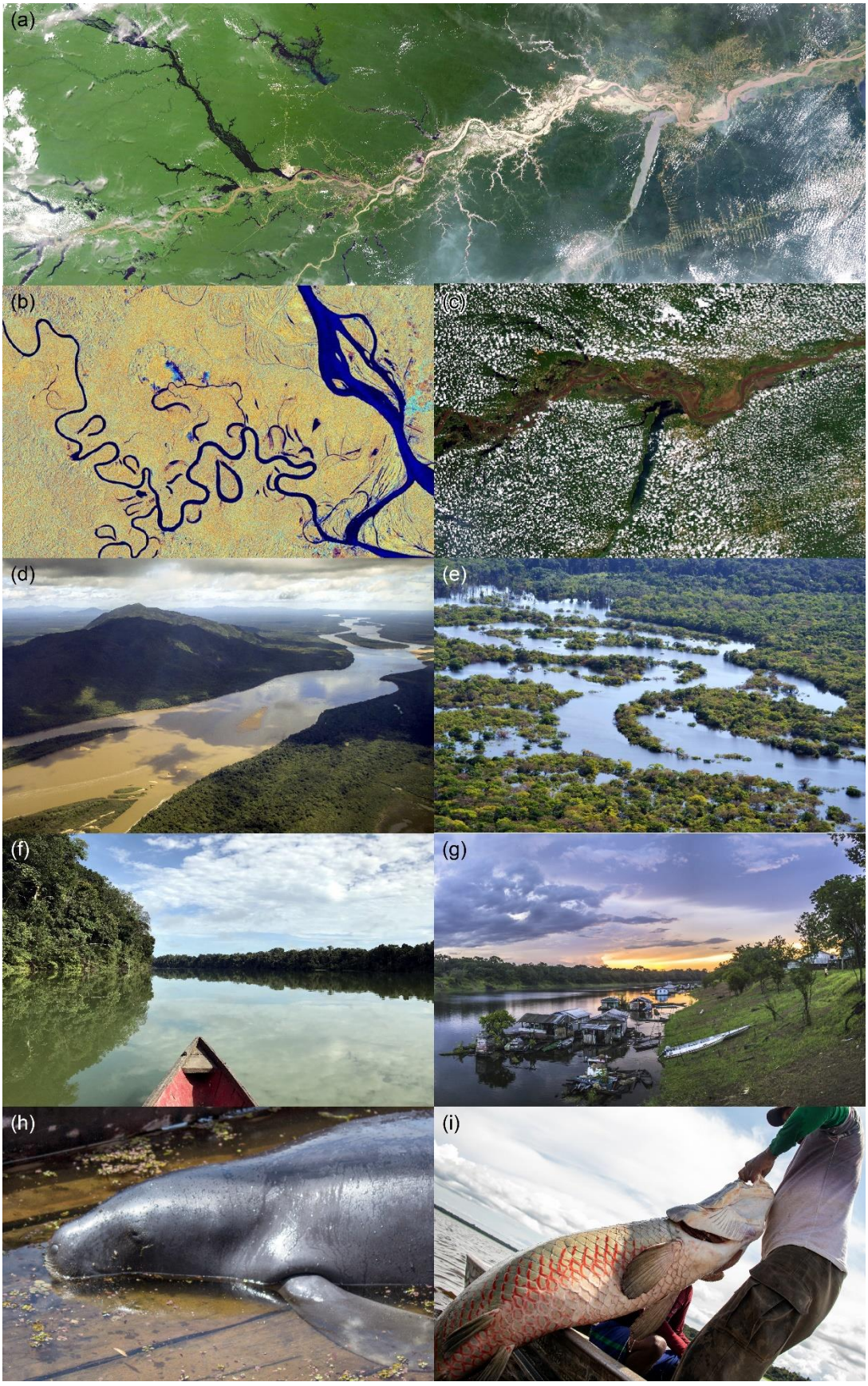
(a)
(b)
(c)
(d)
(e)
(f)
(g)
(h)
(i)

Figure 1. (a) MODIS image of the central AB, characterized by large floodplains (Source: NASA catalog; https://visibleearth.nasa.gov/images/62101/the-amazon-brazil/62104l); (b) Sentinel-1 image of rivers and lakes of the upper Solimões River (Source: ESA catalog; https://www.esa.int/ESA_Multimedia/Images/2020/09/Amazon_River); (c) MODIS image showing the reduced cloud cover over water bodies (Source: NASA catalog; https://earthobservatory.nasa.gov/images/145649/mapping-the-amazon); (d) Aerial view of Rio Branco (Photo by Thiago Laranjeira); (e) Floodplain during the high water (Photo by João Paulo Borges Pedro); (f) Channel (Photo by Jefferson Ferreira-Ferreira); (g) Community at the river bank (Photo by Thiago Laranjeira); (h) Manatee (Photo by Amanda Lelis); (i) Arapaima (Pirarucu) fish, the largest scaled freshwater in the world (Photo by Bernardo Oliveira).

The region is now facing risks under current climate and anthropogenic changes, and changes in Amazon hydrology could have substantial impacts globally (Jimenez et al., 2019). In the past decades, the AB experienced several intense climatic events, such as extreme droughts and floods, with no equivalent in the last 100 years (Barichivich et al., 2018; Marengo & Espinoza, 2016). Severe droughts can lead to environmental disturbances, from increased fire occurrence (Zeng et al., 2008) to abrupt shifts in fish assemblages (Röpke et al., 2017). Moreover, the accumulated negative impacts of increased human interventions across the region, such as damming (Forsberg et al., 2017; Latrubesse et al., 2017), deforestation (M. E. Arias et al., 2020; Coe et al., 2009; Leite-Filho et al., 2020; Leite et al., 2012), fires (Aragão et al., 2008; Xu et al., 2020; Zeng et al., 2008), and mining (Abe et al., 2019; Lobo et al., 2015), will possibly trigger major modifications that could affect the AB water cycle, although they provide a fundamental basis for calibrating and validating RS data.

Characterizing and understanding the dynamics of the Amazon water cycle is of primary importance for climate and ecology research and for the management of global water resources. Consequently, there is a need for a comprehensive monitoring of the spatial-temporal dynamic of the Amazon water cycle components and how they interact with climate variability and anthropogenic pressure. In large and remote tropical watersheds such as the AB, in situ observational networks are difficult to operate and maintain, and they are not capable of monitoring all components of the water cycle.

While the AB was in the spotlight of international scientific discussion during the last decades, the understanding of AB hydrology coevolved with another groundbreaking field: the remote sensing (RS) of terrestrial water cycle. In this context, the AB has been an ideal laboratory for the seminal development of RS techniques with the advent of Earth Observation (EO) and these advances have fostered the scientific understanding of AB hydrology, ecosystems and environmental changes. For example, the first applications of altimeter and gravimetric satellites to characterize, respectively, surface water elevation (Guzkowska et al., 1990) and total water storage variations (Tapley et al., 2004) were performed in the AB due to its wide river and large spatial and temporal changes of freshwater. Pioneering RS applications also include microwave, Synthetic-Aperture Radar (SAR) and interferometric mapping of large scale flood inundation and characterization of sediment dynamics (Alsdorf et al., 2000; Hess et al., 2003; Mertes et al., 1993; Sippel et al., 1994). Since then, several applications using RS data have been carried out in other basins worldwide (e.g., Alsdorf et al., 2021). All these important developments have been carried out by a diverse community of scientists with different interests

and views on the AB water cycle, and surprisingly, there is a lack of review articles analyzing the continuous growth of publications that make use of RS observations to study the hydrology of the region.

Here we review the various achievements of more than three decades of scientific advances on the hydrology of the AB from RS (**Figure 2**), and present perspectives, currently fostered by an unprecedented availability of satellite observations and the upcoming launch of dedicated hydrology satellites, such as the Surface Water and Ocean Topography (SWOT) or the NASA-ISRO SAR mission (NISAR). This work reunited experts on RS of different hydrological processes of the AB to review specific topics and discuss paths towards scientific advances as well as the opportunities shaping this field for the next decades. Reviews account for hydrological variables as precipitation, evapotranspiration, surface water elevation, surface water extent, floodplain and river channels topography, water quality (e.g., estimation of sediments, chlorophyll, and dissolved organic matter), total water storage and groundwater storage that are presented in separate sections (**Figure 2**). Each section describes how the variable is retrieved from RS observations, presents the scientific advances that have been achieved from this information, as well as various applications in the AB and discusses future challenges. Then, four sections are dedicated to the integration of RS data in the fields of water budget closure, hydrological and hydraulic modelling, aquatic environments and environmental changes over the Amazon. Section 7 summarizes the scientific advances, the knowledge gaps and the research opportunities regarding AB hydrology and ecosystems, including the forthcoming satellite missions. It also presents how the lessons learnt from AB experiences are benefiting other large river basins worldwide. The two final parts discuss how to move forward from the scientific advances toward a basin-scale water resources planning and new environment monitoring tools, and highlight our recommendations that set forward the research agenda of Amazon hydrology from space for the coming decade.

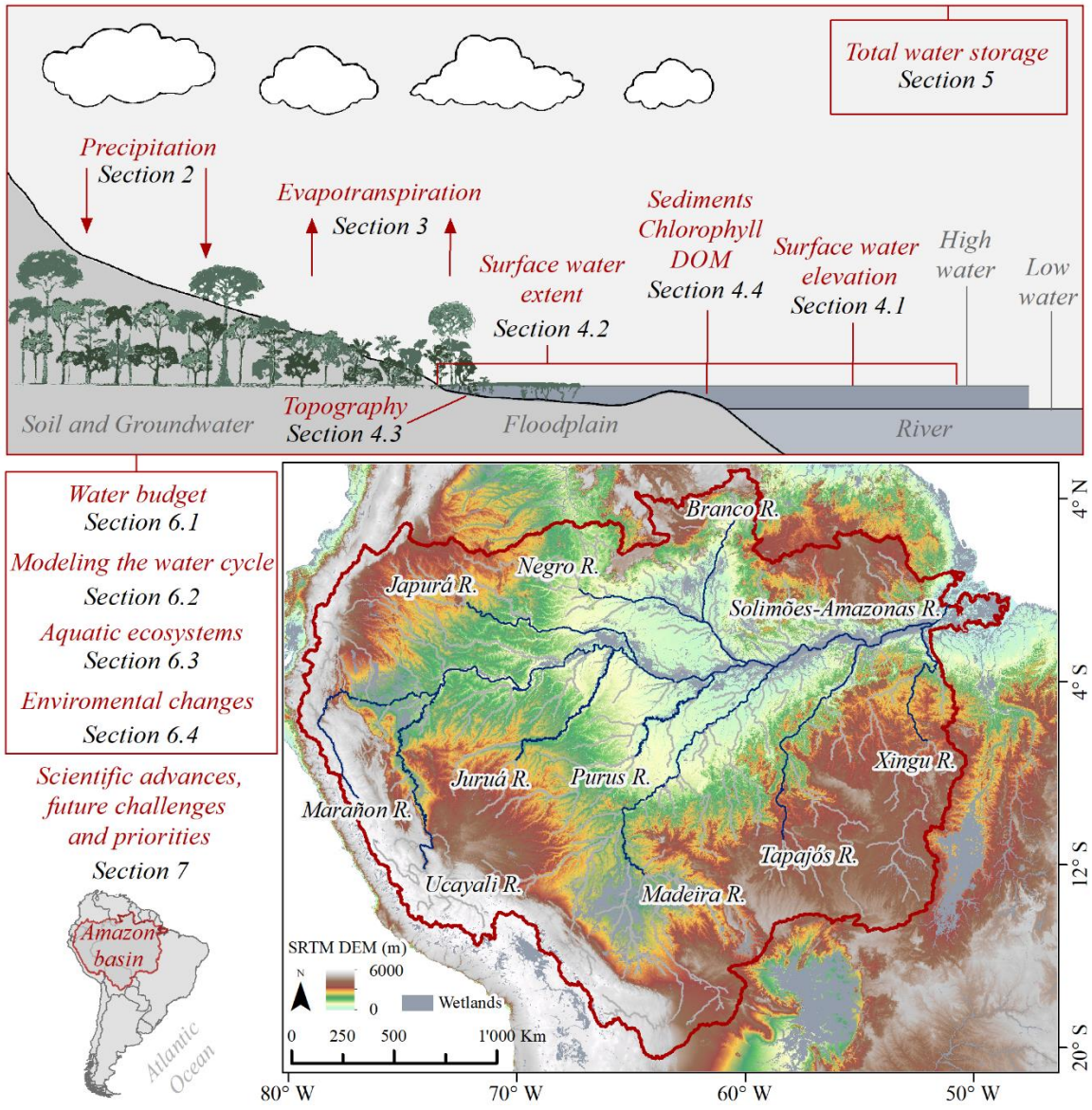

Figure 2. Location of the AB in South America, and representation of the hydrological variables observed by RS techniques, with the respective section numbers as addressed in this review.

2. Precipitation

Precipitation is a crucial component of the water cycle (Bookhagen & Strecker, 2008; J. C. Espinoza Villar, Ronchail, et al., 2009; Salati & Vose, 1984; Trenberth, 2011), characterized by high spatial and temporal variability. In the AB, precipitation is related to complex interactions of various large-scale physical and dynamic processes as well as local features, which are responsible for the temporal and spatial distribution of precipitation (Figueroa & Nobre, 1990). For instance, in addition to the orographic rains that occur in the transition between the Andes mountains and the Amazon, the substantial transpiration from the forest contributes to abundant water fluxes to the atmosphere, which eventually returns to the land as

recycled precipitation and contributes up to around 30% of the basin's rainfall (Bosilovich & Chern, 2006; Eltahir & Bras, 1994; Van Der Ent et al., 2010; Fisher et al., 2009; Salati & Nobre, 1991; Staal et al., 2018; Yang & Dominguez, 2019; Zemp et al., 2014). This contribution is normally presented as a convection process, which helps maintaining a climatological upper-level, large-scale circulation known as the Bolivian high (Lenters & Cook, 1997; Virji, 1981), and together with other related precipitation patterns are affected by both global-scale phenomena (e.g., El Niño–Southern Oscillation -ENSO, Tropical Atlantic sea surface temperature -SSTemp) and local forcing, such as land cover structures (Aceituno, 1988; Koren et al., 2008; Leite-Filho et al., 2020; Lin et al., 2006).

Mainly because of its large extent, precipitation regimes in the AB differ from one region to another in terms of seasonal pattern (**Figure 3**c to f) and on a more local scale, rainfall regimes are highly variable in space (P. A. Arias et al., 2021; Espinoza et al., 2009). Therefore, accurate and reliable rainfall measurements are crucial for the study of climate trends and variability, and also for the management of water resources and weather, climate and hydrological forecasting in this region (S. Jiang et al., 2012; X. Liu et al., 2017; Yilmaz et al., 2005).

Gauge observations are traditionally used to measure precipitation directly at the land surface (Kidd, 2001), and various large-scale datasets at different scales have been developed from these in situ observations (A. Becker et al., 2013; Kidd et al., 2017). However, in situ measurements have several drawbacks, such as incomplete cover over sparsely populated areas, a common feature of Amazonian countries. In addition, the variability of rainfall means that the measurements from in situ stations are typically not representative of the surrounding areas, or may be inaccurate (Kidd et al., 2017; Prabhakara et al., 1986). In the AB, for instance, rainfall stations are typically located in the cities, placed near to the main tributaries, and low density of stations are observed in tropical forest and in regions not accessible. Therefore, the low density of the rain gauge network and the lack of homogeneity in the time series prevent reliable monitoring using ground data (Debortoli et al., 2015; Delahaye et al., 2015; J. C. Espinoza Villar, Ronchail, et al., 2009; Ronchail et al., 2002). Collecting complementary observations to in situ measurements is then fundamental to obtain estimation of rainfall over the continent’s surfaces (Van Dijk & Renzullo, 2011; Kidd & Levizzani, 2011; Wanders et al., 2014).

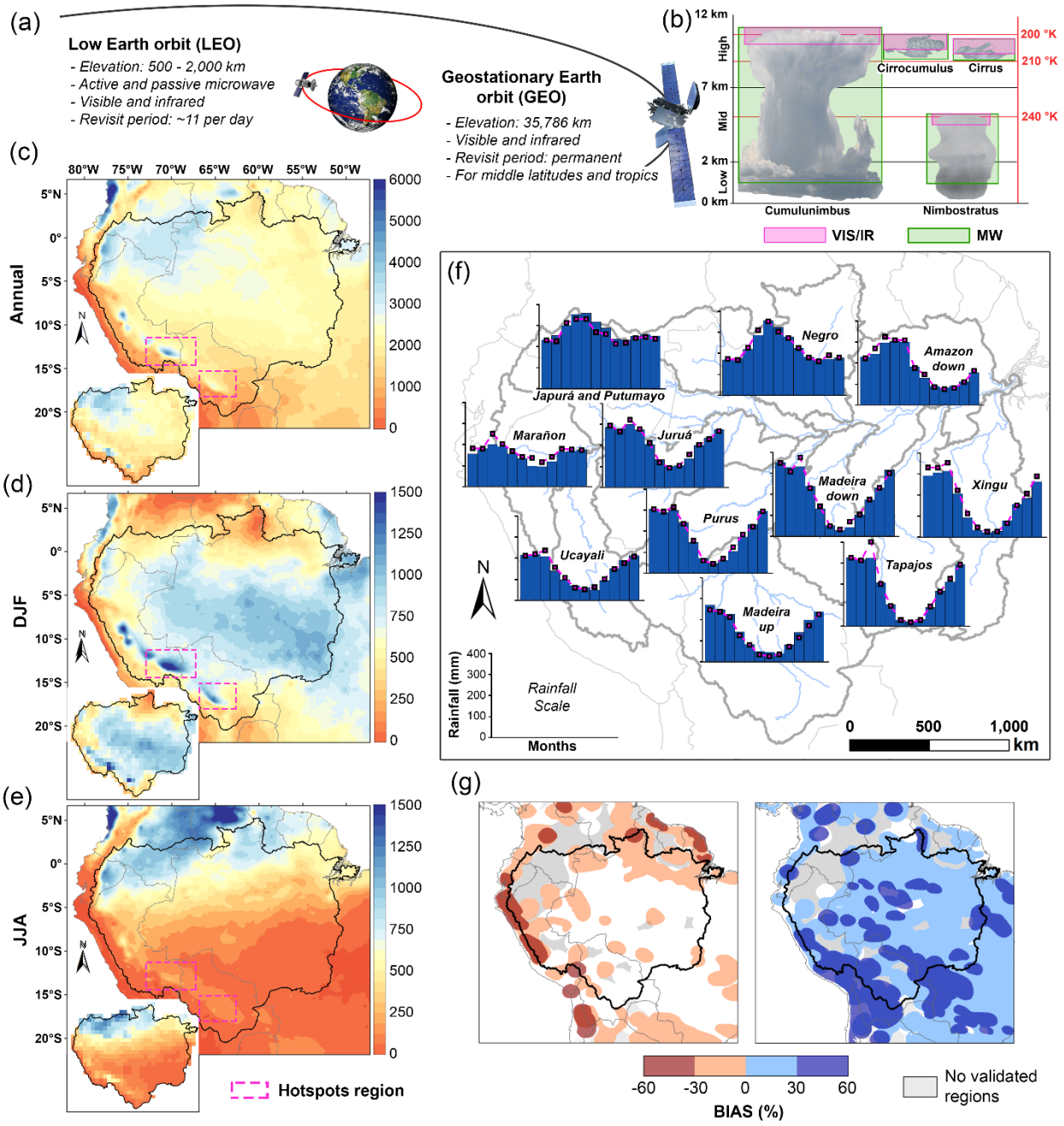

Figure 3. (a) Schematic representation of remote sensors for precipitation estimation on board satellites. (b) Illustration of the VIS/IR and MW coverage range for different cloud types. Precipitation climatology for (c) annual, (d) austral summer - DJF, and (e) austral winter - JJA from CHIRP v2 dataset (1981-2020) at 5 km spatial resolution and HOP dataset (1981-2009) (Espinoza et al., 2016; Guimberteau et al., 2012) in small boxes at left-bottom at ~100 km spatial resolution. (f) The annual regime for eleven large basins of the Amazon, based on HOP datasets (1981-2009) (bars) and the CHIRP based (1981-2020) in magenta lines. (g) Annual average negative (red scale) and positive (blue scale) bias of six precipitation RS-based and non-gauged-

corrected products in the AB for the period 2000-2016, adapted from (Beck, Vergopolan, et al., 2017).

Satellite observations of precipitation have become available on a global scale in recent decades. These satellites mainly use infrared (IR) and microwave (MW) sensors to provide precipitation estimates using different techniques (Kidd & Huffman, 2011). The sensors used to estimate precipitation can be classified in three categories (Prigent, 2010): (i) visible/IR (VIS/IR) sensors on geostationary (GEO) and low Earth orbit (LEO) satellites, (ii) passive MW (PMW) sensors on LEO satellites, and (iii) active MW (AMW) sensors on LEO satellites. Imaging systems on GEO provide the rapid temporal update cycle needed to capture the growth and decay of precipitating cloud systems on a scale of several kilometers. Current systems provide rapid hourly updates in the VIS and IR spectrum, and for optically thick clouds the precipitation can be inferred from the energy reflected by the clouds and the temperature of the cloud top, respectively. MW based imagers on board LEO satellites are better suited than IR sensors for quantitative measurements of precipitation due to the well-established physical connection between the upwelling radiation and the underlying cloud precipitation structure (Turk et al., 2000; **Figure 3**a and b).

From these sensors a diverse range of retrieval algorithms has been developed to estimate precipitation, which require careful validation and provide information about their quality, limitations and associated uncertainties. These algorithms are mainly divided into the so-called "microwave-calibrated" and "morphing" methods (Huffman et al., 2007; Joyce et al., 2004; Kidd et al., 2003; Marzano et al., 2004; Paola et al., 2012). However, there are differences among these datasets due to shortcomings in the sources and in the generation of the products. Therefore, LEO MW, GEO VIS/IR, gauge-based and reanalysis data have been blended together to take advantage of the inherent relative benefits of each type of sensor and product (**Figure 3**a). This can increase accuracy, coverage, spatial-temporal resolution, spatial homogeneity and temporal continuity (Adler et al., 1994; Huffman et al., 1995; Joyce et al., 2004; Levizzani et al., 2007; Sorooshian et al., 2002; Tapiador et al., 2004; Vicente et al., 1998; Xie et al., 2003).

In terms of operationally available datasets, these include the Tropical Rainfall Measuring Mission (TRMM; Huffman et al., 2007), the Climate Hazards group InfraRed Precipitation (CHIRP; Funk et al., 2015), the Precipitation Estimation from Remotely Sensed Information using Artificial Neural Networks (PERSIANN; Ashouri et al., 2015), Integrated Multi-satellite Retrievals for GPM (IMERG; Huffman, Bolvin, & Nelkin, 2015; Huffman, Bolvin, Braithwaite, et al., 2015), Multi-Source Weighted-Ensemble Precipitation near-real-time (MSWEP-NRT; Beck et al., 2018) and the Climate Prediction Center (CPC) morphing technique (CMORPH; Joyce et al., 2004) products, among others. Although an increasing number of precipitation data sets with higher spatial and temporal resolution have been constructed and compared directly or through the application of hydrological models, uncertainty and inconsistency are found among the different data sets (Beck et al., 2018; Beck, Vergopolan, et al., 2017; Collischonn et al., 2008; Correa et al., 2017; Sun et al., 2018; Tapiador et al., 2017). A summary of satellite-derived rainfall data sets currently available for the AB region is provided in **Table 1**.

297 **Table 1.** Missions and products that provide rainfall estimates derived from RS data, including
298 temporal-spatial resolution, data record, satellites used, algorithm retrieval and repository links
299 (NRT - Near Real Time)

Name	Extended name	Satellite adjusted with	Coverage	Spatial resolution	Temporal resolution	Temporal coverage	Reference / Link
CMORPH v1.0	CPC MORPHing technique (CMORPH) V1.0	-	60° N/S	0.07°	30 min	1998–NRT	(Joyce et al., 2004; Joyce & Xie, 2011; Xie et al., 2017) www.cpc.ncep.noaa.gov https://rda.ucar.edu/datasets/ds502.2 ftp://ftp.cpc.ncep.noaa.gov/precip/CMORPH_V1.0/CRT/
CMORPH-CRT v1.0	CPC MORPHing technique (CMORPH) bias corrected (CRT) V1.0	Gauge	60° N/S	0.07°	30 min	1998–2019	
GSMaP-Std v6	Global Satellite Mapping of Precipitation (GSMaP) Moving Vector with Kalman MVK) Standard V6	-	60° N/S	0.1°	Hourly	2000–NRT	(Ushio et al., 2009) http://sharaku.eorc.jaxa.jp/GSMaP/
GSMaP-Std Gauge v7	Global Satellite Mapping of Precipitation (GSMaP) Moving Vector with Kalman (MVK) Standard gauge-corrected V7	Gauge	60° N/S	0.1°	Hourly	2000–NRT	
IMERGHHE v06	Integrated Multi-satellitE Retrievals for GPM (IMERG) early run V06	-	Global	0.1°	30 min	2010-NRT	(Huffman, Bolvin, & Nelkin, 2015; Huffman, Bolvin, Braithwaite, et al., 2015; Tan et al., 2019) https://gpm1.gesdisc.eosdis.nasa.gov/data/GPM_L3/GPM_3IMERGHHE.06/ https://gpm1.gesdisc.eosdis.nasa.gov/data/GPM_L3/GPM_3IMERGDF.06/
IMERGDF v06	Integrated Multi-satellitE Retrievals for GPM (IMERG) final run V06	Gauge	Global	0.1°	Daily	06/2000 - present	
PERSIANN	Precipitation Estimation from Remotely Sensed Information using Artificial Neural Networks (PERSIANN)	-	60° N/S	0.25°	Hourly	03/2000–NRT	(Ashouri et al., 2015; Nguyen et al., 2019; Sorooshian et al., 2000)https://chrsdata.eng.uci.edu/
PERSIANN-CCS	Precipitation Estimation from Remotely Sensed Information using Artificial Neural Networks (PERSIANN) Cloud Classification System (CCS)	-	60° N/S	0.04°	Hourly	01/2003–NRT	
PERSIANN CDR v1R1	Precipitation Estimation from Remotely Sensed Information using Artificial Neural Networks (PERSIANN) Climate Data Record (CDR) V1R1	Gauge	60° N/S	0.25°	Daily	1983–present	
SM2RAIN-CCI v2	Rainfall inferred from European Space Agency's Climate Change Initiative (CCI) satellite near-surface soil moisture V2	Soil Moisture	Quasi Global / Land	0.25°	Daily	01/1998–12/2015	(Brocca et al., 2014; Ciabatta et al., 2018) https://zenodo.org/record/846260 https://doi.org/10.5281/zenodo.846259
SM2RAIN-ASCAT v1.2	Rainfall inferred from Advanced SCATterometer soil moisture	Soil Moisture	Global	12.5 km	Daily	2007-2019	(Brocca et al., 2019) https://doi.org/10.5281/zenodo.3635932
GPM+SM2RAIN v0.1	Rainfall inferred from ASCAT H113 H-SAF, SMOS L3 and SMAP L3 soil moisture	Soil Moisture	Global	0.25°	Daily	2007-2018	(Massari, 2020) https://doi.org/10.5281/zenodo.3854817

TMPA-3B42RT v7	TRMM Multi-satellite Precipitation Analysis (TMPA) 3B42RT V7	-	60° N/S	0.25°	3-hourly	03/2000–NRT	(Huffman et al., 2007) https://disc.gsfc.nasa.gov/datasets/TRMM_3B42RT_7/summary https://disc.gsfc.nasa.gov/datasets/TRMM_3B42_7/summary
TMPA-3B42 v7	TRMM Multi-satellite Precipitation Analysis (TMPA) 3B42 V7	Gauge	50° N/S	0.25°	3-hourly	12/1997–01/2020	
TMPA-3B43 v7	TRMM Multi-satellite Precipitation Analysis (TMPA) 3B43 V7	Gauge	50N-50S	0.25°	Monthly	1998-2020	(Huffman et al., 2010) https://disc2.gesdisc.eosdis.nasa.gov/data/TRMM_L3/TRMM_3B43.7/
GridSat v1.0	P derived from the Gridded Satellite (GridSat) B1 thermal infrared archive v02r01	-	< 50°	0.1°	3-hourly	1983–2016	(Knapp et al., 2011) https://www.ncdc.noaa.gov/gridsat/
ERA5 -HRES	European Centre for Medium-range Weather Forecasts ReAnalysis 5 (ERA5) High RESolution (HRES)	Reanalysis	Global	0.28° (~31 Km)	Hourly	2008–NRT	(Hersbach et al., 2018, 2020)
ERA5 – EDA	European Centre for Medium-range Weather Forecasts ReAnalysis 5 (ERA5) Ensemble Data Assimilation (EDA) ensemble mean	Reanalysis	Global	~0.56°	Hourly	2008–NRT	
ERA5-Land	European Centre for Medium-range Weather Forecasts ReAnalysis 5 (ERA5)	Reanalysis	Global	0.1°	Hourly	01/1981-present	https://cds.climate.copernicus.eu/cdsapp#!/dataset/reanalysis-era5-land
CHIRP v2.0	Climate Hazards group InfraRed Precipitation (CHIRP) V2.0	Reanalysis	50° N/S	0.05°	Daily	1981–NRT	(Funk et al., 2015) https://data.chc.ucsb.edu/products/CHIRP/daily/netcdf/ https://data.chc.ucsb.edu/products/CHIRPS-2.0/global_daily/netcdf/
CHIRPS v2.0	Climate Hazards group InfraRed Precipitation with Stations (CHIRPS) V2.0	Gauge + Reanalysis	50° N/S	0.05°	Daily	01/1981-present	
GPCP-1DD v1.2	Global Precipitation Climatology Project (GPCP) 1-Degree Daily (1DD) Combination V1.2	Gauge	Global	1°	Daily	10/1996-11/2015	(Huffman et al., 2001, 2016) https://rda.ucar.edu/datasets/ds728.3
GPCP-PEN v2.2	Global Precipitation Climatology Project (GPCP) pentad precipitation analysis (PEN)	Gauge	Global	2.5°	5-daily	01/1979-06/2017	Xie, Pingping, R.F. Adler, G.J. Huffman, D. Bolvin (2011): Global Precipitation Climatology Project - Pentad, Version 2.2. NOAA National Climatic Data Center. [07-2020]. https://cmr.earthdata.nasa.gov/search/concepts/C1214566485-NOAA_NCEI http://apdrc.soest.hawaii.edu/dchart/index.html?dsetid=e53e32f2c760e6375a4de86bd4718cba
MERRA-2	Modern-Era Retrospective Analysis for Research and Applications 2	Gauge + Reanalysis	Global	~0.5°	Hourly	1980-NRT	(Gelaro et al., 2017; Reichle et al., 2017)
MSWEP v2.2	Multi-Source Weighted-Ensemble Precipitation (MSWEP) V2.2	Gauge + Reanalysis	Global	0.1°	3-hourly	01/1979–NRT	(Beck et al., 2019; Beck, Van Dijk, et al., 2017) www.gloh2o.org
CMAP	CPC Merged Analysis of Precipitation (CMAP)	Gauge	Global	2.5°	Monthly	1979–present	(Huffman et al., 1997) ftp://ftp.cpc.ncep.noaa.gov/precip/cmap/

CPC-Global	CPC Unified Gauge-Based Analysis of Global Daily Precipitation	Gauge	Global	0.5°	Daily	2006-present	(M. Chen et al., 2008) https://ftp.cpc.ncep.noaa.gov/precip/CPC_UNI_PRCP/
PISCOp v2.1	Peruvian Interpolated data of the SENAMHI's Climatological and hydrological Observations	Gauge + CHIRP v2.0	Peruvian Amazon	0.1°	Daily	01/1981 – 12/2016	(Aybar et al., 2019) https://piscoprec.github.io/

Precipitation information based on RS has contributed substantially in the last decades to the understanding of key processes causing spatial and temporal variability of precipitation, as well as local and regional atmospheric processes related to precipitations. These global or quasi global data sets generally provide records of precipitation suitable for climate and hydrological studies, such as hydrological reanalysis initiatives evaluated in the Amazon on regional (e.g., Correa et al., 2017; Wongchuig et al., 2019) and global scales (e.g. Balsamo et al., 2015; Rodell et al., 2004; Van Huijgevoort et al., 2013). For instance, many studies have used satellite rainfall databases to force hydrological models. One of the first studies was done in the Tapajós River basin, one of the major tributaries of the AB, using TRMM precipitation estimates as input to a precipitation-runoff model (Collischonn et al., 2008). In order to represent the interannual, intraseasonal (30 to 70 days, Kiladis and Mo, 1998) and multidecadal series in the AB, different research has been evaluated (Correa et al., 2017). Satellite-based data sets were also used in water balance approaches to evaluate long term trends (Heerspink et al., 2020) and monthly variations of runoff (Builes-Jaramillo & Poveda, 2018). In addition, hydrological extreme events have been reported in the AB during last decades, which has been possible by using satellite-based rainfall estimates (Barichivich et al., 2018; Espinoza et al., 2012; Gloor et al., 2013; Marengo & Espinoza, 2016; Satyamurty, da Costa, Manzi, et al., 2013; Sena et al., 2012). Applications of precipitation databases to understanding of the hydrologic cycle through modeling is described in Section 6.2.

However, due to inconsistencies between different databases, several evaluations of rainfall datasets were performed that consider the AB, from global evaluations (e.g. Beck et al., 2018, 2017; Sun et al., 2018), only Amazon (e.g., Cavalcante et al., 2020; Correa et al., 2017; Espinoza, Ronchail, et al., 2019; Haghtalab et al., 2020; Paca et al., 2019; Zubieta et al., 2019) and in particular regions of Amazon (e.g., Avila-Diaz et al., 2020; Bookhagen & Strecker, 2008; Chavez & Takahashi, 2017; Espinoza et al., 2015; Killeen et al., 2007; Manz et al., 2017; Paccini et al., 2018; Zed Zulkafli et al., 2014; Getirana et al., 2011). These datasets perform differently according to the region and the time scale analyzed, which will be described in the following subsections together with the main scientific advances that have been elucidated.

Figure 3c-e show the cumulative rainfall for the annual, wet (DJF) and dry (JJA) period, respectively, for the AB. In these figures the Hydro-geodynamics of the AB Observatory (HYBAM) observed precipitation dataset (HOP), comprised of 752 daily rain gauge stations throughout the AB at 1° spatial resolution (Espinoza et al., 2016; Guimberteau et al., 2012), and the 5 km resolution CHIRP dataset, a non-gauged-corrected product, have been used.

Climatological studies in the AB that consider spatial patterns began in the 1980s. For instance, the evaluation of the outgoing longwave radiation (OLR) from polar orbiting satellites (mainly from NOAA), started in 1974, have been particularly useful for routine monitoring of cloudiness and deep convection areas over the tropics with pioneering work by Gruber & Krueger (1984) and Liebmann & Smith (1996). More regional rainfall patterns were revealed in

the transition between the Andes and the Amazon in the so-called "rainfall hotspots" region, where rainfall can reach values higher than 6000 mm yr^{-1}, the highest rainfall in the AB (Chavez & Takahashi, 2017; Espinoza et al., 2015). This region is among the rainiest areas in the world according to the IMERG Grand Average Climatology dataset that covers June 2000 to May 2019 and has the world's largest squall lines (quasi-linear convective systems; Garstang et al., 1994). Extreme vertical and horizontal structures occur due to the interactions between large-scale atmospheric circulation and massive topography that affect atmospheric convection, producing the rainfall hotspots during almost the whole year (Bookhagen & Strecker, 2008; J. C. Espinoza Villar, Guyot, et al., 2009; Killeen et al., 2007). In addition, changes in forest cover in the southern Amazon have been considered as a factor that may affect processes such as the presence of convective cells, resulting in marked spatial and temporal variability (Durieux et al., 2003; Funatsu et al., 2012; Laurance & Bruce Williamson, 2001; Staal et al., 2020).

Figure 3f shows the spatial distribution of the annual cycle of precipitation based on the CHIRP and HOP datasets. Annual cycles of precipitation over the AB vary significantly, mainly related to latitude, orography, and the influence of the large-scale atmospheric features (e.g., Intertropical Convergence Zone (ITCZ), South American Monsoon System (SAMS), South Atlantic convergence zone (SACZ; J. C. Espinoza Villar, Ronchail, et al., 2009). The bias performance of the datasets is shown in **Figure 3**g, which considers six non-gauged-corrected datasets (PERSIANN-CCS, MSWEP-ng v2, CHIRP v2.0, CMORPH v1.0, SM2RAIN-ASCAT and TMPA 3B42RT v7, adapted from Beck, Vergopolan, et al., 2017). The bias of total annual rainfall for the period 2000-2016 is plotted for negative and positive values, where at least one of these databases has detected an equal or greater value of bias. These satellite datasets were validated for the AB against global and local in situ stations (e.g., GHCN, the Global Summary of the Day (GSOD) database, the Latin American Climate Assessment & Dataset). The evaluation of these datasets showed large biases in the occidental and southern AB, covered by the Andean headwaters.

Over the Andes-Amazon transition region RS rainfall data have contributed to understanding the main orographic processes related to anabatic and katabatic winds, which are essential to explain the diurnal cycle of precipitation in this region (Junquas et al., 2018). In this specific region the bias patterns of the datasets are in agreement with other research (Chavez & Takahashi, 2017; Espinoza et al., 2015) only in the Peruvian rainfall hotspots, which underestimated total annual precipitation by about 35% to 40% from the TRMM-PR data set for the period 1998-2012. The general bias in some Andes regions can be explained, in part, by the predominance of cirrus clouds (confused by satellites sensors with convective clouds such as cumulonimbus that have similar cloud top temperature (Paredes Trejo et al., 2016; Thiemig et al., 2013, **Figure 3**b), what occurs, for instance, over the east of the southern Andes mountains (Altiplano Plateau, which extends between 15°S and 22°S). This mainly happens during the wet austral summer (Barahona et al., 2017; Dinku et al., 2011; Viale et al., 2019), and where these cloud formations are orographically dependent (Chavez & Takahashi, 2017; Giovannettone & Barros, 2009; Junquas et al., 2018; Saavedra et al., 2020; Satgé et al., 2016, 2017).

Mesoscale circulation between land surface and large water bodies in the AB produce river and coastal breeze. These systems affect the moisture transport and the spatial rainfall pattern at local scale (Fitzjarrald et al., 2008; M. J. Santos et al., 2019; Silva Dias et al., 2004).

RS data helped to reveal that river breezes reduced rainfall over the Amazon water bodies (rivers and large reservoirs) through the use of TRMM (Paiva et al., 2011).

Changes in land cover can produce complex mesoscale circulation patterns, including the so-called "deforestation breeze" that can happen over small deforested patches but loses strength at deforestation scales of around 100 km (Lawrence & Vandecar, 2015; Saad et al., 2010). These deforestation-induced circulation patterns can significantly alter rainfall patterns at local to continental scales, with such changes being observed over the AB in recent decades (Butt et al., 2011; Khanna et al., 2017; Leite-Filho et al., 2019). The effects of deforestation on rainfall will be further discussed in Section 6.4.

Remotely sensed data have been used to evaluate the temporal variability on different time scales. For instance, spatial synoptic changes in rainfall patterns were evaluated using RS information due to the heterogeneous spatial distribution of weather stations and inconsistent temporal measurements of gauge data (Arvor et al., 2017; Silva Junior et al., 2018). Other studies on a daily scale focused on evaluating the performance of the TMPA V7, TMPA RT, CMORPH and PERSIANN datasets to represent the precipitation concentration index during the period 2001–2009 (Zubieta et al., 2019). This index is an indicator for temporal precipitation distribution. The authors concluded that the best products (CMORPH and TMPA V7) can be an alternative source of data to detect changes in daily precipitation concentration during dry or wet seasons in regions of the AB that experience extreme events.

Considering that one of the main characteristics of convection processes in tropical regions is their strong relationship with the diurnal cycle (Duvel & Kandel, 1985; Minnis & Harrison, 1984), pioneer studies were performed since the 1990s for the understanding of convective patterns in the AB. Based on nine years (1983–1991) of data from GEO IR satellites (i.e., the B3 ISCCP product) with 3-h temporal resolution, Garreaud & Wallace (1997) documented several features of the diurnal march of the frequency of convective cloudiness. Data from SSM/I onboard the Defense Meteorological Satellite Program via application of the Goddard Profiling algorithm were also used to characterize the climatology (10-yr) and the diurnal variability (6-yr) of the rainfall in the AB (Negri et al., 2000). R. Oliveira et al. (2016) evaluated two GPM products in order to reproduce the diurnal cycle of precipitation in the central AB and obtained similar results to Angelis et al. (2004), who showed that rain tends to occur mainly during the afternoon in the central AB.

Rainfall information from RS has helped to identify the time of wet season beginning and ending (Wright et al., 2017), which is especially important because the prolongation of the dry season increases the vulnerability of local ecosystems and agriculture to drought and fire events (P. A. Arias et al., 2015; Fu et al., 2013; Marengo et al., 2011). One of the first RS-based assessments found that the onset of the AB wet season typically occurs within a single month (Horel et al., 1989). Negri et al. (1994) produced a regional precipitation climatology over the AB during the wet season (January–May) using three years of the twice daily Special Sensor Microwave/Imager (SSM/I) data. Changes in the seasonal cycle amplitude were also observed with the TRMM data (Liang et al., 2020).

RS information supported important developments in the understanding of the processes governing the seasonality of rainfall in the AB. The availability of satellite-derived precipitation, OLR and reanalysis allowed the description of the thermally-driven seasonal patterns that form the SAMS, which was previously not understood as a monsoon partly because it lacks the

426 classical seasonal inversion of absolute zonal winds (J. Zhou & Lau, 1998). An uncommon
427 characteristic of the monsoon over the AB elucidated by these RS products is that the onset of
428 rains occurs before the southward migration of the ITCZ, and that the Bolivian high pressure
429 zone characteristic of the SAMS is partly generated by the latent heat release from precipitation
430 over the AB before the traditional monsoon onset (Fu et al., 1999).

431 At seasonal to intraseasonal scales, OLR data from NOAA polar-orbiting satellites was
432 used to identify the intensity and spatial features of the SACZ in the Brazilian AB region (L. M.
433 V. Carvalho et al., 2004). The SACZ is a northwest-southwest convection band that extends from
434 the AB to the southeastern Atlantic Ocean, and its intensity and geographical distribution are
435 associated with extreme rainfall events in the southern AB. At the intraseasonal scale, the large-
436 scale Madden–Julian oscillation (MJO; Madden & Julian, 1994) has been established as the
437 dominant mode of variability across the tropics, modulating the SACZ and other climatological
438 features over the AB. Mayta et al. (2019) and Vera et al. (2018) used OLR data as a proxy of
439 convection to analyze the intraseasonal variability of precipitation in South America, and, in
440 particular, E. B. De Souza & Ambrizzi (2006) showed that the MJO is the main atmospheric
441 mechanism of rainfall variability on intraseasonal timescales over the eastern Amazon during the
442 wet season, which was confirmed through the use of rain gauge network by Mayta et al. (2019).
443 Moreover, RS information has contributed to understanding the mechanisms of atmospheric
444 circulation and rainfall datasets performance of seasonal and intraseasonal precipitation data sets.
445 For instance, in the Andes-Amazon transition region, particular atmospheric circulation patterns
446 (CP) were described by Paccini et al. (2018), where large underestimations of rainfall from
447 TRMM 3B42, TRMM 2A25 RP and CHIRPS occur when the CP is dominated by northerly
448 wind anomalies over tropical South America. In addition, large overestimations occur in the
449 southern Amazonia, during a CP with intermediate state between the northern and southern wind
450 anomalies and where the convergence of winds are predominant in the central and western
451 Amazon.

452 Changes in spatial and temporal distribution of rainfall in the AB may provide an
453 indicator of climate variability and in turn are an indicator of hydrological variability, including
454 extreme events, such as floods and droughts (e.g., Lewis et al., 2011; Marengo & Espinoza,
455 2016). Direct evaluation of these datasets have been done to assess the temporal evolution of
456 rainfall through analysis of occurrence indexes such as the dry-day frequency and the wet-day
457 frequency through the CHIRPS dataset (Espinoza, Ronchail, et al., 2019); or the assessment of
458 the trend in the length of the wet season in southern AB with the PERSIANN-CDR dataset
459 (Arvor et al., 2017). The interannual evolution of the hydrological processes was evaluated
460 through a water balance analysis by using CHIRPS dataset (Espinoza, Sörensson, et al., 2019). A
461 similar approach, the long-term surface water balance over the Andes-Amazonia system, was
462 performed by Builes-Jaramillo & Poveda (2018) through the use of in situ (precipitation from
463 GPCC and runoff from HYBAM) and RS-based information (evapotranspiration from
464 ORCHIDEE, GLEAM, MPI and MOD16), which pointed out that failures and scarcity of
465 information in the high Andes induce uncertainties and errors in the water budget. In addition,
466 CHIRPS v2.0 was used to analyze precipitation anomalies for the identification of spatial
467 patterns of drought over the AB related to the tropical Atlantic and Pacific SSTemp anomalies
468 and different ENSO events (Jimenez et al., 2019).

Rainfall estimations by RS since the 1980s in the AB have depicted more amounts of rain in the north (Espinoza, Ronchail, et al., 2019; Paca et al., 2020; G. Wang et al., 2018) and lower amounts in the south (Espinoza, Ronchail, et al., 2019; Leite-Filho et al., 2019). This north-south contrasting pattern is translated to the hydrological behavior of the main basins that show an intensification of the hydrological regime in the main course of the AB (Barichivich et al., 2018; Heerspink et al., 2020).

AB characteristics pose unique challenges to satellite rainfall retrieval algorithms, both from IR and MW sensors, considering the contrast in terms of orography, climate and changes in vegetative cover. For IR, challenges occur mainly for warm orographic rains (shown north of 10°S), where fixed brightness temperature thresholds (cooler than warm orographic clouds) tend to underestimate rainfall amounts. This would be happening in the hot-spots regions in the Peruvian and Bolivian Andes-Amazon transition (Espinoza et al., 2015). For the MW algorithms, rain overestimation comes from cold surfaces and ice over mountain tops which can be interpreted as precipitation (Dinku et al., 2011; Toté et al., 2015).

Since satellite-based rainfall estimates are adjusted based on observations from rain gauges, the accuracy of estimated rainfall values can be increased. However, this requires a network of rain gauges with adequate spatial coverage in key areas of the Amazonia and high-quality records for proper calibration and validation. In the case of in situ stations, some aspects should be considered, for instance, that rainfall estimates are likely to be biased by river breeze at some times of the year, as meteorological stations are usually located near large rivers and close to most cities (Paiva, Buarque, et al., 2011; M. J. Santos et al., 2019; Silva Dias et al., 2004).

Current satellite-borne radar missions, such as TRMM Precipitation Radar, CloudSat's Cloud Profiling Radar, or GPM Dual frequency Precipitation Radar, have low temporal resolution, therefore are unable to observe the short-time evolution of weather processes. To overcome this limitation, using only radars on LEO, it is necessary to have a constellation of them. In recent years nanosatellites (e.g., SmallSat or CubeSat platforms) have the capability to miniaturize, reduce cost and simultaneously preserve the fundamental requirements of their larger and more expensive peers. In this sense, RainCube is a potential technology demonstration mission to enable precipitation radar technologies on a low-cost platform (Peral et al., 2019).

Ground-based radars can measure the vertical structure of rain since its structure depends on the type of rain, but with better temporal resolution than MW on board satellites (Kumar et al., 2020). A recent example is the operational algorithm RAdar INfrared Blending algorithm for Operational Weather monitoring, which merges ground radar network with VIS and IR images from satellites to provide rainfall pattern and intensity over Italy (Adderio et al., 2020).New methods have emerged that take advantage of the global cell phone network and its density to estimate rainfall intensities, mainly in urban areas, but which can also be used in regions with high topographical variability (Gosset et al., 2016; Overeem et al., 2013, 2016; van het Schip et al., 2017), however they have not yet been explored in the AB. In general, monthly and annual datasets are useful because they have an adequate agreement to the observations, but not with daily and much less sub-daily data.

3. Evapotranspiration

Evapotranspiration (ET) has a considerable importance for the terrestrial climate system, providing moisture to the atmosphere, linking the water, energy, and carbon cycles (Fisher et al., 2017; M. Jung et al., 2010), and driving precipitation and temperature at local and regional scales (Marengo et al., 2018). Studies have shown that around half of the precipitation in the AB is recycled by local ET (Salati et al., 1979; Satyamurty, da Costa, & Manzi, 2013; Zemp et al., 2017). In addition, Amazon ET constitutes an important source of moisture for southeastern South America through atmospheric low-level (often referred to as “flying rivers"), providing around 70% of the precipitation in this region (Van Der Ent et al., 2010; Pearce, 2020). Especially during the dry season, Amazon ET seems to be more efficiently converted to precipitation in the La Plata River Basin than local ET (J. A. Martinez & Dominguez, 2014).

With the advent of satellite observations, ET has been estimated at multiple spatial and temporal scales. RS models to estimate ET can be divided into two main approaches: one based on surface energy balance (SEB) and another using physical equations. One well known energy balance models is the Surface Energy Balance Algorithm for Land (SEBAL), proposed by Bastiaanssen (1995) to overcome most of the problems of the early surface energy balance models, which were suitable only for local scale due to their dependence of local measurements for calibration. Based on principles and methods adopted in SEBAL, R. G. Allen et al. (2007) proposed the Mapping evapotranspiration at high Resolution with Internalized Calibration (METRIC) algorithm, including an internal calibration using Inverse Modeling at Extreme Conditions (CIMEC) and micrometeorological measurements to reduce computational biases inherent to energy models that use RS data (R. G. Allen et al., 2007, 2011). Other surface energy balance models were also proposed to use RS data, such as Surface Energy Balance Index (SEBI; Menenti & Choudhury, 1993), Simplified Surface Energy Balance Index (S-SEBI; Roerink et al., 2000), and Surface Energy Balance System (SEBS; Su et al., 2001).

SEB algorithms are generally defined as “One Source Surface Energy Balance” models, since they do not distinguish between soil evaporation and canopy transpiration, whereas the land surface is treated as a big leaf and as a single uniform layer (Tang et al., 2013; Ke Zhang et al., 2016). In contrast, in the Two-Source Energy Balance (TSEB) models (Kustas & Norman, 1999; Norman et al., 1995), the soil-vegetation system is approximated as a two-layer model, where the energy fluxes are partitioned into soil and vegetation components (Norman et al., 1995). Based on the TSEB approach, the Atmosphere-Land Exchange Inverse model (Alexi) was developed by Anderson et al. (1997), designed to represent land-atmosphere exchange over a wide range of land cover conditions. Both approaches rely on thermal RS data, using meteorological inputs as ancillary data (Ke Zhang et al., 2016).

RS models based on physical equations are generally divided into Penman-Monteith and Priestley and Taylor equation-based approaches. Penman (1948) was the first to formulate an equation to calculate evaporation based on a physical approach using two terms, an energy term related to radiation and an aerodynamic term related to the vapor pressure deficit and wind speed (Shuttleworth, 2012). While this equation represented open water evaporation, Monteith (1965) presented an extension by adding surface and aerodynamic resistances, and thus the equation became more consistent with estimation of ET from vegetated surfaces, resulting in the well-known Penman-Monteith equation (Monteith & Unsworth, 2013). Based on this approach, the MOD16 algorithm was formulated by Mu et al. (2007, 2011), previously proposed by Cleugh et al. (2007), to calculate ET through the integrated use of global meteorological reanalysis and RS

555 data from the Moderate Resolution Imaging Spectroradiometer (MODIS) sensor, including leaf
556 area index (LAI), fraction of absorbed photosynthetically active radiation (fPAR), albedo and
557 land cover classification. Leuning et al. (2008) also proposed a similar ET algorithm based on
558 this equation, the Penman-Monteith-Leuning (PML) using a simple biophysical model to
559 calculate surface conductance from MODIS LAI. Another approach is the Priestley and Taylor
560 equation (Priestley & Taylor, 1972). This model uses an empirical parameter to simplify the
561 Penman-Monteith approach, minimizing the uncertainties related to estimating aerodynamic and
562 surface resistances. Based on this equation, Fisher et al. (2008) developed the JPL-PT model, and
563 Miralles et al. (2011) proposed the Global Land-Surface Evaporation Amsterdam Model
564 (GLEAM), designed to estimate daily terrestrial evaporative fluxes and the root-zone soil
565 moisture using maximum observations derived from RS (Martens et al., 2017). A summary of
566 the main RS-based models to estimate ET in the South American tropics, with applications in the
567 AB, is presented in **Table 2**.

568

569 **Table 2.** Summary of the main RS-based models to estimate ET, with applications in the
570 Amazon (*Global applications including Amazon analysis)

Model	Physical principles	Spatial resolution	Usual RS sources	RS main drivers	Ancillary data	Model advantages	Model limitations	Applications in the AB
ALEXI (Anderson et al., 1997)	Surface Energy Balance	375 meters to 0.05º	GOES, MODIS, VIIRS	1) Thermal (land surface temperature) 2) Multispectral data (surface reflectance)	1) Meteorological (global reanalysis) 2) Surface data (land cover)	1) Energy fluxes are partitioned into soil and vegetation components 2) Representation of surface processes in areas with high water availability	1) High complexity for implementation 2) Require clear sky conditions 3) Require many meteorological variables	Paca et al. (2019)
BESS (Ryu et al., 2011)	Biophysical model	1 to 5 km	MODIS	1) Atmospheric data (aerosol, water vapor, cloud, atmospheric profile) 2) Surface properties (land surface temperature, land cover, LAI, albedo)	1) Meteorological (global reanalysis) 2) Surface data (global climates and vegetation)	1) Global spatial coverage and public data availability 2) Entirely independent from flux tower data, 3) Moderate spatial resolution to cover large areas 4) Multiple atmospheric and land surface data used as inputs 5) Linkage between carbon and water fluxes	1) Require many data (surface RS and meteorological variables) 2) Soil moisture effect and water evaporation from rainfall intercepted by the canopy are not explicitly include in the model 3) Complex terrain and heterogeneity of land surface are not considered, 4) Uncertainties in inputs datasets and gap-filling methods can influence in the results of the model.	Swann and Koven (2017)
MOD16 (Mu et al., 2007; 2011)	Physical approach - Penman-Monteith equation	500 meters to 0.05º		1) Vegetation phenology (LAI, fPAR) 2) surface properties (land cover, albedo)	Meteorological (global reanalysis)	1) Global spatial coverage and public data availability 2) Low complexity for implementation	1) Parametrizations of surface conductance 2) Require measured data for model calibration/parameterization	Baker and Spracklen (2019); da Silva et al. (2019); Maeda et al. (2017); Miralles et al. (2016)*; Oliveira et al.

							3) Limitations in areas with high soil and water evaporation 4) Moderate to high meteorological inputs	(2017); Swann and Koven (2017); Vergopolan and Fisher (2016); Xu et al. (2019), Paca et al. (2019)
PML (Leuning et al., 2008)		500 meters						Zhang et al. (2016)*
GLEAM (Miralles et al., 2011)	Physical approach - Priestley and Taylor equation	0.25º	AIRS, CERES, MODIS, multi-source soil moisture (ES-CCI), vegetation optical depht (VODCA)	1) Atmospheric data (radiation, precipitation, air temperature, lightning frequency) 2) surface properties (snow-water equivalent, soil moisture, vegetation cover fraction, vegetation optical depth)	Meteorological (global reanalysis)	1) Can be driven only with RS inputs 2) Moderate meteorological inputs requirements 3) Global spatial coverage and public data availability	1) Simplification of some physical processes 2) Over-dependence on water availability 3) Limitations in areas with high soil and water evaporation 4) Low spatial resolution	Baker and Spracklen (2019); Miralles et al. (2016)*, Paca et al. (2019), Wu et al. (2020)
PT-JPL (Fisher et al, 2008)		1º	AVHRR, MODIS	Vegetation phenology (NDVI, SAVI)	Meteorological (global reanalysis) and Satellite land surface climatology	1) Global spatial coverage and public data availability 2) Can be driven only with RS data 3) Moderate meteorological inputs requirements	1) Simplification of some physical processes 2) Many ecophysiological parameterization 3) Limitations in areas with high soil and water evaporation 4) Low spatial resolution	Fisher et al., 2009; Miralles et al. (2016)*
METRIC (Allen et al., 2007)	Surface Energy Balance	30 meters to 1 km	MODIS, Landsat	1) Thermal (land surface temperature) 2) multispectral data (surface reflectance)	Meteorological (from ground measurements to global meteorology)	1) Applications for regional scale in moderate to high spatial resolution 2) Less surface parameterization 3) Useful to evaluate land cover changes impacts 4) Low meteorological inputs requirements (SEBAL) 5) Higher accuracy in areas with ground measurements available (METRIC)	1) Require clear sky conditions 2) There is no distinguish between soil evaporation and canopy transpiration 3) Require the presence of hot and cold extreme conditions on the domain area 4) Domain-area dependence, with limitations for large-scale applications 5) Moderate to high meteorological inputs requirements (METRIC) 6) Higher uncertainty in data scarce areas (METRIC)	Khand et al. (2017), Numata et al. (2017), Nobrega et al. (2017)
SEBAL (Bastiaanssen, 1995)			AVHRR, MODIS, Landsat, ASTER					Laipelt et al (2020); Oliveira et al. (2019), Nobrega et al. (2017)
SEBS (Su et al., 2001)			MODIS, Landsat			1) Accuracy related to land surface temperature 2) Low requirement for meteorological inputs	1) High requiremtent for surface parameterization 2) Moderate to high complexity for implementation	Paca et al. (2019)

SSEBop (Senay et al., 2013)	Simplified surface energy balance					1) Low complexity for implementation 2) Global spatial coverage and public data availability	1) Simplified energy balance 2) Moderate to high meteorological inputs requirements (METRIC) 3) Higher uncertainty in data scarce areas	Paca et al. (2019), Senay et al. (2020)*

RS-based ET models have improved our understanding of ET processes worldwide, allowing us to understand hydrological processes from local to large spatial and multiple temporal scales. Energy balance models have the advantage to map ET at fine spatial resolution. These models can estimate human impacts on the energy and water cycles and on the land-surface interactions. However, since they are dependent on thermal RS data, they are generally restricted to clear-sky or cloud-free conditions, which is a major drawback, especially in tropical humid areas, such as the Amazon (Rocha et al., 2009). In addition, SEB models usually require the presence of hot and cold conditions in the satellite domain area. This requirement is a disadvantage since the selection of the hot and cold endmembers for internal calibration using the CIMEC process on RS images can generate subjective results, especially under wet regions such as the AB, where the selection of hot endmembers during both wet and dry seasons is a challenge (Khand et al., 2017). Physically-based equations have the advantage to map ET at high temporal resolution, enabling long-term and large-scale assessments of land-surface interactions. However, some limitations include the uncertainty in parameterizing physical processes, as surface resistance and conductance, and, therefore, are dependent on the use of look-up tables biome-properties (Ruhoff et al., 2013). Error propagation derived from meteorological forcing data is also an issue (Gomis-Cebolla et al., 2019; Miralles et al., 2016; Panday et al., 2015; Talsma et al., 2018), since it can introduce large uncertainties in ET estimates, especially in the tropics.

In the AB, the spatial and temporal drivers of ET are not fully understood, and these uncertainties are reflected on how RS models estimate ET (Maeda et al., 2017; Sörensson & Ruscica, 2018). ET measurements have provided valuable information about seasonality and dynamics at local scales (Rocha et al., 2009). Some national initiatives, as the Brazilian National Water Resource Information System (SINGREH) and the Meteorological Database for Research from the Brazilian National Water and Sanitation Agency (ANA) and the National Institute of Meteorology (INMET), respectively, and international research projects, as the Large-Scale Biosphere-Atmosphere Experiment in Amazonia (LBA; E. A. Davidson & Artaxo, 2004), provided standardized hydrometeorological and surface flux measurements to understand energy, water and carbon exchanges across different tropical ecosystems (Gonçalves et al., 2013; Saleska et al., 2013). However, due the high cost of eddy covariance measurements and maintenance difficulties, there are only a few towers located across the basin, and these do not cover the whole Amazon climate-vegetation complexity. Hence, through the calibration and validation of RS-based ET models it has been possible to extend the spatial coverage of the ET, improving our knowledge about seasonality and patterns in data scarce areas, covering long-term assessments.

RS models have shown that ET spatial pattern (**Figure 4a**), seasonality (**Figure 4b**), and main ET drivers vary across the AB, with monthly averages rates ranging from 80 mm in the southern part (including Madeira and Tapajos basin) up to 160 mm in the northern part of the

basin (Negro basin). Most models, as MOD16, usually show an increase in ET and forest greenness as the dry season progresses in the northeastern and central Amazon, where equatorial wet areas prevail, and spatial and temporal ET seasonality is mainly driven by incident radiation and LAI (Maeda et al., 2017), corroborating with eddy covariance measurements (Christoffersen et al., 2014), despite not all models agree with this pattern (**Figure 4c**). For instance, while MOD16 ET seasonality is consistent with eddy covariance measurements (at K34 and K83), with higher rates during the dry season, seasonality of the GLEAM model (at K34), peaking during the wet season, implying that for wet regions in Amazon, this model has a dependence on water availability, since GLEAM tends to follow the rainfall seasonality (Miralles et al., 2016). Furthermore, in the south and southeastern parts of the AS (at Madeira and Tapajos basin), most of the RS-based models consistently indicate a decrease in ET during the dry season, following water availability (Maeda et al., 2017; H. J. F. da Silva et al., 2019). However, when RS-based models estimates are compared to eddy covariance measurements (at local scale) or water balance estimates (at large scale), the representation of the ET seasonality is still uncertain, since most of the models are unable to consistently reproduce the seasonal cycles in tropical areas, considering that multiple drivers operate simultaneously across the AB. Overall, in the tropics, ET seasonality is mainly regulated by water and energy availability and how vegetation assimilates both (Christoffersen et al., 2014; Restrepo-Coupe et al., 2013). Alternatively, in large data scarce areas, estimating ET using multi-model ensembles and a dense observational network across the Amazon, RS-based models can be improved through calibration and validation, helping assess model uncertainties and to understand the land surface interactions in the tropics (Gonçalves et al., 2013; Paca et al., 2019).

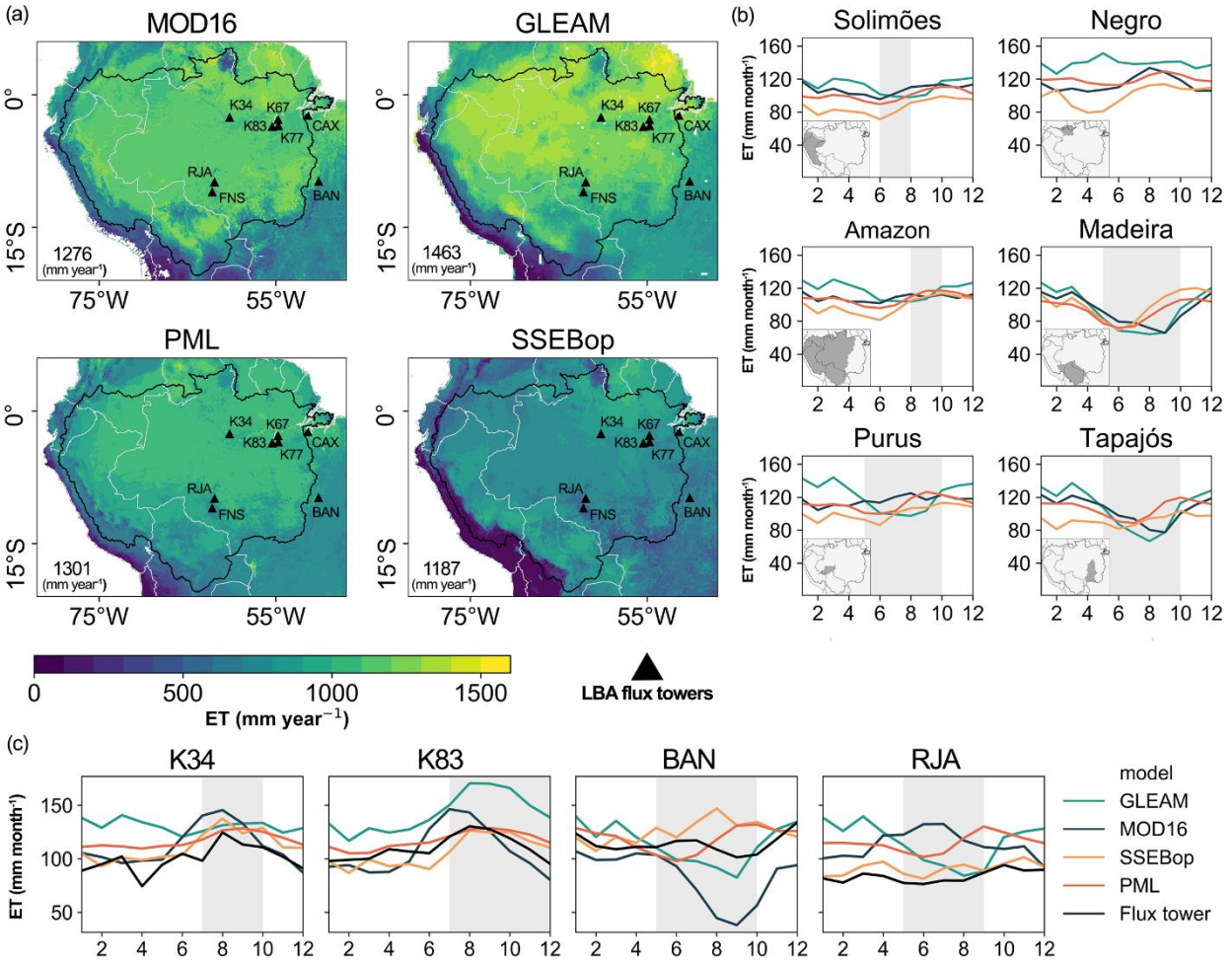

Figure 4. Spatial and temporal patterns of *ET* are differently represented by RS models. (a) Spatial variability of *ET* annual average (2003-2017) for GLEAM, SSEBop, MOD16 and PML models; the numbers on the lower left corner of each subplot represent the annual average *ET*. (b) *ET* seasonality for major Amazon sub-basins. (c) Monthly average comparison between estimates and eddy covariance measurements from the LBA project, using data from Saleska et al. (2013). The dry season is highlighted in gray as monthly precipitation rates < 100 mm month^{-1}

While flux tower measurements have shown, at local scales, that land cover changes can impact water and energy fluxes (C. von Randow et al., 2004), large scale assessment with satellites based on both energy balance and physical-based equations driven by vegetation phenology and meteorological reanalysis have reinforced these findings (Baker & Spracklen, 2019; Khand et al., 2017; Laipelt et al., 2020; G. de Oliveira et al., 2019). All these studies demonstrated significantly lower *ET* rates under pasture, agricultural, and deforested areas than in primary and secondary forests (R. de C. S. von Randow et al., 2020). These results indicate that less water returns to the atmosphere, thus affecting the precipitation recycling and contributing to changes in the dry-to-wet season, possibly making the dry season longer (M. H. Costa & Pires, 2010), while more of the precipitated water goes to runoff (Panday et al., 2015). In addition, RS-based assessments demonstrated that drought events tend to affect anthropogenic

systems as pasture and agriculture areas more than primary and secondary forests, leading to an increase in air temperature, and a decrease in LAI and ET (Baker & Spracklen, 2019; G. de Oliveira et al., 2019). Results from MOD16 ET may assist in monitoring deforested areas in the Brazilian Amazon (H. J. F. da Silva et al., 2019). However, global remotely sensed ET, such as GLEAM, better reflect changes in vegetation greening and in air temperature increase than to deforestation, may due the lack of deforestation account in these models (Wu et al., 2020). Influence of land use changes on the water cycle will be discussed further in Section 6.4.

Our understanding about energy partitioning in the Amazon biome has improved through RS models (Laipelt et al., 2020; G. de Oliveira et al., 2019). For example, high resolution ET estimates using SEBAL in the south-western Amazon demonstrated significant differences among energy and water fluxes in forests and non-forest areas, such as pasture and cropland. In these anthropogenic areas, soil and sensible heat fluxes were from two to four times higher than in forested areas (G. de Oliveira et al., 2019). In a transitional region between Amazon and Cerrado biomes, converted areas can substantially change the energy and water fluxes, where latent heat flux is the major component in forested areas, while in deforested areas an increase in sensible heat flux is observed (Laipelt et al., 2020). These studies showed that change in land use and land cover, can significantly affect ET rates, and observed ET rates was almost two times lower in pasture than in tropical forest (Laipelt et al., 2020), and up to three times lower in non-forested areas (G. de Oliveira et al., 2019).

Fisher et al. (2017) summarized in ten scientific questions the main outstanding knowledge gaps for the ET-based science. To address these questions, ET estimations need to be improved, aiming for high accuracy, high spatial and temporal scales, covering large spatial and long-term monitoring. Recent research demonstrated that RS models can estimate ET with reasonable accuracy and consistent agreement (Gomis-Cebolla et al., 2019; Martens et al., 2017; Michel et al., 2016; Kun Zhang et al., 2019). However, for the individual ET components (soil evaporation, transpiration, and interception), they diverge considerably (Miralles et al., 2016; Talsma et al., 2018). For example, Miralles et al. (2016) showed that in tropical forests, soil evaporation is almost non-existent in GLEAM and JPL models, whereas with MOD16 this component may exceed transpiration. In the Amazon, canopy interception from JPL and MOD16 is nearly two times higher than in GLEAM model. Beyond the uncertainties related to canopy transpiration and soil evaporation, open water evaporation and ETestimation over Amazon wetlands is also a major knowledge gap. Wetland ET can be a complex process as it involves fluxes at different vegetation conditions for transpiration, evaporation from water intercepted in the canopy and from open and vegetated surface water. Changes in latent heat patterns over water bodies (rivers, wetlands, lakes and artificial reservoirs) affect the local climate circulation patterns through a breeze effect (Silva Dias et al., 2004), and have the potential to affect regional climate through precipitation suppression over the wetlands and convection initiation over wetland borders (Taylor et al., 2018).Wetland-upland differences in ET are still poorly understood over the AB, and only a few in situ monitoring gauges are available on floodable environments (Borma et al., 2009) that could be used for model validation. Improvements of accuracy of ET components estimates lead us to better understand ET processes, and how these components are impacted by changes in temperature, green-house gases concentration, and in the hydrologic cycle (Fisher et al., 2017; Talsma et al., 2018).

Another challenge to satellite-based models overcome is to minimize the use of parameterization and to improve input data accuracy. While the performance of Penman-Monteith models can be strongly influenced by resistance parameterizations, Priestley and Taylor models estimates have dependence on Priestley and Taylor parameter (α) parametrization, as well as errors can also be related in both approaches by forcing data and algorithms structure (Ershadi et al., 2015; Gomis-Cebolla et al., 2019). Moreover, measurements are still a significant limitation. In the Amazon biome, there are only eight public flux towers with data available, from the LBA project (Saleska et al., 2013), and they do not cover all vegetation and climate complexity in the AB. In addition, when we are working on energy balance models, the main challenge, especially in the Amazon, is the requirement of clear sky conditions. However recent efforts to integrate microwave data to energy balance models are promising (Holmes et al., 2018), since microwaves are less affected by cloud cover than the thermal infrared wavelength.

RS is now supported by a range of sensors and satellites which provide thermal infrared images, and meteorological and surface observations, essential to estimate ET. In 2018 the Ecosystem Spaceborne Thermal Radiometer Experiment on Space Station (ECOSTRESS) mission was launched by National Aeronautics and Space Administration (NASA) and will provide information about how vegetation responds to stress and how it uses water, focusing on vegetation temperature measurement, allowing understanding of ET dynamics and processes at a good temporal and spatial resolution (Fisher et al., 2017; Sheffield et al., 2018). Other missions will improve ET estimates and will provide valuable information to validade current models. For example, the Joint Polar Satellite System (JPSS), a mission from National Oceanic and Atmospheric Administration (NOAA) and NASA, includes a range of sensors, such as the Visible Infrared Imaging Radiometer Suite (VIIRS), that collect visible and infrared imagery, providing useful global information to monitor vegetation, and as input to retrieval hydrological variables (McCabe et al., 2017; Sheffield et al., 2018; L. Zhou et al., 2016). The Water Cycle Observation Mission (WCOM) from China aims to acquire consistent measurements of the water cycle components (Levizzani & Cattani, 2019; Shi et al., 2016). The FLourescence EXplorer (FLEX) mission by European Space Agency, that will map vegetation fluorescence, providing information about photosynthetic activity and vegetation stress and health, also helping to improve constraints on transpiration (Drusch et al., 2017; McCabe et al., 2017). Beyond continuity of Landsat (McCorkel et al., 2018) mission, will map long- term ET at high spatial scale, and the Gravity Recovery and Climate Experiment (GRACE) Follow-on that will bring significant opportunity to estimate ET with the water balance approach (Landerer et al., 2020).

RS has been crucial to improve our understanding of surface-atmosphere interactions through ET, despite the challenges that still exist, and these future missions are an excellent opportunity to address important scientific questions from ET-based science, allowing us to improve techniques, approaches and our knowledge about ET processes and how the impact of activities can affect the water cycle throughout the Earth, including the Amazon.

4. Surface water

4.1. Surface water elevation

Surface water is a key resource for all the communities living along the Amazon River. Yet monitoring Surface Water Elevation (SWE) and discharge in the AB is a challenge. While

the AB is facing pressure on its water cycle due to human activities, the number of gauges decreased globally in the last decades (Vörösmarty et al., 2000). This threatens our capacity to understand natural and human-driven impacts of climate change on Amazonian rivers. Although, to this date, no satellite mission have been designed specifically for retrieving inland water elevations, remotely-sensed observations of SWE from radar altimetry are complementary to the historical gauge network (Fekete et al., 2012) and improve monitoring of Amazonian rivers (Calmant & Seyler, 2006; J. S. Da Silva et al., 2014).

The AB has become an ideal laboratory for pioneering studies that have demonstrated the capacity of retrieving accurate SWE at particular locations from radar echoes and adapted retracking procedures. The first studies over the AB used observations from Seasat (Sea Satellite from NASA), launched in 1978, to derive the low water gradient of the Amazon main stem (Guzkowska et al., 1990).

The configuration of the satellite altimeter orbit defines the intersections between the satellite ground tracks and the river reaches, the so-called virtual stations (VSs), where SWE can be estimated. At a given VS, the SWE is retrieved through the inversion of the signal round-trip propagation time that provides the range. Several uncertainty corrections (due to delay in the propagation caused by the atmosphere, dynamics of Earth's surface, etc.) must be applied to this range to retrieve the SWE. Stammer & Cazenave (2017) provide an extensive discussion on SWE estimation from satellite altimetry and the associated errors. Since the first satellites, the accuracy of the orbit, which depends on the density of the atmosphere and on the resolution of the gravitational field, has improved, and is now around one centimeter (against sixty centimeters for Seasat). Yet calculating the correct range remains challenging, as it is necessary to track (on board) or retrack (on the ground) the altimetric waveform (Frappart et al., 2006), using algorithms to best fit the highly variable distribution of the echo energy bounced back by the different types of surfaces in the satellite field of view (Calmant et al., 2016).

Since the first studies using Seasat data, we now have more than 30 years of monitoring of inland waters by satellite altimetry. After Seasat came GEodetic and Oceanographic SATellite (GEOSAT), that was used by Koblinsky et al. (1993) to retrieve SWE time series over the AB, with uncertainties ranging from 0.19 to 1.09 m compared to in situ data. The European Remote Sensing satellite (ERS-1; launched in 1991) initiated a long family of satellites that followed the same 35-day repeat orbit (ERS-1, ERS-2, ENVISAT -Environmental Satellite, and SARAL - Satellite with ARgos and ALtika), which covered the 1991-2016 period. A major advance was made by the Observations des Surfaces Continentales par Altimetrie Radar (OSCAR) project, that evaluated the ICE-2 specific retracking of radar echoes for ice caps (Legresy et al., 2005) for ERS-1, ERS-2 and ENVISAT, and promoted its delivery in the Geophysical Data Records.

The retracking of radar echoes was analyzed by Frappart et al. (2006, 2016) and J. S. Da Silva et al. (2010) over 70 ERS-2 and ENVISAT VSs and a large range of river widths (from tens of meters to kilometers). They reported that the proper selection of the data considered as representative of the water body is as important as the choice of the retracking algorithm. The data from the 10-day repeat orbit of Topex/Poseidon (T/P) and Jason-2/3 have also been assessed in the AB. Seyler et al. (2013) highlighted the gain of Jason-2 (ranging from 2008 to 2016 on its nominal orbit) in comparison to T/P (from late 1992 to 2005), with an uncertainty around 0.35 m, possibly due to the sensor's better capacity to discriminate the surrounding floodplain from the river.

All these missions operated in low resolution mode, i.e., the footprint on ground is large (some kilometers, depending on radar operating band) and the echoes returning to the antenna are influenced by the surroundings. The SAR mode, active on Sentinel-3 satellites, allows a reduction of the surrounding contributions by slicing the disc illuminated by the echo at a given time (Raney, 1998). This reduction provides a much better along track resolution, however it does not resolve some issues such as cross-track sloping measurements (Bercher et al., 2013). The addition of a second antenna, as on Cryosat-2, allows the SAR Interferometric mode to correct these cross-track measurements, hence allowing an improvement in the accuracy of SWE time series. However, Croysat-2 is not popular for SWE monitoring over rivers since its orbit shifts around 7 km every month and comes back to the same place every 369 days. Indeed, most of the studies on the use of satellite altimetry in the AB have focused on repetitive orbits, even though some studies have explored the use of missions in drifting or long-term repetitive ones and found good accuracy for SWE monitoring (e.g., Bogning et al., 2018). Such missions, instead of providing a SWE observation on a 10-day or almost monthly basis with a large intertrack distance at the equator (between 60 km and 100 km), provide a much denser spatial span but with observations separated from another in time. The use of ICESat (Ice, Cloud, and land Elevation Satellite) laser altimetry data was investigated by Hall et al. (2012). They concluded that this mission can be a valuable source of data for monitoring rivers from the AB, with accuracies of some tens of centimeters when compared to gauges. The ICESat mission was continued by ICESat-2, launched in 2018. Studies by Bercher et al. (2013) and L. Jiang et al. (2017) concluded that the SAR mission CryoSat-2 offers new opportunities to monitor narrow rivers in the AB, and should help linking the present and future altimetry missions.

The differential interferometry technique with SAR data allows obtaining information about changes in surface displacements, such as topographic changes. Centimeter-scale measurements of water level changes throughout inundated floodplain vegetation using interferometric SAR were obtained over the Amazon floodplains for the first time (Alsdorf et al., 2000; Alsdorf, Birkett, et al., 2001; Alsdorf, Smith, et al., 2001). This estimation is possible due to the radar pulse interactions with the water surface and the trunks of flooded vegetation causing a double-bounce path (Alsdorf et al., 2000; Hess et al., 1995). H. Lee et al., 2020 and Mohammadimanesh et al. (2018) reviewed the methods and limitations of the technique for applications in wetlands.

To date, SWE information is available as raw data and as processed data. Some groups or institutions provide processed SWE time series (see **Table 3**). Each dataset provides SWE on selected water bodies, all over the world or in specific regions, and have different objectives in terms of operability. Processing and filtering procedures vary between each group, and time series of the same VSs can vary from one group to another.

Table 3. Datasets of surface water elevation time series over the water bodies

Name	Producer	Weblink	Reference	Target	Delivery time
G-REALM	USDA NASA	https://ipad.fas.usda.gov/cropexplorer/global_reservoir/Default.aspx#SatelliteRadarAltimetry	(Birkett et al., 2017)	Lakes and reservoirs	NTC

River & Lake	De Montfort University	http://altimetry.esa.int/riverlake/shared/main.html	(Berry et al., 2005)	Rivers, Lakes and reservoirs	SCT (discontinued)
DAHITI database	German Geodetic Research Institute	https://dahiti.dgfi.tum.de/en/	(Schwatke et al., 2015)	Rivers, lakes reservoirs and wetlands	NTC & reanalysis
GRRATS product	Ohio State University	https://podaac.jpl.nasa.gov/dataset/PRESWOT_HYDRO_GRRATS_L2_VIRTUAL_STATION_HEIGHTS_V2	(Coss et al., 2020)	Rivers	Reanalysis only
Hidrosat	ORE-HYBAM and ANA	http://hidrosat.ana.gov.br/	(J. C. Carvalho et al., 2015)	Rivers	NTC
Hydroweb	IRD/LEGOS, CNES (French Space Agency), and Universidade do Estado de Amazonas	http://hydroweb.theia-land.fr/	(Crétaux et al., 2011; J. S. Da Silva et al., 2010)	Rivers, lakes and reservoirs	STC & reanalysis

STC: Slow-Time Critical - delivered at maximum after three days; NTC: Non-Time Critical - delivered typically within one month.

Figure 5 provides the location of all virtual stations in the AB from the Hydroweb website. **Figure 5**a is a representation of the median amplitude of SWE at each VS. Amplitude of SWE measured by the satellites is lower in the headwaters (0-3 m) and medium size rivers (3-6 m) compared to Solimões-Amazonas main stem and its tributaries (9 - 12 m). Largest values are found for the Purus River (> 15 m), a right bank tributary. **Figure 5**b and c provide the mean month for high and low flows, respectively, indicating the influence of rainfall partition in the northern and southern parts of the basin and the gradual shift due to the flood travel time along the rivers and floodplains (~ 1- 3 months). **Figure 5**d and e provide multi-mission SWE time series ranging from 2002 to now with ENVISAT and Sentinel3-B and from 2008 to 2020 with Jason-2 and Jason-3, respectively. It shows the strong seasonal signal of the gradual flood of the Amazon rivers, and interannual variability of maximum and minimum stages.

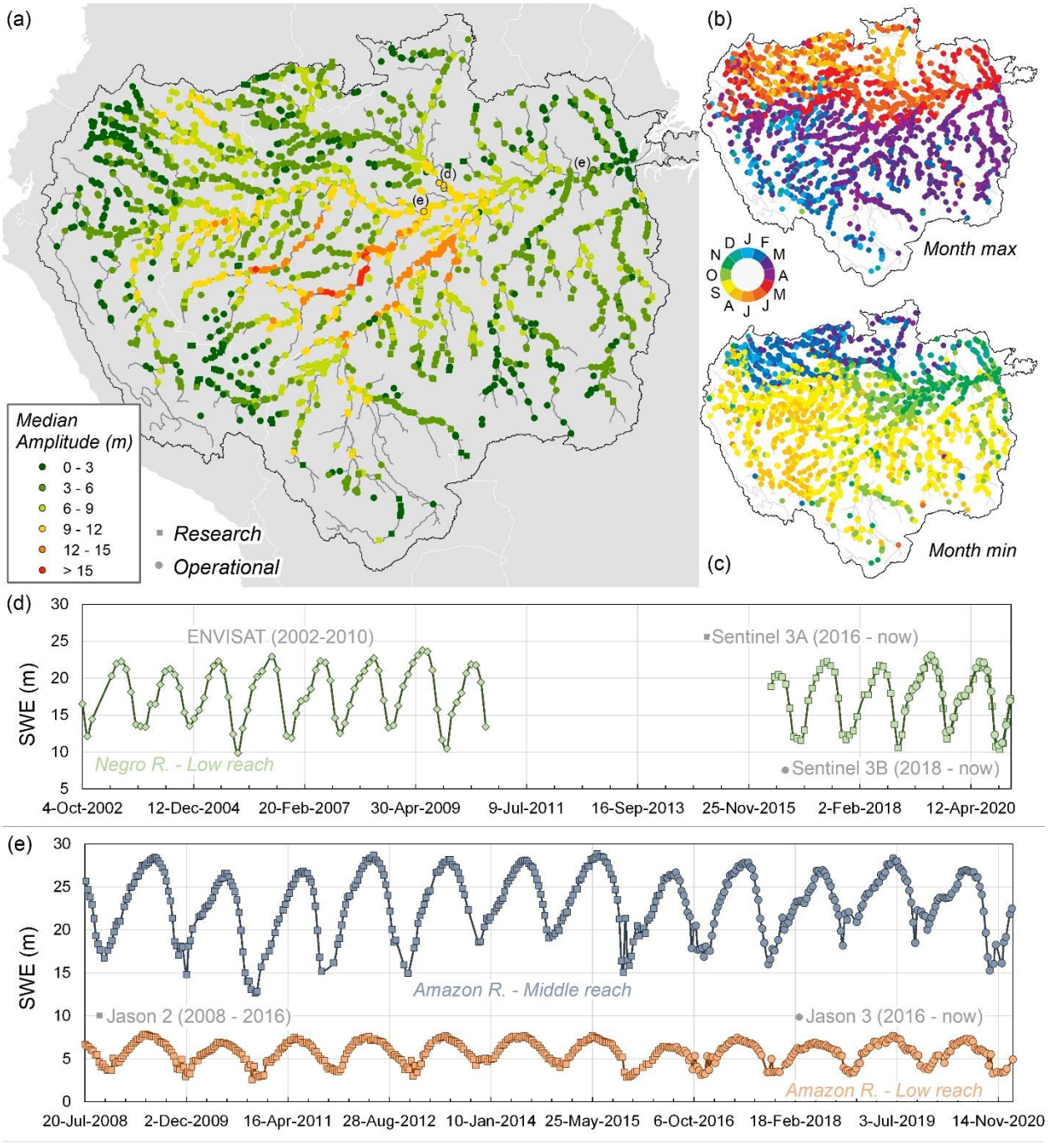

Figure 5. a) Location of the virtual stations freely available on Theia-hydroweb (http://hydroweb.theia-land.fr/) and median amplitude of the time series. Dots are operational VSs (from currently flying missions and updated in near real time) and squares are research VSs (identified as reanalysis in table W). VSs rounded in black are drawn in d and e; b) month of maximum SWE for the mean monthly time series at each VS; c) month of the minimum SWE for the mean monthly time series; d) composite time series of the VSs close one to each other on the lower Negro River, VSs NEGRO_KM1444, NEGRO_KM1420 and NEGRO_KM1404, e)

time series on the Amazon middle reach and Amazon lower reach composed of Jason-2 and Jason-3 observation at VS AMAZONAS_KM1534 and AMAZONAS_KM0397 respectively.

Owing to its relatively dense spatial cover (see **Figure 5**), satellite altimetry has been used for deriving the altimetric profiles of rivers throughout the basin. These profiles, computed for low and high waters for the Negro River from T/P VSs (Frappart et al., 2005) and ENVISAT VSs (Leon et al., 2006), indicated a lower slope for the Negro River over more than 500 km (from its mouth to upstream reaches) than for the Solimões River (confirmed by Callède et al., 2013). Such a difference explains the strong backwater effect that occurs in the lower section of the Negro River and alters the time of peak and low flows. Other backwater effects, mainly from the Amazon main stem on its tributaries, were evident in the river profiles from satellite altimetry. However sparse in time, satellite altimetry observations now provide a dense enough network to monitor extreme events such as those that occurred in 2005 and 2010 in the AB (Frappart et al., 2012; J. S. Da Silva et al., 2012).

A straightforward application of these profiles is to derive the spatiotemporal variations of the water surface slope. While former studies focused on the spatial variations of the surface water gradient, a first try to estimate the temporal variations of the Amazon main stem slope was performed in Birkett et al. (2002) using VSs from the T/P mission. They revealed changes in the sign of the rate of slope variation that were explained by the river not reaching equilibrium. Although the slopes from Birkett et al. (2002) compared well with slopes from the Shuttle Radar Topography Mission (SRTM) Digital Elevation Model (DEM) - a snapshot of profiles and slopes in February 2000 (LeFavour & Alsdorf, 2005) - and with gauge data (Calmant et al., 2013), these breaks in slope variation rate were not found in profiles extracted from more recent and complete altimetric databases (Calmant et al., 2016). Paris et al. (2016) estimated two different time series of slopes from satellite altimetry in the lower Negro River: the first was calculated using a daily interpolation of upstream and downstream SWE time series, providing a daily slope time series, and the second was calculated using the mean climatology of upstream and downstream VSs. Although the stage to discharge relationship was improved when considering the variation of slope with time estimated through both methods, it is the monthly means that provided the best improvement. This illustrates the difficulty in inferring slopes from non-daily uncertain observations.

By coupling satellite altimetry and a hydrologic and hydraulic model through stage to discharge rating curves, Paris et al. (2016) provided a map of estimated bottom of river in the entire AB using data from ENVISAT and Jason-2 missions. This map was then used by Garambois et al. (2017) on a reach of the Xingu River to parameterize a hydraulic model. Such cases where the satellite ground-track crosscuts several times the same river reach allow a more refined analysis of water surface slope. This occurs in sinuous rivers flowing from north to south (or the contrary) like the Xingu River, a right margin tributary of the Amazon River (**Figure 2**). Given these conditions, the authors verified that the presence of an obstacle in the river bed produces temporal changes in water surface slope observed by satellite altimetry. Brêda et al. (2019) proposed a benchmark of methods of altimetric data assimilation, ranging from direct insertion to a hydraulically based Kalman filter, to improve bathymetry estimates of the Madeira River. They concluded that satellite altimetry can be used for better constraining SWE and flood inundation simulations. An analysis of SWE from the ENVISAT mission revealed water passing

886 from the Negro River to the Solimões River through their interconnected floodplains at high
887 stages (J. S. Da Silva et al., 2012).

888 The capacity to observe channel-floodplain connectivity through altimetry was
889 investigated by Park (2020). By observing seasonal changes in SWE in rivers and surrounding
890 floodplains, they separated the role of channelized flows and of overbanks flows, which
891 contributes to surface water storage and smooths the channelized-induced topography. The
892 floodplain located between the Madre-de-Dios, the Beni, the Guapore and the Mamore rivers in
893 the upper Maderia basin was characterized using ENVISAT and SARAL data (Ovando et al.,
894 2018). Water level differences between the frequently flooded regions, with no direct connection
895 to the Andes, and the regions subject to sporadic though large flood events were distinguished.

896 Alsdorf et al. (2000, 2005, 2007) applied for the first time interferometric SAR (InSAR)
897 in the central Amazon floodplains and showed that the water flows in the floodplains are
898 dynamic in space and time, changing the direction with the flood wave of the river. Before the
899 flood, the flows are controlled by the local topography and the surface water elevation in the
900 floodplain is not equivalent to the river level (Alsdorf et al., 2007). By assuming that the water
901 surface in the floodplain is equivalent to those in the main channel, estimates of water storage
902 derived from flood routing can be overestimated, as shown by Alsdorf (2003). H. C. Jung et al.
903 (2010) compared temporal changes in floodplain water in the Amazon and Congo river basins.
904 While the Amazon River is connected by many channels to the floodplains and has complex
905 flow patterns, the Congo Rivers (and especially the Cuvette Centrale) have sparse connections
906 with interfluvial areas and flow patterns that are not well defined and have diffuse boundaries.
907 The patterns of water surface variations in the floodplains located on the Tapajós and Solimões
908 rivers were examined by C. Wang et al. (2011) and Cao et al. (2018), respectively. The most
909 recent SAR missions allowed monitoring of smaller water bodies. Recently, Fleischmann et al.
910 (2020) produced SWE time series in the complex Negro River interfluvial wetlands from
911 Sentinel3-A data. For the first time, they reported < 1 m water level variations in these complex
912 areas. Their results show that satellite altimetry can help understanding the hydraulic behavior of
913 complex ungaged areas and help validate hydrologic and hydraulics models.

914 Through direct assessment or combination with other RS products, satellite altimetry can
915 be used to derive non-measured hydrological variables. Pfeffer et al. (2014) were able to infer
916 the varying exchanges between surface water and the groundwater base-level from 491
917 ENVISAT VSs located all over the basin. Estimates of deviations from groundwater base-level
918 reached up to 5 m. Frappart et al. (2012) made a joint use of satellite altimetry and inundation
919 extent to derive variations of surface continental water storage (see Section 5). These two
920 variables were used in Frappart et al. (2019) to estimate the spatiotemporal variability of
921 groundwater storage in the AB. de Oliveira Campos et al. (2001) and M. V. Silva et al. (2019)
922 found signatures of global climatic events such as ENSO and sea surface temperature variations
923 in the T/P and Jason-2 SWE time series, respectively. Since the SWE estimates are now
924 delivered in near real time, rating curves that relate SWE with discharge and depth, have been
925 the focus of several studies (see details in Section 6.2). These rating curves were either computed
926 using local gauges (Zakharova et al., 2006) or model outputs (Getirana et al., 2012; Leon et al.,
927 2006). By constraining the rating curve parameters into Manning-realistic bounds, Paris et al.
928 (2016) showed that discharges predicted from satellite altimetry are comparable to those
929 measured in situ. The original SWE time series or their conversion into discharge offer an

independent tool to validate hydrological models (Paris et al., 2016) and their rainfall inputs, and in situ data (J. S. Da Silva et al., 2014).

With its disruptive technology based on swath altimetry, almost-global coverage and joint observation of SWE, River width and slope, the SWOT mission , due to be launched in 2022, will permit an unprecedented observation of SWE all over the AB, As highlighted by Biancamaria et al. (2016), SWOT observation of SWE will permit a better monitoring of transboundary waters and wetlands in the AB. Dedicated to sample all rivers wider than 100 m and lakes larger than 250 x 250 m, the mission will permit a consequent reduction of global and regional models, noteworthy through data assimilation (Emery et al., 2020; Wongchuig et al., 2020). The estimate of discharge from altimetry will benefit from SWOT data, both thanks to the global coverage and the observation of slopes, allowing a better constraining of uncertain hydraulics (Wilson et al., 2015).

Thanks to more than twenty years of studies, EO datasets, especially satellite altimetry, have been revealed as an unprecedented tool to monitor continental watersheds and their droughts and floods (Lopez et al., 2020). The current satellite altimetry missions opened the era of operational monitoring from space at large scale, and this will be of critical importance in the coming decades in the large tropical transboundary watershed that is the AB. With almost two thousand VSs distributed all over the basin and available for free on websites, and potentially hundreds more, satellite altimetry can favorably complement the traditional in situ network, whose location usually depends on the proximity to a city or town. However, to operationally monitor non-open waters such as permanently or seasonally flooded vegetated floodplains remains challenging. In fact, few lakes and reservoirs are monitored by altimetry routinely in the AB though more could be (Crétaux et al., 2011; Crétaux & Birkett, 2006). The forthcoming missions will benefit from past research to improve the accuracy of SWE time series and promote its use for monitoring more local phenomena, such as floodplain-channel exchanges. Although limited due to availability of appropriate data, InSAR datasets help characterize floodplains/rivers connectivity and dynamics. The global coverage of the forthcoming SWOT mission will increase greatly our understanding on the global water cycle and should allow a better quantification of past and current inter-mission biases, helping turning satellite altimetry archives into a unique climatic dataset and understanding the impacts of climate change and human activities on the basin. Such a task will benefit of the ongoing VASHYB project (Validation of Altimetric Satellites for HYdrology in Brazil, https://swot.jpl.nasa.gov/documents/1054/), which aims to validate SAR and InSAR observations. The SWOT mission will dramatically increase our capacity to model the AB and the variations of its water cycle, thanks to the new capacity to monitor hydrological variables (height, width, slope, and associated discharge) of hundreds of rivers 100 m wide (Biancamaria et al., 2016). The centimetric accuracy in SWE and slope (Desai, 2018) should provide new insights on water fluxes in the AB. Since the main limitation for a broader use of satellite altimetry remains its relatively low temporal sampling, future missions such as the SMASH mission (SMall Altimetry Satellites for Hydrology, Blumstein et al., 2019), broadcasted together with the current constellation, should help tackle this issue.

4.2. Surface water extent

Characterizing the extent and variation of surface water bodies and aquatic ecosystems, which include rivers, streams, lakes, wetlands, as well as seasonally inundated floodplains, forests and savannas, is of primary importance to the study of the water, energy and biogeochemical cycles of the Amazon River basin (Junk, 1997; Melack et al., 2009). Indeed, covering about 20% of basin's surface area, with large temporal variability, the surface waters of the Amazon play a key role in the climate and in the maintenance of biodiversity. Amazon surface waters are a major source and sink of carbon dioxide (Abril et al., 2014; Amaral et al., 2020; Raymond et al., 2013) and the largest natural geographic source of methane in the tropics (Kirschke et al., 2013; Melack et al., 2004; Pangala et al., 2017; Pison et al., 2013). In this context, understanding the dynamics of surface water extent is of primary importance to Amazon hydrology, biogeochemistry processes and their link with climate, for effective management of water and fisheries resources (see Section 6.3) and for a disaster management for cities which are under flood risk (e.g., Iquitos, Porto Velho, Rio Branco, Cruzeiro do Sul). This is particularly true in the context of current global changes that impact the AB (see Section 6.4), with intense drought and flood events that recently affected large areas of this region (E. A. Davidson et al., 2012; Jiménez-Muñoz et al., 2013; Marengo et al., 2008, 2011). In addition, monitoring the variations of surface water hydrological conditions is key to support the development of models of the Amazon water cycle and its surface hydrology (see Section 6.2).

Characterizing the distribution and quantifying seasonal and interannual variations in the extent of surface waters at the scale of the AB is a challenge given their large variety and variability, and the presence of cloud cover and forest vegetation. Early estimates of the distribution of surface water for large areas were based on static databases from aeronautical charts and aerial photographs, which often reflected the maximum open water extent (Cogley, 2013; E. Matthews & Fung, 1987) and did not provide information on their temporal and spatial variations. The Global Lakes and Wetlands Database (Lehner & Döll, 2004) estimates the extent of floodplains and wetlands in the AB of ~300-350 $x10^3$ km², but with large uncertainties (N. C. Davidson et al., 2018). The advent of satellite observations now allow monitoring the large-scale dynamic of surface waters, including those in the AB (Alsdorf et al., 2007; Prigent et al., 2007) enabling progress on understanding of the associated physical, biogeochemical, environmental and ecological processes.

Different RS-based techniques, using observations made in a wide range of the electromagnetic spectrum (visible, infrared, and microwave; Melack et al., 2004; Prigent et al., 2016), have been developed, with varying degrees of success, to derive quantitative estimates of the extent and dynamics of surface waters and aquatic systems in the Amazon (**Table 4**). They encompass a wide range of spatial and temporal resolutions, often based on a trade-off between temporal and spatial coverages. Observations with low spatial resolution (e.g., ~10-50 km from passive microwave sensors) are generally limited to the detection of relatively large inundated areas, or regions where the cumulative area of small areas represents a fairly large portion of the satellite footprint. They have the advantage of frequent temporal coverage, sometimes daily. High-resolution observations (e.g., <100 m from SAR for instance) provide information at a fine spatial scale but have low temporal frequency, often limiting observations over large areas to a few times per season. Optical and infrared observations offer good spatial and temporal resolution but have limited capabilities in the tropical Amazon region as they are unable to penetrate clouds and dense vegetation.

Table 4. Summary of RS-based approaches developed to monitor the extent of surface water in the Amazon (non-exhaustive list). References, sensor/satellite name, product name (when available), original area of study, spatial/temporal resolution and time span of data availability are shown.

RS Approaches	References	Sensors/Satellites (product name)	Original Area of Study	Spatial/temporal resolution	Time span
Passive Microwaves	Giddings and Choudhury (1989)	SMMR on Nimbus 7	4 major river basins of SA	~25km / Monthly	1979-1985
	Sippel et al., (1994)	SMMR on Nimbus 7	Central Amazon and floodplains	~25km/ Monthly	1979-1985
	Sippel et al., (1998)	SMMR on Nimbus 7	Amazon River and tributaries	~25km/ Monthly	1979-1985 (and 1902-1995 reconstruction)
	Hamilton et al., (2002)	SMMR on Nimbus 7	6 major floodplains over SA.	~25km/ Monthly	1979-1987
	Brakenridge et al., (2007)	AMSR/E on Aqua	Global	~25km/ daily	2002-2011
	Parrens et al., (2017)	SMOS (SWAF)	AB	~25-50km/ 3-day	2009-present
Active Microwaves	Hess et al., (2003)	SAR on JERS-1	Central Amazon	100m/Sep-Oct 95 and May-Jun 96	Sept-Oct 95 and May-Jun 96
	Bourrel et al., (2009)	SAR on ERS-2 / RADARSAT	Bolivian Amazon	2 RADARSAT (50m)/ 3 ERS (15m) images	1996–1998
	Arnesen et al., (2013)	ScanSAR mode on ALOS/PALSAR	Lower Amazon River floodplain	100m/ Twelve ScanSAR images	2007-2010
	Ferreira-Ferreira et al., (2015)	SAR on ALOS/PALSAR	Central Amazon floodplain	12.5m / 13 ScanSAR fine bream images	2007-2010
	Hess et al., (2015)	SAR on JERS-1	AB	100m/ Sept-Oct 1995 and May-Jun 1996	Sept-Oct 1995 and May-Jun 1996
	Chapman et al., (2015)	ScanSAR mode on ALOS/PALSAR	AB	100m / 323 ScanSAR images	2007-2010
	Ovando et al., (2016, 2018)	ScanSAR mode on ALOS/PALSAR and MODIS reflectance	Bolivian Amazon wetlands	100m/Forty-five ScanSAR and 500m/ 8-day MODIS images	2007-2009 and 2001-2014
	Park et Latrubesse (2017)	SAR on ALOS/PALSAR	Amazon floodplain (Miratuba)	12-350m / 19 images	2006-2008
	Pinel (2019)	SAR on ALOS/PALSAR	Amazon/Solimoes River (Janauaca)	30m/ 23 images	2007-2011
	Resende et al. (2019)	SAR on ALOS/PALSAR	Central Amazon	25m / 56 images	2006-2011
	Rosenqvist et al. (2020)	ScanSAR on ALOS-2 PALSAR-2	AB	50m / Yearly minimum and maximum	2014-2017
Optical and infrared	Yamazaki et al. (2015)	Landsat (G3WBM)	Global	90m / 4 scenes of surface body freq. at 5-year interval	1990-2010
	Pekel et al. (2016)	Landsat (GSW)	Global	30m/ Surface water occurence	1984-2015

	Allen et al., (2018)	Landsat (GRWL)	Global	30m / static widths and areas	--
	Souza et al (2019)				
Multi-satellite techniques	Prigent et al., (2007, 2020)	SSMI/AVHRR/ERS (GIEMS)	Global	~25km/ monthly	1992-2016
	Schroeder et al., (2015)	Landsat	AB	30m/Surface water changes	1985-2017
	Aires et al., (2013)	GIEMS/JERS-1 SAR	Central Amazon	500m/ monthly	1993-2007
	Fluet-Chouinard et al., (2015)	GIEMS downscalled (named GIEMS-D15)	Global	500m/ max./min./average	1993-2007
	Aires et al., (2017)	GIEMS downscalled (named GIEMS-D15)	Global	90m/ monthly	1993-2007
	Parrens et al. (2019)	SMOS downscalled (named SWAF-HR)	AB	1km/ 3-day	2010-2016

Passive microwave observations have demonstrated their usefulness for observing surface water and flood extent and provided some of the first estimates of Amazon surface water extent from satellite (Giddings & Choudhury, 1989) as reviewed in Kandus et al. (2018). Emissivities (and brightness temperatures) are sensitive to the presence of surface water (Choudhury, 1991; Sippel et al., 1994) with a decrease in emissivity in both linear polarizations (horizontal and vertical) and an increase for the difference in polarization, especially at low frequencies, due to the different dielectric properties between water, soil and vegetation. Surface water and inundation patterns in the large floodplains of the central AB (Sippe et al., 1998) and South America (Hamilton et al., 2002) were derived by analysis of the 37-GHz polarization difference observed by the Scanning Multichannel Microwave Radiometer (SMMR; Nimbus-7 satellite, 1979-1987). By developing a relationship between the total flooded area along the Amazon river main stem and the monthly means of river stage at Manaus, they provided the first 94-year reconstruction of flooded area from the river stage in situ record, estimating the long-term mean of the flooded area along the Amazon River main stem to be ~ 47000 km^2. Those studies have been followed by passive microwave-derived products of surface water extent over the AB, using Special Sensor Microwave/Imager (SSM/I), Advanced Microwave Scanning Radiometer (AMSR-E; Brakenridge et al., 2007) and most recently Soil Moisture Ocean Salinity (SMOS) observations (Parrens et al., 2017). Parrens et al. (2017) used the microwave L-band (1.4 GHz) observations from 2010 to 2017 to map the temporal evolution of the Amazon water bodies at coarse spatial resolution (~50 km) and weekly temporal resolution (product named SWAF) with the ability, thanks to the L-Band frequency, to better retrieve water under dense canopy. Passive microwave observations have inherent limitations because of their ground footprints in the typical order of 25-50 km, and their relatively low spatial resolution is often insufficient to observe small water bodies.

Multi-satellite methodologies that combine the complementary strengths of different types of satellite observations to retrieve surface water extent and their dynamics expand the information provided by passive microwave radiometers (**Table 4**). Though designed originally for global scale applications, these approaches have been evaluated in the AB. The Global Inundation Extent from Multi-Satellite (GIEMS, Papa et al., 2010; Prigent et al., 2007, 2016,

2020) or the Surface WAter Microwave Product Series (SWAMPS) Inundated Area Fraction (Schroeder et al., 2015) detect and quantify multi-decadal variability of surface water extent over tropical environments (Frappart et al., 2008; Papa et al., 2008, 2013). The current version of GIEMS is available at ~25 km spatial resolution on a monthly basis for 1992 to 2015 (GIEMS-2, Prigent et al., 2020, **Figure 6**a), while SWAMPS offers current and near-real time information (Jensen et al., 2018). The use of these passive microwave-derived datasets helped reveal the sources and characteristics of the flood pulse and annual flood wave along the Amazon River and major tributaries. They contributed to show at basin scale the water extent seasonality, with a high flood season in May-June and low flood season in November in the central Amazon floodplain. At basin-scale, Amazon surface water extent (**Figure 6**b) varies from ~100,000 km² (low season) to almost ~400,000 km² (high season), but with a large interannual variability, mainly driven by droughts (1998, 2005, 2010) or floods (1997, 2014) extreme events (Papa et al., 2010; Prigent et al., 2020). However, the maximum surface water extent from GIEMS and SWAMPS are lower than those from SAR estimates (**Figure 6**b).

Prigent et al. (2007) showed that seasonal flooding differed between the north and south part of the basin due to seasonal differences in precipitation. Papa et al. (2008) reported a phase lag in precipitation, flood extent and peak flows at the basin scale, suggesting as in Richey et al. (1989), that floodplains in large basins such as the Amazon can store large volume of water and alter the water transport. Richey et al. (1989) applied a simple water routing scheme and estimated that up to 30% of the discharge of the Amazon River is routed through the floodplains. However, studies such as Getirana et al. (2012), based on large-scale hydrological model that used GIEMS to evaluate their floodplains simulations, suggested instead that the actual value might be more below 5%. Furthermore, Sorribas et al. (2020) reported that the ratio between river-floodplain discharge and basin discharge ranged between 5 and 40%, which is comparable to the range estimated from observations by Richey et al. (1989) and Alsdorf et al. (2010) who used gravimetric and imaging satellite methods to estimate the amounts of water seasonally filling and draining from the mainstem Amazon floodplain. Hence, there is a need to better understand the processes that control Amazon inundations in order to quantify the various fluxes across floodplain environments, as is evident in applications of regional-scale flooding models (Rudorff et al., 2014b).

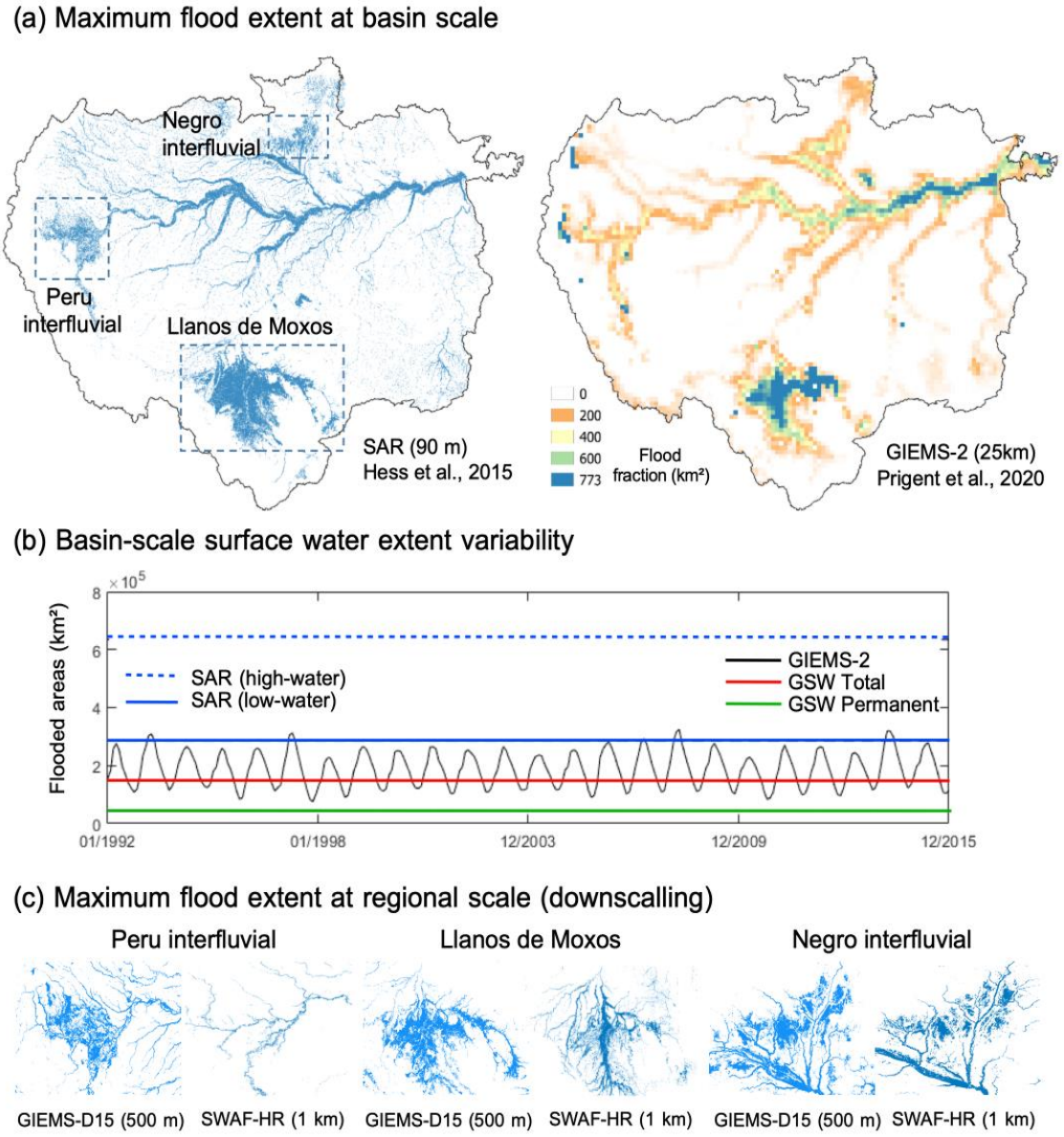

Figure 6. Surface water extent of the AB. (a) Map of maximum wetland and surface water extent (high water season) from JERS-1 SAR (Hess et al., 2015) and map of annual maximum surface water extent (fraction in km^2 for each 773 km^2 pixel) averaged over 1992– 2015 from GIEMS2 (Prigent et al., 2020). (b) Basin-scale monthly mean surface water extent variability for 1992–2015 from GIEMS2 (solid black line) along with estimates of JERS-1 SAR-derived wetland and flooded area for high-water (dashed blue line) and low-water (solid blue line) seasons. Also shown are the Global Surface Water (GSW, Pekel et al., 2016) permanent surface water extent (green line, GSW permanent) and the total (permanent plus transitory) surface water extent at maximum (red line, GSW Total). (c) Map of maximum surface water extent at regional scale (boxes in (a) indicate the locations) from GIEMS-D15 (Fluet-Chouinard et al., 2015) and SWAF-HR (Parrens et al., 2019).

Synthetic aperture radars are active radar instruments that measure the backscatter of the observed surface at an angle of incidence (off-nadir), regardless of cloud cover, and allow delineation of open surface waters and inundated area with vegetation with a typical spatial resolution of 10-100 m (Behnamian et al., 2017; Hess et al., 1990; Kasischke et al., 1997) The Spaceborne Imaging Radar-C (SIR-C) experiment provided high quality, multi-band and multi-polarization data for the Amazon that led to the development of new approaches using SAR. Alsdorf et al. (2000) demonstrated the ability of interferometric analyses to detect centimeter-scale variations in slope across the Amazon rivers and floodplains (see Section 4.1). Hess et al. (1995) developed algorithms to detect inundation and vegetation within Amazon wetlands that benefitted from modeling of interactions between vegetation and radar, including the double-bounce effect, also done as part of SIR-C (Y. Wang et al., 1995). Understanding derived from this led to use of data provided by the Japan Earth Resources Satellite-1 (JERS-1) to produce the first high-resolution wetland map for the central Amazon region under low-water and high-water conditions at 100-m resolution (Hess et al., 2003). These results were validated with airborne, high-resolution, videography transects throughout the imaged area (Hess et al., 2003). Hess et al., (2003) found that 17% of the 1.77 million km^2 study area is occupied by wetlands, of which 96% are inundated at high water and 26% at low water. Flooded forests accounted for nearly 70% of the overall wetland area, but proportions of the wetland habitats showed large regional variations related to floodplain geomorphology. Those new estimates of large inundated area were of major importance to understand the outgassing of methane and carbon dioxide from Amazon flooded areas (see Section 6.3).

The JERS-1 SAR estimates were extended to the entire wetlands of the lowland AB (region < 500 m asl) (**Figure 6**a; Hess et al., 2015), currently one of the standards for comparison with other satellite-derived products. It estimates flooded extent (**Figure 6**b) to be of ~2.85 $x10^5$ km^2 for low water season (Oct-Nov 1995) and of ~6.34 $x10^5$ km^2 for high water season (May-July 1996). An interesting comparison is one made for the central corridor of the AB (Prigent et al., 2007) between GIEMS and the 100 m resolution L-band JERS-1 SAR mosaic of Hess et al. (2003) for low water (September-October 1995) and high water (May-June 1996). For both seasons, the spatial structures are similar but estimates of the surface water extent observed by SAR (118,000 km^2 for the low water season, 243,000 km^2 for the high water season) are larger than the area estimated by GIEMS (105,000 km^2 for the low water season, 171,000 km^2 for the high water season). Thanks to its better spatial resolution, the SAR estimates are capable to discriminate smaller water bodies than GIEMS (typically water bodies smaller than 80 km^2 i.e, 10% of a GIEMS pixel), especially for the low water season. For the entire AB, the basin-wide estimates from GIEMS do not match the basin-wide SAR (**Figure 6**a and b) as reported in Hess et al. (2015) which suggested that global datasets derived from lower-resolution sensors or optical sensors capture less than 25% of the wetland area mapped by the SAR.

The use of multi-temporal SAR coverage, such as the ScanSAR mode of ALOS/PALSAR, provide variations of flood extent at the scale of floodplain units, e.g., Curuai floodplain along lower Amazon River (Arnesen et al., 2013), Mamiraua floodplain (Ferreira-Ferreira et al., 2015) or inundation patterns in central Amazon (Pinel et al., 2019; Resende et al., 2019). Rosenqvist et al. (2020) generated annual maximum and minimum inundation extent maps over the AB using ALOS-2/PALSAR-2 ScanSAR, in line with previous inundation maps

by L-band JERS-1 and ALOS/PALSAR radar classifications of the inundation (Chapman et al., 2015). At the regional scale, Bourrel et al. (2009) mapped the floods in the Bolivian Amazon from SAR C-Band microwave data of RADARSAT and ERS-2. Over the same region, the surface water dynamics of the Bolivian Amazon wetlands (Ovando et al., 2018), as well as the characterization of extreme flood events (Ovando et al., 2016) were investigated by combining ALOS/PALSAR SAR observations with MODIS multi-temporal flood maps and altimetry-derived water level variations (ENVISAT & SARAL). Other SAR satellite missions, such as the Copernicus Sentinel-1 SAR (launched in 2014), which offer a global revisit of 6-12 days, have not been yet fully exploited in the AB but offers new opportunities for mapping the spatial and temporal variations of surface waters at a fine scale in tropical environments. The near-future launch of SAR satellites, such as NISAR and SWOT (Prigent et al., 2016), will offer new opportunities to monitor Amazon surface water with dedicated sensors.

Optical and infrared imagery observations (e.g., Landsat, SPOT, QuickBird, Ikonos, AVHRR, MODIS, Sentinel 2A/B) offer high spatial and temporal resolutions (~1-500 m, sub-daily to weekly) but in tropical environments they are generally limited by the inability to penetrate clouds and dense vegetation. Therefore, assembling cloud-free coverage during the rising flood season of the central AB remains challenging (Asner, 2001; Hess et al., 2015; Klein et al., 2015). Nevertheless, classification of optical imagery using water indexes and related methods, as reviewed by Huang et al. (2018), enables to estimate flood frequency based on temporal maps of surface water cover, and despite the limitations from vegetation canopy and cloud cover, this type of data can be of value to monitor open surface water. Several studies (**Table 4**) based on Landsat observations created global databases of the area of rivers (Global River Widths from Landsat -GRWL; Allen & Pavelsky, 2018) and surface water (Pekel et al., 2016; Yamazaki et al., 2015) which can be used at the AB scale. Based on the decadal-scale monitoring of Landsat missions, the Global Surface Water dataset (GSW, Pekel et al., 2016) uses three million images over 32 years (from 1984 to 2015) at a 30 m spatial resolution to derive a monthly record of water presence in classifying each Landsat pixel as open water, land, or non-valid observation using an expert system. In the AB, GSW estimates of surface water extent (permanent and total as the sum of permanent and transitory water bodies) are lower than the estimates from other RS-based technique such as SAR or GIEMS (**Figure 6**b) and comparison of GSW with GIEMS-D3 (see further below) found seasonal water bodies in savannas and forest floodplains were not detected properly (Filipe Aires et al., 2018). C. M. Souza et al. (2019) developed another Landsat classification to estimate long-term changes in Amazon surface waters revealing the recent increase in areas associated to hydropower lakes. Recent satellite missions such as Sentinel 2A/B (since 2015, with 10 m spatial resolution at 5–10-day intervals, Pham-Duc et al., 2020) or programs such as the RapidEye (since 2008, 5 m spatial resolution and a temporal resolution of 1–5.5 days, Garousi-Nejad et al., 2019) or the PlanetScope (CubeSats, since 2014, with 3–5 m spatial resolution and daily revisit time; Cooley et al., 2019) constellations might bring new opportunities to study fine scale surface water extent of the Amazon.

In order to take advantage of the complementary strengths of various observations, for instance the low resolution but long term estimates of passive microwave versus the high resolution but limited in time observations from SAR, a downscaling methodology combining both estimates has been developed to retrieve monthly central Amazon at ~500 m spatial for the 1993-2007 period (Filipe Aires et al., 2013). Several other studies based on downscaling

approaches using a floodability index provide high resolution maps of surface water extent over the Amazon, such as GIEMS-D15 (Fluet-Chouinard et al., 2015; ~500 m spatial resolution and its 1-km adaptation as in Reis et al., 2019) and GIEMS-D3 (Aires et al., 2017, 90m). Similarly, Parrens et al. (2019) proposed a downscaling methodology based on multi-source RS data (SMOS SWAF; combined with a global DEM and GSW dataset) to map Amazon inland water under vegetation at ~1 km spatial resolution every 3 days for the 2010–2016 (named SWAF-HR). **Figure 6**c shows maps of maximum surface water extent from GIEMS-D15 and SWAF-HR for three regions, including interfluvial wetlands. Such observations are valuable to wetland conservation decisions, as the timing and duration of inundation often determine ecological characteristics and the provision of ecosystem services. For instance, Reis et al. (2019) classified Amazon wetlands according to the timing and duration (months per year) of inundation detected with GIEMS-D15, and their link to precipitation regimes. It revealed that permanently inundated wetlands account for the largest area and are mainly floodplains located in the lowlands of the catchment. Seasonally inundated wetlands varied in the duration of inundation reflecting different rainfall and hydrological regimes. These regional differences in inundation characteristics are important to conservation planning and wetland management especially in the context of anthropogenic interventions such as dams and waterway construction.

Finally, new RS techniques and methodologies are continuing to be developed and can help monitor the surface water extent of the AB. The potential for Global Navigation Satellite System-Reflectometry (GNSS-R) has been explored (Chew & Small, 2020; Jensen et al., 2018; Rodriguez-Alvarez et al., 2019) using Cyclone GNSS (CYGNSS) constellation of GNSS-R satellites and a simple forward model that demonstrate how surface reflectivity measured by CYGNSS can capture flooding dynamic over the region.

In Section 5.1 “Methods for Measuring Area” of Alsdorf et al. (2007), the authors suggested that "*Perhaps the best opportunity in the next few years for routine measurements of inundated area will result from the Japan Aerospace Exploration Agency’s ALOS mission*". More than a decade later, it is worth noting that the extent and variability of surface water of the Amazon are still one of the most studied variables of the hydrological cycle, but that studies using ALOS observations remain recent and limited. Further studies and new observations are required to fully characterize Amazon surface water extent and the processes that drive the patterns and dynamic. In particular, polarimetric and interferometric L-band SAR data from the forthcoming NASA/ISRO L-band SAR mission and the Ka-band Radar Interferometer (KaRIn) swath observations from the forthcoming SWOT mission will be capable of enhanced monitoring and comprehensive survey of large-scale surface water extent and dynamics of the AB.

4.3. Floodplain and river channels topography

Along the Amazon River, the floodplain has many lakes and channels that vary in extent, depth, and connectivity (Hess et al., 2015; Rudorff et al., 2014b; Trigg et al., 2012). This complex topography affects the water flow through river-floodplain water exchanges, which in turn, are important for carbon, nutrients, and sediment fluxes (Melack et al., 2009). Accurate topographic information is essential for the characterization of the surface water in the floodplain, particularly for hydraulic numerical modeling (Baugh et al., 2013; Paiva, Buarque, et

al., 2013; Rudorff et al., 2014a). Furthermore, topographic mapping is required for understanding the morphology and morphodynamics of the river channels and lakes. The SRTM DEM is a global topographic dataset generated from C-band interferometry (Farr et al., 2007) and has been widely used in hydraulic simulations and geomorphic characterization of the Amazon floodplains (**Figure 7**a). However, the data are affected by vegetation cover, and has errors such as absolute bias, speckle noise (granular aspect in the image due to the random presence of pixels with extreme values), and stripe noise (Rodríguez et al., 2006). It is also not capable of describing bathymetry of inland water bodies as it observed surface water elevation only once.

The application of topographic data, such as SRTM DEM, together with radar (e.g., RADAM, JERS-1) and optical (e.g., Landsat) images allowed the geomorphological characterization of floodplains and river channels of the AB. Sippel et al. (1992) described lakes of different shapes based on RADAM maps along different sections of the main stem Solimoes/Amazonas rivers and their major tributaries. Latrubesse & Franzinelli (2002) and Mertes et al. (1996), described geomorphologically distinct regions along the upper and middle reach of the Amazon River. Scroll-bar topography, which forms long and narrow lakes, and oxbow lakes, located in abandoned river meanders, are dominant in the upstream reaches (Mertes et al., 1996; **Figure 7**). Downstream reaches are characterized by large, shallow lakes formed by the overbank deposition of fine sediments in a very flat floodplain topography (Latrubesse & Franzinelli, 2002; Mertes et al., 1996; **Figure 7**). Active deposition of sediments across the floodplains was also identified and described by Lewin et al. (2017) using RS data. Constantine et al. (2014), Peixoto et al. (2009) and Rozo et al. (2012) characterized the channel's migration of rivers and floodplains. Sediment supplies play an important role in the evolution of Amazonian rivers, as the rivers with high sediment loads experience faster meander migration and higher cutoff rates than rivers with lower sediment loads (Constantine et al., 2014). Large and rapid geomorphological changes can also arise due to anthropogenic pressures such as livestock and channel irrigation. These may be the causes of the progressive erosion of a channel along the lower Amazon River that captured almost all discharge from the lower Araguari River, which previously had flowed directly to the Atlantic Ocean (E. S. dos Santos et al., 2018; described in more details in Section 6.4).

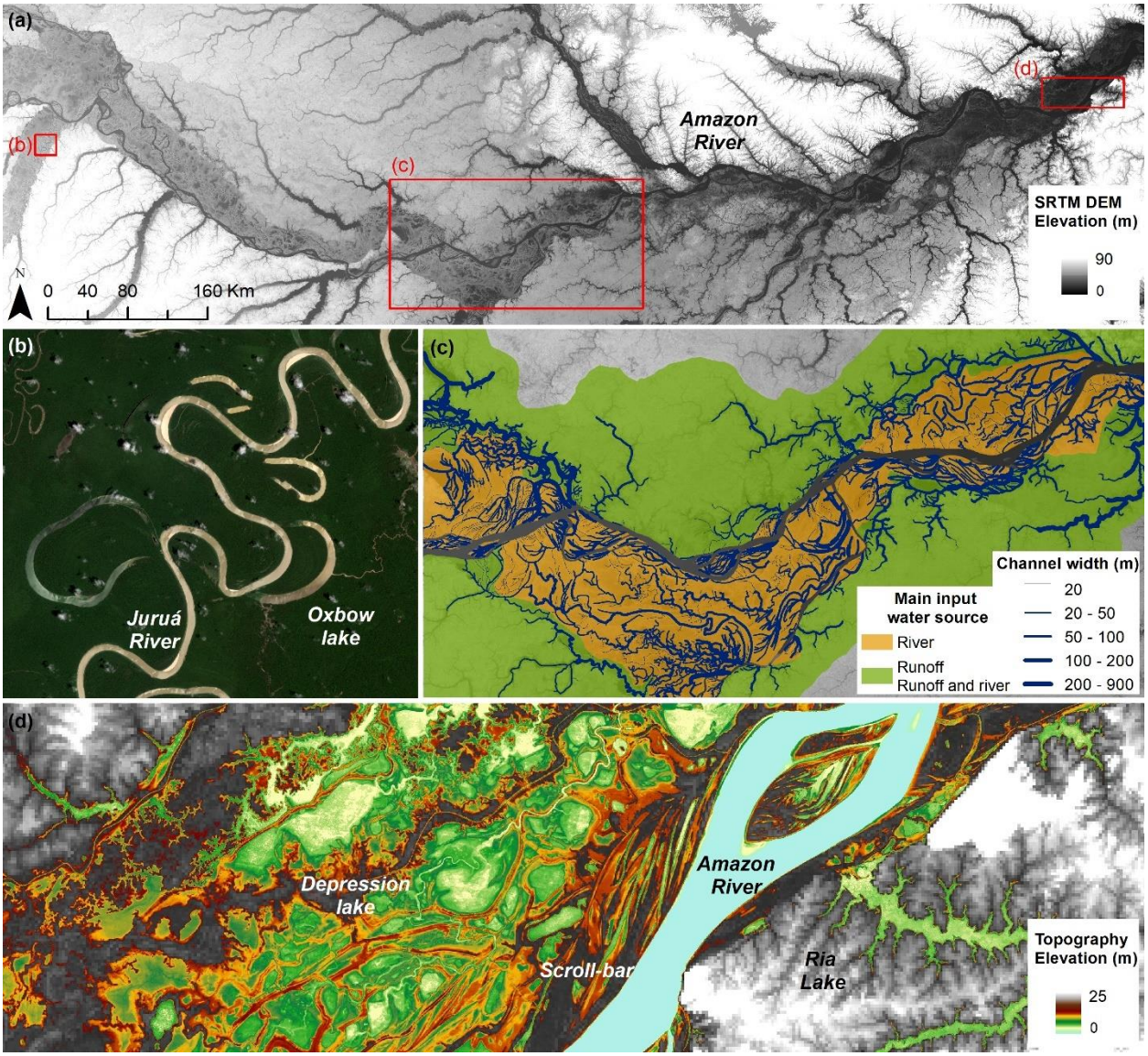

Figure 7. (a) SRTM DEM in central Amazon. (b) Oxbow lakes in Juruá River (Sentinel-2, October of 2020). (c) Channel width in the floodplain (Adapted from Trigg et al., 2012). (d) Topography elevation of the floodplain channels and lakes (Adapted from Fassoni-Andrade, Paiva, Rudorff, et al., 2020).

In order to improve the applicability of SRTM data to hydraulic modeling of the AB, various techniques were developed such as the removal of the vegetation height (Baugh et al., 2013; O'Loughlin et al., 2016; Paiva, Buarque, et al., 2013; Paiva, Collischonn, et al., 2011; Pinel et al., 2015; Rudorff et al., 2014a; Yamazaki et al., 2017), the interferometric bias (Pinel et al., 2015; Rudorff et al., 2014a), as well as smoothing as pit removal (Yamazaki, Baugh, et al., 2012). Despite the better topographic representation achieved by these methods, topographic information below the water surface cannot be recovered from SRTM. Also, SRTM dataset relies on one only overpass in February 2000. Therefore, some processes, such as infilling and

drainage of the floodplain, may not be well represented in the numerical models. River bathymetry is also key information that is not systematically resolved. Recently Brêda et al. (2019) demonstrated the potential of assimilating satellite altimetry data into hydraulic models for its estimation. To estimate the topography in seasonally flooded areas, Bonnet et al. (2008) combined SWE with flood extents derived from JERS-1 images to estimate a bathymetric DEM of the Curuai floodplain. Park et al. (2020) related water depth and a flood frequency map, derived from surface water mapping, to infer the Curuai bathymetry. Fassoni-Andrade, Paiva, Rudorff, et al. (2020) developed and applied a systematic method to estimate floodplain topography using a combination of flood frequency maps derived from optical RS and ancillary in situ water level data archives (**Figure 7**d). This was the first systematic and extensive mapping of a seasonally flooded area in a wetland, showing floodplain depths less than 5 m (15 m) in low (high) water, and that active storage volume in the open-water floodplain varies 104.3 km^3 on average each year. This dataset was complemented over permanently flooded regions by a compilation of digitized nautical charts from the Brazilian Navy. Recently, Fassoni-Andrade et al. (2021) applied this methodology to the Amazon estuary showing the morphology of the intertidal floodplain.

The bathymetric information in permanently flooded areas relies on in situ field surveys. Among the studies cited here, only a few obtained in situ bathymetric information (Bonnet et al., 2008; Fricke et al., 2019; Pinel et al., 2015). Additional studies with detailed bathymetry include Lesack & Melack (1995), Barbosa et al. (2006), Panosso et al. (1995), and Trigg et al. (2012). As part of the first hydrological budget of an Amazon floodplain lake, Lesack & Melack (1995) surveyed the lake's bathymetry, which was subsequently used in the hydrological model of Ji et al. (2019). Panosso et al. (1995) conducted a bathymetric survey of Lake Batata, located near the confluence of the Trombetas River and the Amazon River. This lake received tailings from bauxite processing and the estimate was used for conservation and recovery studies. Barbosa et al. (2006) conducted an extensive bathymetric survey of the Lake Grande do Curuai floodplain, in the eastern AB. The bathymetry was used to estimate volume, in hydraulic simulation (Rudorff et al., 2014a) and topographic assessment (Fassoni-Andrade, Paiva, & Fleischmann, 2020). Trigg et al. (2012) illustrated the first systematic characterization of floodplain channels in central Amazon based on Landsat imagery and field survey (**Figure 7**c). Floodplain channel widths vary considerably (10–1000 m), and channel depths are related to the local amplitude of the Amazon river flood wave (~10 m), and deeper when subject to local runoff.

Many advances have been made to characterize the topography of rivers and floodplains using RS techniques, among the promising prospects for new DEMs (eg.. The L-band reduces the systematic positive bias of vegetation due to its ability of penetrating the canopy. Images from the NISAR mission, a bi-band SAR satellite to be launched in 2022 with global coverage and revisiting periods of 12 days will improve the availability of L-band radar data. The SWOT mission will simultaneously measure the SWE and water extent, opening up new opportunities to create and improve new techniques. New unexplored data from ICESat-2 satellite (launched in 2018) could be useful for topography estimation and validation.

4.4. Water quality: Sediments, chlorophyll and colored dissolved organic matter

According to their physical and chemical water characteristics, rivers of the AB are classified into three types: white, black, and clear-waters rivers (Junk et al., 2011; Sioli, 1956). Nutrient-rich whitewater rivers, such as Madeira and Solimões rivers, which account for 98% of Amazon River's sediment discharge to the Atlantic Ocean are dominated by inorganic sediments mainly originated from the Andes (Almeida et al., 2015; Meade, 1994). Blackwater rivers (e.g. Negro River; **Figure 8a**) are rich in dissolved organic matter derived from podzolic soils (Bouchez et al., 2011). Clear-water rivers (e.g. Tapajós River; **Figure 8b**) are characterized by nutrient-poor, low sediment, and dissolved organic matter concentration (Junk et al., 2015). The water-type diversity and the pathways throughout the Amazon floodplain have significant implications for floodplain lakes and contribute to their high biodiversity (Junk et al., 2011; Thom et al., 2020).

A feasible way to monitor the aquatic system's biogeochemical properties and water paths between the rivers and floodplain lakes is through satellite RS. The interaction between electromagnetic radiation and water bodies, described by radiative transfer theory (Kirk, 2010; Mobley, 1994), allows the development and calibration of algorithms for estimating optically active constituents (OACs: Total Suspended Sediments -TSS; Phytoplankton pigments such as Chlorophyll-a - Chl-a - and Phycocyanin; and Colored Dissolved Organic Matter – CDOM) in the water bodies. These OACs influence the underwater light field and, therefore, the inherent (e.g., absorption and backscattering coefficient) and apparent optical properties (e.g., Remote Sensing Reflectance – R_{rs}) of the water bodies.

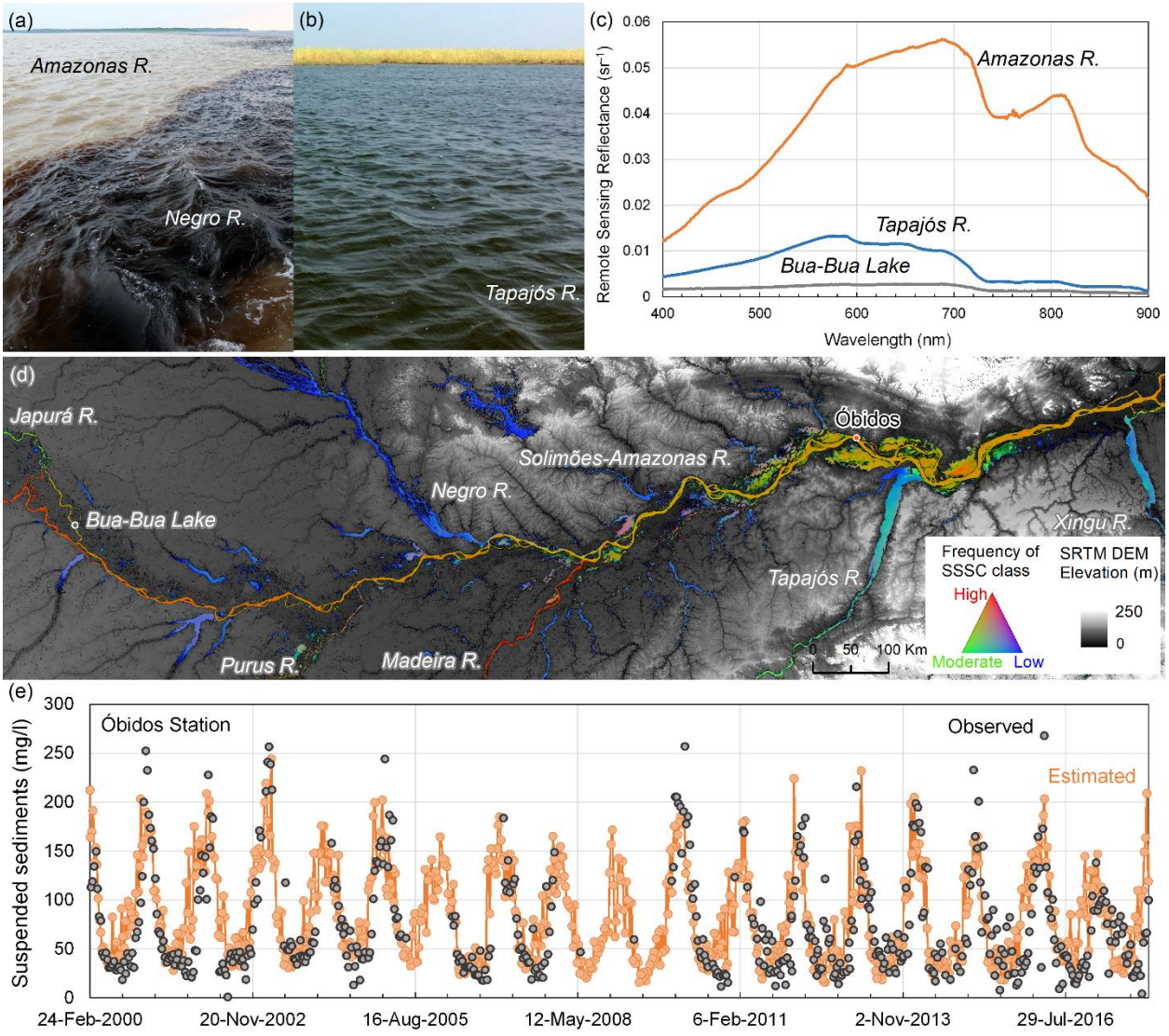

Figure 8. a) Examples of white and black, and b) clear waters. c) Examples of spectra of three water types (Source: Labisa; http://www.dpi.inpe.br/labisa/): white water - Amazon River (TSS of 288.5 mg L^{-1}; Chl-a of 2.0 µg L^{-1}; aCDOM in 440 nm of 1.3 m^{-1}); clear water - Tapajós River (TSS 5.7 mg L^{-1}; Chl-a of 10.8 µg L^{-1}; aCDOM in 440 nm of 1.2 m^{-1}); black water - Bua-Bua Lake (TSS 7.4 mg L^{-1}; Chl-a of 3.6 µg L^{-1}; aCDOM in 440 nm of 2.9 m^{-1}). d) Spatial variability of suspended sediments in the central Amazon (Adapted from Fassoni-Andrade & Paiva, 2019). e) Suspended sediment time-series in situ (observed) and satellite-based MODIS (estimated) obtained from the HYBAM monitoring system (http://hidrosat.ana.gov.br).

There are significant challenges applying RS to monitoring of AB aquatic ecosystems: i) frequent cloud cover makes it difficult to acquire images; ii) the optical complexity of the waters that flow throughout the AB, characterized by high variability in the concentration of the OACs; iii) the lack of sensors with high radiometric, spectral, spatial resolution and signal-to-noise ratio to detect the small changes in upwelling radiance from the water column; and iv) the difficulty of

using RS in narrow rivers and small lakes. These challenges have existed since the beginning of RS applications to study of Amazonian aquatic ecosystems in the early 1980s, that focused on calibration/validation of algorithms based on in situ data. These methods were based mostly on empirical approaches (Bayley & Moreira, 1978; Bradley, 1980; Mertes et al., 1993), with acceptable accuracy limited in time and space to the dataset for which the algorithm was developed (M. W. Matthews, 2011; Odermatt et al., 2012). In the last decade, efforts have been made to adapt ocean color protocols (Mueller et al., 2003) to acquire inherent optical properties (IOPs) of the Amazonian waters (L. A. S. de Carvalho et al., 2015; M. P. F. Costa et al., 2013; Jorge et al., 2017; Maciel, Barbosa, et al., 2020; Pinet et al., 2017; Valerio et al., 2018), allowing for the development of semi-analytical algorithms (SAA). As the apparent optical properties (AOPs) are proportional to the IOPs, SAA uses an inversion process based on radiative transfer theory to obtain IOPs from the AOPs. Once the IOPs are known, they are used to retrieve the OAC concentrations. Therefore, SAA algorithms better identify each constituent contribution, providing more comprehensive temporal and spatial coverage (Dekker, 1993; Novoa et al., 2017).

The flourishing of satellite RS in the second decade of the 21st century is due to two crucial technological advances. First, a new generation of sensors was better designed to study complex aquatic environments, with improved spectral and radiometric resolution (Landsat-8, Sentinel-2, CBERS-04A). Second, the unprecedented increase in computing performance and data storage has improved image processing capability. However, the low radiometric resolution provided by sensors onboard earlier Landsat (Landsat-5 and Landsat-7) satellites has not prevented the development of studies taking advantage of the substantial temporal database available (1972 to now) as reported in Lobo et al. (2015) and Montanher et al. (2018).

In preparation for new sensors, studies of spectral behavior of Amazon water types among a wide range of OAC concentrations have been done (C. C. F. Barbosa, 2005; Nobrega, 2002; Rudorff, 2006). Those spectra were organized into a spectral library linked to OACs data to create reference spectra for water types classification (Lobo et al., 2012). The spectral library is an input to a Spectral Angle Mapper algorithm for deriving water type maps from Hyperion and Medium Resolution Imaging Spectrometer (MERIS) images acquired simultaneously with field campaigns, with reasonable accuracies (48% and 67% for Hyperion and MERIS respectively). This updated library was applied to classify Brazilian water types (E. F. F. da Silva et al., 2020). In proof of concept studies, MODIS images from AQUA and TERRA satellites were successfully used for estimating Chl-a (Novo et al., 2006) and TSS (Espinoza-Villar et al., 2018; Fassoni-Andrade & Paiva, 2019; Marinho et al., 2018; J. M. Martinez et al., 2009) in Amazonian water bodies with a size compatible with the spatial resolution of the sensors.

Chl-a estimation, a proxy for phytoplankton abundance, remains challenging in the Amazon floodplain lakes due to high TSS masking chl-a spectral features (Z.-P. Lee et al., 2016) at some times (C. C. F. Barbosa et al., 2009, 2015; Bourgoin et al., 2007; R. D. Ferreira et al., 2013; Maciel et al., 2019). A spectral mixture algorithm can overcome this problem in some cases (Novo et al., 2006; Rudorff et al., 2006). Highest chlorophyll concentrations were observed in low water periods (November and December) in the middle reach of the Amazon floodplain, as a result of lakes enriched by dissolved nutrients in less turbid waters (Novo et al., 2006). However, the empirical nature of those algorithms prevents their wide application. Therefore, new approaches have been investigated, including the use of semi-analytical algorithms (Flores Júnior, 2019). CDOM retrieval based on satellite imagery is scarce in Amazon lakes since the isolation of CDOM

signature from the water leaving signal is complex in turbid waters (Kutser et al., 2016). M. P. da Silva et al. (2019) proposed an empirical algorithm for estimating CDOM absorption at 440nm from Sentinel-2/MSI images. **Table 5** presents a summary of these studies.

There are many studies on sediment retrieval from satellite data. These studies are mainly focused on TSS estimates for rivers (Bernini et al., 2019; Espinoza-Villar et al., 2018; Kilham & Roberts, 2011; Lobo et al., 2015; Maciel et al., 2019; Maciel, Novo, et al., 2020; Montanher et al., 2014; Park & Latrubesse, 2014; Villar et al., 2013; Yepez et al., 2018) rather than for Amazon floodplain lakes (Alcântara et al., 2009; Fassoni-Andrade & Paiva, 2019; Maciel et al., 2019; Rudorff et al., 2006, 2007). Most of them are based on empirical algorithms, and only recently, some semi-analytical algorithms became available (**Table 5**). The HYBAM observatory provides an example of systematically derived TSS concentration using empirical algorithms from MODIS at 16 stations (TSS time-series; http://hidrosat.ana.gov.br) in the main sediment-contributing rivers, including Amazon-Andean rivers in Peru and Bolivia (Espinoza-Villar et al., 2018; R. Espinoza Villar et al., 2012; J. M. Martinez et al., 2009; Villar et al., 2013). **Figure 8**e is an example of a suspended sediment time-series obtained from the HYBAM monitoring system in Amazon River between 1999 and 2017 and illustrates substantial variability of TSS concentration, ranging from 25 up to 250 mg L^{-1}.

Montanher et al. (2014) mapped TSS in five Amazonian rivers using multiple regression and observed that regional-calibrated algorithms performed better than global algorithms due to changes in optical properties of rivers. Park & Latrubesse (2014) also observed that calibrating a separate empirical algorithm for low and high-water seasons provided better results for the Amazonian river waters. High variability in the OACs in floodplain lakes makes algorithm parametrizations difficult. For example, in the Curuai floodplain (lower reach of the AB), TSS concentrations can vary from ~5 mg L^{-1} in the high-water season up to 1000 mg L^{-1} in the low water season due to sediment resuspension by winds. Despite those issues, recent work provide successful TSS estimates in the floodplains of the lower Amazon River (Maciel et al., 2019; Maciel, Novo, et al., 2020).

TSS trends have been documented in the Amazon River (J. M. Martinez et al., 2009; Montanher et al., 2018) and the Madeira River (Latrubesse et al., 2017; Li et al., 2020) that might be related to dam construction (see Section 6.4 for details). RS data in AB were also used to evaluate siltation impacts caused by artisanal gold mining in the Tapajós River basin (Lobo et al., 2015, 2016; see Section 6.4 for details). Furthermore, Fassoni-Andrade & Paiva (2019) mapped for the first time the spatial-temporal pattern of sediment in clear, white, and black water of the Amazon rivers (**Figure 8d**). Despite errors in the empirical model, temporally filtered reflectance in red and infrared revealed sediment variations in rivers and lakes. Therefore, it was possible to characterize hydrological processes, such as backwater effects, overbank flow, and sediment resuspension in lakes. It was observed that depression lakes of the middle reach receive sediments-rich water by overbank flow during the flood, and resuspension of sediments occurs in the low water period, as previously documented (Bourgoin et al., 2007). In ria lakes, the main water source comes from the local basin (surface runoff and local rainfall) with river inflows adding sediment during the low water period.

Table 5. OACs algorithms for the AB. OAC range refers to the minimum and maximum values; Algorithm Type (AT) refers to Empirical (E) or Semi-Analytical (SAA). In algorithm equation

column, f_{phy} refers to phytoplankton fraction from Linear Mixture Model, R_{rs} (λ) is the RS reflectance, $p(\lambda)$ is water reflectance. R^2 is the coefficient of determination, SE is the Standard Error, MSE is the mean square error, %NMSE is the normalized mean squared error, MAPE is the Mean Absolute Percentage Error, RMSE is the root mean square error, PE is the percentage error. For the equations of statistical metrics, the reader is referred to each reference.

Study Area	Sensor Name	OAC	OAC Range	AT	Algorithm Equation	Validation Statistical Results	Reference
Low Amazon	MODIS Terra	Chl-a	10-120 μgL^{-1}	E	$Chl = 3.9 * e^{0.0175 * fphy}$	R^2 = 0.76 SE = 19 μgL^{-1}	(Novo et al., 2006)
Mamirauá Sustainable Development Reserve	Sentinel-2	CDOM	~1 – 6 m^{-1}	E	$a_{cdom}(440) = 4.39^{\frac{B2}{B3}} + 0.59^{\frac{B6}{B5}} - 6.67$	R^2 = 0.75 MSE = 0.53 m^{-1} %NMSE = 15.12%	(M. P. da Silva et al., 2019)
Curuai Lake	Sentinel-2 and Landsat-8	TSS and TSI	7-43.5 mgL^{-1} (TSS) 3.4-33.8 mgL^{-1} (TSI)	E	$\ln(TSS_{OLI}) = 9.656 + 1.672 * \ln(R_{rs}(550))$ $\ln(TSI_{OLI}) = 10.73 + 2.08 * \ln(R_{rs}(550)$ $\ln(TSS_{MSI}) = 8.318 + 1.336 * \ln(R_{rs}(550))$ $\ln(TSI_{MSI}) = 8.447 + 1.511 * \ln(R_{rs}(550)$	R^2 = 0.71, MAPE = 16.81%, RMSE = 3.54 R^2 = 0.86, MAPE = 18.08, RMSE = 1.97 R^2 = 0.69, MAPE = 16.67, RMSE = 3.58 R^2 = 0.81, MAPE = 18.62, RMSE = 3.1	(Maciel et al., 2019)
Curuai Lake	WFI CBERS-4	TSS	9-28 mgL^{-1}	SAA	$TSS = \frac{293.930 * p550}{1 - p/0.345} + 1.341$	R^2 = 0.75 MAPE = 27.08% RMSE = 5.73 mgL^{-1}	(Maciel et al., 2019)
Tapajós River	Landsat-5/TM LISS-III	TSS	~0 – 120 mgL^{-1}	E	$p_{surf(Red)} = 2.64 * (TSS - 2.27)^{0.45}$	R^2 = 0.94 RMSE = 1.39 mgL^{-1}	(Lobo et al., 2015)
Solimões River	MODIS	TSS	50-700 mgL^{-1}	E	$TSS = 759.12 * \left(\frac{p_{nir}}{p_{red}}\right)^{1.92}$	r = 0.89 RMSE = 70.23 mgL^{-1}	(Villar et al., 2018)
Orinoco River	Landsat-8	TSS	~25-210 mgL^{-1}	E	$TSS = 1.35512 * p_{nir} * 1000 - 2.9385$	R^2 = 0.94 MAPE = 19.8% RMSE = 12.8 mgL^{-1}	(Yepez et al., 2018)
Madeira River	MODIS	TSS	25-622 mgL^{-1}	E	$TSS = 1020 * \left(\frac{p_{nir}}{p_{red}}\right)^{2.94}$	r = 0.79	(Villar et al., 2013)
Amazon River	MODIS	TSS	7-130 mgL^{-1}	E	TSS Fraction from spectral unmixing model	RE = 10 mgL^{-1} (estimated)	(Kilham & Roberts, 2011)
Amazon White water rivers	Landsat-5	TSS	0-3561 mgL^{-1}	E	Multiple regression	R^2 = 0.76	(Montanher et al., 2014)
Madeira River	TriOS Ramses (In situ)	TSS	0-450 mgL^{-1}	SAA	Relationship between *backscattering coefficient* at 550nm and TSS	R^2 = 0.7345	(Bernini et al., 2019)
Amazon white water rivers	TriOS Ramses (In situ)	TSS	5-620 mgL^{-1}	E	$TSS = 20.41 * (p_{860})^{1.173}$	R^2 = 0.89	(J. Martinez et al., 2015)
Amazon rivers and lakes	MODIS Terra and Aqua	TSS	0-600 mgL^{-1}	E	$TSS = exp^{20 * p_{red} + 7.68 * p_{nir} + 0.31 * \frac{p_{red}}{p_{nir}}}$	R^2 = 0.7 RMSE = 75.6 mgL^{-1}	(Fassoni-Andrade & Paiva, 2019)

One of the main challenges regarding water color RS is identifying and separating each constituent contribution from the water column emerging signal. The high sediment concentrations, which can mask the contributions of Chl-a and CDOM, makes this challenge especially significant in Amazonian waters. The semi-analytical approach, which has performed well in other complex waters (Gholizadeh et al., 2016; Werdell et al., 2018; Zheng & DiGiacomo, 2017), is an alternative to overcome this challenge. However, it depends on sensors with spectral, radiometric, and spatial characteristics suitable for inland waters for calibrating high-performance algorithms. Initial applications of this approach in Amazonian waters, using Landsat-8/OLI,

Sentinel-2/MSI, and Sentinel-3/OLCI data, have shown promising results (Bernini et al., 2019; L. A. S. de Carvalho et al., 2015; Jorge et al., 2017; Maciel, Barbosa, et al., 2020). Furthermore, hyperspectral sensors missions such as NASA's Plankton, Aerosol, Cloud, ocean Ecosystem (PACE; Werdell et al., 2019) and recently launched ones such as PRISMA (Giardino et al., 2020; Niroumand-Jadidi et al., 2020) may help to overcome this challenge. Due to the extensive temporal variability in the constituent concentration, a promising approach is to integrate hybrid and semi-analytical algorithms to obtain adequate accuracy in a wide range of OACs concentration. To cope with the frequent cloud coverage and obtain data compatible with aquatic dynamics, the concomitant use of inter-calibrated sensors data (Landsat-8/OLI, Sentinel-2/MSI, Sentinel-3/OLCI, CBERS-4A/MUX), called the virtual constellation, can be a solution. In this sense, two ongoing initiatives are the Brazil Data Cube project (http://brazildatacube.dpi.inpe.br/portal/explore) and the Harmonized Landsat Sentinel (Claverie et al., 2018), which propose to provide intercalibrated data from different sensors. Moreover, to investigate dynamic processes in aquatic ecosystems, high spatiotemporal resolution nanosatellites represent a promising tool for understanding the short-term responses of floodplain lakes' biota to hydrological changes (Maciel, Novo, et al., 2020; Nagel et al., 2020).

All the improvements in RS technologies in the last decades have supported more accurate algorithms for suspended sediment retrieval in the AB. However, as demonstrated in **Table 5**, Chl-a and CDOM estimates are still a challenge in those optically complex waters. The accurate retrieval of Chl-a and CDOM is dependent on precise RS data, which demands the inversion of those OACs. In this sense, new sensors with high radiometric and spectral resolution are imperative. Finally, more robust techniques, such as semi-analytical algorithms, machine learning approaches, and cloud computing platforms (e.g., Google Earth Engine), can improve water quality RS studies in the AB.

5. Total water storage and groundwater storage

Water mass redistribution is a key parameter needed to understand the climate system and its temporal variations at monthly to multi-decadal time-scales. Over land, it corresponds to the continuous exchange of water masses between surface (i.e., rivers, lakes, wetlands, snow cover, and mountain glaciers) and sub-surface (soil moisture and groundwater) storages, and with the atmosphere and the ocean through rainfall, evapotranspiration, and runoff. Total water storage is the sum of the water contained in the different hydrological reservoirs. The importance of surface water in the AB was presented in Section 4. Groundwater storage also plays a major role in the hydrology of the AB and exerts a large influence on climate variability and rainforest ecosystems (Pokhrel et al., 2013). Strong memory effects of the Amazon groundwater system propagate climate anomalies over the region for several years (Frappart et al., 2019; Miguez-Macho & Fan, 2012; Pfeffer et al., 2014).

The GRACE mission, in operation from March 2002 to June 2017, and the GRACE Follow-On mission (GRACE FO), in orbit since May 2018, enable the monitoring of the spatio-temporal changes of Terrestrial Water Storage (TWS) (Tapley et al., 2004). Its temporal anomaly is derived from GRACE observations which measure the very small variations in the Earth's gravity field (Tapley et al., 2004). GRACE-derived TWS Anomaly (TWSA) observations, in spite of their coarse spatial resolution of ~200-300 km, have been widely used to analyze the

impact of climate variability and global changes on the water masses redistribution over land (Tapley et al., 2019), and groundwater storages in combination with external observations (Frappart & Ramillien, 2018).

Over the whole AB, GRACE-derived TWS annual amplitude was found to range from 300 to 450 mm (**Figure 9**; J. L. Chen et al., 2009; Crowley et al., 2008; Frappart, Seoane, et al., 2013; Xavier et al., 2010). This range corresponds to twice the annual amplitude of surface water storage of the whole basin (Frappart et al., 2012; Ndehedehe & Ferreira, 2020), meaning that the annual amplitude of the subsurface storage variations (soil moisture and groundwater) also represents half of the TWS annual amplitude. Large variations of this value were observed among the major Amazon sub-basins depending on the extent of floodplains (Frappart et al., 2011, 2019; Papa et al., 2013). Rainfall and GRACE-based TWSA were found to be highly correlated in the AB and its major sub-basins (over 2003-2010), even at interannual time-scales with Pearson's correlation coefficients generally higher than 0.7 (except in the basins located in the Andes) with a time-lag varying from 0 to 3 months (Frappart, Ramillien, et al., 2013; Ndehedehe & Ferreira, 2020). Similar results were obtained between TWSA and river discharges over the same time spans (Frappart, Ramillien, et al., 2013). Good agreement was also observed between TWS and satellite-derived surface water extent (from GIEMS), rainfall, and discharge over various time-span (Papa et al., 2008; Prigent et al., 2007, 2012; Tourian et al., 2018). These studies revealed the complexity of water transport among the different sub-basins of the Amazon with the presence of hysteresis in the relationship between surface water extent and TWSA.

The analysis of the spatio-temporal patterns of TWS changes provided new information on the impact of the extreme climate events (exceptional droughts and floods which occurred in 2005, 2010, 2012-2015, and 2009, 2012, respectively) on land water storage in the whole AB or in its major sub-basins (J. L. Chen et al., 2009, 2010; Espinoza et al., 2013; V. G. Ferreira et al., 2018; Frappart, Ramillien, et al., 2013). Examples of maps of difference in TWSA between a given month and its climatological mean are presented in **Figure 9**a-b for May 2009, and October 2010, respectively. These months were chosen as they correspond to the extremum of these climate events (droughts of 2005, 2010, and 2015, flood of 2009). This information has revealed to be complementary to what can be obtained using spatialized rainfall and in situ water levels and discharges. For instance, the patterns of minimum TWSA during the droughts of 2005 and 2010 were found to be in good coincidence across the basin with the areas with large fire activity (Aragão et al., 2008; Zeng et al., 2008) and of considerable tree mortality (Phillips et al., 2009) as reported in Frappart, Ramillien, et al. (2013). TWSA also helped, jointly with hydrological modeling, to characterize the recent extreme droughts which occurred in the Amazon, highlighting the importance of the interactions between subsurface and surface water storages to mitigate the deficit in surface reservoirs (Chaudhari et al., 2019).

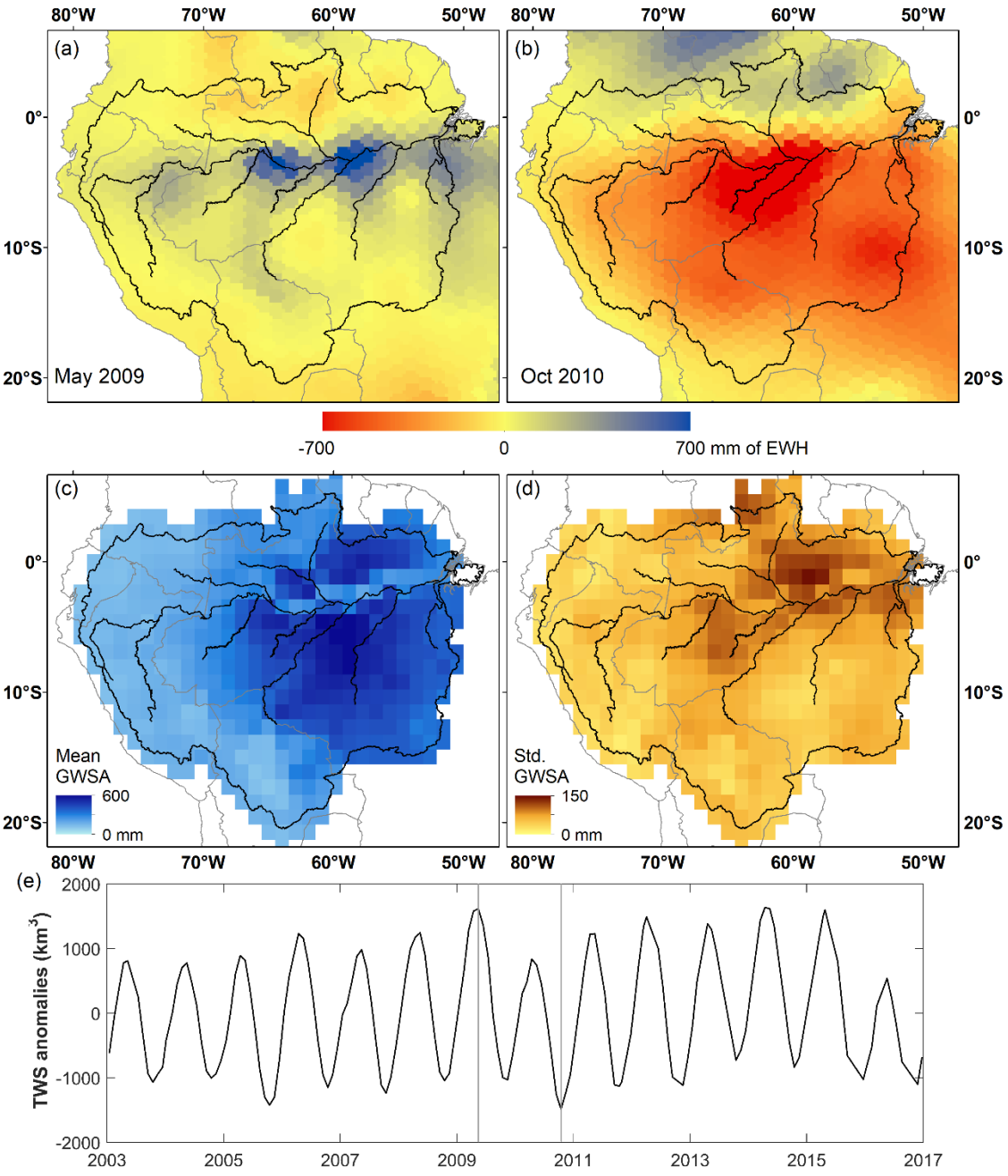

Figure 9. Maps of TWSA during two extreme events (a) the flood in May 2009, and (b) the drought in October 2010. Mean annual changes in groundwater storage anomaly - GWSA (c) and associated standard deviation (d) over 2003–2010 (adapted from Frappart et al., 2019). (e) Time series of GRACE-based TWSA (km^3) over the AB between 2003-2016. The vertical lines show the months of maximum (May 2009) and minimum (October 2010) values.

A direct approach to estimate GW storage anomalies is to remove the contribution of the different hydrological compartments from GRACE-based TWSA as follows:

$$\Delta GW = \Delta TWS - \Delta SW - \Delta SM - \Delta CW - \Delta SWE \quad (2)$$

where Δ represents the anomaly of water storage in the different hydrological compartments, SW is the surface water storage, SM is the soil moisture or water contained in the root zone, CW is the water contained in the canopy, and SWE is the snow water equivalent. This latter term was neglected in the studies performed in the AB as no reliable information on this water storage was available. In most of the cases, water from the other compartments (SW and SM) are provided by model outputs and/or in situ measurements. For the Amazon, it is necessary to accurately take into account the SW component as it represents around half of the TWSA (Frappart et al., 2012, 2019). Using external information from hydrological models for SW, SM, and CW, groundwater storage anomalies were estimated over 2003-2015, revealing a strong link between geological properties and GW storage: the largest groundwater storage capacity in Brazil was found in regions with the highest permeability of the rock layers (e.g., the Guarani and Alter do Chão aquifers; Hu et al., 2017). But in these cases, SW storage was limited to river storage, neglecting the storage in the extensive floodplains of the AB. In order to adequately take into account the contribution of SW components, methodologies were developed to estimate SW storage variations from RS observations (Frappart et al., 2008, 2012; Ndehedehe & Ferreira, 2020). SW storage anomalies were obtained by combining surface water extent (generally from GIEMS, see Section 4.2) and altimetry-based time series of water levels (see Section 4.1) over rivers and floodplains. Frappart et al. (2012) estimated the monthly variations of SW storage at the basin scale during the 2005 drought and found that the amount of water stored in the river and floodplains of AB during this extreme event was 130 km^3 (70%) below its 2003–2007 average, representing almost a half of the anomaly of minimum TWS as estimated by GRACE.

Using this newly external information on SW storage variations, along with SM storage estimates from hydrological models, GW storage anomalies were first estimated over 2003-2004 in the Negro River Basin, one of the largest tributaries to the AB (Frappart et al., 2011). The spatial pattern of the annual amplitude of GW anomalies agrees well with the regional hydrogeological maps and the amplitude are consistent with observations of water level at local wells and altimetry-based time series of water levels in two adjacent wetlands where the groundwater table reaches the surface during the whole hydrological cycle (Frappart et al., 2011).

This approach was then extended to the whole AB over 2003-2010, using about 1000 ENVISAT RA-2 altimetry VSs of surface water elevation (Frappart et al., 2019). SW storage over the entire basin had an annual amplitude ranging between 900 and 1300 km^3 (Frappart et al., 2012). GW estimates had good agreement with scarce in situ groundwater observations and low-water maps of GW table (Frappart et al., 2008). At basin-scale, the results have realistic spatial patterns when compared to hydrogeological maps of Brazil (e.g., porosity maps, aquifer boundaries, GW recharge). The seasonal amplitude of GW was estimated to contribute between 20 to 35% of the GRACE-derived TWS amplitude in the AB (Frappart et al., 2019). The impact of the 2005 extreme drought on GW storage was also observed and lasted several years (Frappart et al., 2019).

Radar altimetry was used to estimate low-water maps of GW table in the central part of the AB (Frappart et al., 2008). Owing to the connection between surface and groundwater during the low water period in the alluvial plains of the central Amazon (54°-70° W, 0°-5°S), annual lower water levels of 593 altimetry VSs were interpolated to generate yearly maps of groundwater base level (GWBL) between 2003 and 2009. The results show that GWBL is governed by the surface topography and that several years were needed for GWBL to recover from the extreme drought of 2005 (Pfeffer et al., 2014).

The recent launch of the GRACE Follow-On (GRACE-FO) offers an opportunity to extend the monitoring of TWS and GWS changes after 2018. Despite a lack of data between October 2017 (end of GRACE operation) and May 2018 (launch of GRACE-FO), two decades of TWSA will be soon available, allowing analysis of the impact of multi-year climatic events such as ENSO on land and ground water storages. The major drawbacks of these data are their low spatial (~200 km) and temporal (1 month) temporal resolutions which are not sufficient to study the dynamics of fast hydrological events. To overcome these drawbacks, the GRACE-FO payload contains advanced versions of the sensors present on-board GRACE and a novel laser ranging interferometer (LRI), measuring the satellite-to-satellite distance in parallel with the K-band radar instrument. The LRI is expected to be 26-times more accurate than the K-band radar instrumenton on-board GRACE (Tapley et al., 2019). This better expected accuracy is likely to improve the quality and the spatial resolution of the retrieved TWSA. New approaches based on the use of Kalman filter were developed to increase the TWSA temporal resolution to quasi-daily without degrading the spatial resolution (Ramillien et al., 2015, 2020).

6. Integrative and interdisciplinary studies

RS data have provided breakthrough advances in understanding of the AB's hydrology and associated aquatic environments. In Sections 2 to 5 we have presented and discussed scientific advances for individual components. In this Section we introduce research agendas that have benefited from the integration of observations from multiple components of the Amazon water cycle. These include the computation of the water budget (6.1), application of hydrological models (6.2), understanding of aquatic ecosystems (6.3) and past and ongoing environmental changes over the AB (6.4).

6.1. Water budget

In order to better understand the complex hydrological processes in the AB, it is necessary to monitor each component of the water cycle, and to understand how these components link and interact. Thus, studying the AB water budget (WB) requires use of a large variety of observations, especially because the AB includes complex local environments (e.g., floodplains) and processes (e.g., soil moisture and canopy transpiration) which are difficult to characterize by satellite observations.

Among the WB literature, the AB has been one major region among global analyses of the water cycle (Munier & Aires, 2018; Pan et al., 2012; Sahoo et al., 2011; Y. Zhang et al., 2018) or the main focus of the analysis (Azarderakhsh et al., 2011; Builes-Jaramillo & Poveda, 2018; Moreira et al., 2019; P. T. S. Oliveira et al., 2014). Most WB studies used only one

satellite product for each water component (Azarderakhsh et al., 2011; Builes-Jaramillo & Poveda, 2018; Maeda et al., 2015; Moreira et al., 2019; P. T. S. Oliveira et al., 2014; Rodell et al., 2011). Use of a multiplicity of the satellite products for each water component can reduce uncertainties, through an approach that is based on observations only (Filipe Aires, 2014) or integrating model simulations and re-analyses (Pan et al., 2012; Y. Zhang et al., 2018).

Continuous quality improvement and increased use of satellite products, associated with more sophisticated integration techniques, have allowed better characterization the water cycle. WB analyses have been used to i) directly estimate a missing water component such as ET (Maeda et al., 2017; Rodell et al., 2011), R (Azarderakhsh et al., 2011; P. T. S. Oliveira et al., 2014), and terrestrial water storage change dS (Moreira et al., 2019); ii) diagnose the hydrological coherence of a combination of RS-based estimates and investigating discrepancies (Builes-Jaramillo & Poveda, 2018; Moreira et al., 2019; P. T. S. Oliveira et al., 2014); and iii) to optimize RS-based estimates to obtain a hydrologically coherent water cycle (Munier & Aires, 2018; Pan et al., 2012; Pan & Wood, 2006; Pellet et al., 2021; Sahoo et al., 2011). The three main uses of WB closure are detailed in the following paragraphs.

When estimating missing water components, the objective can be to investigate seasonal patterns (Azarderakhsh et al., 2011; Moreira et al., 2019) and more complex features such as trends and impacts due to land use and land cover changes (P. T. S. Oliveira et al., 2014). The studies provide uncertainties for their estimates based on the relative uncertainties of the other components (Rodell et al., 2011). When focusing on ET, the literature stresses that ET is controlled by both P and radiation without being limited by one of these two (Maeda et al., 2017); but the seasonality remains unclear due to large uncertainty in P. Nevertheless, the indirect estimation of ET has been used by Rodell et al. (2011) to evaluate model ET outputs over the Tocantins basin and the authors concluded that much effort are still required on the ET modeling.

Diagnosing WB coherency by combining RS products is a useful tool to assess the quality of the RS products. For instance, Moreira et al. (2019) demonstrated that the MSWEP and GLEAM datasets reduce the WB imbalance. P. T. S. Oliveira et al. (2014) showed that recent versions of the TMPA also improve WB closure compared to older versions. Builes-Jaramillo & Poveda (2018) have jointly evaluated the surface and atmospheric water balances over the Amazon, and their diagnostic of the discrepancy between various ET estimate showed that RS-based ET products balance better the WB than the model and reanalysis outputs. As reported in Builes-Jaramillo & Poveda (2018) and Moreira et al. (2019), the WB imbalance relates at sub-basin to the drainage area and the climatic conditions (i.e. tropical or mountainous) which impact the signal-to-noise ratio of each water component.

Several studies have used the WB closure as a constraint for the optimization of satellite estimates, jointly for each water component. Pan & Wood (2006) developed an optimization of the satellite products using an assimilation scheme within a land surface model at the basin scale. This method has then been applied to the AB (Pan et al., 2012; Sahoo et al., 2011). Zhang et al. (2018) extended this scheme to the pixel scale by considering only simulated R. Similarly, Aires (2014) described several approaches to integrate satellite observation (simple weighting, optimal interpolation, post-filtering and neural networks) with the WB closure constraint but without the use of surface or hydrological models to obtain an observational database. Munier & Aires (2018) investigated AB hydrology using this framework, and Pellet et al. (2021) added inter-

basins constraints on the budget closure using river discharges over several stations in the basin. This technical framework allows for the optimization of the satellite datasets and can be used to develop new tools in hydrology such as the assimilation of GRACE data (Y. Zhang et al., 2018). For instance, in Pellet et al. (2021), the spatial patterns of P, ET and dS were used to estimate the river discharge along the river network.

The estimation of the uncertainty of each water component is one of the main objectives of a WB analysis. Such characterizations are generally component- and site-specific. For instance, Moreira et al. (2019) extensively evaluated the satellite estimate uncertainty of P and ET using in situ data (i.e., 300 precipitation gauges and fourteen eddy-covariance monitoring sites), however this approach is limited due to the sparsity of the observation network. Sahoo et al. (2011) used the distance to non-satellite estimate while Y. Zhang et al. (2018) and Pellet et al. (2021) used the spread of the satellite as a proxy for uncertainty. Azarderakhsh et al. (2011) or Munier and Aires (2018) used a literature review based on RS expertise to quantify the uncertainties of the satellite products. Studies generally assume a value of 5% to 10% of error for R while dS errors from GRACE are often computed following the specifications for leakage and measurement covariance errors (Rodell et al., 2004). All the studies agree in the relatively high contribution of the P estimate in the total WB imbalance (~40%). Moreira et al. (2019) and P. T. S. Oliveira et al. (2014) found a positive bias in P when comparing them to in situ data, but all the integration approaches (Pan et al., 2012; Pellet et al., 2021; Sahoo et al., 2011) result in an increased P estimate. Furthermore, Moreira et al. (2019) considered that dS is the second contributor to the WB imbalance (~25%) while Sahoo et al. (2011) and Pellet et al. (2021) found a higher contribution from ET (~30%). All the optimization strategies have shown that the WB can be balanced within the range of the RS-based uncertainties.

Figure 10a represents the climatology of the four water components in three basins and using several datasets for each water component. The three basins are: northern Negro catchment upstream of the Serrinha station, the central basin upstream of the Manacapuru station (including the drainage area upstream of the Tabatinga station) and the southern basin upstream of the Fazenda (Fz) Vista Alegre station (including the drainage area upstream of Porto-Velho station). The climatological season (i.e., annual cycle) of all the water components are represented in mm/month. All satellite products have bias and uncertainties, but this multi-component analysis can isolate the spatial patterns over the AB. For instance, the annual cycles of the WB differ on the northern and southern basins. As reported in the literature (Espinoza, Sörensson, et al., 2019; Marengo, 2005), over southern basin, P is driven by the monsoon with a peak in January and has larger seasonal variations (e.g. min-max range) and lower annual average than on the northern basin, where P peaks in May. The P seasonality drives R over all basins (north and south) with a time-lag of one-two months. Over the central-western basin, R can be higher than P for a particular month and P-R peak is about 4 months related to the runoff and river discharge travel times inside the basin (Sorribas et al., 2020). dS is in phase with P in the southern basin, but shows a particular season over the Negro and Branco river basins: dS is equal to zero during the dry season and a linear transition exists between maximum and minimum. Over these basins, dS become negative while R was increasing, and reached its maximum 2 months later. This illustrates the effect of water storage in floodplain before releasing it into the river. ET seasonal variation is weaker but ET peak seems to be in phase with P over southern basin arguing for a water-limited behavior while ET peak follows the P minimum month in northern basin of an

energy-limited system (Maeda et al., 2017). In Pellet et al. (2021), the correction of ET based on the closure of the water cycle enhances the water limitation regime over the central AB and the energy limitation over the northern AB. In the south, during dry months (JJA), ET is higher than P, and water that evaporates is provided by the soil storage which continues to lose water until November. For this season, the role of ET on the water cycle is relatively more important in the dry season than in the rainy season (Marengo, 2005).

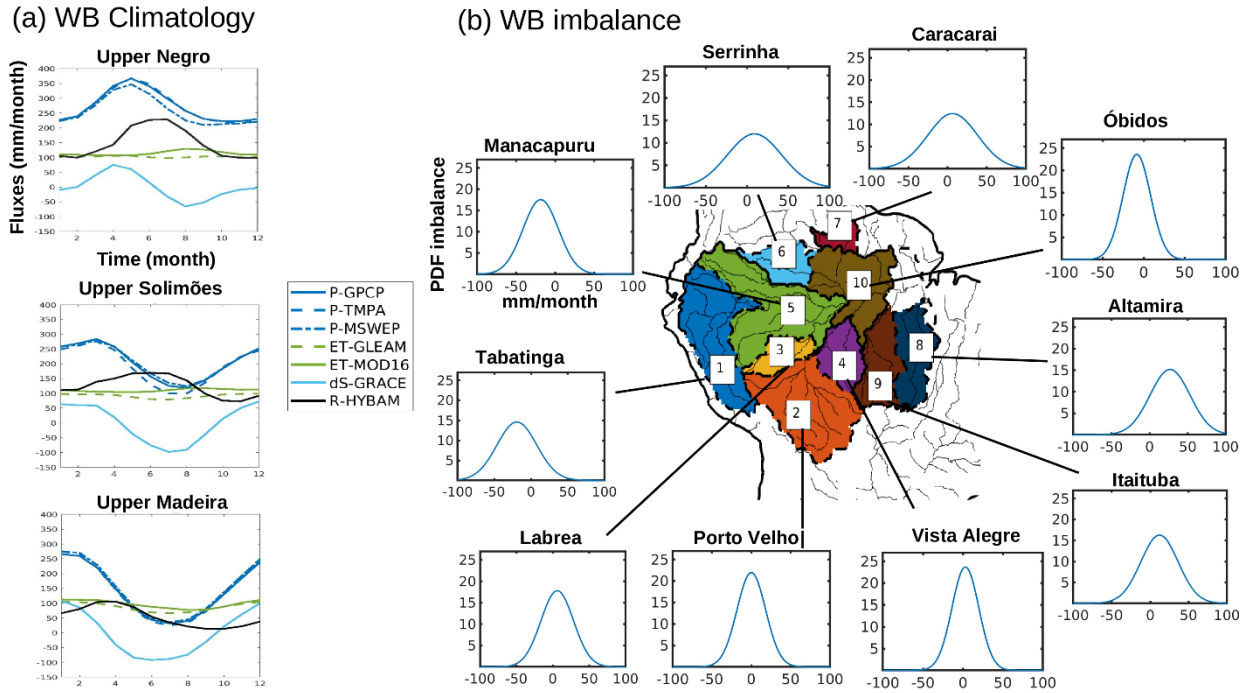

Figure 10. a) seasonal climatology of all the water component: precipitation (P), evapotranspiration (ET), water storage change (dS) and discharge measured at in situ gauges (R) described by one or multiple datasets. b) Probability Density Function (PDF) of the resulting WB imbalances are shown at sub-basin scale (right). PDF provides the bias and variance of the imbalance.

To investigate the overall WB imbalance related to the bias and uncertainty of the all the water components, **Figure 10**b shows the Probability Density Function (PDF) of these imbalances at sub-basins scale. Spatially, there is a gradient in the mean of the PDF between the western and southern sub-basins. Western sub-basins have a lack of water (negative bias in the PDF), while southern sub-basins have an excess of water (positive bias). This gradient was reported by Builes-Jaramillo & Poveda (2018). Furthermore, the variance of the WB imbalance increases from south to north with the annual mean of P suggesting that a large part of imbalance is due to P (Moreira et al., 2019; Pellet et al., 2021). The optimization strategy based on the closure of the WB leads to a bigger correction of the water component over western and central sub-basins (Pellet et al., 2021).

The remaining precipitation uncertainties of the globally calibrated satellite products are mainly due to the increase of the precipitation measurement errors by satellite products during the rainy season, and the lack of in situ gauges used in calibration (Moreira et al., 2019). The AB hydrology could benefit from the use of a dedicated network of precipitation gauges such as HYBAM Observatory Precipitation (J. C. Espinoza Villar, Ronchail, et al., 2009; Guimberteau et al., 2012) to obtain a regionally-calibrated satellite product for precipitation. Its gauges density over the AB is higher than the global gridded rainfall dataset generally used to calibrate satellite products (Guimberteau et al., 2012).

Estimating ET in the AB remains a challenge (see Section 3). In **Figure 10**, the use of different ET datasets can lead to a difference of 30-50 mm/month which represent up to 50% of the ET value. Following Moreira et al. (2019), the establishment of generic methods for estimating uncertainties is of importance for improving our understanding of the terrestrial water cycle. As for P, one source of the improvement will be the extensive use and increase of an eddy covariance network to better understand the uncertainties in ET models.

One technical improvement in the WB based optimization approach might come with the spatial resolution of the analysis. WB analysis has been mostly done at the basin scale over the AB (Munier & Aires, 2018; Sahoo et al., 2011) even if several studies have been conducted in sub-basins defined by river discharge stations (Azarderakhsh et al., 2011; Pellet et al., 2021). Using topography information, it should be possible to consider the runoff over land and downscale the satellite products while closing the WB at a pixel level. The satellite datasets could even be downscaled temporally to obtain a better time resolution.

As discussed in Section 5, attempts have been made to decompose the TWS from GRACE into its surface (Frappart et al., 2012; Papa et al., 2013) and groundwater (Frappart et al., 2019) components. Such decomposition could also be attempted within a full terrestrial WB analysis, especially when reliable soil moisture satellite estimates over the AB will become available. As mentioned in Section 4, long-term surface water datasets would also be necessary (Filipe Aires et al., 2017; Parrens et al., 2019; Prigent et al., 2020).

The GRACE-FO mission launched in 2018, extension of the TRMM data record with the GPM mission, and the launch of the SWOT mission will provide a comprehensive set of new observations. The continuity of these satellite missions monitoring the water components is mandatory to improve our understanding of spatial hydrology patterns through more precise WB analyses, and assess potential long-term trends.

6.2. Modeling the Amazon water cycle and its wetlands

Hydrologic and hydraulic models represent the water cycle storages and fluxes through a set of mathematical equations. Such process-based models are suitable tools to understand Amazon hydrological processes such as river-floodplain water exchange and groundwater-surface water interactions (Miguez-Macho & Fan, 2012; Paiva, Buarque, et al., 2013) and past floods and droughts (Wongchuig et al., 2017), to estimate variables in ungauged regions (e.g., distributed river discharge for the last century; Wongchuig et al., 2019), and to perform scenarios of hydrological alteration due to deforestation, flow regulation by reservoirs, and climate change (M. E. Arias et al., 2020; Guimberteau et al., 2017; Júnior et al., 2015; Lima et al., 2014; Mohor

et al., 2015; Pokhrel et al., 2014; Pontes et al., 2019; Sorribas et al., 2016; Zed Zulkafli et al., 2016).

During the last decades, many models have been applied in the Amazon at different scales, from reach (i.e., more detailed studies addressing a few kilometers long river-floodplain area) to the whole basin scale. Because of the basin's remoteness and vast dimensions, RS datasets are usually adopted as either forcings (e.g., precipitation), a priori information to estimate parameter values (e.g., topographic data), validation, or calibration/assimilation data (e.g., discharge, river water levels). A major distinction can be made between (i) hydrological models that simulate vertical processes as evapotranspiration, soil water infiltration and runoff generation mechanisms, and (ii) hydraulic models of surface waters, which represent flow propagation along rivers and floodplains with physically-based equations, and allow the computation of variables such as surface water elevation and slope, river discharge, and surface water extent and storage (**Figure 11**). More recently, the so-called hydrologic- hydraulic models have been developed to couple the strengths of both approaches (Fleischmann et al., 2020; Hoch et al., 2016; Paiva, Buarque, et al., 2013), and there may be cases where simplified inundation schemes are represented within hydrologic models to estimate wetland flooding dynamics. **Table 6** summarizes the differences between the two approaches.

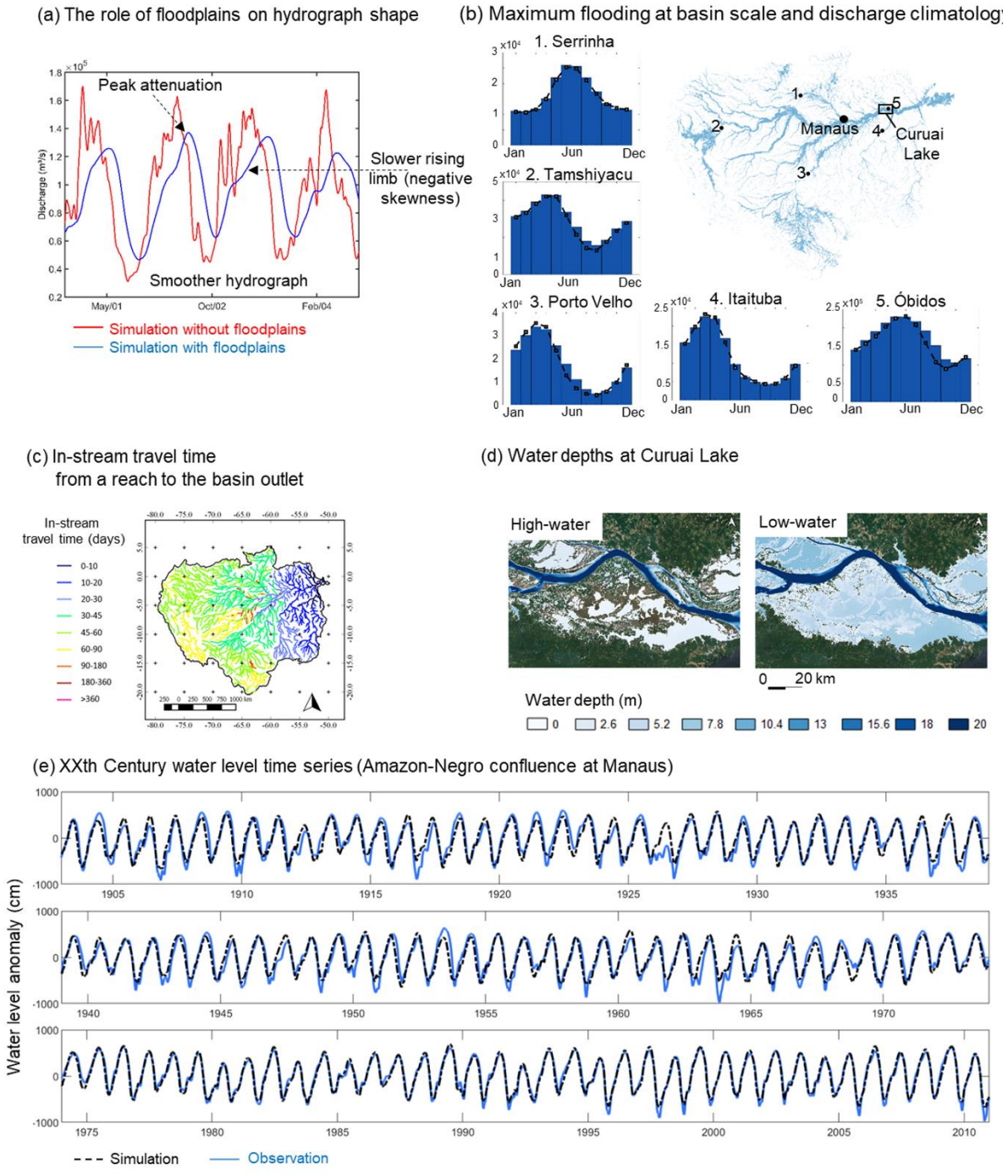

Figure 11. Recent applications of hydrologic and hydraulic models in the AB have added insights into the role of river floodplains on (a) hydrograph shape (Fleischmann et al., 2016) and (c) in-stream travel times (Sorribas et al., 2020), and provided the estimation of (b) long-term discharge climatology (Paiva, Buarque, et al., 2013), (c) long-term water level time series (example for the location of Manaus; Wongchuig et al., 2019), and (d) floodplain water depths (example for the Curuai Lake, 2014 high and low water seasons; Rudorff et al., 2014a).

Table 6. Summary of main differences between hydrologic and hydraulic models of surface waters, with examples of model applications in the AB. Some examples are provided in both categories since they refer to hydrologic-hydraulic models.

	Hydrological models	**Hydraulic models of surface waters**
Main simulated process	Vertical processes (e.g., evapotranspiration, soil water infiltration and runoff generation mechanisms) and groundwater dynamics	River-floodplain interaction (e.g., floodplain storage, backwater effects)
Main forcing (boundary conditions)	Precipitation	River discharge, river water level and precipitation
Main output variables	Water balance, evapotranspiration, soil water and groundwater storage, river discharges	Inundation maps, river-floodplain water depths, longitudinal water levels along rivers, river discharges
Typical scientific outcomes	Quantification of water balance components, water storage partition between surface and subsurface reservoirs, evapotranspiration dynamics, impacts of human alteration on water balance components (e.g., changes in precipitation partition into ET and runoff)	Floodplain water storage and residence time, water travel times across river-floodplain systems, rating curves (water level-discharge relationships) for operational use, impacts of human alteration on flood dynamics
Examples of studies	Beighley et al., 2009; Coe et al., 2002; M. H. Costa & Foley, 1997; Cuartas et al., 2012; Miguez-Macho & Fan, 2012; Paiva, Buarque, et al., 2013; Vörösmarty et al., 1989	Fleischmann et al., 2020; Garambois et al., 2017; Getirana et al., 2012; Miguez-Macho & Fan, 2012; Paiva, Buarque, et al., 2013; Paris et al., 2016; Pinel et al., 2019; Rudorff et al., 2014a; Sorribas et al., 2020; Trigg et al., 2009; Wilson et al., 2007; Yamazaki, Lee, et al., 2012

The first generation of models in the Amazon involved the development of large scale hydrological models, starting with the studies by Vörösmarty et al. (1989), Costa and Foley (1997) and Coe et al. (2002). With the advent of RS datasets and higher computational capacity, several models have been developed, improving the physical representation of hydrological processes, increasing the model spatial resolution and moving from monthly to daily estimates (Beighley et al., 2009; Coe et al., 2008; Luo et al., 2017; Miguez-Macho & Fan, 2012; Paiva, Buarque, et al., 2013). These models usually adopt the following RS-based input data: precipitation with the TMPA product (Collischonn et al., 2008; Getirana et al., 2012; Zubieta et al., 2015), and more recently GPM-IMERG (Zubieta et al., 2017) and MSWEP (Beck, Van Dijk, et al., 2017); landscape properties including terrain lengths and slopes, based on DEMs (most studies using SRTM DEM); and land use and vegetation maps (global maps as FAO, or regional ones as the Brazilian RadamBrasil soil maps). The most common validation datasets from RS are

water level from satellite altimetry (Section 4.1), surface water extent (Section 4.2), and total water storage (Section 5).

These model applications deepened our comprehension of the water partition between soil, surface water and groundwater, and acted as laboratories to improve global hydrological models, which in turn are fundamental elements of Earth System models. The assessment of land surface and global hydrological models in the Amazon has been a standard procedure in geoscientific model development and in model intercomparison projects (Alkama et al., 2010; Bertrand Decharme et al., 2008; Getirana et al., 2012, 2014; Getirana, Peters-Lidard, et al., 2017; Guimberteau et al., 2014, 2017; Pilotto et al., 2015; Towner et al., 2019; Yamazaki, Baugh, et al., 2012; Yamazaki et al., 2011; Z. Zulkafli et al., 2013). At the basin scale, the fraction of the total water storage corresponding to surface waters was estimated as 56%, 41% and 27% by Paiva, Buarque, et al. (2013), Getirana et al. (2017) and Pokhrel et al. (2013), respectively. These values have been compared to RS-based estimates (Frappart et al., 2012, 2019; Papa et al., 2013). Furthermore, basin-scale average ET estimated as 2.39 to 3.26 mm/day by an ensemble of land surface models (Getirana et al., 2014), and as 2.72 mm/day by Paiva, Buarque, et al. (2013), were slightly lower than values by basin-scale RS (Paca et al., 2019) and an in situ eddy-covariance network (M. H. Costa et al., 2010), which estimated values of 3.11 to 3.58 mm/day across a gradient from southern dry to equatorial wet Amazon forests. The role of soil water storage to sustain dry season ET in the Amazon was shown by modeling experiments at local (Fang et al., 2017) and basin scale (Getirana et al., 2014). Some studies addressed the role of groundwater and soil storage on the water balance, and the importance of its representation into hydrological models. Applications at headwater basins showed the predominance of groundwater on headwater water storage (Cuartas et al., 2012; Niu et al., 2017), in agreement with in situ monitoring studies (Hodnett et al., 1997). Miguez-Macho & Fan (2012) suggested the same pattern at the whole basin scale. Their model also indicated an important two-way feedback between floodwater and groundwater, and the existence of large areas not subject to surface flooding across the basin, but where a high water table level would be responsible for keeping high soil water content year-round. The simulation of multiple soil layers in the ORCHIDEE land surface model, in contrast to a simple 2-layer "bucket" model, was also shown to improve the representation of the soil water dynamics and the total water storage in the Amazon, especially for the drier regions in the southern sub-basins (Guimberteau et al., 2014).

Among hydraulic models of surface waters, a pioneer study by Wilson et al. (2007) is one of the first hydraulic modeling experiments performed over large domains. The authors applied the LISFLOOD-FP model to a 260 km reach of the Solimões River, and estimated the river-floodplain water exchange as at least 40% of the river volume in that reach. For a relatively different reach in the Central Amazon (from São Paulo de Olivença to Óbidos), Richey et al. (1989) estimated this ratio as 30% based on a simpler routing method, while Sorribas et al. (2020) estimated a value of 40% for the AB system, based on large scale hydraulic modeling (see below). The authors also found the model accuracy to be higher for the high water period, as has been also reported by recent studies (Pinel et al., 2019; Rudorff et al., 2014a), likely due to misrepresentation of the terrain heterogeneities and small disconnected lakes during the dry season. Furthermore, since the river-floodplain water exchange often occurs through floodplain channels and breached levees that hinder its conceptualization as a simple overbanking flow (Trigg et al., 2012), hydraulic models have the challenge to estimate effective channel parameters that represent these complex processes (Fleischmann et al., 2018; Trigg et al., 2009).

Other applications at reach or floodplain lake scale were developed by Bonnet et al. (2008, 2017), Ji et al. (2019), Trigg et al. (2009) and Wilson et al. (2007), and addressed the relative role of local runoff and river inflow as the main water input, ranging from local runoff-dominated systems in the Lago Calado (Ji et al., 2019; Lesack & Melack, 1995) to river-dominated ones in the Curuai (**Figure 11**d) and Janauacá systems (Bonnet et al., 2008, 2017; Pinel et al., 2019; Rudorff et al., 2014b, 2014a), through either channelized or diffuse flow patterns. In the case of Curuai and Janauacá, the Amazon or Solimões river was responsible for 82% and 93% of the floodplain annual influxes, respectively (Bonnet et al., 2017; Rudorff et al., 2014b).

The first basin-scale inundation model was introduced by Coe et al. (2002), and numerous hydrologic models were developed and coupled to inundation schemes afterwards (Coe et al., 2008; Getirana et al., 2012; Getirana, Peters-Lidard, et al., 2017; Hoch et al., 2016; Luo et al., 2017; Miguez-Macho & Fan, 2012; Paiva, Buarque, et al., 2013; Yamazaki et al., 2011; Yamazaki, Lee, et al., 2012). The models featured varying degrees of physics representation, with the simulation of floodplains moving from simple storage components to dynamic hydraulic schemes, which can represent relevant processes such as backwater effects. For hydraulic models, additional RS-based information required as input data includes river channel geometry as width, and floodplain topography from DEMs (mainly SRTM and its derivatives with vegetation removal to represent the bare terrain; see Baugh et al. (2013), O'Loughlin et al. (2016), Yamazaki et al. (2019) and Fassoni-Andrade, Paiva, Rudorff, et al. (2020). For local scale hydraulic models, additional parameterization usually involves the definition of floodplain roughness based on land cover maps (Pinel et al., 2019; Rudorff et al., 2014a). RS validation datasets are typically surface water elevation and surface water extent (Hall et al., 2011; Schumann et al., 2009).

These hydraulic model applications revealed the combination of backwater effects and floodplain storage to drive the flood wave behavior along Amazon rivers (Paiva, Buarque, et al., 2013), causing strong attenuation and delay up to 2.5 months. Floodplain storage is also responsible for the general negative hydrograph skewness in the main Amazon rivers, with a slower rising and a faster falling limb (Fleischmann et al., 2016; **Figure 11**a). Sorribas et al. (2020) used particle tracking methods to estimate surface water travel times along the AB as 45 days (median), with 20% of Amazon river waters flowing through floodplains (**Figure 11**c). While basin-scale applications have employed 1D models (longitudinal direction along rivers), the necessity of representing the 2D diffuse flow in floodplains, especially during receding waters, was highlighted by Alsdorf et al. (2005), who combined interferometry data with a simple continuity-based model to show that floodplain storage changes decrease with distance from the main channel. Generally, the water level in the river-floodplain system is not horizontal, and the river-floodplain is not homogeneously mixed (Alsdorf et al., 2007), as assumed by several 1D models. While a proper characterization of the complex river-floodplain interactions with hydraulic models has been done at local scales (Pinel et al., 2019; Rudorff et al., 2014a), it is still to be developed for the regional scale – for instance, to be able to infer hyperresolution (e.g., 30 m spatial resolution) flooding patterns for the whole central Amazon at weekly to monthly resolution. Finally, the full coupling between hydrologic and hydraulic models has been suggested to improve the representation of the floodplain-upland interactions, for instance through a more proper representation of open water evaporation in flooded areas (Getirana, Kumar, et al., 2017). However, recent studies have suggested that this process has relatively low

impact on the total ET estimates because of the general energy-limited (and not water-limited) ET in the Amazon (Fleischmann et al., 2020; Paiva, Buarque, et al., 2013). A different conclusion is expected for semi-arid wetlands (Fleischmann et al., 2018).

Regional scale validation of inundation models has been done with surface water extent (Getirana et al., 2012; Luo et al., 2017; Paiva, Collischonn, et al., 2013; Wilson et al., 2007; Yamazaki et al., 2011) based on the products by Hess et al. (2003), GIEMS from Prigent et al. (2007), and more recently with the SWAF database (Parrens et al., 2017) (see Section 4.2 for a description of these products). Although the flooding seasonal cycle is usually well captured by most models, estimates usually diverge in terms of magnitude (Fleischmann et al., 2020), and the fusion between different techniques is likely the optimal solution. However, more detailed validation experiments, for instance with maps based on SAR data, are needed, although many SAR data classifications were already developed for individual Amazon wetlands (Section 4.2). A recent application used ALOS/PALSAR imagery for a local scale model validation in the Janauacá floodplain system (Pinel et al., 2019).

Regarding surface water elevation, hydraulic models are typically capable of representing anomalies, but estimates of absolute values tend to be less accurate (Fleischmann et al., 2019). The hundreds of virtual stations available (see Section 4.1) have provided breakthrough improvements of modelling systems, especially in terms of distributed model validation with dozens of virtual stations (Fleischmann et al., 2020; Getirana, Peters-Lidard, et al., 2017; Paiva, Buarque, et al., 2013) and recent model calibration and assimilation (Brêda et al., 2019; A. M. Oliveira et al., 2021). Validation exercises yielded Nash-Sutcliffe coefficients higher than 0.6 for 60% of the 212 ENVISAT virtual stations assessed by Paiva, Buarque, et al. (2013), and amplitude errors lower than 0.8 m and absolute bias lower than 2.3 m for most of the stations analyzed by Yamazaki, Lee, et al. (2012). The combination of satellite altimetry with a hydraulic model for an ungauged reach of the Xingu River led Garambois et al. (2017) to propose the concept of hydraulic visibility through RS datasets, i.e., the capability of current and future satellite altimetry data to properly estimate river hydraulic variables. Altimetry data were shown to be relevant for the understanding of the hydraulic functioning of ungauged braided reaches in Amazonian rivers, especially along stretches with heterogeneous bed morphology and strong downstream control, which have major effects on surface water elevation and slope (Birkett et al., 2002).

The main output variables that have been addressed by hydrologic-hydraulic models are ET, soil water storage, river discharge, surface water elevation, and surface water extent. However, other variables are also important for an effective understanding of the water cycle, and need to be better constrained within modeling systems. For instance, only a few studies have addressed simulated water velocity (C. M. Dias et al., 2011; Fassoni-Andrade, 2020; Pinel et al., 2019) and flood storage (Fleischmann et al., 2020; Getirana, Kumar, et al., 2017; Paiva, Buarque, et al., 2013) in the Amazon wetlands, which are fundamental variables to understand flood dynamics, even though the latter (flood storage) was already estimated by different RS methods (see Section 5).

As there are still uncertainties in both models and RS estimates, model calibration and data assimilation (DA) techniques have been developed to improve model predictability, based on the optimal combination/analysis of these two. Model calibration was performed with satellite altimetry by Getirana et al. (2013) and A. M. Oliveira et al. (2021), showing the benefits of using

such datasets toward model general improvement in terms of discharge estimation. In turn, the evaluation of DA techniques (mainly the Kalman Filter-based methods) within the Amazon involved many experiments with RS data (e.g. satellite altimetry), from reach to regional scale (Brêda et al., 2019; Emery et al., 2018; Garambois et al., 2017; Paiva, Collischonn, et al., 2013). These studies showed the applicability of such methods to improve model estimates and representation of the water cycle in general. The usefulness of DA schemes for better estimating discharges was demonstrated for forecasting (Paiva, Collischonn, et al., 2013), comprehension of past extreme events (Wongchuig et al., 2019), and near-real time discharge estimation (Paris et al., 2016). The study by Wongchuig et al. (2019) was the first to show discharge estimation in a spatially distributed way for the last 100 years (**Figure 11**e), estimating extreme drought and flood events in unrecorded locations. They follow a general pattern of significant trend of increasing drought events in the south and flood events in the western and northwestern regions of the Amazon (Callède et al., 2004; Correa et al., 2017; J. C. Espinoza Villar, Guyot, et al., 2009; Lopes et al., 2016; Molina-Carpio et al., 2017). RS data other than discharge and water levels can also be used through DA and could be applied in the Amazon, e.g., soil moisture (Baguis & Roulin, 2017; Crowley et al., 2008; Massari et al., 2015); terrestrial water storage change (Khaki et al., 2018, 2019) and flooded water extent. Additionally, the forthcoming SWOT mission will provide breakthrough information for hydraulic modeling of the Amazon rivers. Many studies have been discussing the utility of the mission to better estimate hydraulic variables in the Amazon, from reach (lower Madeira River; Brêda et al., 2019) to the basin scale (Emery et al., 2020; Wongchuig et al., 2020). New frameworks for the incorporation of satellite altimetry water levels will set up the development of the next generation of hydraulic models for the AB, aiming at better representing local processes as water surface heterogeneities that occur due to hydraulic controls as channel width reductions (Garambois et al., 2017; Montazem et al., 2019; Pujol et al., 2020).

Most model applications in Amazon wetlands focused either on parts of the central Amazon floodplains or the whole AB. The simulation of river floodplains is still poorly performed over complex, dynamic river systems as in the Andes foothills, which are associated to multiple alluvian fans, wetlands disconnected from the main river in terms of surface waters but connected through groundwater (e.g., the groundwater-fed backswamp forests; Hamilton et al., 2007), and relatively quick hydrographs, which in turn hamper RS-based monitoring. In addition to river floodplains, other types of wetlands exist in the AB, which are often named as interfluvial wetlands (Junk et al., 2011). They combine endogenous and exogenous flooding processes to different degrees (Bourrel et al., 2009), and are more subject to local rainfall and less connected to adjacent rivers (V. Reis et al., 2019). They are associated with varying vegetation and ecosystem types (e.g., savanna, forest, grasslands). While 1D hydraulic models have proven satisfactory to simulate flooding along river floodplains (Trigg et al., 2009), interfluvial wetlands require a 2D simulation to properly capture the wetland diffuse flow. Fleischmann et al. (2020) provided a first model assessment focusing on the Negro interfluvial wetlands, which are associated to neotectonic events and savanna environment within the Amazon rainforest (Rossetti et al., 2017), and thus largely differ from the central Amazon in terms of flooding, vegetation and soil characteristics. Belger et al. (2011) used a time series of Radarsat images and in situ measurements of water level and local rainfall to estimate changes in inundation in an interfluvial wetland in the Negro basin. 1D models were shown to be unrealistic for simulating surface water elevation in these areas. Future studies should further address the hydrology of these complex wetland systems, including the Llanos de Moxos (Hamilton et al.,

2004; Ovando et al., 2018), Roraima (Hamilton et al., 2002) and Peruvian (Kvist & Nebel, 2001) interfluvial wetlands, aiming at better understanding the hydrological differences between floodplains and interfluvial wetlands, which in turn will improve our understanding of the various particular Amazon ecosystems relying on them, and the differences in terms of river-wetland connectivity.

The downstream part of the AB remains relatively unexplored in terms of hydraulic modelling and RS. This can be explained by the intricate dynamics of the estuary, which has energetic behaviour over a broad range of timescales from the intra-daily tides propagating upstream from the Atlantic Ocean through the Amazon delta to the seasonal-to-interannual timescales driven by the hydrology of the basin. Moreover, tidal effects remain sensible up to about 900 km upstream of the river mouth (Kosuth et al., 2009). One of the challenges in the hydraulic continuum of the lower Amazon is the understanding of the relative roles of the upstream forcing and of the oceanic influence in shaping the spatial and temporal patterns of variability of water level, flow velocity and flooding extent along the course of the estuary. Promising initiatives have been made to model this complex estuary, mostly relying on coastal ocean circulation models, either in two-dimensional configurations (Gabioux et al., 2005; Gallo & Vinzon, 2005), or more recently through full-blown tri-dimensional modeling (Molinas et al., 2020). These studies in particular shed light on the distinct behaviour of the tidal waves during their upstream propagation in the Amazon estuary. However, to date a comprehensive, high-resolution hydraulic modeling framework embracing the complex geometry of the whole hydraulic continuum of the lower Amazon, and accounting for the full range of interactions between oceanic and riverine forcing factors, is lacking. This can be explained, at least partly, by the fact that the monitoring of water level variability is instrumental in the success of a hydraulic modeling of the lower Amazon for calibration/validation purposes; however, spaceborne altimetry has been hardly used in the Amazon estuary.

Finally, new EO data as SWOT-derived water levels (Biancamaria et al., 2016), channel water widths (G. H. Allen & Pavelsky, 2018; Yamazaki et al., 2014), floodplain topography (Fassoni-Andrade, Paiva, Rudorff, et al., 2020), and soil moisture estimates (SMOS, SMAP), as well as new precipitation datasets (e.g., rainfall estimation using soil moisture data as the SM2RAIN Brocca et al., 2013, 2014), gravimetry missions (GRACE-FO), and techniques to retrieve groundwater storages (e.g., Frappart et al., 2019), open great opportunities for the next decade of hydrological and hydraulic modeling development in the AB. A major goal of the Amazon modeling community should be to move towards hyper resolution models, capable of providing locally relevant estimates everywhere (Bierkens et al., 2015; Fleischmann et al., 2019; Wood et al., 2011), as well as better representing all processes within the water cycle, including groundwater dynamics which has been misrepresented in most surface water-oriented hydrological models (Miguez-Macho & Fan, 2012; Sutanudjaja et al., 2018). Such modeling systems could then be coupled to models of other processes, as recently done by researchers aiming at understanding flooding impacts on photosynthesis and biosphere in general (Castro et al., 2018), feedbacks between surface waters and atmosphere (M. J. Santos et al., 2019), sediment exports and floodplain trapping (Fagundes et al., 2021; Rudorff et al., 2017), carbon storage and emissions through wetlands and uplands (Hastie et al., 2019; Lauerwald et al., 2020), and dynamics of biogeochemistry cycles at the basin scale or over wetlands (Guilhen et al., 2020). All these efforts will require additional RS data, and will move forward our predictability of the effects of ongoing environmental changes in the AB.

6.3. Aquatic ecosystems

Floodplains are the largest aquatic system in the AB, support a diverse biota and are important to the biogeochemistry and economy (Hess et al., 2015; Junk, 1997; Junk et al., 2011; Melack et al., 2009). Amazon floodplains contain thousands of lakes, thousands of km^2 of vegetated wetlands and are characterized by large seasonal and inter-annual variations in depth and extent of inundation. Hydrological conditions are central to the ecological structure and function of these aquatic ecosystems, and floodplain hydrology is complex because it combines local inputs and regional-scale fluxes with large spatial variability. Applications of innovations in RS and hydrological measurements and modeling to the investigation of Amazon floodplains have led to advances in understanding of the ecology of floodplains, in general.

Key aspects of hydrology relevant to floodplain ecosystems in the Amazon and elsewhere are the amplitude, duration, frequency, and predictability of variations in discharge and inundation (Melack & Coe, 2021). Two conceptual frameworks of general relevance to river systems were motivated by studies in the Amazon. Junk et al. (1989) emphasized the flood pulse and defined floodplains in terms of river stage, associated physical and chemical conditions, and adaptions of organisms to these conditions; Junk (1997) elaborated these concepts for the central Amazon. Mertes (1997) examined hydrologic aspects of inundation of floodplain systems with RS and simple models, and introduced the concept of the perirheic zone, the mixing zone of water from the river and local catchment. Both these conceptual developments are supported by hydrological measurements of Amazon floodplain lakes, the first by Lesack & Melack (1995), subsequent modeled by Ji et al. (2019) and Bonnet et al. (2008, 2017). Floodplains play an important role in the carbon balance and nitrogen biogeochemistry of the AB and are sites of large fluxes of methane and carbon dioxide to the troposphere and high rates of aquatic plant production. Studies designed to estimate the magnitude and variability of gas fluxes and productivity in the Amazon have combined RS with field data in innovative ways applicable to aquatic ecosystems in general. Melack et al. (2004) used habitat-specific methane fluxes in combination with seasonal changes in the surface water extent of the aquatic habitats derived from active and passive microwave RS to estimate regional methane fluxes. On the mainstem Solimões-Amazonas rivers and their fringing floodplains, annual methane emissions were estimated to vary between approximately 0.7 to 2.4 TgC yr-1 (Melack et al., 2004). Furthermore, methane fluxes per m^2 were higher during lower water levels than during high water in an Amazon floodplain lake, and fluxes in proximity to vegetation were higher than those from habitats in open water (P. M. Barbosa et al., 2020). Richey et al. (2002) and Melack (2016) also used estimates of surface water extent to calculate carbon dioxide fluxes. Guilhen et al. (2020) estimated N_2O emissions from denitrification in Amazonian wetlands by adapting a simple denitrification model forced by open water surface extent from the Soil Moisture and Ocean Salinity (SMOS) satellite, and reported a pattern in denitrification linked to inundation.

Seminal approaches with RS data were used to delineate inundated area and extent of flooded forests, open water and herbaceous plants (e.g., Hamilton et al., 2002; Hess et al., 1995, 2003, 2015); Section 4.2) and used to improve estimates of seasonal and interannual variations in methane fluxes. As described in Section 4.2, new satellite-borne sensors and remote-sensing products can now be used to update such approaches (e.g., Parrens et al., 2019; Prigent et al., 2020). These data can be combined with remotely sensed changes in aquatic habitats, recent field

measurements (e.g., Amaral et al., 2020; P. M. Barbosa et al., 2020), and modeling (e.g., Potter et al., 2014) to significantly improve estimates of emissions. More generally, the vegetative-hydrologic classification scheme used in these analyses meets the criteria for a "functional parameterization" of wetlands (Sahagian & Melack, 1998), with classes suitable for biogeochemical and biodiversity applications

The primary productivity of aquatic plants is often high but challenging to measure, especially for herbaceous plants with large seasonal and spatial variations. On Amazon floodplains, productivity of herbaceous aquatic plants is strongly influenced by hydrological variations (Engle et al., 2008; Junk, 1997). For instance, growth of herbaceous aquatic plants in floodplain lakes follows water level variation. Extending field measurements of plant productivity to a regional scale was first done by M. Costa (2005) using SAR estimates of plant biomass. Lower values were found in regions where plants developed only in the beginning of the flood season, and higher values in areas closer to the Amazon River, where the availability and influence of nutrient-rich water is greater. Further work by T. S. F. Silva et al. (2010) and T. S. F. Silva et al. (2013) used C-band SAR combined and optical data to investigate responses of horizontal expansion and vertical growth of herbaceous plants to variations in the flooded area and water level in two large floodplains along the Amazon River. Over the period from 1970 to 2011 vertical growth varied by a factor of 2 and maximum annual cover varied by a factor 1.5. Years with exceptionally large changes in water level resulted in the highest productivity because horizontal expansion and vertical growth were both enhanced.

The productivity of Amazon aquatic ecosystems is also related to nutrient supply and optical conditions within the water (Melack & Forsberg, 2001). Applications of satellite-borne imaging spectrometers to the optically complex waters of the Amazon have reviled chlorophyll and suspended sediment levels (e.g., C. C. F. Barbosa et al., 2009; Novo et al., 2006; Section 4.4), which are related to planktonic productivity. Other studies employing data from optical sensors have been used to describe aquatic vegetation (e.g., Josse et al., 2007; Novo & Shimabukuro, 1997; Wittmann et al., 2002), and indicate fluvial dynamics (Constantine et al., 2014; Mertes et al., 1995), both important aspects of aquatic ecosystems. However, observations with optical RS are frequently impeded by cloud cover or smoke, and forest canopies are often too dense to allow detection of flooding. Alternatively, time series of SAR data are available for several subregions within the AB and can be used to generate high-resolution maps of vegetation and inundation. For example, Ferreira-Ferreira et al. (2015) used a hydrologically-based time series of ALOS/PALSAR-1 SAR data to distinguish between land cover classes and map water extent and mean flood duration (**Figure 12**). The authors depicted the uneven distribution of flooded areas at different water levels, i.e., some water level stages result in large expansions of the inundated areas while other stages have less effect.

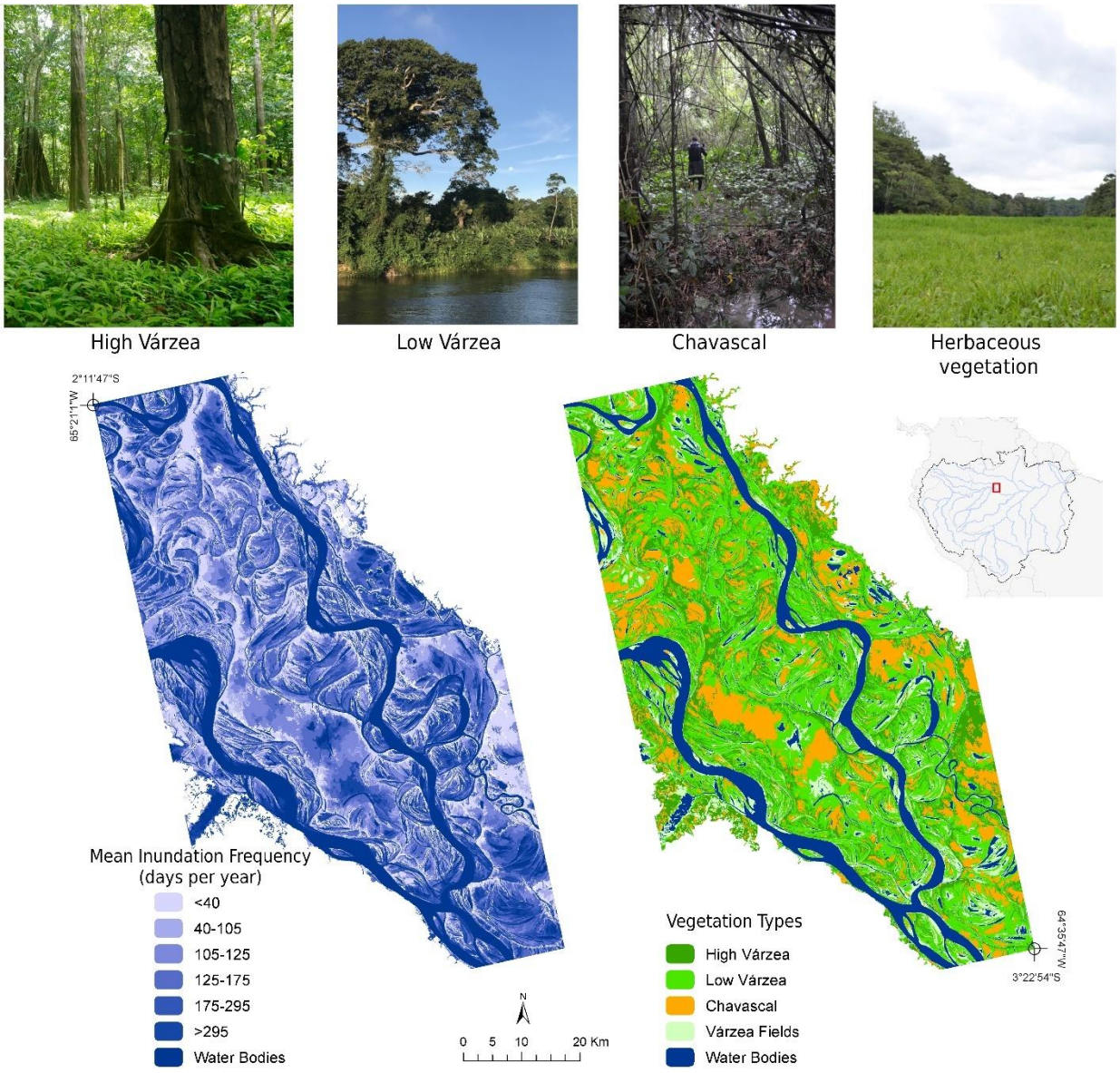

Figure 12. Major vegetation types and estimated mean flood duration maps in the Mamirauá Sustainable Development Reserve, Central Amazon, Brazil (Adapted from Ferreira-Ferreira et al., 2015). The maps were based on a time series of ALOS/ PALSAR-1 image data comprising nine dates between 2007 and 2010 chosen to provide the largest and most uniform range of water level conditions within the available imagery for the area. The water bodies were derived from the flood class of 365 days per year on average, i.e., permanent water bodies. More details on Ferreira-Ferreira et al. (2015).

Complex flow patterns, revealed by interferometric SAR analyses (Alsdorf et al., 2007), and differences in sources of water, evident in hydrological models (Bonnet et al., 2017; Ji et al., 2019), account, in part, for the variations in nutrients, suspended sediments, and productivity (Forsberg et al., 2017). A further example of how advances in hydrological modeling contributed

to the understanding of Amazon floodplains is provided by Rudorff et al. (2014a, 2014b). They added a simple model of hydrological balance to the LISFLOOD-FP hydraulic flooding model and applied it over 15 years. This work also emphasized the importance of detailed topography which they derived from a combination of data from the SRTM with extensive echo-sounding. The model simulated well changes in water level, flooding extent, and river-floodplain flows. Rudorff et al. (2017) combined these results with measurements of suspended sediments to demonstrate variations in sediments supply and loss from the floodplain.

Variations in the distribution and inundation of floodplain habitats play a key role in the ecology and production of many commercially important fish in Amazonia. Lobón-Cerviá et al. (2015) demonstrated that number of fish species and their abundance were directly related to presence of flooded forests and inversely related to distance from the river. Arantes et al. (2018) used both Landsat and SAR data to characterize aquatic habitats and found that spatial patterns of fish biodiversity on Amazon floodplains were associated with forest cover and landscape gradients. Additional examples of connections between fisheries and fish ecology are provided in Melack et al. (2009) and Melack et al. (2021).

Tree phenology on both fertile, eutrophic floodplains (várzea) and nutrient-poor, oligotrophic floodplains (igapó) follow variations in inundation (Junk et al., 2010). Seasonal inundation also provides connectivity that is critical for gamma diversity (Thomaz et al., 2007; Ward et al., 2002). Avian diversity varies among the aquatic habitats (Cintra, 2015; Laranjeiras et al., 2021). At the community level on large river floodplains, birds and fishes have more stable communities in environments with rhythmic annual floods (Jardine et al., 2015; Luz-Agostinho et al., 2009). In a floodplain lake near the confluence of Amazon and Negro rivers, for instance, Röpke et al. (2017) detected an abrupt and persistent change in fish assemblage structure that lasted for more than a decade after the extreme drought of 2005.

Disturbances of the natural variations of flooded area, hydrological connectivity or land cover are disruptive for wetland systems. Resende et al. (2019) used SAR RS to assess the impacts of the Balbina dam to the downstream igapó forests in the Uatumã River. The authors showed that 12% of the floodplain forests died because of the altered flood pulse and another 29% of the remaining living forest stands may be undergoing mortality. Schöngart et al. (2021) provide further evidence for changes in floodplain forests below the Balbina dam over 35 years. Castello et al. (2018) combined fisheries data and habitat coverage derived from SAR analyses to determine effects of land cover change on fishery yields. They showed that removal of flooded forests can reduce fish yields and that other floodplain habitats cannot replace forest removal to improve fish yields.

Several challenges and knowledge gaps remain in the linkage of hydrology to the functioning of aquatic ecosystems in the AB and elsewhere. Wet soil without standing can have high rates of biogeochemical processes such as methane release. While difficult to detect with RS, models offer promise if operating at the correct scales. Streams and small rivers as well as ponds can release disproportionally high amounts of carbon dioxide, but their surface areas are seldom known; high spatial resolution RS products will help alleviate this problem. Interfluvial and savanna wetlands, often inundated by rain rather than rivers, are not well represented by basin-scale hydrological models and will require fine-scale topographic data combined with multi-temporal RS of inundation. Within the AB, particularly large data gaps exist in the Llanos

de Moxos (Bolivia), peatlands in the Pastaza-Marañón foreland basin (Peru), and coastal freshwater wetlands.

6.4. Environmental changes

In the last decades, the Amazon has been subject to large environmental changes. Extensive rainforest areas have been deforested, being converted to pasturelands, croplands, or mining. These land cover changes alter the partitioning of precipitation into evapotranspiration, surface runoff and deep drainage, transport of sediments, river discharge and river color, and influence the processes of formation of rainfall in Amazonia. At the same time, forest areas have been flooded by artificial dams to produce hydropower, affecting flood pulses downstream of the dam, while the forests' ecohydrology has adapted to the flood patterns. RS has been an important tool to detect and map these environmental changes and their impacts on the hydrological cycle.

The role of deforestation on the AB hydrological cycle could only be understood after large-scale mapping of land use and land cover (LULC) in Amazonia. The first of these maps were produced by Cardille et al. (2002). They merged RS imagery from AVHRR with agricultural census data to produce a spatially-explicit LULC map for the Amazon and Tocantins basins for 1995. Based on this dataset and agricultural census data for 1960, M. H. Costa et al. (2003) evaluated how land use increases in the upper Tocantins basin affected its discharge from 1949-1969 to 1979-1999. Although precipitation did not change significantly from the former to the latter period, the annual mean discharge increased by 24% ($P < 0.02$), while the rainy season discharge increased by 28% ($P < 0.01$), and seasonal peaks occurred about one month earlier. Such variations could be credited both to reduced ET and reduced infiltration during the rainy season. The reduction in evapotranspiration is a consequence of three factors: the increased albedo reduces the net radiation at the surface; the reduced roughness length decreases atmospheric turbulence, weakening vertical motions; and the reduced root depth leaves less soil moisture available to plants. Additional factors that can also influence local evapotranspiration include compaction of the soil surface or sub-surface and reduction of leaf area index through grazing (M. H. Costa, 2005).

Other LULC maps were produced for the Brazilian Amazon using similar techniques (Leite et al., 2011 for 1940-1995; L. C. P. Dias et al., 2016 for 1940-2012). Purely RS products are available for more recent periods, like the MODIS MOD44 tree cover product (2002-recent), Landsat-based PRODES (1988-recent, http://www.obt.inpe.br/prodes/) and TerraClass (2004-2014, https://www.terraclass.gov.br/) official government products for the Brazilian Amazon, and MapBiomas for the Pan-Amazonia (1985-recent, https://mapbiomas.org/). Several authors have used these datasets to study the effects of LULC changes on the hydrological regime of several of the Amazon tributaries and the Amazon-Cerrado arc-of-deforestation as a whole (M. E. Arias et al., 2018; Cavalcante et al., 2019; Coe et al., 2011; Levy et al., 2018; Panday et al., 2015), generally finding increased mean and low-flow discharge with deforestation.

In addition to river discharge, LULC changes may also affect the precipitation, particularly during the beginning and end of the rainy season. The first evidence of this was provided by Butt et al. (2011). They compared four Landsat-based land cover maps from 1975 to 2005 against the rainy season onset dates calculated from daily rain gauge data, concluding that, for stations that lie inside the major deforested area, the rainy season's onset has significantly

shifted to, on average, 11 days (and up to 18 days) later in the year over the last three decades. However, for stations that lie in areas that have not been heavily deforested, the onset has not shifted significantly. Recent studies confirmed these results. Repeating the same analysis for southern Amazonia from 1974 to 2012, and after removing regional trends and interannual variability, Leite-Filho et al. (2019) confirmed a delay in the onset of 1.2–1.7 days per each 10% increase in deforestation. In addition, the probability of occurrence of dry spells in the early and late rainy season is higher in areas with greater deforestation.

Moreover, using daily rainfall data from the Tropical Rainfall Measurement Mission 3B42 product and the L. C. P. Dias et al. (2016) 1-km land-use dataset, Leite-Filho et al. (2020) evaluated the quantitative effects of deforestation on the onset, demise, and length of the rainy season in southern Amazon for 1998–2012. After removing the effects of geographical position and year, they verified a relationship between onset, demise, and length of the rainy season and deforestation. Onset delays ~0.4 ± 0.12 day, demise advances ~1.0 ± 0.22 day, and length decreases ~0.9 ± 0.34 day per each 10% deforestation increase relative to the existing forested area ($P < 10\text{-}5$ in all three trends).

Another breakthrough owned to RS was identifying the "deforestation breeze" effect, which affects rainfall distribution. Khanna et al. (2017) used remotely-sensed land-use, precipitation, and cloudiness data combined with a regional climate model, finding that small-scale deforestation patches trigger thermally-driven atmospheric circulation cells in Rondônia. This circulation creates a precipitation anomaly dipole over the deforested area, with enhanced precipitation downwind and suppressed precipitation upwind in the thermal cell's descending branch. The observed dipole in Rondônia is substantial, with the precipitation change in the two regions being ±25% of the deforested area mean.

Although several techniques to infer surface water and channel properties from RS have been developed in recent years (as described in Section 4), there are still relatively few studies that apply these techniques to assess how anthropic and natural environmental changes affect these properties in the AB. Latrubesse et al. (2017) used tree cover data from Hansen et al. (2013), Landsat images, and RS estimates of TSS of Park & Latrubesse (2014) to investigate the current and potential impacts of dams in the basin. They found that the Santo Antônio and Jirau dams caused a 20% reduction in mean surface suspended sediment concentration in the Madeira River, despite unusually high flood discharges in the years analyzed after their start-of-operation. They also used Landsat images to calculate channel migration rates for each sub-basin, finding an average migration rate of 0.02±20% channel widths per year.

Satellite retrieval of TSS has also been used to document trends in the Amazon River's main stem, although there is no apparent consensus on the causes of the observed trends. Such techniques allow for expansion and extrapolation of field datasets, being especially useful in the Amazon since runoff and TSS are poorly correlated at the Amazon River's lowest reaches due to asynchronism of the peak water discharges of the Solimões, Madeira, and Negro rivers (Filizola & Guyot, 2009). J. M. Martinez et al. (2009) used 18 TSS sampling campaigns from 1995 to 2003 and MODIS images to obtain a 12-year (1995-2007) continuous series of TSS at the Óbidos station, the last gauge station in the Amazon river before it reaches the Atlantic Ocean. They find a 20% increase in sediment discharge in the period with no discernible trends in water discharge and cite changes in land use and rainfall patterns as likely explanations. Recently, Li et al. (2020) used similar techniques to obtain an updated (1996-2018) time series of TSS and find

that sediment loading increased until 2007 but decreased afterward. They infer that this reversal is due to decreased sediment contribution from the Madeira river after the construction of the Santo Antônio and Jirau dams in the late 2000s, in agreement with Latrubesse et al. (2017).

Montanher et al. (2018) used similar techniques to generate an extended 32-year (1984-2016) time series of suspended sediment transport (SST, the product of TSS by river discharge). They argued that there is a recurrent pattern of SST rising and falling in cycles likely associated with climate fluctuations and that trends such as those observed by J. M. Martinez et al. (2009) are a consequence of short time series. However, SST depends on river discharge variability, and J. M. Martinez et al. (2009) and Li et al. (2020) found no trends in river discharge in their shorter time series.

Some studies also investigated the impact of mining on suspended solids in sub-basins of the Amazon. Artisanal and small-scale mining, especially gold, is common in some regions, such as the Tapajós River basin. These small mining operations often use low-end techniques such as water jets and dredges that can cause proportionally high land degradation levels and water contamination (Lobo et al., 2018). They are also often illegal and unregistered, making RS an important tool for identifying and mapping these activities. The only publicly available dataset (to our knowledge) on mining areas in the AB is the TerraClass project, which is based on visual interpretation of Landsat images and is available only for a few years between 2004-2014. Lobo et al. (2018) combined multiple datasets to develop an automated classification method that can distinguish between industrial and small-scale mining and ore types based on Sentinel-2. They found that in 2017 64% of the total mining area in the several key mining regions in the basin was comprised of small-scale gold and tin mining.

Lobo et al. (2015) estimated total suspended solids (TSS) in the Tapajós River basin based on Landsat images. They found that increases in TSS are strongly associated with reported increases in mining activity at seasonal and decadal timescales. Lobo et al. (2016) updated the Landsat-based identification of mining areas from the TerraClass project. They described the evolution of mining areas in the same basin, identifying different eras of mining impacts on TSS related to the introduction of different technologies and variations in the gold price. Comparing sub-basins with different kinds of land alteration, they also indicated that mining activities have a much higher effect on TSS than deforestation for agricultural purposes.

Landsat images have also been used to document and understand a major hydro-morphological event in the Amazon: the recent capture of almost all of the water flow from the Araguari River by the Amazon River (E. S. dos Santos et al., 2018). The Araguari is a large river, with an average annual discharge >1000 $m^3 s^{-1}$, which used to flow directly to the Atlantic Ocean until the rapid formation of the Urucurituba channel connecting it to the Amazon River in the early 2010s. The initial headwater migration of the proto-Urucurituba was likely associated with deforestation for buffalo farming around 2007. The first connection to the Araguari was attributed to a high flow event in 2011. The rapid growth of the channel, which increased in width by about 5 m per month until 2015, is likely a consequence of complex hydro-morphodynamic processes related to tidal currents and estuarine deposition that ultimately led to the blockage of the Araguari River mouth. This channel's formation caused large changes in the hydraulic pattern, sediment dynamics, and ecosystems in the Araguari estuary, being the first known observation of estuarine distributary network development by headwater erosion.

RS techniques contributed input, calibration, and validation data to many models that provided important insights on the consequences of environmental changes in the AB (see Section 6.2). These models can integrate hydrological, hydraulic, climate, and land-use processes and are important tools in many studies investigating the impacts of past and future changes in the environment. A main application of these models is to analyze future scenarios (e.g., climate change, deforestation). Another application is attributing the effects of different processes in the variability of the observed data.

Sorribas et al. (2016) examined climate change projections on discharge and inundation extent in the AB using the regional hydrological model MGB with 1-dimensional river hydraulic and water storage simulation in floodplains forced by five GCMs IPCC's Fifth Assessment Report CMIP5. The model was validated against a mix of in situ and RS data. Results indicate an increased mean and maximum river discharge for large rivers draining the Andes in the northwest contributes to increased mean and maximum discharge and inundation extent over Peruvian floodplains and Solimões River in western Amazonia. In contrast, decreased river discharges (mostly dry season) are projected for eastern basins and decreased inundation at low water in the central and lower Amazon.

With the renewed interest in the last decades in constructing hydroelectric dams in the AB (Castello & Macedo, 2016), many modeling studies attempted to quantify the environmental impacts of new and existing dam projects. Forsberg et al. (2017) used several models to evaluate the impacts of six planned dams in the Andean region of the Amazon. Since a sizable portion of sediment production in the basin occurs in this region, these dams are predicted to reduce the basin-wide supply of sediments, phosphorus, and nitrogen by 64%, 51%, and 23%, respectively. Along with changes in nutrient and sediment supply, mercury dynamics and flood pulse attenuation are projected by the authors to cause major impacts on downstream aquatic and floodplain fertility and channel geomorphology. Indeed, Resende et al. (2019) found massive tree mortality in floodplain forests (igapó) downstream of the Balbina reservoir using SAR images, with about 40% of the igapó 49 km downstream of the reservoir either dead or undergoing mortality.

Expected environmental changes in the basin, such as deforestation and climate change, can also significantly impact hydropower production itself, often leading to generation well below the dam's expected capacity. Most recent dam designs follow a run-of-the-river concept, avoiding the large environmental impacts of enormous reservoirs from older designs but making power generation more dependent on river discharge variations (M. H. Costa, 2020). M. E. Arias et al. (2020) combine a land-use and a hydrological model to assess the direct impacts of climate change and deforestation on hydropower production of existing and planned dams in the Tapajós basin. Although decreasing evapotranspiration from deforestation tends to increase annual mean discharge, reduced water retention increases surface runoff and flash flows during the rainy season and reduces discharge during the dry season. Since turbines are normally working at maximum capacity in the rainy season, this excess flow is wasted, and generation in the dry season is reduced. M. E. Arias et al. (2020) find that projected climate change and deforestation combined can delay peak energy generation by a month (worsening the mismatch between peak production and consumption), reduce dry season generation by 4-7% and increase interannual variability of power production by 50-69%.

Deforestation has the indirect effect of reducing precipitation and delaying the onset of the rainy season, which further illustrates the dependency of hydropower generation on forests. Stickler et al. (2013) combine land-use, hydrological, and climate models to assess the direct and indirect effects of deforestation alone on hydropower generation of the Belo Monte energy complex in the Xingu River basin. They find that when considering only the direct effects of deforestation on river flow, a 20-40% deforestation of the basin would lead to a 4-12% increase in mean discharge with similar increases in power generation. However, when the climate effects of deforestation of the Amazon region were considered, rainfall inhibition in the basin counterbalanced the direct effects and led to a 6-36% reduction in discharge. Under the business-as-usual deforestation scenario for 2050 (40% of the Amazon forest removed), they simulated that power generation was reduced to 25% of maximum plant output.

7. Synthesis of scientific advances, future challenges and priorities

The various achievements of more than three decades of scientific advances on the hydrology of the AB with satellite data, along with the development of new RS techniques, and some selected research opportunities, are summarized in **Table 7** and **Table 8**. Section 7.1 presents the main findings obtained in the AB, which has been a RS laboratory for hydrology advancement. Section 7.2 highlights how these experiences can be used to foster the understanding of the water cycle in other large river basins worldwide. Section 7.3 discusses the knowledge gaps and research opportunities on AB waters, thanks to an unprecedented and continued monitoring of AB with upcoming and future satellite missions. Finally, Section 7.4 discusses how to move forward from scientific advances toward more sustainable water resources and risk management, and Section 7.5 highlights recommendations for future studies on Amazon waters from space.

Table 7. Synthesis of scientific advances in understanding the Amazon hydrology with RS

Variable	Seminal developments in RS performed in Amazon	Breakthrough lessons about Amazon / General hydrology learnt from RS	Knowledge gaps and new opportunities for the Amazon
Precipitation	1) Spatial distribution of rainfall at regional scale (Espinoza et al. 2009). 2) Rain trend over the last few decades (Paca et al. 2020).	1) Spatial distribution of "hot-spot" regions (Chavez & Takahashi, 2017; Espinoza et al., 2015). 2) Reduced rainfall over main rivers (Paiva et al., 2011). 3) Rainforest inducted early wet season onset (Wright et al., 2017).	1) Improved algorithms for orographic rains (Dinku et al., 2011; Toté et al., 2015). 2) Strategic network of rain gauges. 3) Low-cost satellite constellation (Peral et al., 2019).

Evapotranspiration	1) Water flux estimates in the tropics at large scales (Fisher et al., 2009). 2) Observational data for model calibration and validation and multi-model assessments (Rocha et al., 2009; Goncalves et al., 2013).	1) Understanding of environmental drivers and ET seasonality basin-wide, with more energy limitation and small seasonality in the wettest parts (central Amazon), and the opposite in southern ones. 2) Decreasing ET due to deforestation and cropland expansion (Spera et al., 2016; Zemp et al., 2017; Oliveira et al., 2019).	1) Modeling high spatial resolution (< 30 m) ET estimates on long time series (> 40 yr). 2) Combining surface energy balance (SEB) models and models less dependent on land cover parameterization. 3) New data fusion techniques using multiple RS sources (multispectral, thermal and microwave) to reduce the cloud cover effects on SEB approaches.
Surface water elevation (SWE)	1) Large scale water level and slope estimates by radar altimetry (Guskowska et al 1990; Birkett et al 2002). 2) Water level changes from interferometry estimates (Alsdorf et al 2000; 2007). 3) Monitoring of SWE and level-discharge rating curves in ungauged rivers (Silva et al 2014; Paris et al 2016).	1) Characterization of water level variation in rivers and wetland forests (Birkett et al 2002; Alsdorf et al 2003, 2007). 2) River-floodplain connectivity (Park et al 2020, Alsdorf et al 2003). 3) Flood storage in river-wetland systems (Frappart et al 2005, Alsdorf, 2003).	1) 2D characterization of water levels (SWOT swath data; Biancamaria et al 2016). 2) Finer spatio-temporal resolution for water level and slope. 3) New techniques for fusion with local to regional modeling (Yamazaki et al 2011; Paiva et al 2013).
Surface water extent	1) First large scale extent and variability of surface water and inundations in floodplains (Sippel et al., 1994; Hess et al. 2003). 2) Relationship between surface water extent and discharge (Sippel et al., 1998). 3) High resolution floodplains dynamic and discrimination of aquatic vegetation types for large area (Ferreira-Ferreira 2015).	1) Seasonal and interannual inundation patterns in the AB (Hamilton et al., 2004; Hess et al., 2015, Aires et al., 2017). 2) Contribution of inland water and floodplains variability to the Amazon Carbon cycle and emissions (Richey et al., 2002, Raymond et al. 2013, Melack et al., 2004).	1) Finer spatio-temporal resolution of surface water and floodplain inundation extent variability with SWOT and NISAR. 2) New development of fusion techniques with IA to combine various RS observations (visible, IR, microwave, GNSS-R). 3) Ensure long term observations to monitor climate/anthropgenic changes.
Floodplain and river channels topography	1) Adjustment of Digital Elevation Models (Yamazaki et al 2012, Baugh 2013). 2) Topography estimates in seasonally flooded areas (Fassoni et al 2020).	1) Characterization of floodplain channels and lakes (Sippel 1997, Trigg 2012; Fassoni 2020). 2) Assessment of river channel migration (Constantine et al., 2014; Santos et al., 2018).	1) Characterization of topography in flooded forests. 2) Long term estimation to monitor geomorphological changes in floodplain and river channels.
Water quality: Sediments, chlorophyll and colored dissolved organic matter	1) Estimates of sediment concentration in rivers (Bayley & Moreira, 1978; Mertes et al., 1993), chlorophyll in floodplain lakes (Novo, 2006), and colored dissolved organic material in lakes (M. P. da Silva et al., 2019). 2) Semi-analytical algorithms for water quality estimates (Bernini et al. 2019, Maciel et al. 2020, Sander de Carvalho et al. 2015).	1) Spatiotemporal dynamics maps of the underwater light field and optically active constituents (Novo et al. 2006, Martinez et al. 2009, Maciel et al. 2019, 2020; Fassoni et al., 2019). 2) Extended time-series of suspended sediments in the Amazon Region (Montanher et al. 2018, Martinez et al. 2009, Li et al. 2020).	1) Evaluation of phytoplankton community dynamics using RS as a proxy for biodiversity indicator in Amazon waters. 2) Robust algorithms for CDOM and Chlorophyll-a retrieval in optically complex inland waters.

Total water storage (TWS) and groundwater storage (GWS)	1) Large scale estimates of the TWS using GRACE data (Tapley et al., 2004). 2) Determination of GWS changes using RS products and model outputs (Frappart et al., 2011).	1) Spatial signatures of droughts and floods in TWS (Chen et al., 2009). 2) Spatio-temporal signatures of droughts on surface water storage (Frappart et al., 2012; Papa et al., 2013). 3) Temporal variations of GWS (Frappart et al., 2019).	1) More accurate estimates of surface water storage from SWOT will improve the determination of GWS anomalies. 2) Long-term monitoring of TWS and GWS (GRACE and GRACE-FO).

Table 8. Synthesis of scientific advances in multidisciplinary and integrative efforts in understanding of the AB hydrology and ecosystems

	Breakthrough lessons about Amazon / General hydrology learnt	**Knowledge gaps and new opportunities for the Amazon**
Water budget	1) Sub-basin scale water cycle analysis (Azarderakhsh et al. 2011). 2) Water budget closure enforcement (Pan et al 2012). 3) Continuous river discharge estimate based on water cycle closure with satellite estimate.	1) Finer spatio-temporal resolution of the water budget analysis using river map information. 2) Sensitivity of the closure to the water component bias in particular ET estimate. 3) Groundwater exchange estimate might be obtained at fine scale in constraining the water cycle at the surface.
Modeling the Amazon water cycle and its wetlands	1) River-floodplain hydrodynamic interactions at local and large scales (Wilson et al., 2007; Paiva et al., 2013; Rudorff et al., 2014; Sorribas et al 2020). 2) Groundwater dynamics across scales and climates, and floodplain-groundwater interaction (Miguez-Macho & Fan, 2012). 3) TWS components (surface, subsurface) at basin scale (Paiva et al., 2013; Pokhrel et al, 2013).	1) Finer spatio-temporal resolution of flood dynamics, considering sedimentation processes, in diverse wetland types (floodplains and interfluvial). 2) Better parameterization of groundwater processes across the AB. 3) Lack of convergence among water storage partition (e.g., divergent estimates of surface water fraction).
Aquatic ecosystems	1) Integration of temporal and spatial variations of inundation and associated aquatic habitats into estimation of carbon dioxide and methane fluxes to the atmosphere (Richey et al. 2002; Melack et al. 2004). 2) Areal estimation of major aquatic habitats in Amazon, and seasonal and interannual variations in the areas (Melack and Hess 2010; Hess et al. 2015). 3) Biomass and growth of aquatic plants on floodplains (Costa 2010, Silva et al. 2014).	1) Extent of saturated soils under forests and in riparian corridors. 2) Modeling of inundation variations in interfluvial wetlands and savanna wetlands. 3) Areal extent of streams and small rivers, especially in Andean region. 4) High-resolution topographic data on floodplains.
Environmental changes	1) Effects of changes in land use on the river discharge (Costa et al. 2003). 2) Influence on changes in land use on onset of the rainy season (Butt et al. 2011; Leite-Filho et al. 2019) and duration of the rainy season (Leite-Filho et al. 2020).	1) Need to better understand the interactions between local changes in land use and large-scale climate mechanisms on the water cycle of the AB. 2) Initiate monitoring of forest degradation in its different forms, so that the long-term effects on forest hydrology can be studied. 3) Apply existing techniques to assess changes in water and floodplain properties caused by anthropic changes (land use change, damming, mining).

7.1. The Amazon Basin as a remote sensing laboratory for hydrology

As the largest river basin in the world, characterized by strong hydrological signals in precipitation, evapotranspiration, water storage change and discharge, the AB has been an ideal laboratory for the seminal development of RS techniques and their applications to foster our understanding of hydrological processes. **Table 7** summarizes for various hydrological variables key seminal developments made in the RS field over AB along with breakthrough lessons learnt regarding AB hydrological functioning. Additionally, **Figure 13** illustrates the major characteristics of AB hydrological storages and fluxes as characterized by RS observations and analyses. Over the past decades, the need to understand the ongoing environmental changes in the AB, that could impact the global water, energy and carbon cycles, has motivated a series of multidisciplinary and integrative efforts that foster scientific advances in our understanding of AB hydrology and ecosystems (**Table 8**).

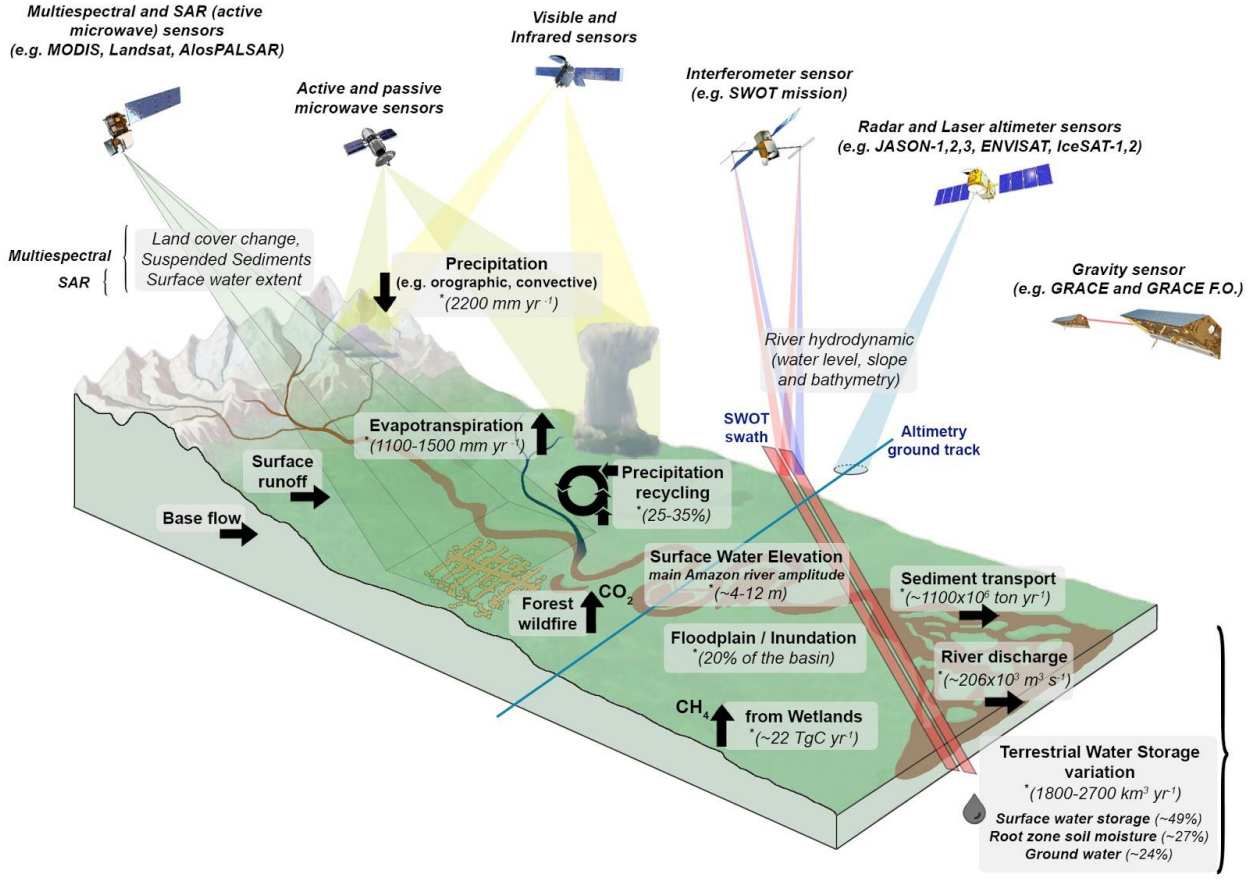

Figure 13. Schematic illustration of the integrated hydrological processes of the water cycle in the AB. The main sensors on board orbiting satellites that have helped measure these processes are indicated. The annual estimates of each component averaged over the entire basin are shown. The references (*) related to these estimates are provided along the text in Section 7.1.

Advances in precipitation estimates from RS have allowed the characterization of the spatial and temporal distributions of rainfall at local to regional scale over AB and provide records long enough to assess rainfall trends over the last few decades (**Table 7** and **Table 2** for developed precipitation products). The average rainfall in the AB was estimated as 2200 mm yr^{-1} (**Figure 3**), and the heaviest rainfall occurs in hot-spot regions in the Andes mountain ranges initiated by convection processes altered by the topography, where rainfall can reach values higher than 6000 mm yr^{-1} (Chavez & Takahashi, 2017; Espinoza et al., 2015; **Figure 3**). Large-scale analysis of RS-derived precipitation revealed the effect of winds over large water bodies that causes reduced rainfall over these areas (Paiva et al., 2011).

RS observations were key to providing the first large-scale estimates of evapotranspiration in tropical regions, especially over AB, and also provided unprecedented observational data for the evaluation, calibration and validation of models (**Table 2**). Furthermore, RS allowed the characterization of ET temporal and spatial variability over the AB (**Figure 4**) and the understanding of its environmental drivers, revealing contrasting regimes between the more energy-limited ones in the equatorial part of the basin, and more water-limited regimes in the southern areas (Maeda et al., 2017). AB annual average evapotranspiration is estimated as 1100 to 1500 mm yr^{-1} (based on SSEBOp, MOD16, PML, and GLEAM global models - **Figure 4**, and water balance by Builes-Jaramillo & Poveda (2018), with higher rates in the northern portions, as in the Negro River basin, decreasing towards the southern parts (Baker et al., 2020; Maeda et al., 2017). Various RS-based approaches result in significant divergences in the estimation of evapotranspiration over AB (**Figure 4** and **Figure 10**). For instance, RS-based ET annual rates at the AB scale were 15-37% higher than those obtained from water balances (Baker et al., 2020).

The characterization of continental water surfaces, including their elevation and extent, was possible thanks to adaptations of satellite techniques not primarily designed for applications to hydrology or inland water monitoring. A striking example is that of altimetry satellite missions, initially designed for the observation of the ocean, but with promising applications to the large rivers of the Amazon (Guzkowska et al., 1990) and with the potential to derive SWE of rivers and lakes. Since then, various altimetry databases for the global monitoring of lakes and rivers have been developed (**Table 3**). The SAR differential interferometry technique, originally developed in geophysics, was also tested and applied for the first time in central Amazon floodplains to characterize SWE changes (Alsdorf et al., 2000). Both altimetry and SAR techniques were important to characterize SWE variations in AB rivers and their connectivity with the floodplains (Park, 2020). The water surface gradient of the Amazon River varies both spatially and temporally, with values ranging from 1.5 cm km^{-1} (800–1020 km upstream) to 4.0 cm km^{-1} (2900–4000 km upstream; Birkett et al., 2002). The monomodal flood pulse of the main Amazon River is well captured with radar altimetry (~4-12 m amplitude; **Figure 5**). This pulse controls the SWE variations in the central Amazon floodplains. During the annual flood, the SWE variations in rivers and adjacent floodplains, as seen from SAR or altimetry, are similar (Alsdorf et al., 2007), but connectivity is reduced during the low-water period (Park, 2020) as the flows are controlled by the local topography (Alsdorf et al., 2007) and SWE in both environments is not always equivalent (Alsdorf, 2003).

The first large-scale surface water extent mapping from RS was also carried out for the AB (Sippel et al., 1994). Many estimates and databases, using a wide range of sensors, have been developed since then at different spatial and temporal scales (**Table 4**). These include innovative high resolution mapping of wetlands and flooded vegetation using L-band SAR (Hess et al., 2003), which provided the first estimates of flood extent in the entire Amazon wetlands, ranging between 285 x 10^3 and 635 x 10^3 km^2 in periods of low (Oct-Dec) and high waters (Apr-Jun), respectively (Hess et al., 2015; **Figure 6**). Significant differences among various RS-based estimates of surface water extent exist over AB (**Figure 6**), with in general lower maximum flooded area found by coarse scale products as compared to SAR-derived maps. Seminal approaches with RS data were used to delineate AB large-scale surface water area and extent of flooded forests, open water and herbaceous plants, revealing their complex seasonal and interannual patterns influenced by local and regional-scale variability (Filipe Aires et al., 2017; Hamilton et al., 2004; Hess et al., 2015; Melack & Hess, 2010). While the width of the Amazon River floodplain is similar throughout the central Amazon, the area of flooded forest decreases from upstream to downstream, where both the number and size of open water lakes increases (Hess et al., 2015; Mertes et al., 1996).

Mapping surface water extent in the AB, in combination with field data, enabled pioneering regional estimates of methane emissions (**Table 7**), with an estimate of methane emissions of ~22 Tg C yr^{-1} for the lowland basin (Melack et al., 2004). The spatial configuration of the Amazon floodplain habitats in relation to vegetation types is related to flooding patterns (**Figure 13**; Ferreira-Ferreira et al., 2015). Herbaceous aquatic plants on central Amazon floodplains have a growth related to water level variation and the flood extent (M. Costa, 2005; T. S. F. Silva et al., 2013). Furthermore, the increasing effect of dams in the AB has been assessed through analyses of flood extent dynamics (Li et al., 2020; C. M. Souza et al., 2019) and impacts on tree mortality (Resende et al., 2019).

The first morphometric characterization in AB using RS data showed that 11% of the floodplain along the Amazon River and lower reaches of major tributaries is covered with lakes (Sippel et al., 1992). In fact, the floodplain topography along the Amazon River is complex with several channels and lakes connected to the river (Latrubesse, 2012; Mertes et al., 1996). Floodplain channel widths vary largely (10–1000 m), and channel depths are tied closely to the local amplitude of the Amazon River flood pulse (Trigg et al., 2012; **Figure 7**). The recent capture of almost all of the water flow from the Araguari River by the Amazon River, the first known observation of estuarine distributary network development by headwater erosion, was also documented with RS techniques (E. S. dos Santos et al., 2018). The need for accurate topographic data for hydrological applications was emphasized in several studies in the central Amazon (Baugh et al., 2013; Wilson et al., 2007; Yamazaki, Baugh, et al., 2012), in which key improvements such as vegetation removal were made. Global DEMs still do not accurately represent the floodplain topography, but surface water extent data combined with WSE allowed the first topographic mapping in seasonally flooded areas in the central Amazon (Fassoni-Andrade, Paiva, Rudorff, et al., 2020). In these areas 75% of the open-water areas have depth of less than 2 m (8 m) in the low (high) water period (Fassoni-Andrade, Paiva, Rudorff, et al., 2020).

The Amazon River exports the largest sedimentary supply to the world's ocean (1.1 x 109 tons per year; (Armijos et al., 2020; **Figure 13**). Several seminal studies and algorithm

developments using RS to characterize water composition of rivers and lakes were primarily conducted in AB (see **Table 5**), such as the pioneering estimates of sediment concentration in rivers (Bayley & Moreira, 1978; Mertes et al., 1993), chlorophyll in floodplain lakes (Novo et al., 2006) and colored dissolved organic material (M. P. da Silva et al., 2019). The spatio-temporal pattern of these components is related to SWE variations and mixing processes from different sources. The shallow depths during the low water period and the large area of floodplain lakes favor conditions for sediment resuspension (Bourgoin et al., 2007; Fassoni-Andrade & Paiva, 2019; **Figure 8**). The mapping of chlorophyll in floodplain lakes showed higher pigment concentrations during the low water season (Novo et al., 2006). Increasing trends in sediment concentration in rivers were linked to changes in land use (J. M. Martinez et al., 2009; Amazon River) and the impact of mining (Lobo et al., 2015, 2016; Tapajós River). Conversely, the construction of the Santo Antônio and Jirau dams seems to have contributed to a reduction of sediment concentration in the Madeira River (Latrubesse et al., 2017; Li et al., 2020).

Due to large spatial and temporal changes of freshwater stored in surface, soil root zone and aquifers, AB is the ideal laboratory to explore measurements of gravity field variations from the GRACE satellite mission and derive TWS variations, linked to the redistribution of water mass over the continental surfaces (**Figure 9**). The first GRACE-derived estimates of TWS variations (Tapley et al., 2004) and groundwater storage changes (Frappart et al., 2011) were presented for the AB. TWS change in the AB is estimated as ~1800-2700 $km^3\ yr^{-1}$ (**Figure 13**) with different contributions from surface water storage (~49%), root zone soil moisture (~27%), and groundwater (~24%) (Frappart et al., 2019). The residence time of the water stored in the AB, i.e., the average time that the water remains in the AB before leaving by runoff or evapotranspiration, was estimated at two months (Tourian et al., 2018). GRACE data helped to monitor periods of extreme droughts (e.g., 2009) and floods (e.g., 2005, 2010; J. L. Chen et al., 2009), quantify water deficit during such events (Frappart et al., 2012), understand groundwater dynamics across different scales and climates, and the interaction between floodplains and groundwater (Miguez-Macho & Fan, 2012).

RS has proven to be a great complement to in situ observations that have traditionally been used to calibrate/assimilate and validate hydrologic and hydrodynamic models (**Table 6** and **Figure 11**). In the case of the AB, the pioneering development or application of models have provided major understanding of basin-wide river-floodplain systems (Coe et al., 2002; Paiva, Buarque, et al., 2013; Rudorff et al., 2014a; Sorribas et al., 2020; Trigg et al., 2009; Wilson et al., 2007; Yamazaki et al., 2011), the role of groundwater in hydrological buffering and headwater basin dynamics (Cuartas et al., 2012), and partitioning of total water storage (Paiva, Buarque, et al., 2013; Pokhrel et al., 2013). The study by Wilson et al. (2007) was one of the first large scale hydraulic models developed, while with the first large-scale hydrologic-hydrodynamic model of the AB by Paiva, Buarque, et al. (2013) it was possible to represent physical processes such as the backwater effects in the main river and the attenuation of the flood wave due to water storage in the floodplains. Applications of two-dimensional models in a reach of the Amazon River showed that the floodplain receives large amounts of water from the river, and small increases in peak discharge promote large changes in this flow (Rudorff et al., 2014b). Recently, Sorribas et al. (2020) estimated, using an innovative hydrological tracking model, surface water travel times along the AB as 45 days (median), with 20% of Amazon River waters flowing through floodplains. Furthermore, with the integration of RS data and hydrological

modeling, the assessment of past floods and droughts was possible (Frappart et al., 2012; Wongchuig et al., 2019).

RS techniques were also important for understanding how the hydrological cycle responds to environmental changes. Long-term changes in discharge could be attributed to changes in land cover via changes in evapotranspiration, as first shown for the Tocantins River (M. H. Costa et al., 2003). The average annual discharge increased by 24% between 1949-1986 and 1979-1998, associated with increased agricultural land use in the basin (from 30% to 49%). The presence of the forest was established as important for determining precipitation patterns both in and outside the region. The deep roots, low albedo and high ET rates of the rainforest induce the wet season onset to be several weeks before what it would be without it, in a mechanism dubbed 'shallow convection moisture pump'(Wright et al., 2017). The changes in land-surface fluxes caused by deforestation were found to cause reductions in precipitation totals, delays on the rainy season onset and longer dry spells during the wet season, with negative consequences for hydropower generation, regional agriculture and the resilience of the forest itself (M. E. Arias et al., 2020; Butt et al., 2011; M. H. Costa, 2020; Leite-Filho et al., 2020; Spera et al., 2014; Stickler et al., 2013).

7.2. The benefits of the lessons learnt in the Amazon to understand the hydrology of other large tropical river basins

AB can be seen as a RS laboratory for fostering the understanding of the water cycle and hydrology in general. While these advances have prompted the scientific understanding of AB hydrology, they have also set up new developments, techniques and analysis that contribute to a better understanding of the hydrological cycle of other large basins worldwide, and at the global scale. Without being exhaustive, we discuss here some key studies that benefit from such advances and how they have contributed to hydrological progress in other regions. In particular, as the second largest river basin in the world, with similar environmental characteristics as AB such as extensive floodplains and dense forests, the Congo River Basin is the new frontier of tropical hydrological research (Alsdorf et al., 2016), gaining more scientific attention in recent years and benefiting from the lessons learnt from AB hydrology. The "Hydrologic Research in the Congo Basin" conference in Washington, D.C (USA) in 2018 delineated new research opportunities for the basin. This effort to gather African and international communities around a joint objective of a better understanding of the Congo basin response to climate change led to an extensive monograph (Alsdorf et al., 2021) that indicates the usefulness of RS and model methodologies built for AB.

The first development of satellite altimetry datasets (Section 4.1) in AB was turned into freely available global datasets providing long-term WSE at thousands of virtual stations (**Table 3**) enabling the characterization of the surface hydrology variability from altimetry in the Congo basin (Paris et al., 2020), Indian inland waters (Ghosh et al., 2017) and the Niger River basin (Normandin et al., 2018). The integration of satellite altimetry and hydrological modeling had seminal advances in the AB, including model validation and development of rating curves for near real-time monitoring of discharges from the space (Section 6.2), that were further performed in other tropical basins as the Congo (Paris et al., 2020), Tsiribihina in Madagascar

(Andriambeloson et al., 2020), Niger (Fleischmann et al., 2018), and Ogooué (Bogning et al., 2020).

Studies based on initial RS developments in the Amazon further performed comparative hydrology approaches, for instance by studying jointly the floodplain dynamics in the central Amazon, the Congo and the Brahmaputra wetlands with SAR (H. C. Jung et al., 2010), highlighting the unique features of each of these river systems. AB, with its extensive river floodplains, largely contrasts with Congo Cuvette Centrale, mainly dominated by interfluvial wetlands, with less river-wetland interaction (H. C. Jung et al., 2010). Following studies using SAR observations to map flood and wetlands extent and distinguish vegetation types in AB (Section 4.2), seasonal flooding dynamics, water level variations and vegetation types over the Congo basin were derived from JERS-1 (Å. Rosenqvist & Birkett, 2002) or ALOS-PALSAR SAR and Envisat altimetry data (Kim et al., 2017).

The development of large scale, multi-satellite RS techniques to monitor surface water storage variability, with initial techniques and analysis developed and assessed for AB (Sections 4.1 and 5) were further applied to the Orinoco River in South America (Frappart et al., 2015), to study droughts in the Ganges-Brahmaputra River (Papa et al., 2015) and to quantify the relative contribution of surface and groundwater variations in the Mekong (Pham-Duc et al., 2019), the Chad (Pham-Duc et al., 2020) and the Congo (M. Becker et al., 2018; Yuan et al., 2017) basins.

Given the global relevance in terms of climate and ecosystems, the presence of large floodplains and dimensions in accordance with the resolution of coarse scale models, many advances and developments of land surface and hydrological models were first assessed over AB (Section 6.2), especially the introduction of basin-scale inundation schemes that were later introduced to other river basins (Andriambeloson et al., 2020; Paris et al., 2020), at continental scale (Siqueira et al., 2018) and at the global scale (Alkama et al., 2010; B Decharme et al., 2012; Yamazaki et al., 2011). Recent advances in large-scale sediment transport using RS observations and modeling followed a similar path, with pioneering works in AB (Section 4.4) being followed by progress for all South America (Fagundes et al., 2021).

7.3. Tackling the current knowledge gaps with future satellite missions

This review shows the tremendous achievements made during more than three decades of scientific advance on the hydrology and the water cycle of the AB with the help of RS. It also helped to identify the various knowledge gaps remaining to promote a comprehensive understanding of the AB hydrology. Here, we summarize these knowledge gaps (**Table 7** and **Table 8**), present the new research opportunities with the upcoming and future satellite missions.

Regarding RS-based precipitation, current algorithm challenges involve the definition of dynamic thresholds of temperature brightness in IR sensors, and processing of MW data to avoid confusing the summit of the Andes snowy peaks with cold clouds (Dinku et al., 2011; Toté et al., 2015). Better algorithms for the detection of solid precipitation are necessary for improved understanding of local processes in AB headwaters in the Andes mountains (Hurley et al., 2015; Levizzani et al., 2011; Peng et al., 2014). In situ observations are fundamental for the calibration of remote sensors, therefore a strategic network of traditional stations and ground-based radars in key points of the AB must necessarily be part of a future agenda. Finally, new low-cost

technologies such as nanosatellites have proven to be viable while maintaining scientific requirements, which should continue to be encouraged for future missions (Peral et al., 2019).

RS models can reasonably estimate average ET rates in the AB, but correctly representing ET seasonality is still a challenge, as well as understanding differences among individual ET components as soil evaporation, transpiration and interception. More studies are needed to disentangle the controls of ET across the basin (water and energy limitation, and vegetation phenology), since multiple drivers operate simultaneously (Maeda et al., 2017). Besides, a major knowledge gap is the difference between ET in Amazon uplands and wetlands, and the effect of open water evaporation on the regional climate. Current satellite-based models need to minimize the use of parameterization (or better constrain it), while the accuracy of input data must be improved. A major limitation of SEB models is their requirement of clear sky conditions, which may be improved by the use of microwave data (Holmes et al., 2018) and the combination with other types of ET models as those based on vegetation index models. In situ measurements are fundamental to achieve this goal, yet today there are only eight flux towers with publicly available data in the AB. For vegetation index-based models (e.g., MOD16, GLEAM), improving the understanding of soil water deficit controls on ET across the basin is also necessary, given the high dependence of these products on soil moisture content. Some breakthrough ongoing and future missions will provide a new understanding of ET dynamics in AB. The ECOSTRESS is addressing the response of vegetation to water deficit with unprecedented details, while the VIIRS collects visible and infrared imagery, extending the time series from its predecessor MODIS and improving its estimates, and the FLEX mission will map vegetation fluorescence, a proxy of photosynthetic activity and vegetation stress and health. The continuity of the Landsat missions will ensure the development of long-term ET at high spatial scale, while the GRACE-FO mission will provide new data for water balance approaches to estimate ET. This will ultimately allow us to model ET at high spatial resolution (< 30 meters) and for long time periods (> 40 years).

The surface water bodies and aquatic ecosystems of AB are still challenging the current available RS observations. Despite the substantial progress in the last decades, there are still limitations. Currently, there is a trade-off over AB between spatial and temporal resolutions in satellite observations, with generally high temporal sampling associated with lower spatial resolution and vice-versa. Therefore, there is a need for finer spatio-temporal resolution to adequately monitor water extent, level and slope of the surface water and floodplain inundation. There is also a need to improve the accuracy of these estimates in order to understand more local phenomena, such as floodplain-river exchanges and dynamics or the complex flooding processes of extensive interfluvial areas. Similarly, only few lakes and reservoirs in AB are monitored routinely from space, using altimetry for instance. The context of the AB, with dense vegetation and cloud cover, makes it still challenging to monitor surface waters such as permanently or seasonally flooded forests and floating herbaceous plants.

The forthcoming NASA/ISRO L-band SAR mission, with its combination of radar wavelengths and polarizations and 12-day orbit passes, will help to precisely measure small changes of SWE in AB, including areas with standing vegetation. Furthermore, with its technology based on swath altimetry from the KaRIn, quasi-global coverage and joint observation of surface water elevation, extent, river width and slope, the SWOT mission, to be launched in 2022, will permit an unprecedented monitoring of AB surface water and rivers at

100 m resolution in two horizontal dimensions. The centimetric accuracy in SWE and slope (Desai, 2018) will help to better characterize freshwater fluxes in the AB. The current satellite altimetry missions, especially the Copernicus program, is now setting the era of operational monitoring from space at large scale for the coming decades, with clear benefits for large tropical transboundary watersheds such as AB. With nearly two thousand virtual stations distributed over the basin, potentially hundreds more, freely available on multiple websites, conventional satellite altimetry can favorably complement the traditional and necessary in situ network. Since the main limitation for a broader use of current satellite altimetry remains its relatively low temporal sampling, future missions in development, such as SMASH (Blumstein et al., 2019), broadcasted together with the current constellation, should help to tackle this issue. Further developments in satellite observations are nevertheless required to fully characterize AB surface water extent and elevation and should combine, in the future, the benefits of SWOT swath global measurements with high temporal sampling of SMASH-like constellation, into a SWOT-like satellite constellation providing global and daily observations.

Besides the concept of new satellite missions, it is worth noticing that the upcoming unprecedented availability of information regarding AB surface water extent and elevations will challenge the current analysis capabilities. New development of analysis tools or fusion techniques with artificial intelligence to combine various RS observations (visible, IR, MW, GNSS-R) are needed. Similarly, new techniques for fusion with local to regional modeling, data assimilation and better constraining of uncertain hydraulics should also dramatically increase our capacity to model the AB and the variations of its water cycle.

Floodplain and river channel topography have not yet been fully characterized in the AB, despite recent efforts with local and regional estimates, preventing a better understanding of habitats related to flood pulse and limiting the accuracy of hydraulic models. In addition, the association between sediment concentration in rivers and channel migration is still poorly understood (Constantine et al., 2014). The development of new techniques and RS data for topography mapping are needed. The main challenge is vegetation removal, as many sensors do not have the ability to penetrate vegetation. LiDAR and altimetric data, such as ICESat-2 (launched in 2018), which allow bare earth mapping, have still been little exploited in the AB for this task. Furthermore, NISAR and SWOT satellites will open opportunities with more accurate estimates of the surface water extent and distributed SWE over water bodies. Thus, new methodologies for topographic mapping, such as the waterline method (Salameh et al., 2019) and Flood2Topo (Fassoni-Andrade, Paiva, & Fleischmann, 2020) can be better developed.

White, black and clear water rivers of AB have particular characteristics with large variation of COA (sediment, chlorophyll and CDOM). Despite the development of many algorithms for estimating these components, little has been explored to implement those algorithms to address scientific questions, as also reported by Topp et al. (2020) worldwide. Sediment concentration estimates could be better exploited to assess the effects of dams, mining, and land use changes in the AB. In addition, the characterization of natural processes, such as the spatio-temporal variation of phytoplankton in lakes, has not been widely explored. On the other hand, there are still technical challenges for these estimates using RS data, such as the high cloud cover in the AB. The main challenge is the discretization of the COA spectra, which can be partially overcome with new sensors with high radiometric and spectral resolution.

The recent launch of the GRACE-FO mission offers an opportunity to extend the monitoring of TWS and GWS changes over more than two decades, allowing to start analyzing the impact of multi-year climatic events such as ENSO on land and groundwater storages over AB. The major drawbacks of these data remain their low spatial and temporal (~200 km and 1 month) resolutions which are not sufficient to study the dynamics of more local and rapid hydrological events. To overcome these drawbacks, the GRACE-FO payload contains advanced versions of the sensors used on-board GRACE, allowing a better expected accuracy to improve the quality and the spatial resolution of the retrieved TWSA. Combined with new methodological approaches based on the use of Kalman filter, it should increase the TWSA temporal resolution to quasi-daily without degrading the spatial resolution (Ramillien et al., 2015, 2020). With the upcoming availability of SWOT observations, unprecedented and finer estimates of surface water storage over large areas will improve the determination of GWS anomalies and will allow us to better understand the interactions between flood dynamics and aquifer recharge in the AB. Groundwater exchange in the AB, which remains poorly characterized with satellites, should also benefit from the integration of these new observations, and could be further estimated in better constraining the water budget at the surface. A comprehensive set of observations dedicated to hydrology, with the continuity of the current satellite missions, is mandatory to improve our understanding of hydrology patterns through more precise water budget analyses and to assess long-term trends.

Given the uncertainties in both hydrological models and RS estimates, model calibration and data assimilation techniques have been recently developed by incorporating mainly water level (satellite altimetry) data and, to a lesser extent, GRACE TWS. Other variables to be better assimilated are flood extent and storage, soil moisture and evapotranspiration. While most hydrologic and hydraulic model applications have been used to estimate variables such as evapotranspiration, soil water storage, river discharge, surface water elevation and extent, new studies must investigate other variables such as water velocity and flood storage. There is also a lack of convergence among water storage partitions (e.g., divergent estimates of surface water fraction), which must be addressed by better constraining models with EO observations, and by performing model intercomparison projects. On the other hand, while the Amazon wetlands were mainly studied for the central Amazon river floodplains, other types of wetlands do exist, as the interfluvial ones in large areas of the Llanos de Moxos, Pacaya-Samiria and Negro, and deserve more efforts from the hydrological community, especially considering their particular flood dynamics, more dependent on local rainfall. Furthermore, high resolution 2D modelling of the full Amazon mainstem mapping velocity fields and detailed river-floodplain interactions was still not explored. The downstream part of the AB also remains relatively unexplored in terms of hydrodynamic modelling and RS, e.g., the relative roles of the upstream forcing and the oceanic influence on the dynamics of the river-estuary-ocean continuum. In addition to a better representation of hydrological processes, e.g., groundwater dynamics which is poorly represented in surface hydrology-oriented models, the future of hydrologic-hydrodynamic models is largely dependent on the growing availability of new EO data. These include SWOT-derived water levels and discharges, channel water widths, floodplain topography, soil moisture (e.g., SMOS, SMAP), precipitation (e.g., SM2RAIN), gravimetry (GRACE-FO), and techniques to retrieve groundwater storages (e.g., Frappart et al., 2019). These data will promote the basis for modeling estimates at high temporal and spatial resolution, aiming ultimately at providing locally relevant hydrological estimates everywhere (Bierkens et al., 2015; Wood et al., 2011).

While most major components of the water cycle have been relatively well addressed in the literature as shown along this review, soil moisture stands out as the less reliable component. This relates to the difficulty to retrieve this variable under densely vegetated areas (Prigent et al., 2005). The relatively poor performance of current soil moisture datasets (e.g., SMAP, AMSR-E and SMOS) on these environments is well known, even when products are combined (Y. Y. Liu et al., 2011) or merged (F Aires et al., 2005; Kolassa et al., 2016). Most soil moisture-oriented studies were performed with hydrological models and in situ data, in a few headwater locations. Moreover, there is an inherent ambiguity in passive microwave observations between water-saturated soils and surface waters. As a consequence, the large surface water fraction in AB affects the soil moisture retrievals by this type of observations. This ambiguity in the satellite observation has triggered the development of a product such as SMOS-based surface water product (Parrens et al., 2017). There is an urgent need to better monitor soil moisture at different spatial-temporal resolutions in the AB, especially considering its major role in controlling the Amazon forest dynamics and phenology, evapotranspiration, and the water cycle in general. This observation supports the development of SMOS-HR, the High Resolution follow-on mission of SMOS, which is currently undergoing feasibility study by the French space agency and which goal is to ensure continuity of L-band measurements while increasing the spatial resolution to ~10 km without degrading the radiometric sensitivity and keeping the revisit time of 3 days unchanged.

Similarly, river discharge, which is historically one of the first hydrological variables that has been observed in situ is still not properly measured from space. This review stresses that there is a need to accurately estimate river discharge using RS in AB with fine spatial and temporal resolution. River discharge has already been estimated indirectly by RS data (e.g., Brakenridge et al., 2007; LeFavour & Alsdorf, 2005; Tarpanelli et al., 2013; Zakharova et al., 2006), but still poorly complements the current in situ network of AB. Upcoming missions, such as SWOT, in combination with current satellite missions, will soon help us move toward a more comprehensive monitoring of river discharge in AB.

The ongoing and future environmental alterations in the AB urge the understanding of the basin hydrology under the perspective of a changing system. The long term effects of multiple human impacts (land use change, climate change, damming, mining, fires) on the Amazon must be better understood. Changes in land-atmosphere feedback due to deforestation will affect the AB water cycle, but the extent is still under debate. There is relatively little understanding of how these interact, especially in terms of how the impact of land-use changes in local climate can be different under large scale meteorological conditions that are changing with the global climate (e.g., Leite-Filho et al., 2020) and how these would affect the land and water ecosystems in the basin. Furthermore, techniques to map forest degradation and discern primary and secondary vegetation are still relatively new, and the impacts of those subtler but pervasive land-use changes on AB hydrology is yet to be understood. Finally, although the influence of the Amazon forest on the hydroclimate outside the AB has been increasingly documented, the consequences of its deforestation and degradation outside the basin is yet to be understood.

Furthermore, the proliferation of dams in tropical basins as the Amazon, Congo and Mekong require basin-scale planning and analysis tools to foster mutual benefits in understanding these changes (e.g. Latrubesse et al., 2017; Schmitt et al., 2019; Winemiller et al., 2016), and RS data stand out as powerful tool to monitor large scale impacts of existing man-

made reservoirs (e.g., Resende et al., 2019), and infer their characteristics, such as water level and stage-area-volume relationships (e.g., Fassoni-Andrade, Paiva, & Fleischmann, 2020; Gao et al., 2012). Better data and knowledge of these impacts are also the base for better hydro-geomorphological models that could be used to quantify the expected impacts of planned reservoirs and therefore aid in creating designs that minimize environmental impacts.

7.4. How to use RS-based scientific advances to foster water resources management in the Amazon basin?

While the AB served as an important laboratory for RS development that produced significant scientific advances related to its hydrological processes in the last decades (**Table 7** and **Table 8**), the Amazon currently undergoing extensive anthropogenic pressure (Section 6.4), and urgently calls for better basin-scale water resources planning and new environment monitoring tools. RS has the potential to democratize essential information for decision makers, for instance to monitor "politically ungauged" regions where information is not publicly available (Gleason & Durand, 2020). Although RS is now a reality and documented knowledge on the AB is much better than decades ago, there is still an open road to move all these advances towards effective applications in decision making and water resources management.

Deforestation and fire monitoring may be the most advanced and promising example in the context of AB environmental management. Since 1988, satellite-based monitoring systems using MODIS, Landsat and CBERS imagery as the DETER (Diniz et al., 2015, http://www.obt.inpe.br/OBT/assuntos/programas/amazonia/deter/), PRODES (http://www.obt.inpe.br/OBT/assuntos/programas/amazonia/prodes), Imazon (https://imazon.org.br/categorias/boletim-do-desmatamento/) and Queimadas (http://queimadas.dgi.inpe.br/queimadas/portal) have been systematically supporting local governments and NGOs on the monitoring and control of deforestation and fires. Technical advances made it possible to monitor deforestation in near real time, on the scale of days, weeks, or months. However, institution building, along with related civil-society engagement, is still needed to facilitate effective actions within complex government frameworks and bridge the gap between technology and policy towards deforestation reduction (Finer et al., 2018).

Amazon neighborhood countries have mature Water Resources Agencies, Geology and Hydrometeorological Services as the ANA, the Peruvian and Bolivian National Meteorology and Hydrology Services (SENAMHIs) and the Brazilian Geological Survey (CPRM). These institutions have dedicated efforts on the challenging task of systematic in situ monitoring of Amazon vast territory and rivers and promoting open hydrological datasets. In this sense, RS is starting to be incorporated into operational monitoring (e.g., SIPAM http://hidro.sipam.gov.br/, Hidrosat, J. C. Carvalho et al., 2015; near real-time flood simulations at sub-daily scale, Llauca et al., 2021). In particular, precipitation has been widely monitored through RS data by multiple meteorological agencies, while other water cycle variables have received less attention. These organizations have been developing technical reports about the national situation and water resources planning including the AB (e.g., Water Resources Situation Report, Agência Nacional de Águas, 2019a; National Water Security Plan, Agência Nacional de Águas, 2019b; flow forecasts at national level and at hourly and daily scale by SENAMHI Peru available at: https://www.senamhi.gob.pe/?&p=pronostico-caudales). Currently, they are mostly supported by

the national hydrometeorological networks that are still scarce and could be greatly enhanced with the data and knowledge produced by RS. Some of these countries also have advanced Water Resources Laws and regulation, such as the Brazilian National Water Resources Management System created by Law 9433, 1997 (Brasil, 1997), but most of the efforts on the development and implementation of such regulation is devoted to river basins in more densely populated regions and not in the context of the complexity of the international/transboundary and larger river basin of the world. Also, even though AB is in the epicenter of international scientific discussion, it appears not to be the main focus of technical and scientific developments on the water resources field in the Amazon countries, as revealed by recent synthesis of advances from Brazilian water community (Paiva, 2020).

Most flooding studies in the Amazon have aimed at understanding ecosystem services and the natural system (Sections 4.2 and 6.2), but many Amazon urban centers are under flood risk (e.g., Amazon River at Iquitos, Madeira River at Porto Velho, Acre River at Rio Branco, Juruá river at Cruzeiro do Sul), and suffer annually from overbanking flow (Fleischmann et al., 2020). While this paper is being drafted, the Brazilian Acre state is recovering from a humanitarian crisis caused by floods at Acre River at Rio Branco and Juruá River at Cruzeiro do Sul, enhanced by the COVID-19 pandemic. Thus, the several developed flood monitoring tools could be translated into effective flood risk mapping and real-time monitoring for disaster management. International initiatives such as the Copernicus Emergency Management Service (https://emergency.copernicus.eu/) and the International Charter “Space and Major Disasters” (https://disasterscharter.org/) have the potential to provide important EO data for real-time disaster management. Furthermore, the transboundary character of many Amazon sub-basins (e.g., Madeira River, with floods at Porto Velho in Brazil being partially generated in upstream Bolivian reaches) makes RS data a fundamental tool to fulfill the disparity in data availability among countries. On the other hand, in many areas of the Amazon, droughts have a larger societal impact than floods, given the adaptation of livelihoods to the annual flooding regime, and the interruption of provision of goods and general transport through rivers during extremely dry periods (Zeng et al., 2008). Recent technical efforts include evaluation of hydrological forecasts from physically based hydrological models supported by RS (Section 6.2), development of site specific statistical forecasting and real-time monitoring systems (e.g. SACE system from http://www.cprm.gov.br/sace/; systems available for the Madeira, Acre, Xingu, Branco and some reaches of the Amazon mainstem), prototypes of hydrological model based monitoring systems (e.g. South America River Discharge Monitor - SARDIM https://sardim.herokuapp.com/; G. G. dos Reis et al., 2020), global flood forecast systems (e.g. GLOFAS, Alfieri et al., 2013) and efforts on monitoring and alerts of natural hazards by centers as CEMADEN from Brazil (Centro Nacional de Alerta e Monitoramento de Desastres Naturais). Drought monitor systems based on in situ and RS-based observations and local community interpretation (e.g., ANA Drought Monitor http://monitordesecas.ana.gov.br/) are evolving and there are no operational hydrological forecasting systems at the AB, national or continental scales (Fan et al., 2016).

Impacts from human activities may propagate through the Amazon River network and neighbor countries, since the ongoing developments of hydropower projects and agricultural expansion alter the hydrological, sediments and ecosystem dynamics (Anderson de Castro et al., 2018; Forsberg et al., 2017). Recent research has explored integrated planning looking for the best hydropower development solutions (Almeida et al., 2020; Winemiller et al., 2016), while

organizations as the Amazon Cooperation Treaty Organization aim at promoting sustainable development of the AB with the participation of its neighborhood countries. However, current national scale policies and regulation do not promote fully integrated water resources planning, as new projects are usually accessed individually. RS can definitely encourage a common and transparent understanding of AB water related issues.

The RS scientific community has now the challenge to promote knowledge, datasets and applications on water-environmental changes, aiming at enhanced water resources management and planning. Potential pathways include: (i) training decision makers and multiple stakeholders on the language of RS (e.g., Applied Remote Sensing Training Program - ARSET https://appliedsciences.nasa.gov/what-we-do/capacity-building/arset); (ii) encouraging local engagement by bridging the gap between RS based science and in situ and traditional knowledge (Runde et al., 2020); (iii) initiatives of science communication and citizen science (Buytaert et al., 2014; e.g. www.amazoniacienciaciudadana.org/, https://www.ufrgs.br/conexoesamazonicas/ , https://ipam.org.br/biblioteca/?biblioteca=artigos-cientificos, https://imazon.org.br/categorias/outros/, https://infoamazonia.org/) (iii) development of open access datasets focused on specific applications (e.g. aquatic ecosystem conservation, Venticinque et al., 2016); (iv) developing monitoring systems focused on environmental changes and water related disasters; (v) developing open hydrological repositories (e.g. HYBAM, https://hybam.obs-mip.fr/, SERVIR-Amazonia, https://servir.ciat.cgiar.org/); (vi) developing a basin-scale research agenda focused on directly supporting water resources decision making (e.g. scenarios of hydropower development; Almeida et al., 2020).

7.5. Recommendations

Based on the knowledge gaps and the perspectives presented in the previous sections, we provide the following recommendations for the future studies on Amazon waters from space.

Recommendation 1: Observations

Current limitations of satellite data for AB are often related to the space-time resolution (e.g., SWE and slope, surface water extent, ET), time span (e.g., surface water extent, TWS, GWS, ET, topography) and accuracy (e.g., surface water extent, GWS anomalies). The largest limitations so far in monitoring the AB hydrology from space refer to soil moisture and river discharge, which have been poorly addressed due to vegetation interference in sensors or by the nature of the variable, respectively, which hampers its estimation from the space. The increasing availability of long term archives of RS datasets should be ensured by national space and water agencies, in complement to existing in situ monitoring networks, which are fundamental to properly calibrate and validate RS estimates. Latency time of RS data distribution (e.g., precipitation and SWE) should be reduced to a few hours to be used by water/risk management. Ensuring satellite observation to be archived into climatic datasets can foster the understanding the impacts of climate change and human activities on the basin.

Recommendation 2: Models, algorithms and integration

Technical limitations are related to the development of algorithms (e.g., orographic rains, CDOM and chlorophyll retrieval, water budget closure, hydrodynamic models), and data fusion (e.g., ET, SWE, surface water extent). The recognition of uncertainties in multiple RS data and

trade-offs between temporal and spatial resolution point to the need of more integrative approaches, e.g., for mapping long term flooding and evapotranspiration patterns at high spatio-temporal resolutions, and artificial intelligence will play a major role in this. The better coupling of EO datasets with hydrological-hydraulic models and land surface models (e.g., data assimilation, spatiotemporal interpolation) is also a necessary step forward in Earth System modeling, by considering the dynamic aspect of AB hydrology.

Recommendation 3: Characterization of hydrological processes in a changing Amazon

Upcoming and future satellite observations will bring new opportunities for the AB regarding the characterization of natural processes, including phytoplankton in waters, floodplain topography, aquatic ecosystems, groundwater dynamics, as well as the monitoring of anthropogenic environmental changes. The development of long term datasets is fundamental to understand Amazon hydrological processes across multiple decades. While RS data currently focus on a set of a few hydrological variables, there are many others that require more attention from the hydrologic community, such as river discharge and water velocity, surface and groundwater storage, soil moisture, CDOM and Chlorophyll-a. Most studies in the AB also focus on a few areas (e.g., the várzea environment in the central Amazon floodplains), and many other complex river-wetland systems or streams and small rivers, especially in Andean region, also require attention.

Recommendation 4: Towards the use of RS to support sustainable science in AB

The AB harbors an incredibly large and still poorly known biodiversity, which provides massive ecosystem services for the globe, as well as some of the most complex and intriguing river-wetland systems in the world. While EO through satellites has provided breakthrough scientific advances on the comprehension of the AB water cycle in the last decades, the forthcoming years with the new hydrology-oriented missions will provide a new milestone on the monitoring of Amazon waters from space. Advance knowledge from RS should be translated into valuable information and indicators to support environmental governance and sustainable science in AB. RS has the potential to democratize essential information for decision makers, moving towards a more sustainable future for the largest basin in the world.

Acknowledgments

We thank Thiago Laranjeiras and the Mamirauá Institute for Sustainable Development for providing the photographs in **Figure 1**. We thank Dr. Mark Trigg and Dr. Conrado Rudorff for providing topographic mapping of the Amazon floodplain (**Figure 7**) and flood maps for the Curuai Lake (**Figure 11**), respectively.

A.C.F-A is supported by EOSC-SYNERGY project (grant number 857647). A.S.F. is supported by the CNPq via grants 141161/2017-5 and 201148/2019-6. J.M.M. received support from NASA (Contract NNX17AK49G) and US National Science Foundation (Division of Environmental Biology, grant number 1753856). F.P., A.P., F.F., F.D., J.F.F. and S.C. received support from CNES (SWOT-ST project SWOT for SOUTH AMERICA, ID: 6018-4500066497). FF and FP also received support from CNES (SWOT-ST project SWOT Wetlands Hydrology Monitoring). F.P., A.P., F.F., F.D. and S.C. are supported by the IRD Groupement De Recherche International SCaHyLab. S.W. and J.C.E. are supported by the French AMANECER-MOPGA

project funded by ANR and IRD (ref. ANR-18-MPGA-0008). V.P was partially supported by the JSPS Kakenhi (N°16H06291) and the French Centre National d'Etudes Spatiales (CNES). G.A. received support from CNPq, process 142230/2017-0. A.A.M is supported from CNPq, process number 141979/2017-8. A.R. is supported by the ANA and by the CAPES Foundation, grant number 88881.178687/2018-01.

Data Availability Statement

This is a review paper, for which no new data was generated. Data supporting the figures are available via the cited references.

References

Abe, C. A., Lobo, F. L., Novo, E. M. L. de M., Costa, M., & Dibike, Y. (2019). Modeling the effects of land cover change on sediment concentrations in a gold-mined Amazonian basin. *Regional Environmental Change*, *19*, 1801–1813. https://doi.org/10.1007/s10113-019-01513-8

Abril, G., Martinez, J. M., Artigas, L. F., Moreira-Turcq, P., Benedetti, M. F., Vidal, L., et al. (2014). Amazon River carbon dioxide outgassing fuelled by wetlands. *Nature*, *505*(7483), 395–398. https://doi.org/10.1038/nature12797

Aceituno, P. (1988). On the Functioning of the Southern Oscillation in the South American Sector. Part I: Surface Climate. *Monthly Weather Review*, *116*(3), 505–524. https://doi.org/10.1175/1520-0493(1988)116<0505:OTFOTS>2.0.CO;2

Adderio, L. P. D., Puca, S., Vulpiani, G., Petracca, M., San, P., & Dietrich, S. (2020). RAINBOW : An Operational Oriented Combined IR-Algorithm, 1–21.

Adler, R. F., Huffman, G. J., & Keehn, P. R. (1994). Global tropical rain estimates from microwave-adjusted geosynchronous IR data. *Remote Sensing Reviews*. https://doi.org/10.1080/02757259409532262

Agência Nacional de Águas. (2019a). *Conjuntura dos recursos hídricos no Brasil 2019*. Brasília. Retrieved from http://conjuntura.ana.gov.br/static/media/conjunturacompleto.bb39ac07.pdf

Agência Nacional de Águas. (2019b). *Plano Nacional de Segurança Hídrica*. Brasília. Retrieved from http://arquivos.ana.gov.br/pnsh/pnsh.pdf

Aires, F, Prigent, C., & Rossow, W. B. (2005). Sensitivity of satellite microwave and infrared observations to soil moisture at a global scale: 2. Global statistical relationships. *Journal of Geophysical Research: Atmospheres*, *110*(D11). https://doi.org/https://doi.org/10.1029/2004JD005094

Aires, Filipe. (2014). Combining Datasets of Satellite-Retrieved Products. Part I: Methodology and Water Budget Closure. *Journal of Hydrometeorology*, *15*(4), 1677–1691. https://doi.org/10.1175/JHM-D-

13-0148.1

Aires, Filipe, Papa, F., & Prigent, C. (2013). A long-term, high-resolution wetland dataset over the amazon basin, downscaled from a multiwavelength retrieval using SAR data. *Journal of Hydrometeorology*, *14*(2), 594–607. https://doi.org/10.1175/JHM-D-12-093.1

Aires, Filipe, Miolane, L., Prigent, C., Pham, B., Fluet-Chouinard, E., Lehner, B., & Papa, F. (2017). A global dynamic long-term inundation extent dataset at high spatial resolution derived through downscaling of satellite observations. *Journal of Hydrometeorology*, *18*(5), 1305–1325. https://doi.org/10.1175/JHM-D-16-0155.1

Aires, Filipe, Prigent, C., Fluet-Chouinard, E., Yamazaki, D., Papa, F., & Lehner, B. (2018). Comparison of visible and multi-satellite global inundation datasets at high-spatial resolution. *Remote Sensing of Environment*, *216*(2018), 427–441. https://doi.org/10.1016/j.rse.2018.06.015

Alcântara, E., Barbosa, C., Stech, J., Novo, E., & Shimabukuro, Y. (2009). Improving the spectral unmixing algorithm to map water turbidity Distributions. *Environmental Modelling and Software*, *24*(9), 1051–1061. https://doi.org/10.1016/j.envsoft.2009.02.013

Alfieri, L., Burek, P., Dutra, E., Krzeminski, B., Muraro, D., Thielen, J., & Pappenberger, F. (2013). GloFAS - global ensemble streamflow forecasting and flood early warning. *Hydrology and Earth System Sciences*, *17*(3), 1161–1175. https://doi.org/10.5194/hess-17-1161-2013

Alkama, R., Decharme, B., Douville, H., Becker, M., Cazenave, A., Sheffield, J., et al. (2010). Global evaluation of the ISBA-TRIP continental hydrological system. Part I: Comparison to GRACE terrestrial water storage estimates and in situ river discharges. *Journal of Hydrometeorology*. https://doi.org/10.1175/2010JHM1211.1

Allen, G. H., & Pavelsky, T. (2018). Global extent of rivers and streams. *Science*, *361*(6402), 585–588. https://doi.org/10.1126/science.aat063

Allen, R. G., Tasumi, M., & Trezza, R. (2007). Satellite-Based Energy Balance for Mapping Evapotranspiration with Internalized Calibration (METRIC)—Model. *Journal of Irrigation and Drainage Engineering*, *133*(4), 380–394. https://doi.org/10.1061/(asce)0733-9437(2007)133:4(380)

Allen, R. G., Irmak, A., Trezza, R., Hendrickx, J. M. H., Bastiaanssen, W., & Kjaersgaard, J. (2011). Satellite-based ET estimation in agriculture using SEBAL and METRIC. *Hydrological Processes*, *25*(26), 4011–4027. https://doi.org/10.1002/hyp.8408

Almeida, R. M., Tranvik, L., Huszar, V. L. M., Sobek, S., Mendonça, R., Barros, N., et al. (2015). Phosphorus transport by the largest Amazon tributary (Madeira River, Brazil) and its sensitivity to precipitation and damming. *Inland Waters*, *5*(3), 275–282. https://doi.org/10.5268/IW-5.3.815

Almeida, R. M., Hamilton, S. K., Rosi, E. J., Barros, N., Doria, C. R. C., Flecker, A. S., et al. (2020).

3030 Hydropeaking Operations of Two Run-of-River Mega-Dams Alter Downstream Hydrology of the
3031 Largest Amazon Tributary. *Frontiers in Environmental Science*, *8*, 120.
3032 https://doi.org/10.3389/fenvs.2020.00120
3033 Alsdorf, D. (2003). Water Storage of the Central Amazon Floodplain Measured with GIS and Remote
3034 Sensing Imagery. *Annals of the Association of American Geographers*, *93*(1), 55–66.
3035 https://doi.org/10.1111/1467-8306.93105
3036 Alsdorf, D., Melack, J. M., Dunne, T., Mertes, L. A. K., Hess, L. L., & Smith, L. C. (2000).
3037 Interferometric radar measurements of water level changes on the Amazon flood plain. *Nature*,
3038 *404*(March), 174–177. https://doi.org/10.1038/35004560
3039 Alsdorf, D., Smith, L. C., & Melack, J. M. (2001). Amazon floodplain water level changes measured with
3040 interferometric SIR-C radar. *IEEE Transactions on Geoscience and Remote Sensing*, *39*(2), 423–
3041 431. https://doi.org/10.1109/36.905250
3042 Alsdorf, D., Birkett, C., Dunne, T., Melack, J., & Hess, L. (2001). Water level changes in a large Amazon
3043 lake measured with spaceborne radar interferometry and altimetry. *Geophysical Research Letters*,
3044 *28*(14), 2671–2674. https://doi.org/10.1029/2001GL012962
3045 Alsdorf, D., Dunne, T., Melack, J., Smith, L., & Hess, L. (2005). Diffusion modeling of recessional flow
3046 on central Amazonian floodplains. *Geophysical Research Letters*, *32*(21), 1–4.
3047 https://doi.org/10.1029/2005GL024412
3048 Alsdorf, D., Bates, P., Melack, J., Wilson, M., & Dunne, T. (2007). Spatial and temporal complexity of
3049 the Amazon flood measured from space. *Geophysical Research Letters*, *34*(8), 1–5.
3050 https://doi.org/10.1029/2007GL029447
3051 Alsdorf, D., Han, S. C., Bates, P., & Melack, J. (2010). Seasonal water storage on the Amazon floodplain
3052 measured from satellites. *Remote Sensing of Environment*, *114*(11), 2448–2456.
3053 https://doi.org/10.1016/j.rse.2010.05.020
3054 Alsdorf, D., Beighley, E., Laraque, A., Lee, H., Tshimanga, R., O'Loughlin, F., et al. (2016).
3055 Opportunities for hydrologic research in the Congo Basin. *Reviews of Geophysics*, *54*(2), 378–409.
3056 https://doi.org/10.1002/2016RG000517
3057 Alsdorf, D., Tshimanga, R. M., & Moukandi, G. D. (Eds.). (2021). *Congo Basin Hydrology, Climate, and*
3058 *Biogeochemistry: A Foundation for the Future*. Wiley-AGU.
3059 Amaral, J. H. F., Melack, J. M., Barbosa, P. M., MacIntyre, S., Kasper, D., Cortés, A., et al. (2020).
3060 Carbon Dioxide Fluxes to the Atmosphere From Waters Within Flooded Forests in the Amazon
3061 Basin. *Journal of Geophysical Research: Biogeosciences*, *125*(3).
3062 https://doi.org/10.1029/2019JG005293

3063 Anderson, A. B., May, P. H., & Balick, M. J. (1991). The subsidy from nature: palm forests, peasantry,
3064 and development on an Amazon frontier. In *The subsidy from nature: palm forests, peasantry, and*
3065 *development on an Amazon frontier*. Columbia University Press. https://doi.org/10.1016/0169-
3066 5347(92)90157-7
3067 Anderson de Castro, A., Cuartas, L. A., Coe, M. T., Von Randow, C., Castanho, A., Ovando, A., et al.
3068 (2018). Coupling the terrestrial hydrology model with biogeochemistry to the integrated LAND
3069 surface model: Amazon Basin applications. *Hydrological Sciences Journal*, *63*(13–14), 1954–1966.
3070 https://doi.org/10.1080/02626667.2018.1538592
3071 Anderson, M. C., Norman, J. M., Diak, G. R., Kustas, W. P., & Mecikalski, J. R. (1997). A two-source
3072 time-integrated model for estimating surface fluxes using thermal infrared remote sensing. *Remote*
3073 *Sensing of Environment*, *60*(2), 195–216. https://doi.org/10.1016/S0034-4257(96)00215-5
3074 Andriambeloson, J. A., Paris, A., Calmant, S., & Rakotondraompiana, S. (2020). Re-initiating depth-
3075 discharge monitoring in small-sized ungauged watersheds by combining remote sensing and
3076 hydrological modelling: a case study in Madagascar. *Hydrological Sciences Journal*, *65*(16), 2709–
3077 2728. https://doi.org/10.1080/02626667.2020.1833013
3078 Angelis, C. F., McGregor, G. R., & Kidd, C. (2004). Diurnal cycle of rainfall over the Brazilian Amazon.
3079 *Climate Research*, *26*(2), 139–149. https://doi.org/10.3354/cr026139
3080 Aragão, L. E. O. ., Malhi, Y., Barbier, N., Lima, A., Shimabukuro, Y., Anderson, L., & Saatchi, S.
3081 (2008). Interactions between rainfall, deforestation and fires during recent years in the Brazilian
3082 Amazonia. In *Philosophical Transactions of the Royal Society B: Biological Sciences* (Vol. 363, pp.
3083 1779–1785). https://doi.org/10.1098/rstb.2007.0026
3084 Arantes, C. C., Winemiller, K. O., Petrere, M., Castello, L., Hess, L. L., & Freitas, C. E. C. (2018).
3085 Relationships between forest cover and fish diversity in the Amazon River floodplain. *Journal of*
3086 *Applied Ecology*, *55*(1), 386–395. https://doi.org/10.1111/1365-2664.12967
3087 Arias, M. E., Lee, E., Farinosi, F., Pereira, F. F., & Moorcroft, P. R. (2018). Decoupling the effects of
3088 deforestation and climate variability in the Tapajós river basin in the Brazilian Amazon.
3089 *Hydrological Processes*, *32*(11), 1648–1663. https://doi.org/10.1002/hyp.11517
3090 Arias, M. E., Farinosi, F., Lee, E., Livino, A., Briscoe, J., & Moorcroft, P. R. (2020). Impacts of climate
3091 change and deforestation on hydropower planning in the Brazilian Amazon. *Nature Sustainability*,
3092 *3*(6), 430–436. https://doi.org/10.1038/s41893-020-0492-y
3093 Arias, P. A., Fu, R., Vera, C., & Rojas, M. (2015). A correlated shortening of the North and South
3094 American monsoon seasons in the past few decades. *Climate Dynamics*, *45*(11–12), 3183–3203.
3095 https://doi.org/10.1007/s00382-015-2533-1

3096 Arias, P. A., Garreaud, R., Poveda, G., Espinoza, J. C., Molina-Carpio, J., Masiokas, M., et al. (2021).
3097 Hydroclimate of the Andes Part II: Hydroclimate Variability and Sub-Continental Patterns.
3098 *Frontiers in Earth Science*, *8*(February), 666. https://doi.org/10.3389/feart.2020.505467
3099 Armijos, E., Crave, A., Espinoza, J. C., Filizola, N., Espinoza-Villar, R., Ayes, et al. (2020). Rainfall
3100 control on Amazon sediment flux: synthesis from 20 years of monitoring. *Environmental Research*
3101 *Communications*, *2*(5), 051008. https://doi.org/10.1088/2515-7620/ab9003
3102 Arnesen, A. S., Silva, T. S. F. F., Hess, L. L., Novo, E. M. L. M. L. M., Rudorff, C. M., Chapman, B. D.,
3103 & McDonald, K. C. (2013). Monitoring flood extent in the lower Amazon River floodplain using
3104 ALOS/PALSAR ScanSAR images. *Remote Sensing of Environment*, *130*, 51–61.
3105 https://doi.org/10.1016/j.rse.2012.10.035
3106 Arvor, D., Funatsu, B. M., Michot, V., & Dubreui, V. (2017). Monitoring rainfall patterns in the southern
3107 amazon with PERSIANN-CDR data: Long-term characteristics and trends. *Remote Sensing*, *9*(9).
3108 https://doi.org/10.3390/rs9090889
3109 Ashouri, H., Hsu, K. L., Sorooshian, S., Braithwaite, D. K., Knapp, K. R., Cecil, L. D., et al. (2015).
3110 PERSIANN-CDR: Daily precipitation climate data record from multisatellite observations for
3111 hydrological and climate studies. *Bulletin of the American Meteorological Society*, *96*(1), 69–83.
3112 https://doi.org/10.1175/BAMS-D-13-00068.1
3113 Asner, G. P. (2001). Cloud cover in Landsat observations of the Brazilian Amazon. *International Journal*
3114 *of Remote Sensing*, *22*, 3855–3862. https://doi.org/10.1080/01431160010006926
3115 Avila-Diaz, A., Benezoli, V., Justino, F., Torres, R., & Wilson, A. (2020). Assessing current and future
3116 trends of climate extremes across Brazil based on reanalyses and earth system model projections.
3117 *Climate Dynamics*, (2017). https://doi.org/10.1007/s00382-020-05333-z
3118 Aybar, C., Fernández, C., Huerta, A., Lavado, W., Vega, F., & Felipe-Obando, O. (2019). Construction of
3119 a high-resolution gridded rainfall dataset for Peru from 1981 to the present day. *Hydrological*
3120 *Sciences Journal*, *0*(0), 1. https://doi.org/10.1080/02626667.2019.1649411
3121 Azarderakhsh, M., Rossow, W. B., Papa, F., Norouzi, H., & Khanbilvardi, R. (2011). Diagnosing water
3122 variations within the Amazon basin using satellite data. *J.\ Geophys.\ Res.*, *116*(D24), n/a--n/a.
3123 https://doi.org/10.1029/2011JD015997
3124 Baguis, P., & Roulin, E. (2017). Soil moisture data assimilation in a hydrological model: A case study in
3125 Belgium using large-scale satellite data. *Remote Sensing*, *9*(8), 1–26.
3126 https://doi.org/10.3390/rs9080820
3127 Baker, J., & Spracklen, D. V. (2019). Climate Benefits of Intact Amazon Forests and the Biophysical
3128 Consequences of Disturbance. *Frontiers in Forests and Global Change*, *2*(August), 1–13.

https://doi.org/10.3389/ffgc.2019.00047

Baker, J., Garcia-Carreras, L., Gloor, M., Marsham, J., Buermann, W., da Rocha, H., et al. (2020). Evapotranspiration in the Amazon: spatial patterns, seasonality and recent trends in observations, reanalysis and CMIP models. *Hydrology and Earth System Sciences Discussions*, 1–32. https://doi.org/10.5194/hess-2020-523

Balsamo, G., Albergel, C., Beljaars, A., Boussetta, S., Brun, E., Cloke, H., et al. (2015). ERA-Interim/Land: A global land surface reanalysis data set. *Hydrology and Earth System Sciences*, *19*(1), 389–407. https://doi.org/10.5194/hess-19-389-2015

Barahona, D., Molod, A., & Kalesse, H. (2017). Direct estimation of the global distribution of vertical velocity within cirrus clouds. *Scientific Reports*, *7*(1), 1–11. https://doi.org/10.1038/s41598-017-07038-6

Barbosa, C. C. F. (2005). Sensoriamento Remoto da dinâmica da circulação da água do sistema planície de Curuaí/Rio Amazonas. *Dissertação*, (January 2005), 255.

Barbosa, C. C. F., Novo, E. M. L. de M., Melack, J. M., Freitas, R. M. de, & Pereira, W. (2006). A methodology for analysis of volume and flooded area dynamics: Lago Grande de Curuai várzea as an example. *Revista Brasileira de Cartografia*, *58*(3), 201–210.

Barbosa, C. C. F., de Moraes Novo, E. M. L., Melack, J. M., Gastil-Buhl, M., & Filho, W. P. (2009). Geospatial analysis of spatiotemporal patterns of pH, total suspended sediment and chlorophyll-a on the Amazon floodplain. *Limnology*, *11*(2), 155–166. https://doi.org/10.1007/s10201-009-0305-5

Barbosa, C. C. F., Novo, E., Ferreira, R., Carvalho, L., Cairo, C., Lopes, F., et al. (2015). Brazilian inland water bio-optical dataset to support carbon budget studies in reservoirs as well as anthropogenic impacts in Amazon floodplain lakes: Preliminary results. *International Archives of the Photogrammetry, Remote Sensing and Spatial Information Sciences - ISPRS Archives*, *40*(7W3), 1439–1446. https://doi.org/10.5194/isprsarchives-XL-7-W3-1439-2015

Barbosa, P. M., Melack, J. M., Amaral, J. H. F., MacIntyre, S., Kasper, D., Cortés, A., et al. (2020). Dissolved methane concentrations and fluxes to the atmosphere from a tropical floodplain lake. *Biogeochemistry*, *148*(2), 129–151. https://doi.org/10.1007/s10533-020-00650-1

Barichivich, J., Gloor, E., Peylin, P., Brienen, R. J. W., Schöngart, J., Espinoza, J. C., & Pattnayak, K. C. (2018). Recent intensification of Amazon flooding extremes driven by strengthened Walker circulation. *Science Advances*, *4*(9). https://doi.org/10.1126/sciadv.aat8785

Bastiaanssen, W. G. M. (1995). *Regionalization of surface flux densities and moisture indicators in composite terrain: a remote sensing approach under clear skies in Mediterranean climates*. *Doctoral thesis, Wageningen Agricultural University, Wageningen The Netherlands.*

Baugh, C. A., Bates, P. D., Schumann, G., & Trigg, M. A. (2013). SRTM vegetation removal and hydrodynamic modeling accuracy. *Water Resources Research*, *49*(9), 5276–5289. https://doi.org/10.1002/wrcr.20412

Bayley, P. B., & Moreira, J. C. (1978). Preliminary interpretations of aquatic resources in the central Amazon Basin using Landsat multispectral imagery. In N. de J. Parada (Ed.), *Anais...* (pp. 854–865). São José dos Campos: Instituto Nacional de Pesquisas Espaciais (INPE). Retrieved from http://urlib.net/rep/dpi.inpe.br/marte@80/2008/09.25.13.57

Beck, H. E., Vergopolan, N., Pan, M., Levizzani, V., van Dijk, A. I. J. M., Weedon, G. P., et al. (2017). Global-scale evaluation of 22 precipitation datasets using gauge observations and hydrological modeling. *Hydrology and Earth System Sciences*, *21*(12), 6201–6217. https://doi.org/10.5194/hess-21-6201-2017

Beck, H. E., Van Dijk, A. I. J. M., Levizzani, V., Schellekens, J., Miralles, D. G., Martens, B., & De Roo, A. (2017). MSWEP: 3-hourly 0.25° global gridded precipitation (1979-2015) by merging gauge, satellite, and reanalysis data. *Hydrology and Earth System Sciences*, *21*(1), 589–615. https://doi.org/10.5194/hess-21-589-2017

Beck, H. E., Pan, M., Roy, T., Weedon, G. P., Pappenberger, F., van Dijk, A. I. J. M., et al. (2018). Daily evaluation of 26 precipitation datasets using Stage-IV gauge-radar data for the CONUS. *Hydrology and Earth System Sciences Discussions*, 1–23. https://doi.org/10.5194/hess-2018-481

Beck, H. E., Wood, E. F., Pan, M., Fisher, C. K., Miralles, D. G., Van Dijk, A. I. J. M., et al. (2019). MSWep v2 Global 3-hourly 0.1° precipitation: Methodology and quantitative assessment. *Bulletin of the American Meteorological Society*, *100*(3), 473–500. https://doi.org/10.1175/BAMS-D-17-0138.1

Becker, A., Finger, P., Meyer-Christoffer, A., Rudolf, B., Schamm, K., Schneider, U., & Ziese, M. (2013). A description of the global land-surface precipitation data products of the Global Precipitation Climatology Centre with sample applications including centennial (trend) analysis from 1901-present. *Earth System Science Data*, *5*(1), 71–99. https://doi.org/10.5194/essd-5-71-2013

Becker, M., Papa, F., Frappart, F., Alsdorf, D., Calmant, S., da Silva, J. S., et al. (2018). Satellite-based estimates of surface water dynamics in the Congo River Basin. *International Journal of Applied Earth Observation and Geoinformation*, *66*, 196–209. https://doi.org/10.1016/j.jag.2017.11.015

Behnamian, A., Banks, S., White, L., Brisco, B., Milard, K., Pasher, J., et al. (2017). Semi-automated surfacewater detection with synthetic aperture radar data: A wetland case study. *Remote Sensing*, *9*, 1209. https://doi.org/10.3390/rs9121209

Beighley, R. E., Eggert, K. G., Dunne, T., He, Y., Gummadi, V., & Verdin, K. L. (2009). Simulating

hydrologic and hydraulic processes throughout the Amazon River Basin. *Hydrological Processes*, *23*, 1221–1235. https://doi.org/10.1002/hyp

Belger, L., Forsberg, B. R., & Melack, J. M. (2011). Carbon dioxide and methane emissions from interfluvial wetlands in the upper Negro River basin, Brazil. *Biogeochemistry*, *105*, 171–183. https://doi.org/10.1007/s10533-010-9536-0

Bercher, N., Dinardo, S., Lucas, B., Fleury, S., Calmant, S., Femenias, P., et al. (2013). A review of Cryosat-2/SIRAL applications for the monitoring of river water levels. *ESA Living Planet Symposium*, *1*(September), 1–30. Retrieved from http://ebooks.cambridge.org/ref/id/CBO9781107415324A009

Bernini, H., Borges, H. D., & Martinez, J. (2019). Quasi-Analytical Algorithm Calibration for Retrieval of Inherent Optical Properties from Extremely Turbid Waters: The Case of Madeira River Basin. In *IGARSS 2019 - 2019 IEEE International Geoscience and Remote Sensing Symposium* (pp. 6150–6153). https://doi.org/10.1109/IGARSS.2019.8897766

Berry, P. A. M., Garlick, J. D., Freeman, J. A., & Mathers, E. L. (2005). Global inland water monitoring from multi-mission altimetry. *Geophysical Research Letters*, *32*(16). https://doi.org/10.1029/2005GL022814

Biancamaria, S., Lettenmaier, D. P., & Pavelsky, T. M. (2016). The SWOT Mission and Its Capabilities for Land Hydrology. *Surveys in Geophysics*, *37*(2), 307–337. https://doi.org/10.1007/s10712-015-9346-y

Bierkens, M. F. P., Bell, V. A., Burek, P., Chaney, N., Condon, L. E., David, C. H., et al. (2015). Hyper-resolution global hydrological modelling: What is next?: "Everywhere and locally relevant" M. F. P. Bierkens et al. Invited Commentary. *Hydrological Processes*, *29*(2), 310–320. https://doi.org/10.1002/hyp.10391

Birkett, C. M., Mertes, L. A. K., Dunne, T., Costa, M. H., & Jasinski, M. J. (2002). Surface water dynamics in the Amazon Basin: Application of satellite radar altimetry. *Journal of Geophysical Research D: Atmospheres*, *107*(20). https://doi.org/10.1029/2001JD000609

Birkett, C. M., Ricko, M., Beckley, B. D., Yang, X., & Tetrault, R. L. (2017). G-REALM: A lake/reservoir monitoring tool for drought monitoring and water resources management. In *AGU Fall Meeting Abstracts* (Vol. 2017, pp. H23P-02).

Blumstein, D., Biancamaria, S., Guérin, A., & Maisongrande, P. (2019). A potential constellation of small altimetry satellites dedicated to continental surface waters (SMASH mission). In *AGU Fall Meeting Abstracts* (Vol. 2019, pp. H43N-2257).

Bogning, S., Frappart, F., Blarel, F., Niño, F., Mahé, G., Bricquet, J.-P., et al. (2018). Monitoring Water

Levels and Discharges Using Radar Altimetry in an Ungauged River Basin: The Case of the Ogooué. *Remote Sensing*, *10*(2). https://doi.org/10.3390/rs10020350

Bogning, S., Frappart, F., Paris, A., Blarel, F., Niño, F., Saux Picart, S., et al. (2020). Hydro-climatology study of the Ogooué River basin using hydrological modeling and satellite altimetry. *Advances in Space Research*. https://doi.org/https://doi.org/10.1016/j.asr.2020.03.045

Bonnet, M. P., Barroux, G., Martinez, J. M., Seyler, F., Moreira-Turcq, P., Cochonneau, G., et al. (2008). Floodplain hydrology in an Amazon floodplain lake (Lago Grande de Curuaí). *Journal of Hydrology*, *349*(1–2), 18–30. https://doi.org/10.1016/j.jhydrol.2007.10.055

Bonnet, M. P., Pinel, S., Garnier, J., Bois, J., Resende Boaventura, G., Seyler, P., & Motta Marques, D. (2017). Amazonian floodplain water balance based on modelling and analyses of hydrologic and electrical conductivity data. *Hydrological Processes*, *31*(9), 1702–1718. https://doi.org/10.1002/hyp.11138

Bookhagen, B., & Strecker, M. R. (2008). Orographic barriers, high-resolution TRMM rainfall, and relief variations along the eastern Andes. *Geophysical Research Letters*, *35*(6), L06403. https://doi.org/10.1029/2007GL032011

Borma, L. S., Da Rocha, H. R., Cabral, O. M., Von Randow, C., Collicchio, E., Kurzatkowski, D., et al. (2009). Atmosphere and hydrological controls of the evapotranspiration over a floodplain forest in the Bananal Island region, Amazonia. *Journal of Geophysical Research: Biogeosciences*, *114*(G1). https://doi.org/10.1029/2007JG000641

Bosilovich, M. G., & Chern, J. D. (2006). Simulation of water sources and precipitation recycling for the MacKenzie, Mississippi, and Amazon River basins. *Journal of Hydrometeorology*, *7*(3), 312–329. https://doi.org/10.1175/JHM501.1

Bouchez, J., Lupker, M., Maurice, L., Perez, M., & Gaillardet, J. (2011). Prediction of depth-integrated fluxes of suspended sediment in the Amazon River: particle aggregation as a complicating factor. *Hydrological Processes*, *794*(October 2010), 778–794. https://doi.org/10.1002/hyp.7868

Bourgoin, L. M., Bonnet, M. P., Martinez, J. M., Kosuth, P., Cochonneau, G., Moreira-Turcq, P., et al. (2007). Temporal dynamics of water and sediment exchanges between the Curuaí floodplain and the Amazon River, Brazil. *Journal of Hydrology*, *335*(1–2), 140–156. https://doi.org/10.1016/j.jhydrol.2006.11.023

Bourrel, L., Phillips, L., & Moreau, S. (2009). The dynamics of floods in the Bolivian Amazon Basin. *Hydrological Processes*, *23*, 3161–3167. https://doi.org/10.1002/hyp.7384

Bradley, J. (1980). *Remote sensing of suspended sediment in Amazonian rivers using satellite multispectral imagery*. Royal Holloway, University of London. Retrieved from

http://isni.org/isni/0000000134753316

Brakenridge, G. R., Nghiem, S. V., Anderson, E., & Mic, R. (2007). Orbital microwave measurement of river discharge and ice status. *Water Resources Research*, *43*. https://doi.org/10.1029/2006WR005238

Brasil. (1997). *Lei nº 9.433, de 8 de janeiro de 1997. Institui a Política Nacional de Recursos Hídricos, cria o Sistema Nacional de Gerenciamento de Recursos Hídricos, regulamenta o inciso XIX do art. 21 da Constituição Federal, e altera o art. 1º da Lei nº 8.001, de 13*. Diário Oficial [da] República Federativa do Brasil, Brasília. Retrieved from http://www.planalto.gov.br/ccivil_03/leis/l9433.htm

Brêda, J. P. L. F., Paiva, R. C. D., Bravo, J. M., Passaia, O. A., & Moreira, D. M. (2019). Assimilation of Satellite Altimetry Data for Effective River Bathymetry. *Water Resources Research*, *55*(9), 7441–7463. https://doi.org/10.1029/2018wr024010

Brocca, L., Moramarco, T., Melone, F., & Wagner, W. (2013). A new method for rainfall estimation through soil moisture observations. *Geophysical Research Letters*, *40*(5), 853–858. https://doi.org/10.1002/grl.50173

Brocca, L., Ciabatta, L., Massari, C., Moramarco, T., Hahn, S., Hasenauer, S., et al. (2014). Soil as a natural rain gauge: Estimating global rainfall from satellite soil moisture data. *Journal of Geophysical Research: Atmospheres*, *119*(9), 5128–5141. https://doi.org/10.1002/2014JD021489

Brocca, L., Filippucci, P., Hahn, S., Ciabatta, L., Massari, C., Camici, S., et al. (2019). SM2RAIN-ASCAT (2007-2018): Global daily satellite rainfall data from ASCAT soil moisture observations. *Earth System Science Data*, *11*(4), 1583–1601. https://doi.org/10.5194/essd-11-1583-2019

Builes-Jaramillo, A., & Poveda, G. (2018). Conjoint Analysis of Surface and Atmospheric Water Balances in the Andes-Amazon System. *Water Resources Research*, *54*(5), 3472–3489. https://doi.org/10.1029/2017WR021338

Butt, N., De Oliveira, P. A., & Costa, M. H. (2011). Evidence that deforestation affects the onset of the rainy season in Rondonia, Brazil. *Journal of Geophysical Research Atmospheres*, *116*(11), 2–9. https://doi.org/10.1029/2010JD015174

Buytaert, W., Zulkafli, Z., Grainger, S., Acosta, L., Alemie, T. C., Bastiaensen, J., et al. (2014). Citizen science in hydrology and water resources: opportunities for knowledge generation, ecosystem service management, and sustainable development. *Frontiers in Earth Science*, *2*, 26. https://doi.org/10.3389/feart.2014.00026

Callède, J., Guyot, J. L., Ronchail, J., L'Hôte, Y., Niel, H., & De Oliveira, E. (2004). Evolution of the River Amazon's discharge at Óbidos from 1903 to 1999. *Hydrological Sciences Journal*, *49*(1), 85–98. https://doi.org/10.1623/hysj.49.1.85.53992

3294 Callède, J., Cochonneau, G., Alves, F. V., Guyot, J.-L., Guimarães, V. S., & De Oliveira, E. (2010). The
3295 River Amazon water contribution to the Atlantic Ocean. *Revue Des Sciences de l'eau*, *23*(3), 247–
3296 273. Retrieved from https://www.erudit.org/en/journals/rseau/2010-v23-n3-
3297 rseau3946/044688ar/abstract/
3298 Callède, J., Moreira, D. M., & Calmant, S. (2013). Détermination de l'altitude du zéro des stations
3299 hydrométriques en amazonie brésilienne. Application aux lignes d'eau des Rios Negro, Solimões et
3300 Amazone. *Revue Des Sciences de l'Eau*, *26*(2), 153–171. https://doi.org/10.7202/1016065ar
3301 Calmant, S., & Seyler, F. (2006). Continental surface waters from satellite altimetry. *Comptes Rendus -*
3302 *Geoscience*, *338*(14–15), 1113–1122. https://doi.org/10.1016/j.crte.2006.05.012
3303 Calmant, S., Da Silva, J. S., Moreira, D. M., Seyler, F., Shum, C. K., Crétaux, J. F., & Gabalda, G.
3304 (2013). Detection of Envisat RA2/ICE-1 retracked radar altimetry bias over the Amazon basin rivers
3305 using GPS. *Advances in Space Research*, *51*(8), 1551–1564.
3306 https://doi.org/10.1016/j.asr.2012.07.033
3307 Calmant, S., Crétaux, J. F., & Rémy, F. (2016). Principles of Radar Satellite Altimetry for Application on
3308 Inland Waters. *Microwave Remote Sensing of Land Surfaces: Techniques and Methods*, 175–218.
3309 https://doi.org/10.1016/B978-1-78548-159-8.50004-9
3310 Campos-Silva, J. V., Hawes, J. E., Freitas, C. T., Andrade, P. C. M., & Peres, C. A. (2020). Community-
3311 Based Management of Amazonian Biodiversity Assets. In C. Baldauf (Ed.), *Participatory*
3312 *Biodiversity Conservation: Concepts, Experiences, and Perspectives* (pp. 99–111). Cham: Springer
3313 International Publishing. https://doi.org/10.1007/978-3-030-41686-7_7
3314 Cao, N., Lee, H., Jung, H. C., & Yu, H. (2018). Estimation of Water Level Changes of Large-Scale
3315 Amazon Wetlands Using ALOS2 ScanSAR Differential Interferometry, *10*(966).
3316 https://doi.org/10.3390/rs10060966
3317 Cardille, J. A., Foley, J. A., & Costa, M. H. (2002). Characterizing patterns of agricultural land use in
3318 Amazonia by merging satellite classifications and census data. *Global Biogeochemical Cycles*,
3319 *16*(3), 18-1-18–14. https://doi.org/10.1029/2000gb001386
3320 Carvalho, J. C., Cochonneau, G., Piscoya, R. de C. C. C. de, Martinez, J., Souza, E. A. De, Antunes, M.
3321 A., et al. (2015). HIDROSAT - Sistema Integrado para Gerenciamento, Processamento e Difusão de
3322 Dados Hidrológicos Obtidos a Partir de Monitoramento por Satélites. In *XXI Simpósio Brasileiro de*
3323 *Recursos Hídricos*. Brasília, DF: ABRH.
3324 de Carvalho, L. A. S., Faria Barbosa, C. C., Leão de Moraes Novo, E. M., & de Moraes Rudorff, C.
3325 (2015). Implications of scatter corrections for absorption measurements on optical closure of
3326 Amazon floodplain lakes using the Spectral Absorption and Attenuation Meter (AC-S-WETLabs).

Remote Sensing of Environment, *157*, 123–137. https://doi.org/10.1016/j.rse.2014.06.018

Carvalho, L. M. V., Jones, C., & Liebmann, B. (2004). The South Atlantic Convergence Zone: Intensity, Form, Persistence, and Relationships with Intraseasonal to Interannual Activity and Extreme Rainfall. *Journal of Climate*, *17*(1), 88–108. https://doi.org/10.1175/1520-0442(2004)017<0088:TSACZI>2.0.CO;2

Castello, L., & Macedo, M. N. (2016). Large-scale degradation of Amazonian freshwater ecosystems. *Global Change Biology*, *22*(3), 990–1007. https://doi.org/10.1111/gcb.13173

Castello, L., Hess, L. L., Thapa, R., McGrath, D. G., Arantes, C. C., Renó, V. F., & Isaac, V. J. (2018). Fishery yields vary with land cover on the Amazon River floodplain. *Fish and Fisheries*, *19*, 431–440. https://doi.org/10.1111/faf.12261

Cavalcante, R. B. L., Pontes, P. R. M., Souza-Filho, P. W. M., & de Souza, E. B. (2019). Opposite Effects of Climate and Land Use Changes on the Annual Water Balance in the Amazon Arc of Deforestation. *Water Resources Research*, *55*(4), 3092–3106. https://doi.org/10.1029/2019WR025083

Cavalcante, R. B. L., Ferreira, D. B. da S., Pontes, P. R. M., Tedeschi, R. G., da Costa, C. P. W., & de Souza, E. B. (2020). Evaluation of extreme rainfall indices from CHIRPS precipitation estimates over the Brazilian Amazonia. *Atmospheric Research*, *238*(October 2019), 104879. https://doi.org/10.1016/j.atmosres.2020.104879

Chapman, B., McDonald, K., Shimada, M., Rosenqvist, A., Schroeder, R., & Hess, L. (2015). Mapping Regional Inundation with Spaceborne L-Band SAR. *Remote Sensing*, *7*(5), 5440–5470. https://doi.org/10.3390/rs70505440

Chaudhari, S., Pokhrel, Y., Moran, E., & Miguez-Macho, G. (2019). Multi-decadal hydrologic change and variability in the Amazon River basin: Understanding terrestrial water storage variations and drought characteristics. *Hydrology and Earth System Sciences*, *23*(7), 2841–2862. https://doi.org/10.5194/hess-23-2841-2019

Chavez, S. P., & Takahashi, K. (2017). Orographic rainfall hot spots in the Andes-Amazon transition according to the TRMM precipitation radar and in situ data. *Journal of Geophysical Research*. https://doi.org/10.1002/2016JD026282

Chen, J. L., Wilson, C. R., Tapley, B. D., Yang, Z. L., & Niu, G. Y. (2009). 2005 drought event in the Amazon River basin as measured by GRACE and estimated by climate models. *Journal of Geophysical Research: Solid Earth*, *114*(5), 1–9. https://doi.org/10.1029/2008JB006056

Chen, J. L., Wilson, C. R., & Tapley, B. D. (2010). The 2009 exceptional Amazon flood and interannual terrestrial water storage change observed by GRACE. *Water Resources Research*, *46*(12), 1–10.

https://doi.org/10.1029/2010WR009383

Chen, M., Shi, W., Xie, P., Silva, V. B. S., Kousky, V. E., Wayne Higgins, R., & Janowiak, J. E. (2008). Assessing objective techniques for gauge-based analyses of global daily precipitation. *Journal of Geophysical Research*, *113*(D4), D04110. https://doi.org/10.1029/2007JD009132

Chew, C., & Small, E. (2020). Estimating inundation extent using CYGNSS data: A conceptual modeling study. *Remote Sensing of Environment*, *246*, 111869. https://doi.org/10.1016/j.rse.2020.111869

Choudhury, B. J. (1991). Passive microwave remote sensing contribution to hydrological variables. *Surveys in Geophysics*, *12*, 63–84. https://doi.org/10.1007/BF01903412

Christoffersen, B. O., Restrepo-Coupe, N., Arain, M. A., Baker, I. T., Cestaro, B. P., Ciais, P., et al. (2014). Mechanisms of water supply and vegetation demand govern the seasonality and magnitude of evapotranspiration in Amazonia and Cerrado. *Agricultural and Forest Meteorology*, *191*(February), 33–50. https://doi.org/10.1016/j.agrformet.2014.02.008

Ciabatta, L., Massari, C., Brocca, L., Gruber, A., Reimer, C., Hahn, S., et al. (2018). SM2RAIN-CCI: A new global long-term rainfall data set derived from ESA CCI soil moisture. *Earth System Science Data*, *10*(1), 267–280. https://doi.org/10.5194/essd-10-267-2018

Cintra, R. (2015). Spatial distribution and composition of waterbirds in relation to limnological conditions in the Amazon basin. *Hydrobiologia*, *747*, 235–252. https://doi.org/10.1007/s10750-014-2148-2

Claverie, M., Ju, J., Masek, J. G., Dungan, J. L., Vermote, E. F., Roger, J., et al. (2018). The Harmonized Landsat and Sentinel-2 surface reflectance data set. *Remote Sensing of Environment*, *219*(August), 145–161. https://doi.org/10.1016/j.rse.2018.09.002

Cleugh, H. A., Leuning, R., Mu, Q., & Running, S. W. (2007). Regional evaporation estimates from flux tower and MODIS satellite data. *Remote Sensing of Environment*, *106*(3), 285–304. https://doi.org/10.1016/j.rse.2006.07.007

Coe, M. T., Costa, M. H., Botta, A., & Birkett, C. (2002). Long-term simulations of discharge and floods in the Amazon Basin. *Journal of Geophysical Research Atmospheres*, *107*(20), 1–17. https://doi.org/10.1029/2001JD000740

Coe, M. T., Costa, M. H., & Howard, E. A. (2008). Simulating the surface waters of the Amazon River basin: Impacts of new river geomorphic and flow parameterizations. *Hydrological Processes*, *22*(14), 2542–2553. https://doi.org/10.1002/hyp.6850

Coe, M. T., Costa, M. H., & Soares-Filho, B. S. (2009). The influence of historical and potential future deforestation on the stream flow of the Amazon River - Land surface processes and atmospheric feedbacks. *Journal of Hydrology*. https://doi.org/10.1016/j.jhydrol.2009.02.043

Coe, M. T., Latrubesse, E. M., Ferreira, M. E., & Amsler, M. L. (2011). The effects of deforestation and

climate variability on the streamflow of the Araguaia River, Brazil. *Biogeochemistry*, *105*(1), 119–131. https://doi.org/10.1007/s10533-011-9582-2

Cogley, J. G. (2013). GGHYDRO - Global Hydrographic Data, Release 2.3.1 Trent Technical Note 2003-1.

Collischonn, B., Collischonn, W., & Tucci, C. E. M. (2008). Daily hydrological modeling in the Amazon basin using TRMM rainfall estimates. *Journal of Hydrology*, *360*(1–4), 207–216. https://doi.org/10.1016/j.jhydrol.2008.07.032

Constantine, J. A., Dunne, T., Ahmed, J., Legleiter, C., & Lazarus, E. D. (2014). Sediment supply as a driver of river meandering and floodplain evolution in the Amazon Basin. *Nature Geoscience*, *7*(12), 899–903. https://doi.org/10.1038/ngeo2282

Cooley, S. W., Smith, L. C., Ryan, J. C., Pitcher, L. H., & Pavelsky, T. M. (2019). Arctic-Boreal Lake Dynamics Revealed Using CubeSat Imagery. *Geophysical Research Letters*, *46*(4), 2111–2120. https://doi.org/10.1029/2018GL081584

Correa, S. W., Paiva, R. C. D. de, Espinoza, J. C., & Collischonn, W. (2017). Multi-decadal Hydrological Retrospective: Case study of Amazon floods and droughts. *Journal of Hydrology*, *549*, 667–684. https://doi.org/10.1016/j.jhydrol.2017.04.019

Coss, S., Durand, M., Yi, Y., Jia, Y., Guo, Q., Tuozzolo, S., et al. (2020). Global River Radar Altimetry Time Series (GRRATS): New river elevation earth science data records for the hydrologic community. *Earth System Science Data*, *12*(1), 137–150. https://doi.org/10.5194/essd-12-137-2020

Costa, M. (2005). Estimate of net primary productivity of aquatic vegetation of the Amazon floodplain using Radarsat and JERS-1. *International Journal of Remote Sensing*, *26*(20), 4527–4536. https://doi.org/10.1080/01431160500213433

Costa, M. H. (2005). Large-scale hydrological impacts of tropical forest conversion. In M. Bonell & L. A. S. Bruijnzeel (Eds.), *Forests, Water and People in the Humid Tropics* (pp. 590–597). Cambridge University Press. https://doi.org/https://doi.org/10.1017/CBO9780511535666

Costa, M. H. (2020). When more trees mean more power. *Nature Sustainability*, *3*(June), 410–411. https://doi.org/10.1038/s41893-020-0511-z

Costa, M. H., & Foley, J. A. (1997). Water balance of the Amazon Basin: Dependence on vegetation cover and canopy conductance. *Journal of Geophysical Research: Atmospheres*, *102*(D20), 23973–23989. https://doi.org/10.1029/97JD01865

Costa, M. H., & Pires, G. F. (2010). Effects of Amazon and Central Brazil deforestation scenarios on the duration of the dry season in the arc of deforestation. *International Journal of Climatology*, *30*(13), 1970–1979. https://doi.org/10.1002/joc.2048

3426 Costa, M. H., Botta, A., & Cardille, J. A. (2003). Effects of large-scale changes in land cover on the
3427 discharge of the Tocantins River, Southeastern Amazonia. *Journal of Hydrology*, *283*(1–4), 206–
3428 217. https://doi.org/10.1016/S0022-1694(03)00267-1
3429 Costa, M. H., Biajoli, M. C., Sanches, L., Malhado, A. C. M., Hutyra, L. R., da Rocha, H. R., et al.
3430 (2010). Atmospheric versus vegetation controls of Amazonian tropical rain forest
3431 evapotranspiration: Are the wet and seasonally dry rain forests any different? *Journal of*
3432 *Geophysical Research*, *115*(G4), G04021. https://doi.org/10.1029/2009JG001179
3433 Costa, M. P. F., Novo, E. M. L. M., & Telmer, K. H. (2013). Spatial and temporal variability of light
3434 attenuation in large rivers of the Amazon. *Hydrobiologia*, *702*(1), 171–190.
3435 https://doi.org/10.1007/s10750-012-1319-2
3436 Crétaux, J. F., & Birkett, C. (2006). Lake studies from satellite radar altimetry. *Comptes Rendus -*
3437 *Geoscience*, *338*(14–15), 1098–1112. https://doi.org/10.1016/j.crte.2006.08.002
3438 Crétaux, J. F., Jelinski, W., Calmant, S., Kouraev, A., Vuglinski, V., Bergé-Nguyen, M., et al. (2011).
3439 SOLS: A lake database to monitor in the Near Real Time water level and storage variations from
3440 remote sensing data. *Advances in Space Research*, *47*(9), 1497–1507.
3441 https://doi.org/10.1016/j.asr.2011.01.004
3442 Crowley, J. W., Mitrovica, J. X., Bailey, R. C., Tamisiea, M. E., & Davis, J. L. (2008). Annual variations
3443 in water storage and precipitation in the Amazon Basin: Bounding sink terms in the terrestrial
3444 hydrological balance using GRACE satellite gravity data. *Journal of Geodesy*, *82*(1), 9–13.
3445 https://doi.org/10.1007/s00190-007-0153-1
3446 Cuartas, L. A., Tomasella, J., Nobre, A. D., Nobre, C. A., Hodnett, M. G., Waterloo, M. J., et al. (2012).
3447 Distributed hydrological modeling of a micro-scale rainforest watershed in Amazonia: Model
3448 evaluation and advances in calibration using the new HAND terrain model. *Journal of Hydrology*,
3449 *462–463*, 15–27. https://doi.org/10.1016/j.jhydrol.2011.12.047
3450 Davidson, E. A., & Artaxo, P. (2004). Globally significant changes in biological processes of the Amazon
3451 Basin: Results of the large-scale Biosphere-Atmosphere Experiment. *Global Change Biology*, *10*(5),
3452 519–529. https://doi.org/10.1111/j.1529-8817.2003.00779.x
3453 Davidson, E. A., De Araüjo, A. C., Artaxo, P., Balch, J. K., Brown, I. F., Mercedes, M. M., et al. (2012).
3454 The Amazon basin in transition. *Nature*, *481*, 312–328. https://doi.org/10.1038/nature10717
3455 Davidson, N. C., Fluet-Chouinard, E., & Finlayson, C. M. (2018). Global extent and distribution of
3456 wetlands: Trends and issues. *Marine and Freshwater Research*, *69*, 620–627.
3457 https://doi.org/10.1071/MF17019
3458 Debortoli, N. S., Dubreuil, V., Funatsu, B., Delahaye, F., de Oliveira, C. H., Rodrigues-Filho, S., et al.

(2015). Rainfall patterns in the Southern Amazon: a chronological perspective (1971–2010). *Climatic Change*, *132*(2), 251–264. https://doi.org/10.1007/s10584-015-1415-1

Decharme, B, Alkama, R., Papa, F., Faroux, S., Douville, H., & Prigent, C. (2012). Global off-line evaluation of the ISBA-TRIP flood model. *Climate Dynamics*, *38*(7), 1389–1412. https://doi.org/10.1007/s00382-011-1054-9

Decharme, Bertrand, Douville, H., Prigent, C., Papa, F., & Aires, F. (2008). A new river flooding scheme for global climate applications: Off-line evaluation over South America. *Journal of Geophysical Research Atmospheres*, *113*(11). https://doi.org/10.1029/2007JD009376

Dekker, A. G. (1993). *Detection of optical water quality parameters for eutrophic waters by high resolution remote sensing*. *Management*.

Delahaye, F., Kirstetter, P. E., Dubreuil, V., Machado, L. A. T., Vila, D. A., & Clark, R. (2015). A consistent gauge database for daily rainfall analysis over the Legal Brazilian Amazon. *Journal of Hydrology*, *527*, 292–304. https://doi.org/10.1016/j.jhydrol.2015.04.012

Desai, S. (2018). *Surface Water and Ocean Topography Mission Project - Science Requirements Document. JPL documentD-61923. Jet Propulsion Laboratory*. Retrieved from https://swot.jpl.nasa.gov/system/documents/files/2176_2176_D-61923_SRD_Rev_B_20181113.pdf

Dias, C. M., Pastore, D. H., Borma, L. S., & Bevilacqua, L. (2011). Modelling and numerical simulation of the velocity field in the Parque Estadual do Cantão (TO), Brazil. *Mathematical and Computer Modelling*, *53*(7–8), 1575–1581. https://doi.org/10.1016/j.mcm.2010.06.021

Dias, L. C. P., Pimenta, F. M., Santos, A. B., Costa, M. H., & Ladle, R. J. (2016). Patterns of land use, extensification, and intensification of Brazilian agriculture. *Global Change Biology*, *22*(8), 2887–2903. https://doi.org/10.1111/gcb.13314

Van Dijk, A. I. J. M., & Renzullo, L. J. (2011). Water resource monitoring systems and the role of satellite observations. *Hydrology and Earth System Sciences*, *15*(1), 39–55. https://doi.org/10.5194/hess-15-39-2011

Diniz, C. G., d. A. Souza, A. A., Santos, D. C., Dias, M. C., d. Luz, N. C., d. Moraes, D. R. V, et al. (2015). DETER-B: The New Amazon Near Real-Time Deforestation Detection System. *IEEE Journal of Selected Topics in Applied Earth Observations and Remote Sensing*, *8*(7), 3619–3628. https://doi.org/10.1109/JSTARS.2015.2437075

Dinku, T., Ceccato, P., & Connor, S. J. (2011). Challenges of satellite rainfall estimation over mountainous and arid parts of east africa. *International Journal of Remote Sensing*, *32*(21), 5965–5979. https://doi.org/10.1080/01431161.2010.499381

Drusch, M., Moreno, J., Del Bello, U., Franco, R., Goulas, Y., Huth, A., et al. (2017). The FLuorescence

EXplorer Mission Concept-ESA's Earth Explorer 8. *IEEE Transactions on Geoscience and Remote Sensing*, *55*(3), 1273–1284. https://doi.org/10.1109/TGRS.2016.2621820

Durieux, L., Toledo Machado, L. A., & Laurent, H. (2003). The impact of deforestation on cloud cover over the Amazon arc of deforestation. *Remote Sensing of Environment*, *86*(1), 132–140. https://doi.org/10.1016/S0034-4257(03)00095-6

Duvel, J. F., & Kandel, R. S. (1985). Regional-Scale Diurnal Variations of Outgoing Infrared Radiation Observed by METEOSAT. *Journal of Climate and Applied Meteorology*, *24*(4), 335–349. https://doi.org/10.1175/1520-0450(1985)024<0335:RSDVOO>2.0.CO;2

Eltahir, E. A. B., & Bras, R. L. (1994). Precipitation recycling in the Amazon basin. *Quarterly Journal of the Royal Meteorological Society*, *120*(518), 861–880. https://doi.org/10.1002/qj.49712051806

Emery, C. M., Paris, A., Biancamaria, S., Boone, A., Calmant, S., Garambois, P. A., & Da Silva, J. S. (2018). Large-scale hydrological model river storage and discharge correction using a satellite altimetry-based discharge product. *Hydrology and Earth System Sciences*. https://doi.org/10.5194/hess-22-2135-2018

Emery, C. M., Biancamaria, S., Boone, A., Ricci, S., Rochoux, M., Pedinotti, V., & David, C. (2020). Assimilation of wide-swath altimetry observations to correct large-scale river routing model parameters. *Hydrology and Earth System Sciences Discussions*, *24*, 2207–2233. https://doi.org/10.5194/hess-2019-242-RC3

Endo, W., Peres, C. A., & Haugaasen, T. (2016). Flood pulse dynamics affects exploitation of both aquatic and terrestrial prey by Amazonian floodplain settlements. *Biological Conservation*, *201*, 129–136. https://doi.org/10.1016/j.biocon.2016.07.006

Engle, D. L., Melack, J. M., Doyle, R. D., & Fisher, T. R. (2008). High rates of net primary production and turnover of floating grasses on the Amazon floodplain: Implications for aquatic respiration and regional CO2 flux. *Global Change Biology*, *14*, 369–381. https://doi.org/10.1111/j.1365-2486.2007.01481.x

Van Der Ent, R. J., Savenije, H. H. G., Schaefli, B., & Steele-Dunne, S. C. (2010). Origin and fate of atmospheric moisture over continents. *Water Resources Research*, *46*(9), 1–12. https://doi.org/10.1029/2010WR009127

Ershadi, A., McCabe, M. F., Evans, J. P., & Wood, E. F. (2015). Impact of model structure and parameterization on Penman-Monteith type evaporation models. *Journal of Hydrology*, *525*, 521–535. https://doi.org/10.1016/j.jhydrol.2015.04.008

Espinoza-Villar, R., Martinez, J. M., Armijos, E., Espinoza, J. C., Filizola, N., Dos Santos, A., et al. (2018). Spatio-temporal monitoring of suspended sediments in the Solimões River (2000-2014).

Comptes Rendus - Geoscience, *350*(1–2), 1–9. https://doi.org/10.1016/j.crte.2017.05.001

Espinoza, J. C., Ronchail, J., Guyot, J. L., Cochonneau, G., Naziano, F., Lavado, W., et al. (2009). Spatio-temporal rainfall variability in the Amazon basin countries (Brazil, Peru, Bolivia, Colombia, and Ecuador). *International Journal of Climatology*, *29*(11), 1574–1594. https://doi.org/10.1002/joc.1791

Espinoza, J. C., Ronchail, J., Guyot, J. L., Junquas, C., Drapeau, G., Martinez, J. M., et al. (2012). From drought to flooding: Understanding the abrupt 2010-11 hydrological annual cycle in the Amazonas River and tributaries. *Environmental Research Letters*, *7*(2). https://doi.org/10.1088/1748-9326/7/2/024008

Espinoza, J. C., Ronchail, J., Frappart, F., Lavado, W., Santini, W., & Guyot, J. L. (2013). The Major Floods in the Amazonas River and Tributaries (Western Amazon Basin) during the 1970-2012 Period: A Focus on the 2012 Flood. *Journal of Hydrometeorology*, *14*(3), 1000–1008. https://doi.org/10.1175/JHM-D-12-0100.1

Espinoza, J. C., Chavez, S., Ronchai, J., Junquas, C., Takahashi, K., & Lavado, W. (2015). Rainfall hotspots over the southern tropical Andes: Spatial distribution, rainfall intensity, and relations with large-scale atmospheric circulation. *Water Resources Research*, 1–27. https://doi.org/10.1002/2015WR017096.Received

Espinoza, J. C., Segura, H., Ronchail, J., Drapeau, G., & Gutierrez-Cori, O. (2016). Evolution of wet-day and dry-day frequency in the western Amazon basin: Relationship with atmospheric circulation and impacts on vegetation. *Water Resources Research*, *52*(11), 8546–8560. https://doi.org/10.1002/2016WR019305

Espinoza, J. C., Ronchail, J., Marengo, J. A., & Segura, H. (2019). Contrasting North–South changes in Amazon wet-day and dry-day frequency and related atmospheric features (1981–2017). *Climate Dynamics*, *52*(9–10), 5413–5430. https://doi.org/10.1007/s00382-018-4462-2

Espinoza, J. C., Sörensson, A. A., Ronchail, J., Molina-Carpio, J., Segura, H., Gutierrez-Cori, O., et al. (2019). Regional hydro-climatic changes in the Southern Amazon Basin (Upper Madeira Basin) during the 1982–2017 period. *Journal of Hydrology: Regional Studies*, *26*(June), 100637. https://doi.org/10.1016/j.ejrh.2019.100637

Espinoza Villar, J. C., Guyot, J. L., Ronchail, J., Cochonneau, G., Filizola, N., Fraizy, P., et al. (2009). Contrasting regional discharge evolutions in the Amazon basin (1974-2004). *Journal of Hydrology*, *375*(3–4), 297–311. https://doi.org/10.1016/j.jhydrol.2009.03.004

Espinoza Villar, J. C., Ronchail, J., Guyot, J. L., Cochonneau, G., Naziano, F., Lavado, W., et al. (2009). Spatio-temporal rainfall variability in the Amazon basin countries (Brazil, Peru, Bolivia, Colombia,

and Ecuador). *International Journal of Climatology*, *29*, 1574–1594. https://doi.org/10.1002/joc.1791

Espinoza Villar, R., Martinez, J. M., Guyot, J. L., Fraizy, P., Armijos, E., Crave, A., et al. (2012). The integration of field measurements and satellite observations to determine river solid loads in poorly monitored basins. *Journal of Hydrology*, *444–445*, 221–228. https://doi.org/10.1016/j.jhydrol.2012.04.024

Fagundes, H. O., Fan, F. M., Paiva, R. C. D., Siqueira, V. A., Buarque, D. C., Kornowski, L. W., et al. (2021). Sediment Flows in South America Supported by Daily Hydrologic-Hydrodynamic Modeling. *Water Resources Research*, *57*(2). https://doi.org/10.1029/2020wr027884

Fan, F. M., Paiva, R. C. D., & Collischonn, W. (2016). Chapter 2 - Hydrological Forecasting Practices in Brazil. In T. E. Adams & T. C. B. T.-F. F. Pagano (Eds.), *Flood Forecasting A Global Perspective* (pp. 41–66). Boston: Academic Press. https://doi.org/https://doi.org/10.1016/B978-0-12-801884-2.00002-5

Fang, Y., Leung, L. R., Duan, Z., Wigmosta, M. S., Maxwell, R. M., Chambers, J. Q., & Tomasella, J. (2017). Influence of landscape heterogeneity on water available to tropical forests in an Amazonian catchment and implications for modeling drought response. *Journal of Geophysical Research: Atmospheres*, *122*(16), 8410–8426. https://doi.org/https://doi.org/10.1002/2017JD027066

Farr, T., Rosen, P., Caro, E., Crippen, R., Duren, R., Hensley, S., et al. (2007). The shuttle radar topography mission. *Reviews of Geophysics*, *45*(2005), 1–33. https://doi.org/10.1029/2005RG000183

Fassoni-Andrade, A. C. (2020). *Mapping and characterization of the central Amazon river-floodplain system by remote sensing and hydraulic modeling*. Universidade Federal do Rio Grande do Sul.

Fassoni-Andrade, A. C., & Paiva, R. C. D. (2019). Mapping spatial-temporal sediment dynamics of river-floodplains in the Amazon. *Remote Sensing of Environment*, *221*(March 2018), 94–107. https://doi.org/10.1016/j.rse.2018.10.038

Fassoni-Andrade, A. C., Paiva, R. C. D., Rudorff, C. M., Barbosa, C. C. F., & Novo, E. M. L. de M. (2020). High-resolution mapping of floodplain topography from space: A case study in the Amazon. *Remote Sensing of Environment*, *251*, 112065. https://doi.org/10.1016/j.rse.2020.112065

Fassoni-Andrade, A. C., Paiva, R. C. D., & Fleischmann, A. S. (2020). Lake topography and active storage from satellite observations of flood frequency. *Water Resources Research*, *56*(7). https://doi.org/10.1029/2019wr026362

Fassoni-Andrade, A. C., Durand, F., Moreira, D., Azevedo, A., Santos, V., Funi, C., & Laraque, A. (2021). Comprehensive bathymetry and intertidal topography of the Amazon estuary. *Earth System*

Science Data. https://doi.org/https://doi.org/10.5194/essd-2021-32

Fekete, B. M., Looser, U., Pietroniro, A., & Robarts, R. D. (2012). Rationale for monitoring discharge on the ground. *Journal of Hydrometeorology*, *13*(6), 1977–1986. https://doi.org/10.1175/JHM-D-11-0126.1

Ferreira-Ferreira, J., Silva, T. S. F., Streher, A. S., Affonso, A. G., De Almeida Furtado, L. F., Forsberg, B. R., et al. (2015). Combining ALOS/PALSAR derived vegetation structure and inundation patterns to characterize major vegetation types in the Mamirauá Sustainable Development Reserve, Central Amazon floodplain, Brazil. *Wetlands Ecology and Management*, *23*(1), 41–59. https://doi.org/10.1007/s11273-014-9359-1

Ferreira, R. D., Barbosa, C. C. F., & Novo, E. M. L. de M. (2013). Assessment of in vivo fluorescence method for chlorophyll-a estimation in optically complex waters (Curuai floodplain, Pará - Brazil). *Acta Limnologica Brasiliensia*, *24*(4), 373–386. https://doi.org/10.1590/s2179-975x2013005000011

Ferreira, V. G., Montecino, H. C., Ndehedehe, C. E., Heck, B., Gong, Z., de Freitas, S. R. C., & Westerhaus, M. (2018). Space-based observations of crustal deflections for drought characterization in Brazil. *Science of the Total Environment*, *644*, 256–273. https://doi.org/10.1016/j.scitotenv.2018.06.277

Figueroa, S. N., & Nobre, C. A. (1990). Precipitation Distribution over Central and Western Tropical South America. *Climanálise*, *6*, 36–40.

Filizola, N., & Guyot, J. (2009). Suspended sediment yields in the Amazon basin: an assessment using the Brazilian national data set. *Hydrological Processes*, *23*, 3207–3215. https://doi.org/10.1002/hyp.7394

Finer, M., Novoa, S., Weisse, M. J., Petersen, R., Mascaro, J., Souto, T., et al. (2018). Combating deforestation: From satellite to intervention. *Science*, *360*(6395), 1303–1305. https://doi.org/10.1126/science.aat1203

Fisher, J. B., Tu, K. P., & Baldocchi, D. D. (2008). Global estimates of the land-atmosphere water flux based on monthly AVHRR and ISLSCP-II data, validated at 16 FLUXNET sites. *Remote Sensing of Environment*, *112*(3), 901–919. https://doi.org/10.1016/j.rse.2007.06.025

Fisher, J. B., Malhi, Y., Bonal, D., Da Rocha, H. R., De Araújo, A. C., Gamo, M., et al. (2009). The land-atmosphere water flux in the tropics. *Global Change Biology*, *15*(11), 2694–2714. https://doi.org/10.1111/j.1365-2486.2008.01813.x

Fisher, J. B., Melton, F., Middleton, E., Hain, C., Anderson, M., Allen, R., et al. (2017, April 1). The future of evapotranspiration: Global requirements for ecosystem functioning, carbon and climate feedbacks, agricultural management, and water resources. *Water Resources Research*. Blackwell

Publishing Ltd. https://doi.org/10.1002/2016WR020175

Fitzjarrald, D. R., Sakai, R. K., Moraes, O. L. L., Cosme de Oliveira, R., Acevedo, O. C., Czikowsky, M. J., & Beldini, T. (2008). Spatial and temporal rainfall variability near the Amazon-Tapajós confluence. *Journal of Geophysical Research: Biogeosciences*, *113*(G1), n/a-n/a. https://doi.org/10.1029/2007JG000596

Fleischmann, A. S., Paiva, R. C. D., Collischonn, W., Sorribas, M. V., & Pontes, P. R. M. (2016). On river-floodplain interaction and hydrograph skewness. *Water Resources Research*, *52*(10), 7615–7630. https://doi.org/10.1002/2016WR019233

Fleischmann, A. S., Siqueira, V., Paris, A., Collischonn, W., Paiva, R., Pontes, P., et al. (2018). Modelling hydrologic and hydrodynamic processes in basins with large semi-arid wetlands. *Journal of Hydrology*, *561*, 943–959. https://doi.org/10.1016/j.jhydrol.2018.04.041

Fleischmann, A. S., Paiva, R., & Collischonn, W. (2019). Can regional to continental river hydrodynamic models be locally relevant? A cross-scale comparison. *Journal of Hydrology X*, *3*, 100027. https://doi.org/10.1016/j.hydroa.2019.100027

Fleischmann, A. S., Paiva, R. C. D., Collischonn, W., Siqueira, V. A., Paris, A., Moreira, D. M., et al. (2020). Trade-Offs Between 1-D and 2-D Regional River Hydrodynamic Models. *Water Resources Research*, *56*(8). https://doi.org/10.1029/2019WR026812

Flores Júnior, R. (2019). *Parametrização de algoritmos empíricos e algoritmo quasi-analítico QAA para estimativa de clorofila-a em lagos da várzea do rio Amazonas*. Instituto Nacional de Pesquisas Espaciais (INPE). Retrieved from http://urlib.net/rep/8JMKD3MGP3W34R/3SUQ3U2

Fluet-Chouinard, E., Lehner, B., Rebelo, L. M., Papa, F., & Hamilton, S. K. (2015). Development of a global inundation map at high spatial resolution from topographic downscaling of coarse-scale remote sensing data. *Remote Sensing of Environment*, *158*, 348–361. https://doi.org/10.1016/j.rse.2014.10.015

Forsberg, B. R., Melack, J. M., Dunne, T., Barthem, R. B., Goulding, M., Paiva, R. C. D., et al. (2017). The potential impact of new Andean dams on Amazon fluvial ecosystems. *PLoS ONE*, *12*(8). https://doi.org/10.1371/journal.pone.0182254

Frappart, F., & Ramillien, G. (2018, May). Monitoring groundwater storage changes using the Gravity Recovery and Climate Experiment (GRACE) satellite mission: A review. *Remote Sensing*. Multidisciplinary Digital Publishing Institute. https://doi.org/10.3390/rs10060829

Frappart, F., Seyler, F., Martinez, J. M., León, J. G., & Cazenave, A. (2005). Floodplain water storage in the Negro River basin estimated from microwave remote sensing of inundation area and water levels. *Remote Sensing of Environment*, *99*(4), 387–399. https://doi.org/10.1016/j.rse.2005.08.016

3657 Frappart, F., Calmant, S., Cauhopé, M., Seyler, F., & Cazenave, A. (2006). Preliminary results of
3658 ENVISAT RA-2-derived water levels validation over the Amazon basin. *Remote Sensing of*
3659 *Environment*, *100*(2), 252–264. https://doi.org/10.1016/j.rse.2005.10.027
3660 Frappart, F., Papa, F., Famiglietti, J. S., Prigent, C., Rossow, W. B., & Seyler, F. (2008). Interannual
3661 variations of river water storage from a multiple satellite approach: A case study for the Rio Negro
3662 River basin. *Journal of Geophysical Research Atmospheres*, *113*(D21).
3663 https://doi.org/10.1029/2007JD009438
3664 Frappart, F., Papa, F., Güntner, A., Werth, S., Santos da Silva, J., Tomasella, J., et al. (2011). Satellite-
3665 based estimates of groundwater storage variations in large drainage basins with extensive
3666 floodplains. *Remote Sensing of Environment*, *115*(6), 1588–1594.
3667 https://doi.org/10.1016/j.rse.2011.02.003
3668 Frappart, F., Papa, F., Santos Da Silva, J., Ramillien, G., Prigent, C., Seyler, F., & Calmant, S. (2012).
3669 Surface freshwater storage and dynamics in the Amazon basin during the 2005 exceptional drought.
3670 *Environmental Research Letters*, *7*(4). https://doi.org/10.1088/1748-9326/7/4/044010
3671 Frappart, F., Ramillien, G., & Ronchail, J. (2013). Changes in terrestrial water storage versus rainfall and
3672 discharges in the Amazon basin. *International Journal of Climatology*, *33*(14), 3029–3046.
3673 https://doi.org/10.1002/joc.3647
3674 Frappart, F., Seoane, L., & Ramillien, G. (2013). Validation of GRACE-derived terrestrial water storage
3675 from a regional approach over South America. *Remote Sensing of Environment*, *137*, 69–83.
3676 https://doi.org/10.1016/j.rse.2013.06.008
3677 Frappart, F., Papa, F., Malbeteau, Y., León, J. G., Ramillien, G., Prigent, C., et al. (2015). Surface
3678 Freshwater Storage Variations in the Orinoco Floodplains Using Multi-Satellite Observations.
3679 *Remote Sensing*, *7*(1), 89–110. https://doi.org/10.3390/rs70100089
3680 Frappart, F., Legrésy, B., Niño, F., Blarel, F., Fuller, N., Fleury, S., et al. (2016). An ERS-2 altimetry
3681 reprocessing compatible with ENVISAT for long-term land and ice sheets studies. *Remote Sensing*
3682 *of Environment*, *184*, 558–581. https://doi.org/10.1016/j.rse.2016.07.037
3683 Frappart, F., Papa, F., Güntner, A., Tomasella, J., Pfeffer, J., Ramillien, G., et al. (2019). The spatio-
3684 temporal variability of groundwater storage in the Amazon River Basin. *Advances in Water*
3685 *Resources*, *124*(October 2016), 41–52. https://doi.org/10.1016/j.advwatres.2018.12.005
3686 Fricke, A. T., Nittrouer, C. A., Ogston, A. S., Nowacki, D. J., Asp, N. E., & Souza Filho, P. W. M.
3687 (2019). Morphology and dynamics of the intertidal floodplain along the Amazon tidal river. *Earth*
3688 *Surface Processes and Landforms*, *44*(1), 204–218. https://doi.org/10.1002/esp.4545
3689 Fu, R., Zhu, B., & Dickinson, R. E. (1999). How Do Atmosphere and Land Surface Influence Seasonal

Changes of Convection in the Tropical Amazon? *Journal of Climate*, *12*(5), 1306–1321. https://doi.org/10.1175/1520-0442(1999)012<1306:HDAALS>2.0.CO;2

Fu, R., Yin, L., Li, W., Arias, P. A., Dickinson, R. E., Huang, L., et al. (2013). Increased dry-season length over southern Amazonia in recent decades and its implication for future climate projection. *Proceedings of the National Academy of Sciences of the United States of America*, *110*(45), 18110–18115. https://doi.org/10.1073/pnas.1302584110

Funatsu, B. M., Dubreuil, V., Claud, C., Arvor, D., & Gan, M. A. (2012). Convective activity in Mato Grosso state (Brazil) from microwave satellite observations: Comparisons between AMSU and TRMM data sets. *Journal of Geophysical Research Atmospheres*, *117*(16), 1–16. https://doi.org/10.1029/2011JD017259

Funk, C., Peterson, P., Landsfeld, M., Pedreros, D., Verdin, J., Shukla, S., et al. (2015). The climate hazards infrared precipitation with stations - A new environmental record for monitoring extremes. *Scientific Data*, *2*, 1–21. https://doi.org/10.1038/sdata.2015.66

Gabioux, M., Vinzon, S. B., & Paiva, A. M. (2005). Tidal propagation over fluid mud layers on the Amazon shelf. *Continental Shelf Research*, *25*(1), 113–125. https://doi.org/10.1016/j.csr.2004.09.001

Gallo, M. N., & Vinzon, S. B. (2005). Generation of overtides and compound tides in Amazon estuary. *Ocean Dynamics*, *55*(5–6), 441–448. https://doi.org/10.1007/s10236-005-0003-8

Gao, H., Birkett, C., & Lettenmaier, D. P. (2012). Global monitoring of large reservoir storage from satellite remote sensing. *Water Resources Research*, *48*(9), 1–12. https://doi.org/10.1029/2012WR012063

Garambois, P. A., Calmant, S., Roux, H., Paris, A., Monnier, J., Finaud-Guyot, P., et al. (2017). Hydraulic visibility: Using satellite altimetry to parameterize a hydraulic model of an ungauged reach of a braided river. *Hydrological Processes*, *31*(4), 756–767. https://doi.org/10.1002/hyp.11033

Garousi-Nejad, I., Tarboton, D. G., Aboutalebi, M., & Torres-Rua, A. F. (2019). *Terrain Analysis Enhancements to the Height Above Nearest Drainage Flood Inundation Mapping Method*. *Water Resources Research* (Vol. 55). https://doi.org/10.1029/2019WR024837

Garreaud, R. D., & Wallace, J. M. (1997). The diurnal march of convective cloudiness over the Americas. *Monthly Weather Review*, *125*(12), 3157–3171. https://doi.org/10.1175/1520-0493(1997)125<3157:TDMOCC>2.0.CO;2

Garstang, M., Massie Jr., H. L., Halverson, J., Greco, S., & Scala, J. (1994). Amazon Coastal Squall Lines. Part I: Structure and Kinematics. *Monthly Weather Review*, *122*(4), 608–622. https://doi.org/10.1175/1520-0493(1994)122<0608:ACSLPI>2.0.CO;2

Gash, J., Keller, M., Bustamante, M., & Dias, P. S. (2013). *Amazonia and Global Change*. *Amazonia and Global Change*. https://doi.org/10.1029/GM186

Gelaro, R., McCarty, W., Suárez, M. J., Todling, R., Molod, A., Takacs, L., et al. (2017). The modern-era retrospective analysis for research and applications, version 2 (MERRA-2). *Journal of Climate*, *30*(14), 5419–5454. https://doi.org/10.1175/JCLI-D-16-0758.1

Getirana, A. C. V., Espinoza, J. C. V., Ronchail, J., & Rotunno Filho, O. C. (2011). Assessment of different precipitation datasets and their impacts on the water balance of the Negro River basin. *Journal of Hydrology*, *404*(3–4), 304–322. https://doi.org/10.1016/j.jhydrol.2011.04.037

Getirana, A. C. V., Boone, A., Yamazaki, D., Decharme, B., Papa, F., & Mognard, N. (2012). The Hydrological Modeling and Analysis Platform (HyMAP): Evaluation in the Amazon Basin. *Journal of Hydrometeorology*, *13*(6), 1641–1665. https://doi.org/10.1175/JHM-D-12-021.1

Getirana, A. C. V., Boone, A., Yamazaki, D., & Mognard, N. (2013). Automatic parameterization of a flow routing scheme driven by radar altimetry data : Evaluation in the Amazon basin. *Water Resources Research*, *49*(1), 614–629. https://doi.org/10.1002/wrcr.20077

Getirana, A. C. V., Dutra, E., Guimberteau, M., Kam, J., Li, H.-Y., Decharme, B., et al. (2014). Water Balance in the Amazon Basin from a Land Surface Model Ensemble. *Journal of Hydrometeorology*, *15*(6), 2586–2614. https://doi.org/10.1175/JHM-D-14-0068.1

Getirana, A. C. V., Kumar, S., Girotto, M., & Rodell, M. (2017). Rivers and Floodplains as Key Components of Global Terrestrial Water Storage Variability. *Geophysical Research Letters*, *44*(20), 10,359-10,368. https://doi.org/10.1002/2017GL074684

Getirana, A. C. V., Peters-Lidard, C., Rodell, M., & Bates, P. D. (2017). Trade-off between cost and accuracy in large-scale surface water dynamic modeling. *Water Resources Research*, *53*(6), 4942–4955. https://doi.org/10.1002/2017WR020519

Gholizadeh, M. H., Melesse, A. M., & Reddi, L. (2016). A comprehensive review on water quality parameters estimation using remote sensing techniques. *Sensors (Switzerland)*, *16*(8). https://doi.org/10.3390/s16081298

Ghosh, S., Thakur, P. K., Sharma, R., Nandy, S., Garg, V., Amarnath, G., & Bhattacharyya, S. (2017). The Potential Applications of Satellite Altimetry with SARAL/AltiKa for Indian Inland Waters. *Proceedings of the National Academy of Sciences, India Section A: Physical Sciences*, *87*(4), 661–677. https://doi.org/10.1007/s40010-017-0463-5

Giardino, C., Bresciani, M., Braga, F., Fabretto, A., Ghirardi, N., Pepe, M., et al. (2020). First evaluation of PRISMA Level 1 data for water applications. *Sensors*, *(SUBMITTED*(August). https://doi.org/10.3390/s20164553

3756 Giddings, L., & Choudhury, B. J. (1989). Observation of hydrological features with Nimbus-7 37 GHz
3757 data, applied to South America. *International Journal of Remote Sensing*, *10*, 1673–1686.
3758 https://doi.org/10.1080/01431168908903998
3759 Giovannettone, J. P., & Barros, A. P. (2009). Probing regional orographic controls of precipitation and
3760 cloudiness in the Central Andes using satellite data. *Journal of Hydrometeorology*, *10*(1), 167–182.
3761 https://doi.org/10.1175/2008JHM973.1
3762 Gleason, C. J., & Durand, M. T. (2020). Remote sensing of river discharge: A review and a framing for
3763 the discipline. *Remote Sensing*, *12*(7), 1–28. https://doi.org/10.3390/rs12071107
3764 Gloor, M., Brienen, R. J. W., Galbraith, D., Feldpausch, T. R., Schöngart, J., Guyot, J.-L., et al. (2013).
3765 Intensification of the Amazon hydrological cycle over the last two decades. *Geophysical Research*
3766 *Letters*, *40*(9), 1729–1733. https://doi.org/10.1002/grl.50377
3767 Gomis-Cebolla, J., Jimenez, J. C., Sobrino, J. A., Corbari, C., & Mancini, M. (2019). Intercomparison of
3768 remote-sensing based evapotranspiration algorithms over amazonian forests. *International Journal*
3769 *of Applied Earth Observation and Geoinformation*, *80*, 280–294.
3770 https://doi.org/10.1016/j.jag.2019.04.009
3771 Gonçalves, L. G., Borak, J. S., Costa, M. H., Saleska, S. R., Baker, I., Restrepo-Coupe, N., et al. (2013).
3772 Overview of the large-scale biosphere-atmosphere experiment in amazonia data model
3773 intercomparison project (LBA-DMIP). *Agricultural and Forest Meteorology*, *182–183*, 111–127.
3774 https://doi.org/10.1016/j.agrformet.2013.04.030
3775 Gosset, M., Kunstmann, H., Zougmore, F., Cazenave, F., Leijnse, H., Uijlenhoet, R., et al. (2016).
3776 Improving rainfall measurement in gauge poor regions thanks to mobile telecommunication
3777 networks. *Bulletin of the American Meteorological Society*, *97*(3), ES49–ES51.
3778 https://doi.org/10.1175/BAMS-D-15-00164.1
3779 Gruber, A., & Krueger, A. F. (1984). The status of the NOAA outgoing longwave radiation data set.
3780 *Bulletin - American Meteorological Society*, *65*(9), 958–962. https://doi.org/10.1175/1520-
3781 0477(1984)065<0958:TSOTNO>2.0.CO;2
3782 Guilhen, J., Al Bitar, A., Sauvage, S., Parrens, M., Martinez, J.-M., Abril, G., et al. (2020). Denitrification
3783 and associated nitrous oxide and carbon dioxide emissions from the Amazonian wetlands.
3784 *Biogeosciences*, *17*(16), 4297–4311. https://doi.org/10.5194/bg-17-4297-2020
3785 Guimberteau, M., Drapeau, G., Ronchail, J., Sultan, B., Polcher, J., Martinez, J. M., et al. (2012).
3786 Discharge simulation in the sub-basins of the Amazon using ORCHIDEE forced by new datasets.
3787 *Hydrology and Earth System Sciences*, *16*, 911–935. https://doi.org/10.5194/hess-16-911-2012
3788 Guimberteau, M., Ducharne, A., Ciais, P., Boisier, J. P., Peng, S., De Weirdt, M., & Verbeeck, H. (2014).

Testing conceptual and physically based soil hydrology schemes against observations for the Amazon Basin. *Geoscientific Model Development*, *7*(3), 1115–1136. https://doi.org/10.5194/gmd-7-1115-2014

Guimberteau, M., Ciais, P., Ducharne, A., Boisier, J. P., Dutra Aguiar, A. P., Biemans, H., et al. (2017). Impacts of future deforestation and climate change on the hydrology of the Amazon Basin: a multi-model analysis with a new set of land-cover change scenarios. *Hydrology and Earth System Sciences*, *21*(3), 1455–1475. https://doi.org/10.5194/hess-21-1455-2017

Guzkowska, M. A. J., Rapley, C. G., Ridley, J. K., Cudlip, W., Birkett, C. M., & Scott, R. F. (1990). *Developments in inland water and land altimetry: University College of London, Mullard Space Science Laboratory, European Space Agency final contract report 7839/88/F/Fl*.

Haghtalab, N., Moore, N., Heerspink, B. P., & Hyndman, D. W. (2020). Evaluating spatial patterns in precipitation trends across the Amazon basin driven by land cover and global scale forcings. *Theoretical and Applied Climatology*, (2017). https://doi.org/10.1007/s00704-019-03085-3

Hall, A. C., Schumann, G. J. P., Bamber, J. L., & Bates, P. D. (2011). Tracking water level changes of the Amazon Basin with space-borne remote sensing and integration with large scale hydrodynamic modelling: A review. *Physics and Chemistry of the Earth*, *36*(7–8), 223–231. https://doi.org/10.1016/j.pce.2010.12.010

Hall, A. C., Schumann, G. J., Bamber, J. L., Bates, P. D., & Trigg, M. A. (2012). Geodetic corrections to Amazon River water level gauges using ICESat altimetry, *48*(6). https://doi.org/10.1029/2011WR010895

Hamilton, S. K., Sippel, S. J., & Melack, J. M. (2002). Comparison of inundation patterns among major South American floodplains. *Journal of Geophysical Research Atmospheres*, *107*(20), 1–14. https://doi.org/10.1029/2000JD000306

Hamilton, S. K., Sippel, S. J., & Melack, J. M. (2004). Seasonal inundation patterns in two large savanna floodplains of South America: The Llanos de Moxos (Bolivia) and the Llanos del Orinoco (Venezuela and Colombia). *Hydrological Processes*, *18*(11), 2103–2116. https://doi.org/10.1002/hyp.5559

Hamilton, S. K., Kellndorfer, J., Lehner, B., & Tobler, M. (2007). Remote sensing of floodplain geomorphology as a surrogate for biodiversity in a tropical river system (Madre de Dios, Peru). *Geomorphology*, *89*(1-2 SPEC. ISS.), 23–38. https://doi.org/10.1016/j.geomorph.2006.07.024

Hansen, M. C., Potapov, P. V., Moore, R., Hancher, M., Turubanova, S. A., Tyukavina, A., et al. (2013). High-Resolution Global Maps of 21st-Century Forest Cover Change. *Science*, *342*(November), 850–854. https://doi.org/10.1126/science.1244693

3822 Hastie, A., Lauerwald, R., Ciais, P., & Regnier, P. (2019). Aquatic carbon fluxes dampen the overall
3823 variation of net ecosystem productivity in the Amazon basin: An analysis of the interannual
3824 variability in the boundless carbon cycle. *Global Change Biology*, *25*(6), 2094–2111.
3825 https://doi.org/10.1111/gcb.14620
3826 Heerspink, B. P., Kendall, A. D., Coe, M. T., & Hyndman, D. W. (2020). Trends in streamflow,
3827 evapotranspiration, and groundwater storage across the Amazon Basin linked to changing
3828 precipitation and land cover. *Journal of Hydrology: Regional Studies*, *32*(March), 100755.
3829 https://doi.org/10.1016/j.ejrh.2020.100755
3830 Hersbach, H., Rosnay, P. de, Bell, B., Schepers, D., Simmons, A., Soci, C., et al. (2018). *Operational*
3831 *global reanalysis: progress, future directions and synergies with NWP* (ERA Report). *ERA Report*
3832 *Series*.
3833 Hersbach, H., Bell, B., Berrisford, P., Hirahara, S., Horányi, A., Muñoz-Sabater, J., et al. (2020). The
3834 ERA5 global reanalysis. *Quarterly Journal of the Royal Meteorological Society*, (September 2019),
3835 1–51. https://doi.org/10.1002/qj.3803
3836 Hess, L. L., Melack, J. M., & Simonett, D. S. (1990). Radar detection of flooding beneath the forest
3837 canopy: A review. *International Journal of Remote Sensing*, *11*, 1313–1325.
3838 https://doi.org/10.1080/01431169008955095
3839 Hess, L. L., Melack, J. M., Melack, J. M., Filoso, S., Wang, Y., & Wang, Y. (1995). Delineation of
3840 Inundated Area and Vegetation Along the Amazon Floodplain with the SIR-C Synthetic Aperture
3841 Radar. *IEEE Transactions on Geoscience and Remote Sensing*, *33*(4), 896–904.
3842 https://doi.org/10.1109/36.406675
3843 Hess, L. L., Melack, J. M., Novo, E. M. L. M. L. M., Barbosa, C. C. F. F., & Gastil, M. (2003). Dual-
3844 season mapping of wetland inundation and vegetation for the central Amazon basin. *Remote Sensing*
3845 *of Environment*, *87*(4), 404–428. https://doi.org/10.1016/j.rse.2003.04.001
3846 Hess, L. L., Melack, J. M., Affonso, A. G., Barbosa, C., Gastil-Buhl, M., & Novo, E. M. L. M. (2015).
3847 Wetlands of the Lowland Amazon Basin: Extent, Vegetative Cover, and Dual-season Inundated
3848 Area as Mapped with JERS-1 Synthetic Aperture Radar. *Wetlands*, *35*(4), 745–756.
3849 https://doi.org/10.1007/s13157-015-0666-y
3850 Hoch, J. M., Haag, A. V., van Dam, A., Winsemius, H. C., van Beek, L. P. H., & Bierkens, M. F. P.
3851 (2016). Assessing the impact of hydrodynamics on large-scale flood wave propagation - a case study
3852 for the Amazon Basin. *Hydrology and Earth System Sciences Discussions*, (August), 1–25.
3853 https://doi.org/10.5194/hess-2016-442
3854 Hodnett, M. G., Vendrame, I., De O. Marques Filho, A., Oyama, M. D., & Tomasella, J. (1997). Soil

water storage and groundwater behaviour in a catenary sequence beneath forest in central Amazonia: I. Comparisons between plateau, slope and valley floor. *Hydrology and Earth System Sciences*, *1*(2), 265–277. https://doi.org/10.5194/hess-1-265-1997

Holmes, T. R. H., Hain, C. R., Crow, W. T., Anderson, M. C., & Kustas, W. P. (2018). Microwave implementation of two-source energy balance approach for estimating evapotranspiration. *Hydrology and Earth System Sciences*, *22*(2), 1351–1369. https://doi.org/10.5194/hess-22-1351-2018

Horel, J. D., Hahmann, A. N., & Geisler, J. E. (1989). An investigation of the Annual Cycle of Convective Activity over the Tropical Americas. *Journal of Climate*, *2*(11), 1388–1403. https://doi.org/10.1175/1520-0442(1989)002<1388:AIOTAC>2.0.CO;2

Hu, K., Awange, J. L., Khandu, Forootan, E., Goncalves, R. M., & Fleming, K. (2017). Hydrogeological characterisation of groundwater over Brazil using remotely sensed and model products. *Science of the Total Environment*, *599–600*, 372–386. https://doi.org/10.1016/j.scitotenv.2017.04.188

Huang, C., Chen, Y., Zhang, S., & Wu, J. (2018). Detecting, Extracting, and Monitoring Surface Water From Space Using Optical Sensors: A Review. *Reviews of Geophysics*, *56*(2), 333–360. https://doi.org/10.1029/2018RG000598

Huffman, G. J., Adler, R. F., Rudolf, B., Schneider, U., & Keehn, P. R. (1995). Global Precipitation Estimates Based on a Technique for Combining Satellite-Based Estimates, Rain Gauge Analysis, and NWP Model Precipitation Information. *Journal of Climate*, *8*(5), 1284–1295. https://doi.org/10.1175/1520-0442(1995)008<1284:GPEBOA>2.0.CO;2

Huffman, G. J., Adler, R. F., Arkin, P., Chang, A., Ferraro, R., Gruber, A., et al. (1997). The Global Precipitation Climatology Project (GPCP) Combined Precipitation Dataset. *Bulletin of the American Meteorological Society*, *78*(1), 5–20. https://doi.org/10.1175/1520-0477(1997)078<0005:TGPCPG>2.0.CO;2

Huffman, G. J., Adler, R. F., Morrissey, M. M., Bolvin, D. T., Curtis, S., Joyce, R., et al. (2001). Global precipitation at one-degree daily resolution from multisatellite observations. *Journal of Hydrometeorology*, *2*(1), 36–50. https://doi.org/10.1175/1525-7541(2001)002<0036:GPAODD>2.0.CO;2

Huffman, G. J., Adler, R. F., Bolvin, D. T., Gu, G., Nelkin, E. J., Bowman, K. P., et al. (2007). The TRMM Multisatellite Precipitation Analysis (TMPA): Quasi-global, multiyear, combined-sensor precipitation estimates at fine scales. *Journal of Hydrometeorology*, *8*(1), 38–55. https://doi.org/10.1175/JHM560.1

Huffman, G. J., Adler, R. F., Bolvin, D. T., & Nelkin, E. J. (2010). *The TRMM Multi-satellite*

Precipitation Analysis (TMPA). Chapter 1 in Satellite Rainfall Applications for Surface Hydrology. (M. Gebremichael & F. Hossain, Eds.). Dordrecht: Springer Netherlands. https://doi.org/10.1007/978-90-481-2915-7

Huffman, G. J., Bolvin, D. T., Braithwaite, D., Hsu, K., Joyce, R., & Xie, P. (2015). *Algorithm Theoretical Basis Document (ATBD) Version 4.5. NASA Global Precipitation Measurement (GPM) Integrated Multi-satellitE Retrievals for GPM (IMERG)*. Retrieved from https://gpm.nasa.gov/sites/default/files/document_files/IMERG_ATBD_V5.2_0.pdf

Huffman, G. J., Bolvin, D. T., & Nelkin, E. J. (2015). *Integrated MultisatellitE Retrievals for GPM (IMERG) technical documentation*. Retrieved from https://gpm.nasa.gov/sites/default/files/document_files/IMERG_doc.pdf

Huffman, G. J., Bolvin, D. T., & Adler, R. F. (2016). GPCP Version 1.2 One-Degree Daily Precipitation Data Set. Boulder, CO: Research Data Archive at the National Center for Atmospheric Research, Computational and Information Systems Laboratory. https://doi.org/10.5065/D6D50K46

Van Huijgevoort, M. H. J., Hazenberg, P., Van Lanen, H. A. J., Teuling, A. J., Clark, D. B., Folwell, S., et al. (2013). Global multimodel analysis of drought in runofffor the second half of the twentieth century. *Journal of Hydrometeorology*, *14*(5), 1535–1552. https://doi.org/10.1175/JHM-D-12-0186.1

Hurley, J. V, Vuille, M., Hardy, D. R., Burns, S. J., & Thompson, L. G. (2015). Cold air incursions, δ18O variability, and monsoon dynamics associated with snow days at Quelccaya Ice Cap, Peru. *Journal of Geophysical Research: Atmospheres*, *120*(15), 7467–7487. https://doi.org/https://doi.org/10.1002/2015JD023323

Jardine, T. D., Bond, N. R., Burford, M. A., Kennard, M. J., Ward, D. P., Bayliss, P., et al. (2015). Does flood rhythm drive ecosystem responses in tropical riverscapes? *Ecology*, *96*(3), 684–692. https://doi.org/10.1890/14-0991.1

Jensen, K., McDonald, K., Podest, E., Rodriguez-Alvarez, N., Horna, V., & Steiner, N. (2018). Assessing L-Band GNSS-reflectometry and imaging radar for detecting sub-canopy inundation dynamics in a tropicalwetlands complex. *Remote Sensing*, *10*(9), 1431. https://doi.org/10.3390/rs10091431

Ji, X., Lesack, L. F. W., Melack, J. M., Wang, S., Riley, W. J., & Shen, C. (2019). Seasonal and inter-annual patterns and controls of hydrological fluxes in an Amazon floodplain lake with a surface-subsurface processes model. *Water Resources Research*, *55*(4), 3056–3075. https://doi.org/10.1029/2018WR023897

Jiang, L., Schneider, R., Andersen, O. B., & Bauer-Gottwein, P. (2017). CryoSat-2 altimetry applications over rivers and lakes. *Water*, *9*(3), 211. https://doi.org/10.3390/w9030211

3921 Jiang, S., Ren, L., Hong, Y., Yong, B., Yang, X., Yuan, F., & Ma, M. (2012). Comprehensive evaluation
3922 of multi-satellite precipitation products with a dense rain gauge network and optimally merging their
3923 simulated hydrological flows using the Bayesian model averaging method. *Journal of Hydrology*,
3924 *452–453*, 213–225. https://doi.org/10.1016/j.jhydrol.2012.05.055
3925 Jiménez-Muñoz, J. C., Sobrino, J. A., Mattar, C., & Malhi, Y. (2013). Spatial and temporal patterns of the
3926 recent warming of the Amazon forest. *Journal of Geophysical Research Atmospheres*, *118*, 5204–
3927 5215. https://doi.org/10.1002/jgrd.50456
3928 Jimenez, J. C., Marengo, J. A., Alves, L. M., Sulca, J. C., Takahashi, K., Ferrett, S., & Collins, M. (2019).
3929 The role of ENSO flavours and TNA on recent droughts over Amazon forests and the Northeast
3930 Brazil region. *International Journal of Climatology*, (December), 1–20.
3931 https://doi.org/10.1002/joc.6453
3932 Jorge, D. S. F., Barbosa, C. C. F., de Carvalho, L. A. S., Affonso, A. G., Lobo, F. D. L., & Novo, E. M. L.
3933 D. M. (2017). SNR (Signal-To-Noise Ratio) Impact on Water Constituent Retrieval from Simulated
3934 Images of Optically Complex Amazon Lakes. *Remote Sensing*, *9*(7), 644.
3935 https://doi.org/10.3390/rs9070644
3936 Josse, C., Navarro, G., Encarnación, F., Tovar, A., Comer, P., Ferreira, W., et al. (2007). *Ecological*
3937 *Systems of the Amazon Basin of Peru and Bolivia: Classification and Mapping*. Virginia:
3938 NatureServe.
3939 Joyce, R. J., & Xie, P. (2011). Kalman filter-based CMORPH. *Journal of Hydrometeorology*, *12*(6),
3940 1547–1563. https://doi.org/10.1175/JHM-D-11-022.1
3941 Joyce, R. J., Janowiak, J. E., Arkin, P. A., & Xie, P. (2004). CMORPH: A method that produces global
3942 precipitation estimates from passive microwave and infrared data at high spatial and temporal
3943 resolution. *Journal of Hydrometeorology*, *5*(3), 487–503. https://doi.org/10.1175/1525-
3944 7541(2004)005<0487:CAMTPG>2.0.CO;2
3945 Jung, H. C., Hamski, J., Durand, M., Alsdorf, D., Hossain, F., Lee, H., et al. (2010). Characterization of
3946 complex fluvial systems using remote sensing of spatial and temporal water level variations in the
3947 Amazon, Congo, and Brahmaputra rivers. *Earth Surface Processes and Landforms*, *35*(3), 294–304.
3948 https://doi.org/10.1002/esp.1914
3949 Jung, M., Reichstein, M., Ciais, P., Seneviratne, S. I., Sheffield, J., Goulden, M. L., et al. (2010). Recent
3950 decline in the global land evapotranspiration trend due to limited moisture supply. *Nature*,
3951 *467*(7318), 951–954. https://doi.org/10.1038/nature09396
3952 Júnior, J. L. S., Tomasella, J., & Rodriguez, D. A. (2015). Impacts of future climatic and land cover
3953 changes on the hydrological regime of the Madeira River basin. *Climatic Change*, *129*(1–2), 117–

129. https://doi.org/10.1007/s10584-015-1338-x

Junk, W. J. (1997). *The Central Amazon Floodplain: ecology of a pulsing system. Ecological Studies* (Vol. 126). Berlin: Springer-Verlag.

Junk, W. J., Bayley, P. B., & Sparks, R. E. (1989). The flood pulse concept in river-floodplain-systems. *Canadian Journal of Fisheries and Aquatic Sciences*, *106*, 110–127. https://doi.org/10.1371/journal.pone.0028909

Junk, W. J., Piedade, M. T. F., Wittmann, F., Schöngart, J., & Parolin, P. (2010). *Amazonian Floodplain Forests: Ecophysiology, ecology, biodiversity and sustainable management*. *Ecological Studies*. Berlin, Germany: Springer. https://doi.org/10.1007/978-90-481-8725-6

Junk, W. J., Piedade, M. T. F., Schöngart, J., Cohn-Haft, M., Adeney, J. M., & Wittmann, F. (2011). A classification of major naturally-occurring amazonian lowland wetlands. *Wetlands*, *31*(4), 623–640. https://doi.org/10.1007/s13157-011-0190-7

Junk, W. J., Wittmann, F., Schöngart, J., & Piedade, M. T. F. (2015). A classification of the major habitats of Amazonian black-water river floodplains and a comparison with their white-water counterparts. *Wetlands Ecology and Management*, *23*(4), 677–693. https://doi.org/10.1007/s11273-015-9412-8

Junquas, C., Takahashi, K., Condom, T., Espinoza, J. C., Chavez, S., Sicart, J. E., & Lebel, T. (2018). Understanding the influence of orography on the precipitation diurnal cycle and the associated atmospheric processes in the central Andes. *Climate Dynamics*, *50*(11–12), 3995–4017. https://doi.org/10.1007/s00382-017-3858-8

Kandus, P., Minotti, P. G., Morandeira, N. S., Grimson, R., Trilla, G. G., González, E. B., et al. (2018). Remote sensing of wetlands in South America: Status and challenges. *International Journal of Remote Sensing*, *39*(4), 993–1016. https://doi.org/10.1080/01431161.2017.1395971

Kasischke, E. S., Melack, J. M., & Dobson, M. C. (1997). The use of imaging radars for ecological applications - A review. *Remote Sensing of Environment*, *59*(2), 141–156. https://doi.org/10.1016/S0034-4257(96)00148-4

Khaki, M., Forootan, E., Kuhn, M., Awange, J., Longuevergne, L., & Wada, Y. (2018). Efficient basin scale filtering of GRACE satellite products. *Remote Sensing of Environment*, *204*(October 2017), 76–93. https://doi.org/10.1016/j.rse.2017.10.040

Khaki, M., Hoteit, I., Kuhn, M., Forootan, E., & Awange, J. (2019). Assessing data assimilation frameworks for using multi-mission satellite products in a hydrological context. *Science of The Total Environment*, *647*(October 2017), 1031–1043. https://doi.org/10.1016/j.scitotenv.2018.08.032

Khand, K., Numata, I., Kjaersgaard, J., & Vourlitis, G. L. (2017). Dry season evapotranspiration

dynamics over human-impacted landscapes in the southern Amazon using the landsat-based METRIC model. *Remote Sensing*, *9*(7). https://doi.org/10.3390/rs9070706

Khanna, J., Medvigy, D., Fueglistaler, S., & Walko, R. (2017). Regional dry-season climate changes due to three decades of Amazonian deforestation. *Nature Climate Change*, *7*(3), 200–204. https://doi.org/10.1038/nclimate3226

Kidd, C. (2001). Satellite rainfall climatology: A review. *International Journal of Climatology*, *21*(9), 1041–1066. https://doi.org/10.1002/joc.635

Kidd, C., & Huffman, G. (2011). Global precipitation measurement. *Meteorological Applications*, *18*(3), 334–353. https://doi.org/10.1002/met.284

Kidd, C., & Levizzani, V. (2011). Status of satellite precipitation retrievals. *Hydrology and Earth System Sciences*, *15*(4), 1109–1116. https://doi.org/10.5194/hess-15-1109-2011

Kidd, C., Kniveton, D. R., Todd, M. C., & Bellerby, T. J. (2003). Satellite Rainfall Estimation Using Combined Passive Microwave and Infrared Algorithms. *Journal of Hydrometeorology*, *4*(6), 1088–1104. https://doi.org/10.1175/1525-7541(2003)004<1088:SREUCP>2.0.CO;2

Kidd, C., Becker, A., Huffman, G. J., Muller, C. L., Joe, P., Skofronick-Jackson, G., & Kirschbaum, D. B. (2017). So, How Much of the Earth's Surface Is Covered by Rain Gauges? *Bulletin of the American Meteorological Society*, *98*(1), 69–78. https://doi.org/10.1175/BAMS-D-14-00283.1

Kilham, N. E., & Roberts, D. (2011). Amazon river time series of surface sediment concentration from MODIS. *International Journal of Remote Sensing*, *32*(10), 2659–2679. https://doi.org/10.1080/01431161003713044

Killeen, T. J., Douglas, M., Consiglio, T., Jørgensen, P. M., & Mejia, J. (2007). Dry spots and wet spots in the Andean hotspot. *Journal of Biogeography*, *34*(8), 1357–1373. https://doi.org/10.1111/j.1365-2699.2006.01682.x

Kim, D., Lee, H., Laraque, A., Tshimanga, R. M., Yuan, T., Jung, H. C., et al. (2017). Mapping spatio-temporal water level variations over the central Congo River using PALSAR ScanSAR and Envisat altimetry data. *International Journal of Remote Sensing*, *38*(23), 7021–7040. https://doi.org/10.1080/01431161.2017.1371867

Kirk, J. T. O. (2010). *Light and Photosynthesis in Aquatic Ecosystems* (3rd ed.). New York: Cambridge University Press.

Kirschke, S., Bousquet, P., Ciais, P., Saunois, M., Canadell, J. G., Dlugokencky, E. J., et al. (2013). Three decades of global methane sources and sinks. *Nature Geoscience*, *6*, 813–823. https://doi.org/10.1038/ngeo1955

Klein, I., Dietz, A., Gessner, U., Dech, S., & Kuenzer, C. (2015). Results of the Global WaterPack: A

4020 novel product to assess inland water body dynamics on a daily basis. *Remote Sensing Letters*, *6*(1).
4021 https://doi.org/10.1080/2150704X.2014.1002945
4022 Knapp, K. R., Ansari, S., Bain, C. L., Bourassa, M. A., Dickinson, M. J., Funk, C., et al. (2011). Globally
4023 Gridded Satellite observations for climate studies. *Bulletin of the American Meteorological Society*,
4024 *92*(7), 893–907. https://doi.org/10.1175/2011BAMS3039.1
4025 Koblinsky, C. J., Clarke, R. T., Brenner, A. C., & Frey, H. (1993). Measurement of river level variations
4026 with satellite altimetry. *Water Resources Research*, *29*(6), 1839–1848.
4027 https://doi.org/10.1029/93WR00542
4028 Kolassa, J., Gentine, P., Prigent, C., & Aires, F. (2016). Soil moisture retrieval from AMSR-E and
4029 ASCAT microwave observation synergy. Part 1: Satellite data analysis. *Remote Sensing of*
4030 *Environment*, *173*, 1–14. https://doi.org/https://doi.org/10.1016/j.rse.2015.11.011
4031 Koren, I., Martins, J. V., Remer, L. A., & Afargan, H. (2008). Smoke Invigoration Versus Inhibition of
4032 Clouds over the Amazon. *Science*, *321*(5891), 946–949. https://doi.org/10.1126/science.1159185
4033 Kosuth, P., Callede, J., Laraque, A., Filizola, N., Guyot, J. L., Seyler, P., et al. (2009). Sea-tide effects on
4034 flows in the lower reaches of the Amazon River. *Hydrological Processes*, *23*(November 2008),
4035 3141–3150. https://doi.org/10.1002/hyp.7387
4036 Kumar, S., Del Castillo-Velarde, C., Prado, J. M. V., Rojas, J. L. F., Gutierrez, S. M. C., Alvarez, A. S.
4037 M., et al. (2020). Rainfall characteristics in the mantaro basin over tropical andes from a vertically
4038 pointed profile rain radar and in-situ field campaign. *Atmosphere*, *11*(3).
4039 https://doi.org/10.3390/atmos11030248
4040 Kustas, W. P., & Norman, J. M. (1999). *Evaluation of soil and vegetation heat ¯ux predictions using a*
4041 *simple two-source model with radiometric temperatures for partial canopy cover*. *Agricultural and*
4042 *Forest Meteorology* (Vol. 94).
4043 Kutser, T., Pascual, G. C., Barbosa, C., & Paavel, B. (2016). Mapping inland water carbon content with
4044 Landsat 8 data. *International Journal of Remote Sensing ISSN:*, (June).
4045 https://doi.org/10.1080/01431161.2016.1186852
4046 Kvist, L. P., & Nebel, G. (2001). A review of Peruvian flood plain forests: Ecosystems, inhabitants and
4047 resource use. *Forest Ecology and Management*, *150*(1–2), 3–26. https://doi.org/10.1016/S0378-
4048 1127(00)00679-4
4049 Laipelt, L., Ruhoff, A. L., Fleischmann, A. S., Bloedow Kayser, R. H., Kich, E. de M., Rocha, H. R. da,
4050 & Usher Neale, C. M. (2020). Assessment of an automated calibration of the SEBAL Algorithm to
4051 estimate dry-season surface-energy partitioning in a Forest-Savanna Transition in Brazil. *Remote*
4052 *Sensing*, *12*(7). https://doi.org/10.3390/rs12071108

4053 Landerer, F. W., Flechtner, F. M., Save, H., Webb, F. H., Bandikova, T., Bertiger, W. I., et al. (2020).
4054 Extending the Global Mass Change Data Record: GRACE Follow-On Instrument and Science Data
4055 Performance. *Geophysical Research Letters*, *47*(12). https://doi.org/10.1029/2020GL088306
4056 Laranjeiras, T. O., Naka, L. N., Leite, G. A., & Cohn-Haft, M. (2021). Effects of a major Amazonian
4057 river confluence on the distribution of floodplain forest avifauna. *Journal of Biogeography*,
4058 (November), 1–14. https://doi.org/10.1111/jbi.14042
4059 Latrubesse, E. M. (2012). Amazon lakes. In L. Bengtsson, R. W. Herschy, & R. W. Fairbridge (Eds.),
4060 *Encyclopedia of Lakes and Reservoirs* (pp. 13–26). Springer Verlag. https://doi.org/10.1007/978-1-
4061 4020-4410-6
4062 Latrubesse, E. M., & Franzinelli, E. (2002). The Holocene alluvial plain of the middle Amazon River,
4063 Brazil. *Geomorphology*, *44*(3–4), 241–257. https://doi.org/10.1016/S0169-555X(01)00177-5
4064 Latrubesse, E. M., Arima, E. Y., Dunne, T., Park, E., Baker, V. R., D'Horta, F. M., et al. (2017).
4065 Damming the rivers of the Amazon basin. *Nature*. Nature Publishing Group.
4066 https://doi.org/10.1038/nature22333
4067 Lauerwald, R., Regnier, P., Guenet, B., Friedlingstein, P., & Ciais, P. (2020). How Simulations of the
4068 Land Carbon Sink Are Biased by Ignoring Fluvial Carbon Transfers: A Case Study for the Amazon
4069 Basin. *One Earth*, *3*(2), 226–236. https://doi.org/10.1016/j.oneear.2020.07.009
4070 Laurance, W. F., & Bruce Williamson, G. (2001). Positive feedbacks among forest fragmentation,
4071 drought, and climate change in the Amazon. *Conservation Biology*, *15*(6), 1529–1535.
4072 https://doi.org/10.1046/j.1523-1739.2001.01093.x
4073 Lawrence, D., & Vandecar, K. (2015). Effects of tropical deforestation on climate and agriculture. *Nature*
4074 *Climate Change*, *5*(1), 27–36. https://doi.org/10.1038/nclimate2430
4075 Lee, H., Yuan, T., Yu, H., & Jung, H. C. (2020). Interferometric SAR for Wetland Hydrology: An
4076 Overview of Methods, Challenges, and Trends. *IEEE Geoscience and Remote Sensing Magazine*,
4077 *8*(1), 120–135. https://doi.org/10.1109/MGRS.2019.2958653
4078 Lee, Z.-P., Shang, S., Lin, G., Chen, J., & Doxaran, D. (2016). On the modeling of hyperspectral remote-
4079 sensing reflectance of high-sediment-load waters in the visible to shortwave-infrared domain.
4080 *Applied Optics*, *55*(7), 1738–1750. https://doi.org/10.1364/AO.55.001738
4081 LeFavour, G., & Alsdorf, D. (2005). Water slope and discharge in the Amazon River estimated using the
4082 shuttle radar topography mission digital elevation model. *Geophysical Research Letters*, *32*(17), 1–
4083 5. https://doi.org/10.1029/2005GL023836
4084 Legresy, B., Papa, F., Remy, F., Vinay, G., Van Den Bosch, M., & Zanife, O. Z. (2005). ENVISAT radar
4085 altimeter measurements over continental surfaces and ice caps using the ICE-2 retracking algorithm.

Remote Sensing of Environment, *95*(2), 150–163. https://doi.org/10.1016/j.rse.2004.11.018

Lehner, B., & Döll, P. (2004). Development and validation of a global database of lakes, reservoirs and wetlands. *Journal of Hydrology*, *296*(1–4), 1–22. https://doi.org/10.1016/j.jhydrol.2004.03.028

Leite-Filho, A. T., Pontes, V. Y. de S., & Costa, M. H. (2019). Effects of Deforestation on the Onset of the Rainy Season and the Duration of Dry Spells in Southern Amazonia. *Journal of Geophysical Research: Atmospheres*, *124*(10), 5268–5281. https://doi.org/10.1029/2018JD029537

Leite-Filho, A. T., Costa, M. H., & Fu, R. (2020). The southern Amazon rainy season: The role of deforestation and its interactions with large-scale mechanisms. *International Journal of Climatology*, *40*(4), 2328–2341. https://doi.org/10.1002/joc.6335

Leite, C. C., Costa, M. H., de Lima, C. A., Ribeiro, C. A. A. S., & Sediyama, G. C. (2011). Historical reconstruction of land use in the Brazilian Amazon (1940–1995). *Journal of Land Use Science*, *6*(1), 33–52. https://doi.org/10.1080/1747423X.2010.501157

Leite, C. C., Costa, M. H., Soares-Filho, B. S., & De Barros Viana Hissa, L. (2012). Historical land use change and associated carbon emissions in Brazil from 1940 to 1995. *Global Biogeochemical Cycles*, *26*(2). https://doi.org/10.1029/2011GB004133

Lenters, J. D., & Cook, K. H. (1997). On the origin of the Bolivian high and related circulation features of the South American climate. *Journal of the Atmospheric Sciences*, *54*(5), 656–677. https://doi.org/10.1175/1520-0469(1997)054<0656:otootb>2.0.co;2

Leon, J. G., Calmant, S., Seyler, F., Bonnet, M. P., Cauhopé, M., Frappart, F., et al. (2006). Rating curves and estimation of average water depth at the upper Negro River based on satellite altimeter data and modeled discharges. *Journal of Hydrology*, *328*(3–4), 481–496. https://doi.org/10.1016/j.jhydrol.2005.12.006

Lesack, F. W., & Melack, J. M. (1995). Flooding hydrology and mixture dynamics of lakewater derived from multiple sources in an Amazon floodplain lake. *Water Resources Research*, *31*(2), 329–345.

Leuning, R., Zhang, Y. Q., Rajaud, A., Cleugh, H., & Tu, K. (2008). A simple surface conductance model to estimate regional evaporation using MODIS leaf area index and the Penman-Monteith equation. *Water Resources Research*, *44*(10). https://doi.org/10.1029/2007WR006562

Levizzani, V., & Cattani, E. (2019, October 1). Satellite remote sensing of precipitation and the terrestrial water cycle in a changing climate. *Remote Sensing*. MDPI AG. https://doi.org/10.3390/rs11192301

Levizzani, V., Porcú, F., Marzano, F. S., Mugnai, A., Smith, E. A., & Prodi, F. (2007). Investigating a SSM/I microwave algorithm to calibrate Meteosat infrared instantaneous rainrate estimates. *Meteorological Applications*, *3*(1), 5–17. https://doi.org/10.1002/met.5060030102

Levizzani, V., Laviola, S., & Cattani, E. (2011). Detection and measurement of snowfall from space.

Remote Sensing, *3*(1), 145–166. https://doi.org/10.3390/rs3010145

Levy, M. C., Lopes, A. V., Cohn, A., Larsen, L. G., & Thompson, S. E. (2018). Land use change increases streamflow across the arc of deforestation in Brazil. *Geophysical Research Letters*, 3520–3530. https://doi.org/10.1002/2017GL076526

Lewin, J., Ashworth, P. J., & Strick, R. J. P. (2017). Spillage sedimentation on large river floodplains. *Earth Surface Processes and Landforms*, *42*(2), 290–305. https://doi.org/10.1002/esp.3996

Lewis, S. L., Brando, P. M., Phillips, O. L., Van Der Heijden, G. M. F., & Nepstad, D. (2011). The 2010 Amazon drought. *Science*, *331*(6017), 554. https://doi.org/10.1126/science.1200807

Li, T., Wang, S., Liu, Y., Fu, B., & Gao, D. (2020). Reversal of the sediment load increase in the Amazon basin influenced by divergent trends of sediment transport from the Solimões and Madeira Rivers. *Catena*, *195*(December 2019), 104804. https://doi.org/10.1016/j.catena.2020.104804

Liang, Y. C., Lo, M. H., Lan, C. W., Seo, H., Ummenhofer, C. C., Yeager, S., et al. (2020). Amplified seasonal cycle in hydroclimate over the Amazon river basin and its plume region. *Nature Communications*, *11*(1), 1–11. https://doi.org/10.1038/s41467-020-18187-0

Liebmann, B., & Smith, C. A. (1996). Description of a complete (interpolated) outgoing longwave radiation dataset. *Bulletin of the American Meteorological Society*.

Lima, L. S., Coe, M. T., Soares Filho, B. S., Cuadra, S. V., Dias, L. C. P., Costa, M. H., et al. (2014). Feedbacks between deforestation, climate, and hydrology in the Southwestern Amazon: Implications for the provision of ecosystem services. *Landscape Ecology*, *29*(2), 261–274. https://doi.org/10.1007/s10980-013-9962-1

Lin, J. C., Matsui, T., Pielke, R. A., & Kummerow, C. (2006). Effects of biomass-burning-derived aerosols on precipitation and clouds in the Amazon Basin: a satellite-based empirical study. *Journal of Geophysical Research*, *111*(D19), D19204. https://doi.org/10.1029/2005JD006884

Liu, X., Yang, T., Hsu, K., Liu, C., & Sorooshian, S. (2017). Evaluating the streamflow simulation capability of PERSIANN-CDR daily rainfall products in two river basins on the Tibetan Plateau. *Hydrology and Earth System Sciences*, *21*(1), 169–181. https://doi.org/10.5194/hess-21-169-2017

Liu, Y. Y., Parinussa, R. M., Dorigo, W. A., De Jeu, R. A. M., Wagner, W., van Dijk, A. I. J. M., et al. (2011). Developing an improved soil moisture dataset by blending passive and active microwave satellite-based retrievals. *Hydrology and Earth System Sciences*, *15*(2), 425–436. https://doi.org/10.5194/hess-15-425-2011

Llauca, H., Lavado-Casimiro, W., León, K., Jimenez, J., Traverso, K., & Rau, P. (2021). Assessing Near Real-Time Satellite Precipitation Products for Flood Simulations at Sub-Daily Scales in a Sparsely Gauged Watershed in Peruvian Andes. *Remote Sensing*, *13*(4), 826.

https://doi.org/10.3390/rs13040826

Lobo, F., Novo, E. M. L. de M., Barbosa, C. C. F., & Galvão, L. S. (2012). Reference spectra to classify Amazon water types. *International Journal of Remote Sensing*, *33*(11), 3422–3442. https://doi.org/10.1080/01431161.2011.627391

Lobo, F., Costa, M. P. F., & Novo, E. M. L. M. (2015). Time-series analysis of Landsat-MSS/TM/OLI images over Amazonian waters impacted by gold mining activities. *Remote Sensing of Environment*, *157*, 170–184. https://doi.org/10.1016/j.rse.2014.04.030

Lobo, F., Costa, M., Novo, E., & Telmer, K. (2016). Distribution of Artisanal and Small-Scale Gold Mining in the Tapajós River Basin (Brazilian Amazon) over the Past 40 Years and Relationship with Water Siltation. *Remote Sensing*, *8*(7), 579. https://doi.org/10.3390/rs8070579

Lobo, F., Souza-Filho, P. W. M., Novo, E. M. L. de M., Carlos, F. M., & Barbosa, C. C. F. (2018). Mapping mining areas in the Brazilian amazon using MSI/Sentinel-2 imagery (2017). *Remote Sensing*, *10*(8). https://doi.org/10.3390/rs10081178

Lobón-Cerviá, J., Hess, L. L., Melack, J. M., & Araujo-Lima, C. A. R. M. (2015). The importance of forest cover for fish richness and abundance on the Amazon floodplain. *Hydrobiologia*, *750*, 245–255. https://doi.org/10.1007/s10750-014-2040-0

Lopes, A. V., Chiang, J. C. H., Thompson, S. A., & Dracup, J. A. (2016). Trend and uncertainty in spatial-temporal patterns of hydrological droughts in the Amazon basin. *Geophysical Research Letters*, *43*(7), 3307–3316. https://doi.org/10.1002/2016GL067738

Lopez, T., Al Bitar, A., Biancamaria, S., Güntner, A., & Jäggi, A. (2020). On the Use of Satellite Remote Sensing to Detect Floods and Droughts at Large Scales. *Surveys in Geophysics*. https://doi.org/10.1007/s10712-020-09618-0

Luo, X., Li, H. Y., Ruby Leung, L., Tesfa, T. K., Getirana, A., Papa, F., & Hess, L. L. (2017). Modeling surface water dynamics in the Amazon Basin using MOSART-Inundation v1.0: Impacts of geomorphological parameters and river flow representation. *Geoscientific Model Development*, *10*(3), 1233–1259. https://doi.org/10.5194/gmd-10-1233-2017

Luz-Agostinho, K. D. G., Agostinho, A. A., Gomes, L. C., Júlio-Jr., H. F., & Fugi, R. (2009). Effects of flooding regime on the feeding activity and body condition of piscivorous fish in the Upper Paraná River floodplain. *Brazilian Journal of Biology*, *69*, 481–490. https://doi.org/10.1590/s1519-69842009000300004

Maciel, D. A., Novo, E., Sander de Carvalho, L., Barbosa, C., Flores Júnior, R., de Lucia Lobo, F., et al. (2019). Retrieving Total and Inorganic Suspended Sediments in Amazon Floodplain Lakes: A Multisensor Approach. *Remote Sensing*, *11*(15), 1744. https://doi.org/10.3390/rs11151744

4185 Maciel, D. A., Novo, E. M. L. de M., Barbosa, C. C. F. C. C. F. C., Martins, V. S. ., Flores Júnior, R.,
4186 Oliveira, A. H., et al. (2020). Evaluating the potential of CubeSats for remote sensing reflectance
4187 retrieval over inland waters. *International Journal of Remote Sensing*, *41*(7), 2807–2817.
4188 https://doi.org/10.1080/2150704X.2019.1697003
4189 Maciel, D. A., Barbosa, C. C. F., Novo, E. M. L. de M., Cherukuru, N., Martins, V. S., Flores Júnior, R.,
4190 et al. (2020). Mapping of diffuse attenuation coefficient in optically complex waters of amazon
4191 floodplain lakes. *ISPRS Journal of Photogrammetry and Remote Sensing*, *170*(October), 72–87.
4192 https://doi.org/10.1016/j.isprsjprs.2020.10.009
4193 Madden, R. A., & Julian, P. R. (1994). Observations of the 40–50-Day Tropical Oscillation—A Review.
4194 *Monthly Weather Review*, *122*(5), 814–837. https://doi.org/10.1175/1520-
4195 0493(1994)122<0814:OOTDTO>2.0.CO;2
4196 Maeda, E. E., Kim, H., Aragão, L. E. O. C., Famiglietti, J. S., & Oki, T. (2015). Disruption of
4197 hydroecological equilibrium in southwest Amazon mediated by drought. *Geophysical Research*
4198 *Letters*, *42*, 7546– 7553. https://doi.org/10.1002/2015GL065252
4199 Maeda, E. E., Ma, X., Wagner, F. H., Kim, H., Oki, T., Eamus, D., & Huete, A. (2017).
4200 Evapotranspiration seasonality across the Amazon Basin. *Earth System Dynamics*, *8*(2), 439–454.
4201 https://doi.org/10.5194/esd-8-439-2017
4202 Manz, B., Páez-Bimos, S., Horna, N., Buytaert, W., Ochoa-Tocachi, B., Lavado-Casimiro, W., &
4203 Willems, B. (2017). Comparative ground validation of IMERG and TMPA at variable
4204 spatiotemporal scales in the tropical Andes. *Journal of Hydrometeorology*, *18*(9), 2469–2489.
4205 https://doi.org/10.1175/JHM-D-16-0277.1
4206 Marengo, J. A. (2005). Characteristics and spatio-temporal variability of the Amazon river basin water
4207 budget. *Climate Dynamics*, *24*(1), 11–22. https://doi.org/10.1007/s00382-004-0461-6
4208 Marengo, J. A., & Espinoza, J. C. (2016). Extreme seasonal droughts and floods in Amazonia: Causes,
4209 trends and impacts. *International Journal of Climatology*, *36*(3), 1033–1050.
4210 https://doi.org/10.1002/joc.4420
4211 Marengo, J. A., Nobre, C. A., Tomasella, J., Cardoso, M. F., & Oyama, M. D. (2008). Hydro-climatic and
4212 ecological behaviour of the drought of Amazonia in 2005. *Philosophical Transactions of the Royal*
4213 *Society B: Biological Sciences*, *363*(1498), 1773–1778. https://doi.org/10.1098/rstb.2007.0015
4214 Marengo, J. A., Tomasella, J., Alves, L. M., Soares, W. R., & Rodriguez, D. A. (2011). The drought of
4215 2010 in the context of historical droughts in the Amazon region. *Geophysical Research Letters*,
4216 *38*(12), 1–5. https://doi.org/10.1029/2011GL047436
4217 Marengo, J. A., Souza, C. M., Thonicke, K., Burton, C., Halladay, K., Betts, R. A., et al. (2018). Changes

in Climate and Land Use Over the Amazon Region: Current and Future Variability and Trends. *Frontiers in Earth Science*. https://doi.org/10.3389/feart.2018.00228

Marinho, T., Filizola, N., Martinez, J. M., Armijos, E., & Nascimento, A. (2018). Suspended sediment variability at the Solimões and negro confluence between May 2013 and February 2014. *Geosciences (Switzerland)*, *8*(7). https://doi.org/10.3390/geosciences8070265

Martens, B., Miralles, D. G., Lievens, H., Van Der Schalie, R., De Jeu, R. A. M., Fernández-Prieto, D., et al. (2017). GLEAM v3: Satellite-based land evaporation and root-zone soil moisture. *Geoscientific Model Development*, *10*(5), 1903–1925. https://doi.org/10.5194/gmd-10-1903-2017

Martinez, J., Espinoza-villar, R., Armijos, E., & Moreira, L. S. (2015). The optical properties of river and floodplain waters in the Amazon River Basin: Implications for satellite-based measurements of suspended particulate matter - Supplemtary ,material. *Journal of Geophysical Research : Earth Surface*, *1*(860), 1–11. https://doi.org/10.1002/2014JF003404.Received

Martinez, J. A., & Dominguez, F. (2014). Sources of Atmospheric Moisture for the La Plata River Basin*. *Journal of Climate*, *27*(17), 6737–6753. https://doi.org/10.1175/JCLI-D-14-00022.s1

Martinez, J. M., Guyot, J. L., Filizola, N., & Sondag, F. (2009). Increase in suspended sediment discharge of the Amazon River assessed by monitoring network and satellite data. *Catena*, *79*(3), 257–264. https://doi.org/10.1016/j.catena.2009.05.011

Marzano, F. S., Member, S., Palmacci, M., Cimini, D., Giuliani, G., & Turk, F. J. (2004). Multivariate Statistical Integration of Satellite Infrared and Microwave Radiometric Measurements for Rainfall Retrieval at the Geostationary Scale, *42*(5), 1018–1032.

Massari, C. (2020, May). GPM+SM2RAIN (2007-2018): quasi-global 25km/daily rainfall product from the integration of GPM and SM2RAIN-based rainfall products. Zenodo. https://doi.org/10.5281/zenodo.3854817

Massari, C., Brocca, L., Tarpanelli, A., & Moramarco, T. (2015). *Data assimilation of satellite soil moisture into rainfall-runoffmodelling: A complex recipe? Remote Sensing* (Vol. 7). https://doi.org/10.3390/rs70911403

Matthews, E., & Fung, I. (1987). Methane emission from natural wetlands: Global distribution, area, and environmental characteristics of sources. *Global Biogeochemical Cycles*, *1*, 61–86. https://doi.org/10.1029/GB001i001p00061

Matthews, M. W. (2011). A current review of empirical procedures of remote sensing in Inland and near-coastal transitional waters. *International Journal of Remote Sensing*, *32*(21), 6855–6899. https://doi.org/10.1080/01431161.2010.512947

Mayta, V. C., Ambrizzi, T., Espinoza, J. C., & Silva Dias, P. L. (2019). The role of the Madden–Julian

4251 oscillation on the Amazon Basin intraseasonal rainfall variability. *International Journal of*
4252 *Climatology*, *39*(1), 343–360. https://doi.org/10.1002/joc.5810
4253 McCabe, M. F., Rodell, M., Alsdorf, D. E., Miralles, D. G., Uijlenhoet, R., Wagner, W., et al. (2017). The
4254 future of Earth observation in hydrology. *Hydrology and Earth System Sciences*, *21*(7), 3879–3914.
4255 https://doi.org/10.5194/hess-21-3879-2017
4256 McCorkel, J., Montanaro, M., Efremova, B., Pearlman, A., Wenny, B., Lunsford, A., et al. (2018).
4257 Landsat 9 Thermal Infrared Sensor 2 Characterization Plan Overview. In *IEEE International*
4258 *Geoscience and Remote Sensing Symposium* (pp. 8845–8848). Valencia, Spain: IEEE.
4259 Meade, R. H. (1994). Suspended sediments of the modern Amazon and Orinoco rivers. *Quaternary*
4260 *International*, *21*(C), 29–39. https://doi.org/10.1016/1040-6182(94)90019-1
4261 Melack, J. M. (2016). Aquatic ecosystems. In L. Nagy, P. Artaxo, & B. R. Forsberg (Eds.), *Interactions*
4262 *Between Biosphere, Atmosphere, and Human Land Use in the Amazon Basin* (pp. 117–145).
4263 Springer. https://doi.org/10.1007/978-3-662-49902-3_1
4264 Melack, J. M., & Coe, M. (2021). Amazon floodplain hydrology and implications for aquatic
4265 conservation. *Aquatic Conservation: Marine and Freshwater Ecosystems*. Retrieved from
4266 Manuscript ID JHMAS-2020-066.R1
4267 Melack, J. M., & Forsberg, B. R. (2001). The Biogeochemistry of the Amazon Floodplain Lakes and
4268 Associated Wetlands. *The Biogeochemistry of the Amazon Basin and Its Role in a Changing World*.
4269 Melack, J. M., & Hess, L. L. (2010). Remote sensing of the distribution and extend of wetlands in the
4270 Amazon Basin. In J. W;, M. T. F. Piedade, F. Wittmann, J. Schöngart, & P. Parolin (Eds.),
4271 *Amazonian Floodplain Forests: Ecophysiology, ecology, biodiversity and sustainable management.*
4272 *Ecological Studies* (Vol. 210, pp. 43–59). Dordrecht: Springer. https://doi.org/10.1007/978-90-481-
4273 8725-6_3
4274 Melack, J. M., Hess, L. L., Gastil, M., Forsberg, B. R., Hamilton, S. K., Lima, I. B. T., & Novo, E. M. L.
4275 M. (2004). Regionalization of methane emissions in the Amazon Basin with microwave remote
4276 sensing. *Global Change Biology*, *10*, 530–544. https://doi.org/10.1111/j.1529-8817.2003.00763.x
4277 Melack, J. M., Novo, E. M. L. M., Forsberg, B. R., Piedade, M. T. F. F., & Maurice, L. (2009).
4278 Floodplain Ecosystem Processes. *Amazonia and Global Change*, (2003), 525–541.
4279 https://doi.org/10.1029/2008GM000727
4280 Melack, J. M., Amaral, J. H. F., Kasper, D., Barbosa, P. M., & Forsberg, B. R. (2021). Limnological
4281 perspectives on conservation of aquatic ecosystems in the Amazon basin. *Aquatic Conservation:*
4282 *Marine and Freshwater Ecosystems*, *30*(12). https://doi.org/10.1002/aqc.3556
4283 Menenti, M., & Choudhury, B. J. (1993). Parameterization of land surface evaporation by means of

location dependent potential evaporation and surface temperature range. In *Exchange Processes at the Land Surface for a Range of Space and Time Scales* (pp. 561–568). Yokohama, Japan: IAHS Publ.

Mertes, L. A. K. (1997). Documentation and significance of the perirheic zone on inundated floodplains. *Water Resources Research*, *33*(7), 1749–1762. https://doi.org/10.1029/97WR00658

Mertes, L. A. K., Smith, M. O., & Adams, J. B. (1993). Estimating suspended sediment concentrations in surface waters of the amazon river wetlands from landsat images. *Remote Sensing of Environment*, *43*(3), 281–301. https://doi.org/10.1016/0034-4257(93)90071-5

Mertes, L. A. K., Daniel, D. L., Melack, J. M., Nelson, B., Martinelli, L. A., & Forsberg, B. R. (1995). Spatial patterns of hydrology, geomorphology, and vegetation on the floodplain of the Amazon river in Brazil from a remote sensing perspective. *Geomorphology*, *13*(1–4), 215–232. https://doi.org/10.1016/0169-555X(95)00038-7

Mertes, L. A. K., Dunne, T., & Martinelli, L. A. (1996). Channel-floodplain geomorphology along the Solimoes-Amazon River, Brazil. *Bulletin of the Geological Society of America*, *108*(9), 1089–1107. https://doi.org/10.1130/0016-7606(1996)108<1089:CFGATS>2.3.CO;2

Michel, D., Jiménez, C., Miralles, D. G., Jung, M., Hirschi, M., Ershadi, A., et al. (2016). The WACMOS-ET project - Part 1: Tower-scale evaluation of four remote-sensing-based evapotranspiration algorithms. *Hydrology and Earth System Sciences*, *20*(2), 803–822. https://doi.org/10.5194/hess-20-803-2016

Miguez-Macho, G., & Fan, Y. (2012). The role of groundwater in the Amazon water cycle: 1. Influence on seasonal streamflow, flooding and wetlands. *Journal of Geophysical Research Atmospheres*, *117*(15), 1–30. https://doi.org/10.1029/2012JD017539

Minnis, P., & Harrison, E. F. (1984). Diurnal Variability of Regional Cloud and Clear-Sky Radiative Parameters Derived from GOES Data. Part II: November 1978 Cloud Distributions. *Journal of Climate and Applied Meteorology*, *23*(7), 1012–1031. https://doi.org/10.1175/1520-0450(1984)023<1012:DVORCA>2.0.CO;2

Miralles, D. G., Holmes, T. R. H., De Jeu, R. A. M., Gash, J. H., Meesters, A. G. C. A., & Dolman, A. J. (2011). Global land-surface evaporation estimated from satellite-based observations. *Hydrology and Earth System Sciences*, *15*(2), 453–469. https://doi.org/10.5194/hess-15-453-2011

Miralles, D. G., Jiménez, C., Jung, M., Michel, D., Ershadi, A., Mccabe, M. F., et al. (2016). The WACMOS-ET project - Part 2: Evaluation of global terrestrial evaporation data sets. *Hydrology and Earth System Sciences*, *20*(2), 823–842. https://doi.org/10.5194/hess-20-823-2016

Mobley, C. D. (1994). *Light and water: radiative transfer in natural waters*. Academic press.

4317 Mohammadimanesh, F., Salehi, B., Mahdianpari, M., Brisco, B., & Motagh, M. (2018). Wetland Water
4318 Level Monitoring Using Interferometric Synthetic Aperture Radar (InSAR): A Review. *Canadian*
4319 *Journal of Remote Sensing*, *0*(0), 1–16. https://doi.org/10.1080/07038992.2018.1477680
4320 Mohor, G. S., Rodriguez, D. A., Tomasella, J., & Siqueira Júnior, J. L. (2015). Exploratory analyses for
4321 the assessment of climate change impacts on the energy production in an Amazon run-of-river
4322 hydropower plant. *Journal of Hydrology: Regional Studies*, *4*(PB), 41–59.
4323 https://doi.org/10.1016/j.ejrh.2015.04.003
4324 Molina-Carpio, J., Espinoza, J. C., Vauchel, P., Ronchail, J., Gutierrez Caloir, B., Guyot, J. L., &
4325 Noriega, L. (2017). Hydroclimatology of the Upper Madeira River basin: spatio-temporal variability
4326 and trends. *Hydrological Sciences Journal*, *62*(6), 911–927.
4327 https://doi.org/10.1080/02626667.2016.1267861
4328 Molinas, E., Carneiro, J. C., & Vinzon, S. (2020). Internal tides as a major process in Amazon continental
4329 shelf fine sediment transport. *Marine Geology*, *430*(June).
4330 https://doi.org/10.1016/j.margeo.2020.106360
4331 Montanher, O. C., Novo, E. M. L. de M., Barbosa, C. C. F. F., Rennó, C. D., & Silva, T. S. F. F. (2014).
4332 Empirical models for estimating the suspended sediment concentration in Amazonian white water
4333 rivers using Landsat 5/TM. *International Journal of Applied Earth Observation and*
4334 *Geoinformation*, *29*(1), 67–77. https://doi.org/10.1016/j.jag.2014.01.001
4335 Montanher, O. C., Novo, E. M. L. de M., & Filho, E. D. S. (2018). Temporal trend of the suspended
4336 sediment transport of the Amazon River (1984 – 2016). *Hydrological Sciences Journal*, *63*(13–14),
4337 1901–1912. https://doi.org/10.1080/02626667.2018.1546387
4338 Montazem, A., Garambois, P., Calmant, S., Finaud-Guyot, P., Monnier, J., Medeiros Moreira, D., et al.
4339 (2019). Wavelet-based river segmentation using hydraulic control-preserving water surface
4340 elevation profile properties. *Geophysical Research Letters*, 2019GL082986.
4341 https://doi.org/10.1029/2019GL082986
4342 Monteith, J. (1965). Evaporation and the Environment in the State and Movement of Water in Living
4343 Organisms. In *Proceedings of the Society for Experimental Biology* (pp. 205–234). Cambridge:
4344 Cambridge University Press.
4345 Monteith, J., & Unsworth, M. (2013). *Principles of Environmental Physics: Plants, Animals, and the*
4346 *Atmosphere*. *Principles of Environmental Physics: Plants, Animals, and the Atmosphere: Fourth*
4347 *Edition* (Fourth). Academic Press. https://doi.org/10.1016/C2010-0-66393-0
4348 Moreira, A. A., Ruhoff, A. L., Roberti, D. R., Souza, V. de A., da Rocha, H. R., & de Paiva, R. C. D.
4349 (2019). Assessment of terrestrial water balance using remote sensing data in South America. *Journal*

4350 *of Hydrology*, *575*(May), 131–147. https://doi.org/10.1016/j.jhydrol.2019.05.021
4351 Mu, Q., Heinsch, F. A., Zhao, M., & Running, S. W. (2007). Development of a global evapotranspiration
4352 algorithm based on MODIS and global meteorology data. *Remote Sensing of Environment*, *111*(4),
4353 519–536. https://doi.org/10.1016/j.rse.2007.04.015
4354 Mu, Q., Zhao, M., & Running, S. W. (2011). Improvements to a MODIS global terrestrial
4355 evapotranspiration algorithm. *Remote Sensing of Environment*, *115*(8), 1781–1800.
4356 https://doi.org/10.1016/j.rse.2011.02.019
4357 Mueller, J. L., Morel, A., Frouin, R., Davis, C. O., Arnone, R. a., Carder, K. L., et al. (2003). Vol 3:
4358 Radiometric Measurements and Data Analysis Protocols. *Ocean Optics Protocols For Satellite*
4359 *Ocean Color Sensor Validation, Revision 4*, *III*(January), 78.
4360 Munier, S., & Aires, F. (2018). A new global method of satellite dataset merging and quality
4361 characterization constrained by the terrestrial water budget. *Remote Sensing of Environment*,
4362 *205*(October 2017), 119–130. https://doi.org/10.1016/j.rse.2017.11.008
4363 Nagel, G. W., Novo, E. M. L. de M., & Kampel, M. (2020). Nanosatellites applied to optical Earth
4364 observation: a review. *Revista Ambiente e Agua*, *9*(3), 445–458. https://doi.org/10.4136/1980-993X
4365 Nagy, L., Artaxo, P., & Forsberg, B. R. (2016). *Interactions between Biosphere, Atmosphere and Human*
4366 *Land Use in the Amazon Basin*. (L. Nagy, P. Artaxo, & B. R. Forsberg, Eds.) (1st ed.). Berlin
4367 Heidelberg: Springer. https://doi.org/10.1007/978-3-662-49902-3
4368 Ndehedehe, C. E., & Ferreira, V. G. (2020). Assessing land water storage dynamics over South America.
4369 *Journal of Hydrology*, *580*. https://doi.org/10.1016/j.jhydrol.2019.124339
4370 Negri, A. J., Adler, R. F., Nelkin, E. J., & Huffman, G. J. (1994). Regional Rainfall Climatologies
4371 Derived from Special Sensor Microwave Imager (SSM/I) Data. *Bulletin of the American*
4372 *Meteorological Society*, *75*(7), 1165–1182. https://doi.org/10.1175/1520-
4373 0477(1994)075<1165:RRCDFS>2.0.CO;2
4374 Negri, A. J., Anagnostou, E. N., & Adler, R. F. (2000). A 10-yr climatology of amazonian rainfall derived
4375 from passive microwave satellite observations. *Journal of Applied Meteorology*, *39*(1), 42–56.
4376 https://doi.org/10.1175/1520-0450(2000)039<0042:AYCOAR>2.0.CO;2
4377 Nguyen, P., Shearer, E. J., Tran, H., Ombadi, M., Hayatbini, N., Palacios, T., et al. (2019). The CHRS
4378 data portal, an easily accessible public repository for PERSIANN global satellite precipitation data.
4379 *Scientific Data*, *6*, 1–10. https://doi.org/10.1038/sdata.2018.296
4380 Niroumand-Jadidi, M., Bovolo, F., & Bruzzone, L. (2020). Water quality retrieval from PRISMA
4381 hyperspectral images: First experience in a turbid lake and comparison with sentinel-2. *Remote*
4382 *Sensing*, *12*(23), 1–21. https://doi.org/10.3390/rs12233984

4383 Niu, J., Shen, C., Chambers, J. Q., Melack, J. M., & Riley, W. J. (2017). Interannual Variation in
4384 Hydrologic Budgets in an Amazonian Watershed with a Coupled Subsurface–Land Surface Process
4385 Model. *Journal of Hydrometeorology*, *18*(9), 2597–2617. https://doi.org/10.1175/JHM-D-17-0108.1
4386 Nobrega, I. W. da. (2002). *Análise espectral de sistemas aquáticos da Amazônia para a identificação de*
4387 *componentes opticamente ativos*. Instituto Nacional de Pesquisas Espaciais (INPE), São José dos
4388 Campos.
4389 Norman, J. M., Kustas, W. P., & Humes, K. S. (1995). *Source approach for estimating soil and*
4390 *vegetation energy fluxes in observations of directional radiometric surface temperature*.
4391 *Agricultural and Forest Meteorology* (Vol. 77).
4392 Normandin, C., Frappart, F., Diepkilé, A. T., Marieu, V., Mougin, E., Blarel, F., et al. (2018). Evolution
4393 of the Performances of Radar Altimetry Missions from ERS-2 to Sentinel-3A over the Inner Niger
4394 Delta. *Remote Sensing*, *10*(6), 833. https://doi.org/10.3390/rs10060833
4395 Novo, E. M. L. de M., & Shimabukuro, Y. E. (1997). Identification and mapping of the Amazon habitats
4396 using a mixing model. *International Journal of Remote Sensing*, *18*, 663–670.
4397 https://doi.org/10.1080/014311697218999
4398 Novo, E. M. L. de M., de Farias Barbosa, C. C., Freitas, R. M., Shimabukuro, Y. E., Melack, J. M., &
4399 Filho, W. P. (2006). Seasonal changes in chlorophyll distributions in Amazon floodplain lakes
4400 derived from MODIS images. *Limnology*, *7*(3), 153–161. https://doi.org/10.1007/s10201-006-0179-
4401 8
4402 Novoa, S., Doxaran, D., Ody, A., Vanhellemont, Q., Lafon, V., Lubac, B., & Gernez, P. (2017).
4403 Atmospheric corrections and multi-conditional algorithm for multi-sensor remote sensing of
4404 suspended particulate matter in low-to-high turbidity levels coastal waters. *Remote Sensing*, *9*(1).
4405 https://doi.org/10.3390/rs9010061
4406 O'Loughlin, F. E., Paiva, R. C. D., Durand, M., Alsdorf, D. E., & Bates, P. D. (2016). A multi-sensor
4407 approach towards a global vegetation corrected SRTM DEM product. *Remote Sensing of*
4408 *Environment*, *182*, 49–59. https://doi.org/10.1016/j.rse.2016.04.018
4409 Odermatt, D., Gitelson, A., Brando, V. E., & Schaepman, M. (2012). Review of constituent retrieval in
4410 optically deep and complex waters from satellite imagery. *Remote Sensing of Environment*,
4411 *118*(March), 116–126. https://doi.org/10.1016/j.rse.2011.11.013
4412 Oliveira, A. M., Fleischmann, A. S., & Paiva, R. C. D. (2021). On the contribution of remote sensing-
4413 based calibration to model hydrological and hydraulic processes in tropical regions. *Journal of*
4414 *Hydrology*, 126184. https://doi.org/https://doi.org/10.1016/j.jhydrol.2021.126184
4415 de Oliveira Campos, I., Mercier, F., Maheu, C., Cochonneau, G., Kosuth, P., Blitzkow, D., & Cazenave,

A. (2001). Temporal variations of river basin waters from Topex/Poseidon satellite altimetry. Application to the Amazon basin. *Comptes Rendus de l'Académie Des Sciences-Series IIA-Earth and Planetary Science*, *333*(10), 633–643.

de Oliveira, G., Brunsell, N. A., Moraes, E. C., Shimabukuro, Y. E., dos Santos, T. V., von Randow, C., et al. (2019). Effects of land-cover changes on the partitioning of surface energy and water fluxes in Amazonia using high-resolution satellite imagery. *Ecohydrology*, *12*(6). https://doi.org/10.1002/eco.2126

Oliveira, P. T. S., Nearing, M. A., Moran, M. S., Goodrich, D. C., Wendland, E., & Gupta, H. V. (2014). Trends in water balance components across the Brazilian Cerrado. *Water Resources Research*, *50*(9), 7100–7114. https://doi.org/10.1002/2013WR015202

Oliveira, R., Maggioni, V., Vila, D., & Morales, C. (2016). Characteristics and diurnal cycle of GPM rainfall estimates over the Central Amazon region. *Remote Sensing*, *8*(7). https://doi.org/10.3390/rs8070544

Ovando, A., Tomasella, J., Rodriguez, D. A., Martinez, J. M., Siqueira-Junior, J. L., Pinto, G. L. N., et al. (2016). Extreme flood events in the Bolivian Amazon wetlands. *Journal of Hydrology: Regional Studies*, *5*, 293–308. https://doi.org/10.1016/j.ejrh.2015.11.004

Ovando, A., Martinez, J. M., Tomasella, J., Rodriguez, D. A., & von Randow, C. (2018). Multi-temporal flood mapping and satellite altimetry used to evaluate the flood dynamics of the Bolivian Amazon wetlands. *International Journal of Applied Earth Observation and Geoinformation*, *69*(January), 27–40. https://doi.org/10.1016/j.jag.2018.02.013

Overeem, A., Leijnse, H., & Uijlenhoet, R. (2013). Country-wide rainfall maps from cellular communication networks. *Proceedings of the National Academy of Sciences of the United States of America*, *110*(8), 2741–2745. https://doi.org/10.1073/pnas.1217961110

Overeem, A., Leijnse, H., & Uijlenhoet, R. (2016). Two and a half years of country-wide rainfall maps using radio links from commercial cellular telecommunication networks. *Water Resources Research*, *52*(10), 8039–8065. https://doi.org/10.1002/2016WR019412

Paca, V. H. da M., Espinoza-Dávalos, G. E., Hessels, T. M., Moreira, D. M., Comair, G. F., & Bastiaanssen, W. G. M. (2019). The spatial variability of actual evapotranspiration across the Amazon River Basin based on remote sensing products validated with flux towers. *Ecological Processes*, *8*(1). https://doi.org/10.1186/s13717-019-0158-8

Paca, V. H. da M., Espinoza-Dávalos, G., Moreira, D., & Comair, G. (2020). Variability of Trends in Precipitation across the Amazon River Basin Determined from the CHIRPS Precipitation Product and from Station Records. *Water*, *12*(5), 1244. https://doi.org/10.3390/w12051244

4449 Paccini, L., Espinoza, J. C., Ronchail, J., & Segura, H. (2018). Intra-seasonal rainfall variability in the
4450 Amazon basin related to large-scale circulation patterns: a focus on western Amazon-Andes
4451 transition region. *International Journal of Climatology*, *38*(5), 2386–2399.
4452 https://doi.org/10.1002/joc.5341
4453 Paiva, R. C. D. de. (2020). Advances and challenges in the water sciences in Brazil : a community
4454 synthesis of the XXIII Brazilian Water Resources Symposium. *Revista Brasileira de Recursos*
4455 *Hídricos*, *5*(50). https://doi.org/10.1590/2318-0331.252020200136
4456 Paiva, R. C. D. de, Collischonn, W., & Tucci, C. E. M. (2011). Large scale hydrologic and hydrodynamic
4457 modeling using limited data and a GIS based approach. *Journal of Hydrology*, *406*(3–4), 170–181.
4458 https://doi.org/10.1016/j.jhydrol.2011.06.007
4459 Paiva, R. C. D. de, Buarque, D. C., Clarke, R. T., Collischonn, W., & Allasia, D. G. (2011). Reduced
4460 precipitation over large water bodies in the Brazilian Amazon shown from TRMM data.
4461 *Geophysical Research Letters*, *38*(4). https://doi.org/10.1029/2010GL045277
4462 Paiva, R. C. D. de, Collischonn, W., Bonnet, M. P., De Gonçalves, L. G. G., Calmant, S., Getirana, A., &
4463 Santos Da Silva, J. (2013). Assimilating in situ and radar altimetry data into a large-scale
4464 hydrologic-hydrodynamic model for streamflow forecast in the Amazon. *Hydrology and Earth*
4465 *System Sciences*, *17*(7), 2929–2946. https://doi.org/10.5194/hess-17-2929-2013
4466 Paiva, R. C. D. de, Buarque, D. C., Collischonn, W., Bonnet, M. P., Frappart, F., Calmant, S., & Bulhões
4467 Mendes, C. A. (2013). Large-scale hydrologic and hydrodynamic modeling of the Amazon River
4468 basin. *Water Resources Research*, *49*(3), 1226–1243. https://doi.org/10.1002/wrcr.20067
4469 Pan, M., & Wood, E. F. (2006). Data Assimilation for Estimating the Terrestrial Water Budget Using a
4470 Constrained Ensemble Kalman Filter. *Journal of Hydrometeorology*, *7*(3), 534–547.
4471 https://doi.org/10.1175/JHM495.1
4472 Pan, M., Sahoo, A. K., Troy, T. J., Vinukollu, R. K., Sheffield, J., & Wood, A. E. F. (2012). Multisource
4473 estimation of long-term terrestrial water budget for major global river basins. *Journal of Climate*,
4474 *25*(9), 3191–3206. https://doi.org/10.1175/JCLI-D-11-00300.1
4475 Panday, P. K., Coe, M. T., Macedo, M. N., Lefebvre, P., & Castanho, A. D. de A. (2015). Deforestation
4476 offsets water balance changes due to climate variability in the Xingu River in eastern Amazonia.
4477 *Journal of Hydrology*, *523*(February 2015), 822–829. https://doi.org/10.1016/j.jhydrol.2015.02.018
4478 Pangala, S. R., Enrich-Prast, A., Basso, L. S., Peixoto, R. B., Bastviken, D., Hornibrook, E. R. C., et al.
4479 (2017). Large emissions from floodplain trees close the Amazon methane budget. *Nature*, *552*, 230–
4480 234. https://doi.org/10.1038/nature24639
4481 Panosso, R. D. F., Muehe, D., & Esteves, F. D. A. (1995). Morphological characteristics of an Amazon

floodplain lake (Lake Batata, Para State, Brazil). *Amazonia*, *13*(3–4), 245–258.

Paola, F. Di, Casella, D., Dietrich, S., Mugnai, A., Ricciardelli, E., Romano, F., et al. (2012). Combined MW-IR Precipitation Evolving Technique (PET) of convective rain fields, 3557–3570. https://doi.org/10.5194/nhess-12-3557-2012

Papa, F., Günther, A., Frappart, F., Prigent, C., Rossow, W. B. B., Güntner, A., et al. (2008). Variations of surface water extent and water storage in large river basins: A comparison of different global data sources. *Geophysical Research Letters*, *35*(11), L11401. https://doi.org/10.1029/2008GL033857

Papa, F., Prigent, C., Aires, F., Jimenez, C., Rossow, W. B., & Matthews, E. (2010). Interannual variability of surface water extent at the global scale, 1993-2004. *Journal of Geophysical Research Atmospheres*, *115*(D12). https://doi.org/10.1029/2009JD012674

Papa, F., Frappart, F., Güntner, A., Prigent, C., Aires, F., Getirana, A. C. V, & Maurer, R. (2013). Surface freshwater storage and variability in the Amazon basin from multi-satellite observations, 1993-2007. *Journal of Geophysical Research Atmospheres*, *118*(21), 11951–11965. https://doi.org/10.1002/2013JD020500

Papa, F., Frappart, F., Malbeteau, Y., Shamsudduha, M., Vuruputur, V., Sekhar, M., et al. (2015). Satellite-derived surface and sub-surface water storage in the Ganges–Brahmaputra River Basin. *Journal of Hydrology: Regional Studies*, *4*, 15–35. https://doi.org/https://doi.org/10.1016/j.ejrh.2015.03.004

Paredes Trejo, F. J., Barbosa, H. A., Peñaloza-Murillo, M. A., Alejandra Moreno, M., & Farías, A. (2016). Intercomparison of improved satellite rainfall estimation with CHIRPS gridded product and rain gauge data over Venezuela. *Atmosfera*, *29*(4), 323–342. https://doi.org/10.20937/ATM.2016.29.04.04

Paris, A., Paiva, R. D. de, Silva, J. S. da, Moreira, D. M., Calmant, S., Garambois, P.-A., et al. (2016). Stage-discharge rating curves based on satellite altimetry and modeled discharge in the Amazon basin. *Water Resources Research*, *52*, 3787–3814. https://doi.org/10.1002/2014WR016618.Received

Paris, A., Calmant, S., Gosset, M., Fleischmann, A., Conchy, T., Bricquet, J.-P., et al. (2020). Monitoring hydrological variables from remote sensing and modelling in the Congo River basin. *Earth and Space Science Open Archive*, 53. https://doi.org/10.1002/essoar.10505518.1

Park, E. (2020). Characterizing channel-floodplain connectivity using satellite altimetry: Mechanism, hydrogeomorphic control, and sediment budget. *Remote Sensing of Environment*, *243*(February), 111783. https://doi.org/10.1016/j.rse.2020.111783

Park, E., & Latrubesse, E. M. (2014). Modeling suspended sediment distribution patterns of the Amazon

River using MODIS data. *Remote Sensing of Environment*, *147*, 232–242. https://doi.org/10.1016/j.rse.2014.03.013

Park, E., Emadzadeh, A., Alcântara, E., Yang, X., & Ho, H. L. (2020). Inferring floodplain bathymetry using inundation frequency. *Journal of Environmental Management*, *273*(July). https://doi.org/10.1016/j.jenvman.2020.111138

Parrens, M., Bitar, A. Al, Frappart, F., Papa, F., Calmant, S., Crétaux, J. F., et al. (2017). Mapping dynamic water fraction under the tropical rain forests of the Amazonian basin from SMOS brightness temperatures. *Water*, *9*(5), 350. https://doi.org/10.3390/w9050350

Parrens, M., Bitar, A. Al, Frappart, F., Paiva, R., Wongchuig, S., Papa, F., et al. (2019). High resolution mapping of inundation area in the Amazon basin from a combination of L-band passive microwave, optical and radar datasets. *International Journal of Applied Earth Observation and Geoinformation*, *81*(August 2018), 58–71. https://doi.org/10.1016/j.jag.2019.04.011

Pearce, F. (2020). Weather makers. *Science*, *368*, 1302–1305. https://doi.org/10.1126/science.368.6497.1302

Peixoto, J. M. A., Nelson, B. W., & Wittmann, F. (2009). Spatial and temporal dynamics of river channel migration and vegetation in central Amazonian white-water floodplains by remote-sensing techniques. *Remote Sensing of Environment*, *113*(10), 2258–2266. https://doi.org/10.1016/j.rse.2009.06.015

Pekel, J. F., Cottam, A., Gorelick, N., & Belward, A. S. (2016). High-resolution mapping of global surface water and its long-term changes. *Nature*, *540*(7633), 418–422. https://doi.org/10.1038/nature20584

Pellet, V., Aires, F., & Yamazaki, D. (2021). Satellite monitoring of the water cycle over the Amazon using upstream / downstream dependency. Part 2 : Mass-conserved reconstruction of total water storage change and river discharge. *Water Resources Research*.

Peng, B., Shi, J., Ni-Meister, W., Zhao, T., & Ji, D. (2014). Evaluation of TRMM multisatellite precipitation analysis (tmpa) products and their potential hydrological application at an arid and semiarid basin in china. *IEEE Journal of Selected Topics in Applied Earth Observations and Remote Sensing*, *7*(9), 3915–3930. https://doi.org/10.1109/JSTARS.2014.2320756

Penman, H. L. (1948). Natural evaporation from open water, hare soil and grass. *Proceedings of the Royal Society of London. Series A, Mathematical and Physical Sciences*, *194*, 120–146. https://doi.org/10.1098/rspa.1948.0037

Peral, E., Tanelli, S., Statham, S., Joshi, S., Imken, T., Price, D., et al. (2019). RainCube: the first ever radar measurements from a CubeSat in space. *Journal of Applied Remote Sensing*, *13*(03), 1.

https://doi.org/10.1117/1.jrs.13.032504

Pfeffer, J., Seyler, F., Bonnet, M.-P., Calmant, S., Frappart, F., Papa, F., et al. (2014). Low-water maps of the groundwater table in the central Amazon by satellite altimetry. *Geophysical Research Letters*, *41*(6), 1981–1987. https://doi.org/10.1002/2013GL059134

Pham-Duc, B., Papa, F., Prigent, C., Aires, F., Biancamaria, S., & Frappart, F. (2019). Variations of Surface and Subsurface Water Storage in the Lower Mekong Basin (Vietnam and Cambodia) from Multisatellite Observations. *Water*, *11*(1). https://doi.org/10.3390/w11010075

Pham-Duc, B., Sylvestre, F., Papa, F., Frappart, F., Bouchez, C., & Crétaux, J. F. (2020). The Lake Chad hydrology under current climate change. *Scientific Reports*, *10*. https://doi.org/10.1038/s41598-020-62417-w

Phillips, O. L., Aragão, L. E. O. C., Lewis, S. L., Fisher, J. B., Lloyd, J., López-González, G., et al. (2009). Drought sensitivity of the amazon rainforest. *Science*, *323*(5919), 1344–1347. https://doi.org/10.1126/science.1164033

Pilotto, I. L., Rodríguez, D. A., Tomasella, J., Sampaio, G., & Chou, S. C. (2015). Comparisons of the Noah-MP land surface model simulations with measurements of forest and crop sites in Amazonia. *Meteorology and Atmospheric Physics*, *127*(6), 711–723. https://doi.org/10.1007/s00703-015-0399-8

Pinel, S., Bonnet, M.-P., Santos Da Silva, J., Moreira, D., Calmant, S., Satgé, F., & Seyler, F. (2015). Correction of Interferometric and Vegetation Biases in the SRTMGL1 Spaceborne DEM with Hydrological Conditioning towards Improved Hydrodynamics Modeling in the Amazon Basin. *Remote Sensing*, *7*(12), 16108–16130. https://doi.org/10.3390/rs71215822

Pinel, S., Bonnet, M., Silva, J. S. Da, Sampaio, T. C., Garnier, J., Fragoso, C. R. J., et al. (2019). Flooding dynamics within a Amazonian floodplain: Water circulation patterns and inundation duration. *Water Resources Research*, 1–23.

Pinet, S. Y. P., Artinez, J. E. A. N. I. M., Uillon, S. Y. O., Runo, B., Artiges, L., & Illar, R. A. U. L. E. S. V. (2017). Variability of apparent and inherent optical properties of sediment-laden waters in large river basins – lessons from in situ measurements and bio-optical modeling. *Optics Express*, *25*(8), 283–310.

Pison, I., Ringeval, B., Bousquet, P., Prigent, C., & Papa, F. (2013). Stable atmospheric methane in the 2000s: Key-role of emissions from natural wetlands. *Atmospheric Chemistry and Physics*, *13*(23), 11609–11623. https://doi.org/10.5194/acp-13-11609-2013

Pokhrel, Y. N., Fan, Y., Miguez-Macho, G., Yeh, P. J. F., & Han, S. C. (2013). The role of groundwater in the Amazon water cycle: 3. Influence on terrestrial water storage computations and comparison

with GRACE. *Journal of Geophysical Research Atmospheres*, *118*(8), 3233–3244. https://doi.org/10.1002/jgrd.50335

Pokhrel, Y. N., Fan, Y., & Miguez-Macho, G. (2014). Potential hydrologic changes in the Amazon by the end of the 21st century and the groundwater buffer. *Environmental Research Letters*, *9*(8), 084004. https://doi.org/10.1088/1748-9326/9/8/084004

Pontes, P. R. M., Cavalcante, R. B. L., Sahoo, P. K., Silva Júnior, R. O. d., da Silva, M. S., Dall'Agnol, R., & Siqueira, J. O. (2019). The role of protected and deforested areas in the hydrological processes of Itacaiúnas River Basin, eastern Amazonia. *Journal of Environmental Management*, *235*, 489–499. https://doi.org/10.1016/j.jenvman.2019.01.090

Potter, C., Melack, J. M., & Engle, D. (2014). Modeling methane emissions from amazon floodplain ecosystems. *Wetlands*, *34*, 501–511. https://doi.org/10.1007/s13157-014-0516-3

Prabhakara, C., Short, D. A., Wiscombe, W., Fraser, R. S., & Vollmer, B. E. (1986). Rainfall over Oceans Inferred from Nimbus 7 SMMR: Application to 1982–83 El Niño. *Journal of Climate and Applied Meteorology*, *25*(10), 1464–1474.

Priestley, C. H. B., & Taylor, R. J. (1972). On the Assessment of Surface Heat Flux and Evaporation Using Large-Scale Parameters. *Monthly Weather Review*, *100*(2), 81–92. https://doi.org/10.1175/1520-0493(1972)100<0081:otaosh>2.3.co;2

Prigent, C. (2010). Precipitation retrieval from space: An overview. *Comptes Rendus - Geoscience*, *342*(4–5), 380–389. https://doi.org/10.1016/j.crte.2010.01.004

Prigent, C., Aires, F., Rossow, W. B., & Robock, A. (2005). Sensitivity of satellite microwave and infrared observations to soil moisture at a global scale: Relationship of satellite observations to in situ soil moisture measurements. *Journal of Geophysical Research: Atmospheres*, *110*(D7). https://doi.org/https://doi.org/10.1029/2004JD005087

Prigent, C., Papa, F., Aires, F., Rossow, W. B., & Matthews, E. (2007). Global inundation dynamics inferred from multiple satellite observations, 1993-2000. *Journal of Geophysical Research Atmospheres*, *112*(12). https://doi.org/10.1029/2006JD007847

Prigent, C., Papa, F., Aires, F., Jimenez, C., Rossow, W. B., & Matthews, E. (2012). Changes in land surface water dynamics since the 1990s and relation to population pressure. *Geophysical Research Letters*, *39*(8). https://doi.org/10.1029/2012GL051276

Prigent, C., Lettenmaier, D. P., Aires, F., & Papa, F. (2016). Toward a High-Resolution Monitoring of Continental Surface Water Extent and Dynamics, at Global Scale: from GIEMS (Global Inundation Extent from Multi-Satellites) to SWOT (Surface Water Ocean Topography). *Surveys in Geophysics*, *37*(2), 339–355. https://doi.org/10.1007/s10712-015-9339-x

4614 Prigent, C., Jimenez, C., & Bousquet, P. (2020). Satellite-Derived Global Surface Water Extent and
4615 Dynamics Over the Last 25 Years (GIEMS-2). *Journal of Geophysical Research: Atmospheres*,
4616 *125*(3). https://doi.org/10.1029/2019JD030711
4617 Pujol, L., Garambois, P.-A., Finaud-Guyot, P., Monnier, J., Larnier, K., Mosé, R., et al. (2020).
4618 Estimation of Multiple Inflows and Effective Channel by Assimilation of Multi-satellite Hydraulic
4619 Signatures: The Ungauged Anabranching Negro River. *Journal of Hydrology*.
4620 https://doi.org/10.1016/j.jhydrol.2020.125331
4621 Ramillien, G., Frappart, F., Gratton, S., & Vasseur, X. (2015). Sequential estimation of surface water
4622 mass changes from daily satellite gravimetry data. *Journal of Geodesy*, *89*(3), 259–282.
4623 https://doi.org/10.1007/s00190-014-0772-2
4624 Ramillien, G., Seoane, L., Schumacher, M., Forootan, E., Frappart, F., & Darrozes, J. (2020). Recovery of
4625 rapid water mass changes (RWMC) by Kalman filtering of GRACE observations. *Remote Sensing*,
4626 *12*(8), 1299. https://doi.org/10.3390/RS12081299
4627 von Randow, C., Manzi, A. O., Kruijt, B., de Oliveira, P. J., Zanchi, F. B., Silva, R. L., et al. (2004).
4628 Comparative measurements and seasonal variations in energy and carbon exchange over forest and
4629 pasture in South West Amazonia. *Theoretical and Applied Climatology*, *78*(1–3), 5–26.
4630 https://doi.org/10.1007/s00704-004-0041-z
4631 von Randow, R. de C. S., Tomasella, J., von Randow, C., de Araújo, A. C., Manzi, A. O., Hutjes, R., &
4632 Kruijt, B. (2020). Evapotranspiration and gross primary productivity of secondary vegetation in
4633 Amazonia inferred by eddy covariance. *Agricultural and Forest Meteorology*, *294*.
4634 https://doi.org/10.1016/j.agrformet.2020.108141
4635 Raney, R. K. (1998). The delay/Doppler radar altimeter. *IEEE Transactions on Geoscience and Remote*
4636 *Sensing*, *36*(5), 1578–1588. https://doi.org/10.1109/36.718861
4637 Raymond, P. A., Hartmann, J., Lauerwald, R., Sobek, S., McDonald, C., Hoover, M., et al. (2013). Global
4638 carbon dioxide emissions from inland waters. *Nature*, *503*, 355–359.
4639 https://doi.org/10.1038/nature12760
4640 Reichle, R. H., Liu, Q., Koster, R. D., Draper, C. S., Mahanama, S. P. P., & Partyka, G. S. (2017). Land
4641 Surface Precipitation in MERRA-2. *Journal of Climate*, *30*(5), 1643–1664.
4642 https://doi.org/10.1175/JCLI-D-16-0570.1
4643 Reis, G. G. dos, Paiva, R. C. D. de, Brêda, J. P. L. F., & Medeiros, M. S. (2020). SARDIM - UMA
4644 PLATAFORMA PARA ACOMPANHAMENTO HIDROLÓGICO EM TEMPO REAL DOS RIOS
4645 DA AMÉRICA DO SUL. In *II END - Encontro Nacional de Desastres da*. Porto Alegre:
4646 Associação Brasileira de Recursos Hídricos. Retrieved from http://anais.abrh.org.br/works/7285

4647 Reis, V., Hermoso, V., Hamilton, S. K., Linke, S., & Bunn, S. E. (2019). Characterizing seasonal
4648 dynamics of Amazonian wetlands for conservation and decision making, (December 2018), 1–10.
4649 https://doi.org/10.1002/aqc.3051
4650 Resende, A. F. de, Schöngart, J., Streher, A. S., Ferreira-Ferreira, J., Piedade, M. T. F., & Silva, T. S. F.
4651 (2019). Massive tree mortality from flood pulse disturbances in Amazonian floodplain forests: The
4652 collateral effects of hydropower production. *Science of the Total Environment*, *659*, 587–598.
4653 https://doi.org/10.1016/j.scitotenv.2018.12.208
4654 Restrepo-Coupe, N., da Rocha, H. R., Hutyra, L. R., da Araujo, A. C., Borma, L. S., Christoffersen, B., et
4655 al. (2013). What drives the seasonality of photosynthesis across the Amazon basin? A cross-site
4656 analysis of eddy flux tower measurements from the Brasil flux network. *Agricultural and Forest*
4657 *Meteorology*, *182–183*, 128–144. https://doi.org/10.1016/j.agrformet.2013.04.031
4658 Richey, J. E., Mertes, L. K., Dunne, T., Victoria, R. L., Forsberg, B. R., Tancredi, A. C. N. S., & Oliveira,
4659 E. de. (1989). Sources and routing of the Amazon River flood wave, *3*(3), 191–204.
4660 Richey, J. E., Melack, J. M., Aufdenkampe, A. K., Ballester, V. M., & Hess, L. L. (2002). Outgassing
4661 from Amazonian rivers and wetlands as a large tropical source of atmospheric CO2. *Nature*,
4662 *416*(6881), 617–620. https://doi.org/10.1038/416617a
4663 Rocha, H. R., Manzi, A. O., Cabral, O. M., Miller, S. D., Goulden, M. L., Saleska, S. R., et al. (2009).
4664 Patterns of water and heat flux across a biome gradient from tropical forest to savanna in brazil.
4665 *Journal of Geophysical Research: Biogeosciences*, *114*(1), 1–8.
4666 https://doi.org/10.1029/2007JG000640
4667 Rodell, M., Houser, P. R., Jambor, U., Gottschalck, J., Mitchell, K., Meng, C. J., et al. (2004). The Global
4668 Land Data Assimilation System. *Bulletin of the American Meteorological Society*, *85*(3), 381–394.
4669 https://doi.org/10.1175/BAMS-85-3-381
4670 Rodell, M., Mcwilliams, E. B., Famiglietti, J. S., Beaudoing, H. K., & Nigro, J. (2011). Estimating
4671 evapotranspiration using an observation based terrestrial water budget. *Hydrological Processes*,
4672 *25*(26), 4082–4092. https://doi.org/10.1002/hyp.8369
4673 Rodriguez-Alvarez, N., Podest, E., Jensen, K., & McDonald, K. C. (2019). Classifying inundation in a
4674 tropical wetlands complex with GNSS-R. *Remote Sensing*, *11*, 1053.
4675 https://doi.org/10.3390/rs11091053
4676 Rodríguez, E., Morris, C. S., & Belz, J. E. (2006). A Global Assessment of the SRTM Performance.
4677 *Photogrammetric Engineering & Remote Sensing*, *72*(3), 249–260.
4678 https://doi.org/10.14358/PERS.72.3.249
4679 Roerink, G. J., Su, Z., & Menenti, M. (2000). *S-SEBI: A Simple Remote Sensing Algorithm to Estimate*

the Surface Energy Balance. *P&s. Chem .Earth (B)* (Vol. 25).

Ronchail, J., Cochonneau, G., Molinier, M., Guyot, J. L., De Miranda Chaves, A. G., Guimarães, V., & De Oliveira, E. (2002). Interannual rainfall variability in the Amazon basin and sea-surface temperatures in the equatorial Pacific and the tropical Atlantic Oceans. *International Journal of Climatology*, *22*(13), 1663–1686. https://doi.org/10.1002/joc.815

Röpke, C. P., Amadio, S., Zuanon, J., Ferreira, E. J. G., De Deus, C. P., Pires, T. H. S., & Winemiller, K. O. (2017). Simultaneous abrupt shifts in hydrology and fish assemblage structure in a floodplain lake in the central Amazon. *Scientific Reports*, *7*, 40170. https://doi.org/10.1038/srep40170

Rosenqvist, Å., & Birkett, C. M. (2002). Evaluation of JERS-1 SAR mosaics for hydrological applications in the Congo river basin. *International Journal of Remote Sensing*, *23*(7), 1283–1302. https://doi.org/10.1080/01431160110092902

Rosenqvist, J., Rosenqvist, A., Jensen, K., & McDonald, K. (2020). Mapping of maximum and minimum inundation extents in the amazon basin 2014-2017 with ALOS-2 PALSAR-2 scan SAR time-series data. *Remote Sensing*, *12*(8). https://doi.org/10.3390/RS12081326

Rossetti, D. F., Gribel, R., Rennó, C. D., Cohen, M. C. L., Moulatlet, G. M., Cordeiro, C. L. de O., & Rodrigues, E. do S. F. (2017). Late Holocene tectonic influence on hydrology and vegetation patterns in a northern Amazonian megafan. *Catena*, *158*(June), 121–130. https://doi.org/10.1016/j.catena.2017.06.022

Rozo, M. G., Nogueira, A. C. R., & Truckenbrodt, W. (2012). The anastomosing pattern and the extensively distributed scroll bars in the middle Amazon River. *Earth Surface Processes and Landforms*, *37*(14), 1471–1488. https://doi.org/10.1002/esp.3249

Rudorff, C. M. (2006). *Estudo da composição das águas da planície amazônica por meio de dados de reflectância do sensor hyperion/EO-1 e de espectrômetro de campo visando a compreensão da variação temporal dos seus constituintes opticamente ativos*. Instituto Nacional de Pesquisas Espaciais (INPE), São José dos Campos.

Rudorff, C. M., Novo, E. M. L. M., & Galvão, L. S. (2006). Spectral Mixture Analysis of Inland Tropical Amazon Floodplain Waters Using EO-1 Hyperion. In *IEEE International Symposium on Geoscience and Remote Sensing* (pp. 128–133). Denver. https://doi.org/10.1109/IGARSS.2006.38

Rudorff, C. M., Novo, E. M. L. M., Galvão, L. S., & Pereira Filho, W. (2007). Análise derivativa de dados hiperespectrais medidos em nível de campo e orbital para caracterizar a composição de águas opticamente complexas na Amazônia. *Acta Amazonica*, *37*(2), 269–280. https://doi.org/10.1590/S0044-59672007000200014

Rudorff, C. M., Melack, J. M., & Bates, P. D. (2014a). Flooding dynamics on the lower Amazon

4713 floodplain: 1. Hydraulic controls on water elevation, inundation extent, and river-floodplain
4714 discharge. *Water Resources Research*, *50*(1), 619–634. https://doi.org/10.1002/2013WR014091
4715 Rudorff, C. M., Melack, J. M., & Bates, P. D. (2014b). Flooding dynamics on the lower Amazon
4716 floodplain: 2. Seasonal and interannual hydrological variability. *Water Resources Research*, *50*(1),
4717 635–649. https://doi.org/10.1002/2013WR014714
4718 Rudorff, C. M., Dunne, T., & Melack, J. M. (2017). Recent increase of river-floodplain suspended
4719 sediment exchange in a reach of the lower Amazon River. *Earth Surface Processes and Landforms*.
4720 https://doi.org/10.1002/esp.4247
4721 Ruhoff, A. L., Paz, A. R., Aragao, L. E. O. C., Mu, Q., Malhi, Y., Collischonn, W., et al. (2013).
4722 Evaluation de l'algorithme MODIS d'estimation de l'évapotranspiration globale utilisant des
4723 mesures de covariance de la turbulence et la modélisation hydrologique dans le bassin du Rio
4724 Grande. *Hydrological Sciences Journal*, *58*(8), 1658–1676.
4725 https://doi.org/10.1080/02626667.2013.837578
4726 Runde, A., Hallwass, G., & Silvano, R. A. M. (2020). Fishers' Knowledge Indicates Extensive
4727 Socioecological Impacts Downstream of Proposed Dams in a Tropical River. *One Earth*, *2*(3), 255–
4728 268. https://doi.org/https://doi.org/10.1016/j.oneear.2020.02.012
4729 Saad, S. I., Da Rocha, H. R., Silva Dias, M. A. F., & Rosolem, R. (2010). Can the deforestation breeze
4730 change the rainfall in Amazonia? A case study for the BR-163 highway region. *Earth Interactions*,
4731 *14*(18). https://doi.org/10.1175/2010EI351.1
4732 Saavedra, M., Junquas, C., Espinoza, J. C., & Silva, Y. (2020). Impacts of topography and land use
4733 changes on the air surface temperature and precipitation over the central Peruvian Andes.
4734 *Atmospheric Research*, *234*, 104711. https://doi.org/10.1016/j.atmosres.2019.104711
4735 Sahagian, D., & Melack, J. (1998). *Global Wetland Distribution and Functional Characterization: Trace*
4736 *Gases and the Hydrologic Cycle*. *Royal Swedish Academy of Sciences*. Stockholm, Sweden.
4737 Sahoo, A. K., Pan, M., Troy, T. J., Vinukollu, R. K., Sheffield, J., & Wood, E. F. (2011). Reconciling the
4738 global terrestrial water budget using satellite remote sensing. *Remote Sensing of Environment*,
4739 *115*(8), 1850–1865. https://doi.org/10.1016/j.rse.2011.03.009
4740 Salameh, E., Frappart, F., Almar, R., Baptista, P., Heygster, G., Lubac, B., et al. (2019). Monitoring
4741 Beach Topography and Nearshore Bathymetry Using Spaceborne Remote Sensing: A Review.
4742 *Remote Sensing*, *11*(19). https://doi.org/10.3390/rs11192212
4743 Salati, E., & Nobre, C. A. (1991). Possible climatic impacts of tropical deforestation. *Climatic Change*,
4744 *19*(1–2), 177–196. https://doi.org/10.1007/BF00142225
4745 Salati, E., & Vose, P. B. (1984). Amazon Basin: A system in equilibrium. *Science*, *225*(4658), 129–138.

https://doi.org/10.1126/science.225.4658.129

Salati, E., Dall'Olio, A., Matsui, E., & Gat, J. R. (1979). Recycling of water in the Amazon Basin: An isotopic study. *Water Resources Research*, *15*(5).

Saleska, S. R., da Rocha, H. R., Huete, A. R., Nobre, A. D., Artaxo, P. E., & Shimabukuro, Y. E. (2013). *LBA-ECO CD-32 Flux Tower Network Data Compilation, Brazilian Amazon: 1999-2006*. Oak Ridge, Tennessee, USA. https://doi.org/doi.org/10.3334/ORNLDAAC/1174

dos Santos, E. S., Lopes, P. P. P., Pereira, H. H. da S., Nascimento, O. de O., Rennie, C. D., Sternberg, L. da S. L. O., & Cunha, A. C. da. (2018). The impact of channel capture on estuarine hydro-morphodynamics and water quality in the Amazon delta. *Science of the Total Environment*, *624*, 887–899. https://doi.org/10.1016/j.scitotenv.2017.12.211

Santos, M. J., Medvigy, D., Silva Dias, M. A. F., Freitas, E. D., & Kim, H. (2019). Seasonal Flooding Causes Intensification of the River Breeze in the Central Amazon. *Journal of Geophysical Research: Atmospheres*, *124*(10), 5178–5197. https://doi.org/10.1029/2018JD029439

Satgé, F., Bonnet, M. P., Gosset, M., Molina, J., Hernan Yuque Lima, W., Pillco Zolá, R., et al. (2016). Assessment of satellite rainfall products over the Andean plateau. *Atmospheric Research*, *167*, 1–14. https://doi.org/10.1016/j.atmosres.2015.07.012

Satgé, F., Xavier, A., Zolá, R. P., Hussain, Y., Timouk, F., Garnier, J., & Bonnet, M. P. (2017). Comparative assessments of the latest GPM mission's spatially enhanced satellite rainfall products over the main bolivian watersheds. *Remote Sensing*, *9*(4), 1–16. https://doi.org/10.3390/rs9040369

Satyamurty, P., da Costa, C. P. W., Manzi, A. O., & Candido, L. A. (2013). A quick look at the 2012 record flood in the Amazon Basin. *Geophysical Research Letters*, *40*(7), 1396–1401. https://doi.org/10.1002/grl.50245

Satyamurty, P., da Costa, C. P. W., & Manzi, A. O. (2013). Moisture source for the Amazon Basin: A study of contrasting years. *Theoretical and Applied Climatology*, *111*(1–2), 195–209. https://doi.org/10.1007/s00704-012-0637-7

van het Schip, T. I., Overeem, A., Leijnse, H., Uijlenhoet, R., Meirink, J. F., & van Delden, A. J. (2017). Rainfall measurement using cell phone links: classification of wet and dry periods using geostationary satellites. *Hydrological Sciences Journal*, *62*(9), 1343–1353. https://doi.org/10.1080/02626667.2017.1329588

Schmitt, R. J. P., Bizzi, S., Castelletti, A., Opperman, J. J., & Kondolf, G. M. (2019). Planning dam portfolios for low sediment trapping shows limits for sustainable hydropower in the Mekong. *Science Advances*, *5*(10). https://doi.org/10.1126/sciadv.aaw2175

Schöngart, J., Wittmann, F., Resende, A. F. de, Assahira, C., Lobo, G. de S., Neves, J. R. D., et al. (2021).

4779 The shadow of the Balbina dam : A synthesis of over 35 years of downstream impacts on floodplain
4780 forests in Central Amazonia. *Aquatic Conservation: Marine and Freshwater Ecosystems*, (Special
4781 Issue), 1–19. https://doi.org/10.1002/aqc.3526
4782 Schroeder, R., McDonald, K. C., Chapman, B. D., Jensen, K., Podest, E., Tessler, Z. D., et al. (2015).
4783 Development and evaluation of a multi-year fractional surface water data set derived from
4784 active/passive microwave remote sensing data. *Remote Sensing*, *7*(12), 16688–16732.
4785 https://doi.org/10.3390/rs71215843
4786 Schumann, G., Bates, P. D., Horritt, M. S., Matgen, P., & Pappenberger, F. (2009). Progress in
4787 Integration of Remote Sensing-Derived Flood Extent and Stage Data and Hydraulic Models.
4788 *Reviews of Geophysics*, *47*(2008), 1–20. https://doi.org/10.1029/2008rg000274
4789 Schwatke, C., Dettmering, D., Bosch, W., & Seitz, F. (2015). DAHITI - An innovative approach for
4790 estimating water level time series over inland waters using multi-mission satellite altimetry.
4791 *Hydrology and Earth System Sciences*, *19*(10), 4345–4364. https://doi.org/10.5194/hess-19-4345-
4792 2015
4793 Sena, J. A., de Deus, L. A. B., Freitas, M. A. V., & Costa, L. (2012). Extreme Events of Droughts and
4794 Floods in Amazonia: 2005 and 2009. *Water Resources Management*, *26*(6), 1665–1676.
4795 https://doi.org/10.1007/s11269-012-9978-3
4796 Seyler, F., Calmant, S., Silva, J. S. Da, Moreira, D. M., Mercier, F., & Shum, C. K. (2013). From
4797 TOPEX/Poseidon to Jason-2/OSTM in the amazon basin. *Advances in Space Research*, *51*(8),
4798 1542–1550. https://doi.org/10.1016/j.asr.2012.11.002
4799 Sheffield, J., Wood, E. F., Pan, M., Beck, H., Coccia, G., Serrat-Capdevila, A., & Verbist, K. (2018,
4800 December 1). Satellite Remote Sensing for Water Resources Management: Potential for Supporting
4801 Sustainable Development in Data-Poor Regions. *Water Resources Research*. Blackwell Publishing
4802 Ltd. https://doi.org/10.1029/2017WR022437
4803 Shi, J., Dong, X., Zhao, T., Du, Y., Liu, H., Wang, Z., et al. (2016). The water cycle observation mission
4804 (WCOM): Overview. In *International Geoscience and Remote Sensing Symposium (IGARSS)* (Vol.
4805 2016-November, pp. 3430–3433). Institute of Electrical and Electronics Engineers Inc.
4806 https://doi.org/10.1109/IGARSS.2016.7729886
4807 Shuttleworth, W. J. (2012). *Terrestrial Hydrometeorology*. *Terrestrial Hydrometeorology*. John Wiley &
4808 Sons. https://doi.org/10.1002/9781119951933
4809 Silva Dias, M. A. F., Silva Dias, P. L., Longo, M., Fitzjarrald, D. R., & Denning, A. S. (2004). River
4810 breeze circulation in eastern Amazonia: Observations and modelling results. *Theoretical and*
4811 *Applied Climatology*, *78*(1–3), 111–121. https://doi.org/10.1007/s00704-004-0047-6

4812 da Silva, E. F. F., Novo, E. M. L. de M., Lobo, F. de L., Barbosa, C. C. F., Noernberg, M. A., Rotta, L. H.
4813 da S., et al. (2020). Optical water types found in Brazilian waters. *Limnology*.
4814 https://doi.org/10.1007/s10201-020-00633-z
4815 Silva, H. J. F. da, Gonçalves, W. A., & Bezerra, B. G. (2019). Comparative analyzes and use of
4816 evapotranspiration obtained through remote sensing to identify deforested areas in the Amazon.
4817 *International Journal of Applied Earth Observation and Geoinformation*, *78*, 163–174.
4818 https://doi.org/10.1016/j.jag.2019.01.015
4819 Silva, J. S. Da, Calmant, S., Seyler, F., Rotunno Filho, O. C., Cochonneau, G., & Mansur, W. J. (2010).
4820 Water levels in the Amazon basin derived from the ERS 2 and ENVISAT radar altimetry missions.
4821 *Remote Sensing of Environment*, *114*(10), 2160–2181. https://doi.org/10.1016/j.rse.2010.04.020
4822 Silva, J. S. Da, Seyler, F., Calmant, S., Filho, O. C. R., Roux, E., Araújo, A. A. M., & Guyot, J. L. (2012).
4823 Water level dynamics of Amazon wetlands at the watershed scale by satellite altimetry.
4824 *International Journal of Remote Sensing*, *33*(11), 3323–3353.
4825 https://doi.org/10.1080/01431161.2010.531914
4826 Silva, J. S. Da, Calmant, S., Seyler, F., Moreira, D. M., Oliveira, D., & Monteiro, A. (2014). Radar
4827 altimetry aids managing gauge networks. *Water Resources Management*, *28*, 587–603.
4828 https://doi.org/10.1007/s11269-013-0484-z
4829 Silva Junior, C. H. L., Almeida, C. T., Santos, J. R. N., Anderson, L. O., Aragão, L. E. O. C., & Silva, F.
4830 B. (2018). Spatiotemporal rainfall trends in the Brazilian legal Amazon between the years 1998 and
4831 2015. *Water*, *10*(9), 1220. https://doi.org/10.3390/w10091220
4832 Silva, M. P. da, Sander de Carvalho, L., Novo, E., Jorge, D., & Barbosa, C. (2019). Use of absorption
4833 optical indices to assess seasonal variability of dissolved organic matter in amazon floodplain lakes.
4834 *Biogeosciences Discussions*, 1–20. https://doi.org/10.5194/bg-2019-324
4835 Silva, M. V., Paris, A., Calmant, S., Cândido, L. A., & Silva, J. S. (2019). Associação do regime
4836 hidrológico do rio xingu com oceanos adjancentes em eventos extremos utilizando dados
4837 altimétricos. *Brazilian Journal of Development*, *5*(11). https://doi.org/10.34117/bjdv5n11-339
4838 Silva, T. S. F., Costa, M. P. F., & Melack, J. M. (2010). Spatial and temporal variability of macrophyte
4839 cover and productivity in the eastern Amazon floodplain: A remote sensing approach. *Remote*
4840 *Sensing of Environment*, *114*(9), 1998–2010. https://doi.org/10.1016/j.rse.2010.04.007
4841 Silva, T. S. F., Melack, J. M., & Novo, E. M. L. M. L. M. (2013). Responses of aquatic macrophyte cover
4842 and productivity to flooding variability on the Amazon floodplain. *Global Change Biology*, *19*(11),
4843 3379–3389. https://doi.org/10.1111/gcb.12308
4844 Sioli, H. (1956). Über natur und mensch im brasilianischen Amazonasgebiet. *Erdkunde*, pp. 89–109.

https://doi.org/http://www.jstor.org/stable/23218158

Sippe, S. J., Hamilton, S. K., Melack, J. M., & Novo, E. M. M. (1998). Passive microwave observations of inundation area and the area/stage relation in the Amazon River floodplain. *International Journal of Remote Sensing*, *19*(16), 3055–3074. https://doi.org/10.1080/014311698214181

Sippel, S. J., Hamilton, S. K., & Melack, J. (1992). Inundation area and morphometry of lakes on the Amazon River floodplain, Brazil. *Archiv Für Hydrobiologie*, *123*, 385–400.

Sippel, S. J., Hamilton, S. K., Melack, J. M., & Choudhury, B. J. (1994). Determination of inundation area in the Amazon River floodplain using the SMMR 37 GHz polarization difference. *Remote Sensing of Environment*, *48*(1), 70–76. https://doi.org/10.1016/0034-4257(94)90115-5

Siqueira, V. A., Paiva, R. C. D., Fleischmann, A. S., Fan, F. M., Ruhoff, A. L., Pontes, P. R. M., et al. (2018). Toward continental hydrologic-hydrodynamic modeling in South America. *Hydrology and Earth System Sciences*, *22*(9), 4815–4842. https://doi.org/10.5194/hess-22-4815-2018

Sörensson, A. A., & Ruscica, R. C. (2018). Intercomparison and Uncertainty Assessment of Nine Evapotranspiration Estimates Over South America. *Water Resources Research*, *54*(4), 2891–2908. https://doi.org/10.1002/2017WR021682

Sorooshian, S., Hsu, K. L., Gao, X., Gupta, H. V., Imam, B., & Braithwaite, D. (2000). Evaluation of PERSIANN system satellite-based estimates of tropical rainfall. *Bulletin of the American Meteorological Society*, *81*(9), 2035–2046. https://doi.org/10.1175/1520-0477(2000)081<2035:EOPSSE>2.3.CO;2

Sorooshian, S., Gao, X., Hsu, K., Maddox, R. A., Hong, Y., Gupta, H. V., & Imam, B. (2002). Diurnal variability of tropical rainfall retrieved from combined GOES and TRMM satellite information. *Journal of Climate*, *15*(9), 983–1001. https://doi.org/10.1175/1520-0442(2002)015<0983:DVOTRR>2.0.CO;2

Sorribas, M. V., Paiva, R. C. D., Melack, J. M., Bravo, J. M., Jones, C., Carvalho, L., et al. (2016). Projections of climate change effects on discharge and inundation in the Amazon basin. *Climatic Change*, *136*(3–4), 555–570. https://doi.org/10.1007/s10584-016-1640-2

Sorribas, M. V., Paiva, R. C. D., Fleischmann, A. S., & Collischonn, W. (2020). *Hydrological Tracking Model for Amazon Surface Waters*. *Water Resources Research* (Vol. 56). https://doi.org/10.1029/2019wr024721

Souza, C. M., Kirchhoff, F. T., Oliveira, B. C., Ribeiro, J. G., & Sales, M. H. (2019). Long-term annual surface water change in the Brazilian Amazon Biome: Potential links with deforestation, infrastructure development and climate change. *Water (Switzerland)*, *11*, 566. https://doi.org/10.3390/w11030566

4878 De Souza, E. B., & Ambrizzi, T. (2006). Modulation of the intraseasonal rainfall over tropical Brazil by
4879 the Madden–Julian oscillation. *International Journal of Climatology*, *26*(13), 1759–1776.
4880 https://doi.org/10.1002/joc.1331
4881 Spera, S. A., Cohn, A. S., Vanwey, L. K., Mustard, J. F., Rudorff, B. F., Risso, J., & Adami, M. (2014).
4882 Recent cropping frequency, expansion, and abandonment in Mato Grosso, Brazil had selective land
4883 characteristics. *Environmental Research Letters*, *9*(6). https://doi.org/10.1088/1748-
4884 9326/9/6/064010
4885 Staal, A., Tuinenburg, O. A., Bosmans, J. H. C., Holmgren, M., Van Nes, E. H., Scheffer, M., et al.
4886 (2018). Forest-rainfall cascades buffer against drought across the Amazon. *Nature Climate Change*,
4887 *8*, 539–543. https://doi.org/10.1038/s41558-018-0177-y
4888 Staal, A., Flores, B. M., Aguiar, A. P. D., Bosmans, J. H. C., Fetzer, I., & Tuinenburg, O. A. (2020).
4889 Feedback between drought and deforestation in the Amazon. *Environmental Research Letters*,
4890 *15*(4). https://doi.org/10.1088/1748-9326/ab738e
4891 Stammer, D., & Cazenave, A. (2017). *Satellite altimetry over oceans and land surfaces*. (D. Stammer &
4892 A. Cazenave, Eds.), *Satellite Altimetry Over Oceans and Land Surfaces*. CRC Press.
4893 https://doi.org/10.1201/9781315151779
4894 Stickler, C. M., Coe, M. T., Costa, M. H., Nepstad, D. C., McGrath, D. G., Dias, L. C. P., et al. (2013).
4895 Dependence of hydropower energy generation on forests in the Amazon Basin at local and regional
4896 scales. *Proceedings of the National Academy of Sciences*, *110*(23), 9601–9606.
4897 https://doi.org/10.1073/pnas.1215331110
4898 Su, Z., Schmugge, T., Kustas, W. P., & Massman, W. J. (2001). An evaluation of two models for
4899 estimation of the roughness height for heat transfer between the land surface and the atmosphere.
4900 *Journal of Applied Meteorology*, *40*(11), 1933–1951. https://doi.org/10.1175/1520-
4901 0450(2001)040<1933:AEOTMF>2.0.CO;2
4902 Sun, Q., Miao, C., Duan, Q., Ashouri, H., Sorooshian, S., & Hsu, K. (2018). A Review of Global
4903 Precipitation Data Sets: Data Sources, Estimation, and Intercomparisons. *Reviews of Geophysics*,
4904 *56*(1), 79–107. https://doi.org/10.1002/2017RG000574
4905 Sutanudjaja, E. H., van Beek, R., Wanders, N., Wada, Y., Bosmans, J. H. C., Drost, N., et al. (2018).
4906 PCR-GLOBWB 2: a 5arcmin global hydrological and water resources model. *Geoscientific Model*
4907 *Development*, *11*(6), 2429–2453. https://doi.org/10.5194/gmd-11-2429-2018
4908 Talsma, C. J., Good, S. P., Jimenez, C., Martens, B., Fisher, J. B., Miralles, D. G., et al. (2018).
4909 Partitioning of evapotranspiration in remote sensing-based models. *Agricultural and Forest*
4910 *Meteorology*, *260–261*, 131–143. https://doi.org/10.1016/j.agrformet.2018.05.010

4911 Tan, J., Huffman, G. J., Bolvin, D. T., & Nelkin, E. J. (2019). IMERG V06: Changes to the morphing
4912 algorithm. *Journal of Atmospheric and Oceanic Technology*, *36*(12), 2471–2482.
4913 https://doi.org/10.1175/JTECH-D-19-0114.1
4914 Tang, R., Li, Z. L., Jia, Y., Li, C., Chen, K. S., Sun, X., & Lou, J. (2013). Evaluating one- and two-source
4915 energy balance models in estimating surface evapotranspiration from Landsat-derived surface
4916 temperature and field measurements. *International Journal of Remote Sensing*, *34*(9–10), 3299–
4917 3313. https://doi.org/10.1080/01431161.2012.716529
4918 Tapiador, F. J., Kidd, C., Levizzani, V., & Marzano, F. S. (2004). A neural networks-based fusion
4919 technique to estimate half-hourly rainfall estimates at 0.1° resolution from satellite passive
4920 microwave and infrared data. *Journal of Applied Meteorology*, *43*(4), 576–594.
4921 https://doi.org/10.1175/1520-0450(2004)043<0576:ANNFTT>2.0.CO;2
4922 Tapiador, F. J., Navarro, A., Levizzani, V., García-Ortega, E., Huffman, G. J., Kidd, C., et al. (2017).
4923 Global precipitation measurements for validating climate models. *Atmospheric Research*, *197*, 1–20.
4924 https://doi.org/10.1016/j.atmosres.2017.06.021
4925 Tapley, B. D., Bettadpur, S., Ries, J. C., Thompson, P. F., & Watkins, M. M. (2004). GRACE
4926 measurements of mass variability in the Earth system. *Science*, *305*(5683), 503–505.
4927 https://doi.org/10.1126/science.1099192
4928 Tapley, B. D., Watkins, M. M., Flechtner, F., Reigber, C., Bettadpur, S., Rodell, M., et al. (2019, May).
4929 Contributions of GRACE to understanding climate change. *Nature Climate Change*. Nature
4930 Publishing Group. https://doi.org/10.1038/s41558-019-0456-2
4931 Tarpanelli, A., Barbetta, S., Brocca, L., & Moramarco, T. (2013). River Discharge Estimation by Using
4932 Altimetry Data and Simplified Flood Routing Modeling, 4145–4162.
4933 https://doi.org/10.3390/rs5094145
4934 Taylor, C. M., Prigent, C., & Dadson, S. J. (2018). Mesoscale rainfall patterns observed around wetlands
4935 in sub-Saharan Africa. *Quarterly Journal of the Royal Meteorological Society*, *144*(716), 2118–
4936 2132. https://doi.org/10.1002/qj.3311
4937 Thiemig, V., Rojas, R., Zambrano-Bigiarini, M., & De Roo, A. (2013). Hydrological evaluation of
4938 satellite-based rainfall estimates over the Volta and Baro-Akobo Basin. *Journal of Hydrology*, *499*,
4939 324–338. https://doi.org/10.1016/j.jhydrol.2013.07.012
4940 Thom, G., Xue, A. T., Sawakuchi, A. O., Ribas, C. C., Hickerson, M. J., Aleixo, A., & Miyaki, C. (2020).
4941 Quaternary climate changes as speciation drivers in the Amazon floodplains. *Science Advances*,
4942 *6*(11). https://doi.org/10.1126/sciadv.aax4718
4943 Thomaz, S. M., Bini, L. M., & Bozelli, R. L. (2007). Floods increase similarity among aquatic habitats in

river-floodplain systems. *Hydrobiologia*, *579*(1), 1–13. https://doi.org/10.1007/s10750-006-0285-y

Topp, S. N., Pavelsky, T. M., Jensen, D., Simard, M., & Ross, M. R. V. (2020). Research trends in the use of remote sensing for inland water quality science: Moving towards multidisciplinary applications. *Water (Switzerland)*, *12*(1), 1–34. https://doi.org/10.3390/w12010169

Toté, C., Patricio, D., Boogaard, H., van der Wijngaart, R., Tarnavsky, E., & Funk, C. (2015). Evaluation of satellite rainfall estimates for drought and flood monitoring in Mozambique. *Remote Sensing*, *7*(2), 1758–1776. https://doi.org/10.3390/rs70201758

Tourian, M. J., Reager, J. T., & Sneeuw, N. (2018). The Total Drainable Water Storage of the Amazon River Basin: A First Estimate Using GRACE. *Water Resources Research*, *54*(5), 1–27. https://doi.org/10.1029/2017WR021674

Towner, J., Cloke, H. L., Zsoter, E., Flamig, Z., Hoch, J. M., Bazo, J., et al. (2019). Assessing the performance of global hydrological models for capturing peak river flows in the Amazon basin. *Hydrology and Earth System Sciences*. https://doi.org/10.5194/hess-23-3057-2019

Trenberth, K. E. (2011). Changes in precipitation with climate change. *Climate Research*, *47*(1–2), 123–138. https://doi.org/10.3354/cr00953

Trigg, M. A., Wilson, M. D., Bates, P. D., Horritt, M. S., Alsdorf, D. E., Forsberg, B. R., & Vega, M. C. (2009). Amazon flood wave hydraulics. *Journal of Hydrology*, *374*(1–2), 92–105. https://doi.org/10.1016/j.jhydrol.2009.06.004

Trigg, M. A., Bates, P. D., Wilson, M. D., Schumann, G., & Baugh, C. (2012). Floodplain channel morphology and networks of the middle Amazon River. *Water Resources Research*, *48*(10), 1–17. https://doi.org/10.1029/2012WR011888

Turk, F. J., Rohaly, G. D., Jeff, H., Smith, E. A., Marzano, F. S., Mugnai, A., & Levizzani, V. (2000). Meteorological applications of precipitation estimation from combined SSM/I, TRMM and infrared geostationary. *Microwave Radiometry and Remote Sensing of the Earth's Surface and Atmosphere*, (January), 353.

Ushio, T., Sasashige, K., Kubota, T., Shige, S., Okamoto, K., Aonashi, K., et al. (2009). A kalman filter approach to the global satellite mapping of precipitation (GSMaP) from combined passive microwave and infrared radiometric data. *Journal of the Meteorological Society of Japan*, *87 A*(November 2008), 137–151. https://doi.org/10.2151/jmsj.87A.137

Valerio, A. de M., Kampel, M., Vantrepotte, V., Ward, N. D., Sawakuchi, H. O., Less, D. F. D. S., et al. (2018). Using CDOM optical properties for estimating DOC concentrations and pCO2 in the Lower Amazon River. *Optics Express*, *26*(14), A657. https://doi.org/10.1364/oe.26.00a657

Venticinque, E., Forsberg, B., Barthem, R., Petry, P., Hess, L., Mercado, A., et al. (2016). An explicit

GIS-based river basin framework for aquatic ecosystem conservation in the Amazon. *Earth System Science Data*, *8*(2), 651–661. https://doi.org/10.5194/essd-8-651-2016

Vera, C. S., Alvarez, M. S., Gonzalez, P. L. M., Liebmann, B., & Kiladis, G. N. (2018). Seasonal cycle of precipitation variability in South America on intraseasonal timescales. *Climate Dynamics*, *51*(5–6), 1991–2001. https://doi.org/10.1007/s00382-017-3994-1

Viale, M., Bianchi, E., Cara, L., Ruiz, L. E., Villalba, R., Pitte, P., et al. (2019). Contrasting climates at both sides of the Andes in Argentina and Chile. *Frontiers in Environmental Science*, *7*(May), 1–15. https://doi.org/10.3389/fenvs.2019.00069

Vicente, G. A., Scofield, R. A., & Menzel, W. P. (1998). The Operational GOES Infrared Rainfall Estimation Technique. *Bulletin of the American Meteorological Society*, *79*(9), 1883–1893. https://doi.org/10.1175/1520-0477(1998)079<1883:togire>2.0.co;2

Villar, R. E., Martinez, J. M., Le Texier, M., Guyot, J. L., Fraizy, P., Meneses, P. R., & Oliveira, E. de. (2013). A study of sediment transport in the Madeira River, Brazil, using MODIS remote-sensing images. *Journal of South American Earth Sciences*, *44*, 45–54. https://doi.org/10.1016/j.jsames.2012.11.006

Villar, R. E., Martinez, J. M., Armijos, E., Espinoza, J. C., Filizola, N., Dos Santos, A., et al. (2018). Spatio-temporal monitoring of suspended sediments in the Solimões River (2000–2014). *Comptes Rendus - Geoscience*, *350*(1–2), 4–12. https://doi.org/10.1016/j.crte.2017.05.001

Virji, H. (1981). A Preliminary Study of Summertime Tropospheric Circulation Patterns over South America Estimated from Cloud Winds. *Monthly Weather Review*, *109*(3), 599–610. https://doi.org/10.1175/1520-0493(1981)109<0599:APSOST>2.0.CO;2

Vörösmarty, C. J., Moore, B., Grace, A. L., Gildea, M. P., Melillo, J. M., Peterson, B. J., et al. (1989). Continental scale models of water balance and fluvial transport: An application to South America. *Global Biogeochemical Cycles*, *3*(3), 241–265. https://doi.org/10.1029/GB003i003p00241

Vörösmarty, C. J., Green, P., Salisbury, J., & Lammers, R. B. (2000). Global water resources: Vulnerability from climate change and population growth. *Science*, *289*(5477), 284–288. https://doi.org/10.1126/science.289.5477.284

Wanders, N., Bierkens, M. F. P., de Jong, S. M., de Roo, A., & Karssenberg, D. (2014). The benefits of using remotely sensed soil moisture in parameter identification of large-scale hydrological models. *Water Resources Research*, *50*(8), 6874–6891. https://doi.org/10.1002/2013WR014639

Wang, C., Li, Z., Zhu, J., Yi, H., & Xie, Q. (2011). Flooded forest water level changes in Amazon measured with ALOS PALSAR polarimetric interferometric SAR data. *Journal of Computational Information Systems*, *7*(8), 2922–2930.

5010 Wang, G., Cao, X., Cai, X., Sun, J., Li, X., & Wang, H. (2018). A new data assimilation method for high-
5011 dimensional models. *PLoS ONE*, *13*(2), 1–15. https://doi.org/10.1371/journal.pone.0191714
5012 Wang, Y., Hess, L. L., Filoso, S., & Melack, J. M. (1995). Understanding the radar backscattering from
5013 flooded and nonflooded Amazonian forests: Results from canopy backscatter modeling. *Remote*
5014 *Sensing of Environment*, *54*, 324–332. https://doi.org/10.1016/0034-4257(95)00140-9
5015 Ward, J. V., Tockner, K., Arscott, D. B., & Claret, C. (2002). Riverine landscape diversity. *Freshwater*
5016 *Biology*, *47*, 517–539. https://doi.org/10.1046/j.1365-2427.2002.00893.x
5017 Werdell, P. J., McKinna, L. I. W., Boss, E., Ackleson, S. G., Craig, S. E., Gregg, W. W., et al. (2018). An
5018 overview of approaches and challenges for retrieving marine inherent optical properties from ocean
5019 color remote sensing. *Progress in Oceanography*, *160*(January), 186–212.
5020 https://doi.org/10.1016/j.pocean.2018.01.001
5021 Werdell, P. J., Behrenfeld, M. J., Bontempi, P. S., Boss, E., Cairns, B., Davis, G. T., et al. (2019). The
5022 plankton, aerosol, cloud, ocean ecosystem mission status, science, advances. *Bulletin of the*
5023 *American Meteorological Society*, *100*(9), 1775–1794. https://doi.org/10.1175/BAMS-D-18-0056.1
5024 Wilson, M. D., Bates, P., Alsdorf, D., Forsberg, B., Horritt, M., Melack, J., et al. (2007). Modeling large-
5025 scale inundation of Amazonian seasonally flooded wetlands. *Geophysical Research Letters*, *34*(15),
5026 4–9. https://doi.org/10.1029/2007GL030156
5027 Wilson, M. D., Durand, M., Jung, H. C., & Alsdorf, D. (2015). Swath-altimetry measurements of the
5028 main stem Amazon River :, 1943–1959. https://doi.org/10.5194/hess-19-1943-2015
5029 Winemiller, K. O., McIntyre, P. B., Castello, L., Fluet-Chouinard, E., Giarrizzo, T., Nam, S., et al. (2016).
5030 Balancing hydropower and biodiversity in the Amazon, Congo, and Mekong. *Science*, *351*(6269),
5031 128–129. https://doi.org/10.1126/science.aac7082
5032 Wittmann, F., Anhuf, D., & Funk, W. J. (2002). Tree species distribution and community structure of
5033 central Amazonian várzea forests by remote-sensing techniques. *Journal of Tropical Ecology*, *18*(6),
5034 805–820. https://doi.org/10.1017/S0266467402002523
5035 Wongchuig, S. C., de Paiva, R. C. D., Siqueira, V., & Collischonn, W. (2019). Hydrological reanalysis
5036 across the 20th century: A case study of the Amazon Basin. *Journal of Hydrology*, *570*, 755–773.
5037 https://doi.org/10.1016/j.jhydrol.2019.01.025
5038 Wongchuig, S. C., Paiva, R. C. D. de, Biancamaria, S., & Collischonn, W. (2020). Assimilation of future
5039 SWOT-based river elevations, surface extent observations and discharge estimations into uncertain
5040 global hydrological models. *Journal of Hydrology*, *590*(125473).
5041 https://doi.org/10.1016/j.jhydrol.2020.125473
5042 Wood, E. F., Roundy, J. K., Troy, T. J., Van Beek, L. P. H., Bierkens, M. F. P., Blyth, E., et al. (2011).

5043 Hyperresolution global land surface modeling: meeting a grand challenge for monitoring Earth's
5044 terrestrial water. *Water Resources Research*, *47*(5), 1–10. https://doi.org/10.1029/2010WR010090
5045 Wright, J. S., Fu, R., Worden, J. R., Chakraborty, S., Clinton, N. E., Risi, C., et al. (2017). Rainforest-
5046 initiated wet season onset over the southern Amazon. *Proceedings of the National Academy of*
5047 *Sciences of the United States of America*, *114*(32), 8481–8486.
5048 https://doi.org/10.1073/pnas.1621516114
5049 Wu, J., Lakshmi, V., Wang, D., Lin, P., Pan, M., Cai, X., et al. (2020). The reliability of global remote
5050 sensing evapotranspiration products over Amazon. *Remote Sensing*, *12*(14).
5051 https://doi.org/10.3390/rs12142211
5052 Xavier, L., Becker, M., Cazenave, A., Longuevergne, L., Llovel, W., & Filho, O. C. R. (2010).
5053 Interannual variability in water storage over 2003–2008 in the Amazon Basin from GRACE space
5054 gravimetry, in situ river level and precipitation data. *Remote Sensing of Environment*, *114*(8), 1629–
5055 1637. https://doi.org/10.1016/J.RSE.2010.02.005
5056 Xie, P., Janowiak, J. E., Arkin, P. A., Adler, R., Gruber, A., Ferraro, R., et al. (2003). GPCP pentad
5057 precipitation analyses: An experimental dataset based on gauge observations and satellite estimates.
5058 *Journal of Climate*, *16*(13), 2197–2214. https://doi.org/10.1175/2769.1
5059 Xie, P., Joyce, R., Wu, S., Yoo, S. H., Yarosh, Y., Sun, F., & Lin, R. (2017). Reprocessed, bias-corrected
5060 CMORPH global high-resolution precipitation estimates from 1998. *Journal of Hydrometeorology*,
5061 *18*(6), 1617–1641. https://doi.org/10.1175/JHM-D-16-0168.1
5062 Xu, X., Jia, G., Zhang, X., Riley, W. J., & Xue, Y. (2020). Climate regime shift and forest loss amplify
5063 fire in Amazonian forests. *Global Change Biology*, *26*(10), 5874–5885.
5064 https://doi.org/10.1111/gcb.15279
5065 Yamazaki, D., Kanae, S., Kim, H., & Oki, T. (2011). A physically based description of floodplain
5066 inundation dynamics in a global river routing model. *Water Resources Research*, *47*(4).
5067 https://doi.org/10.1029/2010WR009726
5068 Yamazaki, D., Baugh, C. A., Bates, P. D., Kanae, S., Alsdorf, D. E., & Oki, T. (2012). Adjustment of a
5069 spaceborne DEM for use in floodplain hydrodynamic modeling. *Journal of Hydrology*, *436–437*,
5070 81–91. https://doi.org/10.1016/j.jhydrol.2012.02.045
5071 Yamazaki, D., Lee, H., Alsdorf, D. E., Dutra, E., Kim, H., Kanae, S., & Oki, T. (2012). Analysis of the
5072 water level dynamics simulated by a global river model: A case study in the Amazon River. *Water*
5073 *Resources Research*, *48*(9), 1–15. https://doi.org/10.1029/2012WR011869
5074 Yamazaki, D., O'Loughlin, F., Trigg, M. A., Miller, Z. F., Pavelsky, T. M., & Bates, P. D. (2014).
5075 Development of the Global Width Database for Large Rivers. *Water Resources Research*, *50*(4),

3467–3480. https://doi.org/10.1002/2013WR014664

Yamazaki, D., Trigg, M. A., & Ikeshima, D. (2015). Development of a global ~90m water body map using multi-temporal Landsat images. *Remote Sensing of Environment*, *171*, 337–351. https://doi.org/10.1016/j.rse.2015.10.014

Yamazaki, D., Ikeshima, D., Tawatari, R., Yamaguchi, T., O'Loughlin, F., Neal, J. C., et al. (2017). A high-accuracy map of global terrain elevations. *Geophysical Research Letters*, *44*(11), 5844–5853. https://doi.org/10.1002/2017GL072874

Yamazaki, D., Ikeshima, D., Sosa, J., Bates, P. D., Allen, G. H., & Pavelsky, T. M. (2019). MERIT Hydro: A High-Resolution Global Hydrography Map Based on Latest Topography Dataset. *Water Resources Research*, *55*(6), 5053–5073. https://doi.org/10.1029/2019WR024873

Yang, Z., & Dominguez, F. (2019). Investigating land surface effects on the moisture transport over South America with a moisture tagging model. *Journal of Climate*, *32*(19), 6627–6644. https://doi.org/10.1175/JCLI-D-18-0700.1

Yepez, S., Laraque, A., Martinez, J. M., Sa, J. De, Manuel, J., Castellanos, B., et al. (2018). Retrieval of suspended sediment concentrations using Landsat-8 OLI satellite images in the Orinoco River (Venezuela). *Comptes Rendus - Geoscience*, *350*(1–2), 20–30. https://doi.org/10.1016/j.crte.2017.08.004

Yilmaz, K. K., Hogue, T. S., Hsu, K. L., Sorooshian, S., Gupta, H. V., & Wagener, T. (2005). Intercomparison of rain gauge, radar, and satellite-based precipitation estimates with emphasis on hydrologic forecasting. *Journal of Hydrometeorology*, *6*(4), 497–517. https://doi.org/10.1175/JHM431.1

Yuan, T., Lee, H., Jung, H. C., Aierken, A., Beighley, E., Alsdorf, D. E., et al. (2017). Absolute water storages in the Congo River floodplains from integration of InSAR and satellite radar altimetry. *Remote Sensing of Environment*, *201*(March), 57–72. https://doi.org/10.1016/j.rse.2017.09.003

Zakharova, E. A., Kouraev, A. V., Cazenave, A., & Seyler, F. (2006). Amazon River discharge estimated from TOPEX/Poseidon altimetry. *Comptes Rendus - Geoscience*, *338*(3), 188–196. https://doi.org/10.1016/j.crte.2005.10.003

Zemp, D. C., Schleussner, C. F., Barbosa, H. M. J., Van Der Ent, R. J., Donges, J. F., Heinke, J., et al. (2014). On the importance of cascading moisture recycling in South America. *Atmospheric Chemistry and Physics*, *14*(23), 13337–13359. https://doi.org/10.5194/acp-14-13337-2014

Zemp, D. C., Schleussner, C. F., Barbosa, H. M. J., Hirota, M., Montade, V., Sampaio, G., et al. (2017). Self-amplified Amazon forest loss due to vegetation-atmosphere feedbacks. *Nature Communications*, *8*(14681). https://doi.org/10.1038/ncomms14681

5109 Zeng, N., Yoon, J. H., Marengo, J. A., Subramaniam, A., Nobre, C. A., Mariotti, A., & Neelin, J. D.
5110 (2008). Causes and impacts of the 2005 Amazon drought. *Environmental Research Letters*, *3*(1),
5111 014002. https://doi.org/10.1088/1748-9326/3/1/014002
5112 Zhang, Ke, Kimball, J. S., & Running, S. W. (2016, November 1). A review of remote sensing based
5113 actual evapotranspiration estimation. *Wiley Interdisciplinary Reviews: Water*. John Wiley and Sons
5114 Inc. https://doi.org/10.1002/wat2.1168
5115 Zhang, Kun, Zhu, G., Ma, J., Yang, Y., Shang, S., & Gu, C. (2019). Parameter Analysis and Estimates for
5116 the MODIS Evapotranspiration Algorithm and Multiscale Verification. *Water Resources Research*,
5117 *55*(3), 2211–2231. https://doi.org/10.1029/2018WR023485
5118 Zhang, Y., Pan, M., Sheffield, J., Siemann, A. L., Fisher, C. K., Liang, M., et al. (2018). A Climate Data
5119 Record (CDR) for the global terrestrial water budget: 1984-2010. *Hydrology and Earth System*
5120 *Sciences*, *22*(1), 241–263. https://doi.org/10.5194/hess-22-241-2018
5121 Zheng, G., & DiGiacomo, P. M. (2017). Remote sensing of chlorophyll-a in coastal waters based on the
5122 light absorption coefficient of phytoplankton. *Remote Sensing of Environment*, *201*(September),
5123 331–341. https://doi.org/10.1016/j.rse.2017.09.008
5124 Zhou, J., & Lau, K. M. (1998). Does a monsoon climate exist over South America? *Journal of Climate*,
5125 *11*(5), 1020–1040. https://doi.org/10.1175/1520-0442(1998)011<1020:DAMCEO>2.0.CO;2
5126 Zhou, L., Divakarla, M., & Liu, X. (2016). An overview of the joint polar satellite system (JPSS) science
5127 data product calibration and validation. *Remote Sensing*, *8*(2). https://doi.org/10.3390/rs8020139
5128 Zubieta, R., Getirana, A., Espinoza, J. C., & Lavado, W. (2015). Impacts of satellite-based precipitation
5129 datasets on rainfall-runoff modeling of the Western Amazon basin of Peru and Ecuador. *Journal of*
5130 *Hydrology*, *528*, 599–612. https://doi.org/10.1016/j.jhydrol.2015.06.064
5131 Zubieta, R., Getirana, A., Espinoza, J. C., Lavado-Casimiro, W., & Aragon, L. (2017). Hydrological
5132 modeling of the Peruvian-Ecuadorian Amazon Basin using GPM-IMERG satellite-based
5133 precipitation dataset. *Hydrology and Earth System Sciences*, *21*(7), 3543–3555.
5134 https://doi.org/10.5194/hess-21-3543-2017
5135 Zubieta, R., Saavedra, M., Espinoza, J. C., Ronchail, J., Sulca, J., Drapeau, G., & Martin-Vide, J. (2019).
5136 Assessing precipitation concentration in the Amazon basin from different satellite-based data sets.
5137 *International Journal of Climatology*, *39*(7), 3171–3187. https://doi.org/10.1002/joc.6009
5138 Zulkafli, Z., Buytaert, W., Onof, C., Lavado, W., & Guyot, J. L. (2013). A critical assessment of the
5139 JULES land surface model hydrology for humid tropical environments. *Hydrology and Earth*
5140 *System Sciences*, *17*(3), 1113–1132. https://doi.org/10.5194/hess-17-1113-2013
5141 Zulkafli, Zed, Buytaert, W., Onof, C., Manz, B., Tarnavsky, E., Lavado, W., & Guyot, J. L. (2014). A

comparative performance analysis of TRMM 3B42 (TMPA) versions 6 and 7 for hydrological applications over Andean-Amazon river basins. *Journal of Hydrometeorology*, *15*(2), 581–592. https://doi.org/10.1175/JHM-D-13-094.1

Zulkafli, Zed, Buytaert, W., Manz, B., Rosas, C. V., Willems, P., Lavado-Casimiro, W., et al. (2016). Projected increases in the annual flood pulse of the Western Amazon. *Environmental Research Letters*, *11*(1). https://doi.org/10.1088/1748-9326/11/1/014013